Methodological Development and Computational Investigations of Metal-Catalyzed Coupling Reactions

Thesis by

Robert L. Anderson

In Partial Fulfillment of the Requirements for

the Degree of

Doctor of Philosophy in Chemistry

CALIFORNITA INSTITUTE OF TECHNOLOGY

Pasadena, California

2026

(Defended September 30th, 2025)

ACKNOWLEDGEMENTS

Earning a PhD in chemistry is no doubt, one of the most difficult things I consider myself to have accomplished. In remembering the struggles, twists of fate, late nights, and flashes of insight, it cannot be forgotten that no amount of any of these would have made achieving this degree possible were it not for the myriad people who helped me with incredible thoughtfulness, companionship, support, and care. While it must be disclaimed that no short epitaph here can give full and proper credit to those who played this role, let it be said that the following work stands as a testament to not only the work described, but also those people who made it possible.

First among these is my advisor, Professor Gregory C. Fu. During my studies, Greg has provided the support I have needed to develop as a chemist, as well as the guidelines needed to pursue the right lines of inquiry. He has challenged me to be an expert and shown me the indispensable nature of expertise. I greatly appreciate the risks he undertook to support my progress and for believing in my potential. His unerring professionalism displayed without coldness enabled a more honest approach to the scientific process, the benefits of which cannot be overstated. I must thank also members of my committee, Professor Sarah Reisnman, Professor Theo Agapie, and Professor Bill Goddard. Their continual willingness to pursue discussion and provide support and ideas was critical to my success.

I have greatly enjoyed working with my coworkers in the Fu lab, who have provided a deep well of knowledge, friendship, and many hilarious stories. I want to especially thank Dr. Dan Tong, who pursued his degree alongside me; his innovation always provided me with inspiration, and his sense of humor proved an excellent addition to lab culture. I appreciate greatly the work of my collaborators, Dr. Jason Rygus, Dr. Asik Hossain, Dr. Feng Zhong, Dr. Hyungdo Cho, Dr. Giuseppe Zuccarello, Ruby Chen, Claudia Zhang, and Carlos Del Angel Aguilar. I want to thank

all the other labmates whose time overlapped with mine, including Dr. Zhaobin Wang, Arianna Ayonon, Dr. Wendy Zhang, Dr. Zepeng Yang, Dr. Socrates Munoz, Dr. Suzanne Batiste, Dr. Robynne Neff, Dr. Dylan Freas, Dr. Felix Schneck, Dr. Caiyou Chen, Dr. Renhe Li, Dr. Dong Liu, Rina Wang, Grace Fleury, Yuxuan Li, Laura Martinez Leal, Kyra Jackson, Dr. Arup Mondal, Dr. Skye Yang, Matt Wong, and Zhuoyan Wang. I also have much appreciation for Julianne Just who has provided stellar support for the lab, as well as Joyce Wu for accomplishing the same.

The wider Caltech community also deserves mention, including my collaborators Dr. Paul Oyala for operating the Caltech EPR facility, Ruby Chen, and Maria Blankenmeyer. Dr. Charles Musgrave provided significant support in teaching me computational techniques. Much thanks goes to Dr. Scott Virgil for providing unestimable support for lab equipment, as well as Dr. David Vander Velde and Dr. Rajan Paranji for maintaining the NMR facility. Thanks go to Nathan Hart for keeping our glassware in working order, and to Joe Drew for keeping the building in order. In addition, thank you to Leslie for keeping our floor clean tirelessly for many years. The administrative staff of Caltech deserves mention, including Alison Ross, Suri Pourmodheji, Annette Luymes, and Grace Liang-Franco, who needs special recognition for updating the periodic table of elements located on the wall of Noyes 153 at my request. Further, Suresh Gupta provided me with technical help at just the right time.

My time at Caltech was also blessed with the company of many friends. I remember fondly times with my roommates Dr. Nick Watkins. Dr. Brian Lee, Dr. Michelle Chan, Dr. Steven Stradley, Andreas Butler, and Tucker Folsom. Other friends found at Caltech include Sari Kerkhove, Dr. Annette Boehme, Jillian Reed, David Fager, Vignesh Bhethanabotla, Krista Dong, Conner Wells, Dr. Jake Rothbaum, and Dr. David Cagan, Mengdi Li, and Sasha Alabugin.

Before my time at Caltech I benefited from the mentorship of many mentors and teachers, including Dr. Noam Saper at Berkeley, and my first chemistry teachers Tony Sartori and Paul Farnham who encouraged me to shoot for the stars. Thanks also to Professor Robert Zoellner, who graciously introduced me to the world of research. I am grateful to the Ammon family and the Mathews family who proved the support of critical encouragement.

Without my family's support I would never have gotten this far. My thanks go to my parents Bill and Theresa Anderson for giving me what I needed to pursue my goals. Much thanks goes to my siblings Danica, Talia, and Stephen, who have each provided key support in their own ways throughout my entire life. Thanks too to my grandmother Sue whose optimism and unconditional support cannot be discounted.

Finally, I want to thank my partner, Lucia Hwang, for her unerring support during my PhD. She has always displayed understanding at the most important times, and humor when it was sorely needed. I am very excited to begin the next phase of our life together, and I hope to make many future mutual discoveries. I would also like to thank the wider Hwang family for their quick acceptance and support, and for making me feel welcome in their lives.

ABSTRACT

Chapter One describes the computational study of the asymmetric arylation of propargylic electrophiles. While previous mechanistic experiments have verified the general scheme of the catalytic cycle, it was still not known what the enantiodetermining step is, or how factors of the ligand and substrate influence reactivity. To answer these questions, a computational study to emulate the entire catalytic cycle was performed. It was determined that radical addition to the nickel catalyst was likely the enantiodetermining step. While the standard substrate and ligand combinations result was well predicted, the computational method was not widely applicable to different ligands. This implies that the catalytic cycle may not go through a discrete radical capture and reductive elimination step, but instead a more concerted process may be operating.

Chapter Two details the development of the asymmetric cross-coupling between tertiary nucleophiles and secondary electrophiles. Specifically, α-zincated benzylic nitriles are asymmetrically coupling with secondary alkyl iodides under the influence of a nickel catalyst and iminopyrox ligand. This study represents the first report of such a ligand being use for any asymmetric nickel-catalyzed cross-couplings.

Chapter Three describes computational work on three separate projects published by coworkers in the Fu lab.

1) The first section details work on the nickel-catalyzed asymmetric coupling of enynes with secondary racemic electrophiles to accomplish for the first time the simultaneous control of axial and point chirality. The computational work probed the possible steps of rearrangement of the putative nickel-propargyl species into nickel allenyl species, as

well as rationalized the different reactivity of the catalyst towards different electrophiles.

2) The second project was investigations into the photocatalytic coupling of secondary and tertiary electrophiles with secondary amines by copper and a dual-ligand system. The computations shed light on possible C—N coupling mechanisms, as well as rationalized the differing photoactivity of the two Cu^{I} complexes present in the system.
3) The final work supported mechanistic studies into the photocatalytic asymmetric azidation of α-bromoamides by a copper-phosphine complex. DFT studies were performed to predict EPR spectra which were used to disambiguate the possible Cu^{II} species present in solution.

CONTRIBUTIONS TO PUBLISHED WORK

1) A. Hossain, **R. L. Anderson**, C. S. Zhang, P.-J. Chen, G. C. Fu*. Nickel-Catalyzed Enantioconvergent and Diastereoselective Allenylation of Alkyl Electrophiles: Simultaneous Control of Central and Axial Chirality. J. Am. Chem. Soc. 2024, 146, 7173-7177. DOI: 10.1021/jacs.4c00593.

   Personal Contribution: I calculated bond dissociation energies for relevant molecular species as well as performed calculations exploring putative reaction intermediates.

2) H. Cho, X. Tong, G. Zuccarello, **R. L. Anderson**, G. C. Fu*. Synthesis of Tertiary Alkyl Amines via Photoinduced Copper-Catalysed Nucleophilic Substitution. Nature Chemistry. 2025, 17, 271-278. DOI: 10.1038/s41557-024-01692-w

   Personal Contributon: I calculated putative catalytic cycles to explain the C-N bond forming step, rationalize observed species in solution, and offer explanations for photocatalyst activity.

3) F. Zhong, **R. L. Anderson**, P. H. Oyala, G. C. Fu*. Photoinduced, Copper-Catalyzed Enantioconvergent Azidation of Alkyl Halides. JACS. https://doi.org/10.1021/jacs.5c10003

   Personal contribution: I performed calculations of EPR properties of putative species to help disambiguate the assignment of EPR spectra of the catalytic reaction.

TABLE OF CONTENTS

LIST OF ABBREVIATIONS

%ee	Enantiomeric excess
2,2-bipy	2,2'-Bipyridine
2-Me-THF	2-methyl tetrahydrofuran
4CzIPN	1,2,3,5-Tetrakis(carbazol-9-yl)-4,6-dicyanobenzene, 2,4,5,6-Tetrakis(9H-carbazol-9-yl) isophthalonitrile
Å	Angstrom
Ac	Acetyl
AI	Artifical Intelligence
Ar	Generic aryl group
BArF4	Tetrakis[3,5-bis(trifluoromethyl)phenyl]borate
BDE	Bond Dissociation Energy
BDFE	Bond Dissociation Free Energy
Biox	Bi-oxazoline
Bn	Benzyl, PhCH2
Boc	tert-butyl caraboxy group
BOX	Bisoxazoline
COD	1,5-Cyclooctadiene
Cy	Cyclohexyl
DCM	Dichloromethane
DFT	Density Functional Theory
diglyme	bis(2-methoxyethyl) ether
DMA	N,N-dimethylacetamide
DME	1,2-Dimethoxyethane
DMF	N,N-dimethylformamide
dtbpy	4,4'-di-tert-butyl-bipyridine
EPR	Electron Paramagnetic Resonance
Et	Ethyl, CH3CH2
Et2O	Diethyl Ether
EtOAc	Ethyl acetate
EWG	Electron Withdrawing Group
FID	Flame Ionization Detector
GC	Gas Chromatography
GCMS	Gas Chromatography-Mass Spectroscopy
glyme	1,2-Dimethoxyethane
HBD	Hydrogen Bond Donor
HTE	High-Throughput Experimentation
i-Pr	Isopropyl fragment, (CH3)2CH
IR	Infrared
kcal	kilocalori
LED	Light Emitting Diode
LG	Leaving Group
LiHMDS	Lithium hexamethyldisilylamide

M	Molar
Me	Methyl, CH3
MeOH	Methanol
MHz	Megahertz
ML	Machine Learning
MLR	Multivariate Linear Regression
mmol	millimole
mol	mole
Ms	Mesylate
mtorr	millitorr
N3	Azidyl
NaDA	Sodium diisopropylamide
n-Bu	Linear n-butyl, CH3CH2CH2CH2
n-BuLi	n-butylithium
NMR	Nuclear Magnetic Resonance
ºC	Degrees Celsius
Ph	Phenyl, C6H5
ppm	parts per million
PTFE	Perfluorotetrafluoroethylene
PyBox	Pyridine-bisoxazoline
s-BuLi	sec-butyllithium
SOMO	Singly Occupied Molecular Orbtal
TBS	Tert-Butyldimethylsilyl
t-Bu	tert-Butyl
TD-DFT	Time-Dependent Density Functional Theory
TFA	Trifluoroacetate
THF	Tetrahydrofuran
TMEDA	N,N,N′,N′-Tetramethylethane-1,2-diamine
TMS	Trimethylsilyl
TMSN3	Trimithylsilyl azide
TMTAU	N,N',N',N''-Tetramethyl-2,6,10-triazaundecane
ΔΔG	Change in the difference of Gibb's free energies

CHAPTER ONE

1. Introduction

1.1: Models of asymmetric induction

A defining feature of the evolution of synthetic organic chemistry is the development of ever more accurate models capable of explaining and anticipating reaction outcomes. The utility of models extends beyond facilitating synthesis: their success or failure itself is a test of their foundational theories. Models can be placed on a spectrum ranging from the empirical, relying on rules derived from observations of many examples to the *ab initio*, those models derived from more fundamental physical laws. The development of empirical models is often top-down, involving the aggregation of data to detect trends. By contrast, the development of *ab initio* models by definition arises from more fundamental physical laws. The former models tend to be motivated by explaining some subset of chemical reactivity, while *ab initio* models attempt to explain a broad class of phenomena from a few laws. In the 19th century, empirical models dominated and include Markovnikov's rule[1], Zaitsev's rule,[2] Hoffman's rule,[3] and Walden's observations of

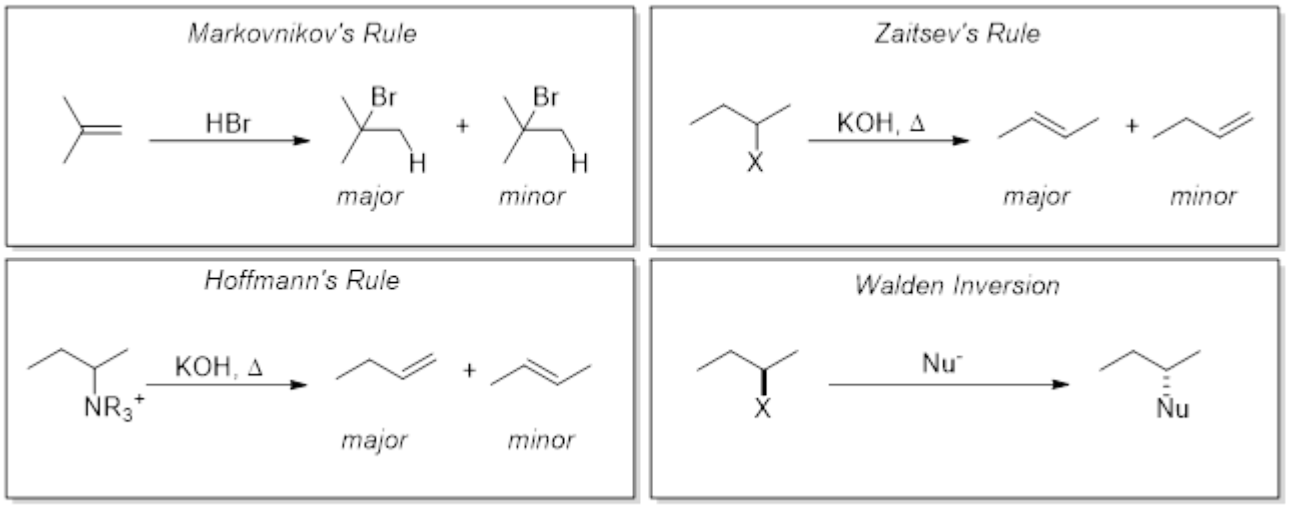

Figure 1.1.1: Early empirical rules for predicting product selectivity.

stereochemical inversion (Fig 1.1.1).[4] The advent of the Schrödinger equation and related developments in quantum mechanics from 1925 marked an explosion of *ab initio* chemical modeling.[5,6] Shortly after its introduction molecular orbital theory offered a new and powerful way to interrogate the nature chemical bonds.[7] This theory in turn led to, among many other things, the Woodward-Hoffman rules, which stand as a tremendous success in the use of theory to predict stereochemical outcomes.[8]

Reactions involving asymmetric induction and stereoselectivity are of particular importance to organic chemists. Early attempts to solve these problems were greatly aided by the advancement of X-ray crystallography techniques alongside quantum theories, which allowed for unprecedented knowledge of the ground-state geometry of molecules. Given however that transition states, and not ground states, are of much more importance to reaction outcomes, early models were more empirical, and it had to be assumed that transition states resembled reactants. Despite this, early success was achieved in the prediction of nucleophilic additions to carbonyl compounds. Additions to carbonyl compounds represent a diverse and powerful method of C—C bond construction, and are relevant to diverse total synthesis, such as that of polyketide natural products.[9] Cram,[10] Felkin,[11] Ahn,[12] Prelog,[13] and others[14] provided pioneering models to explain the stereoselectivity of 1,2 additions to carbonyl compounds (Fig. 1.1.2). These models were expanded to explain additions to β-substituted carbonyls,[15] as well as those with chelating β-groups.[16,17] Advances in

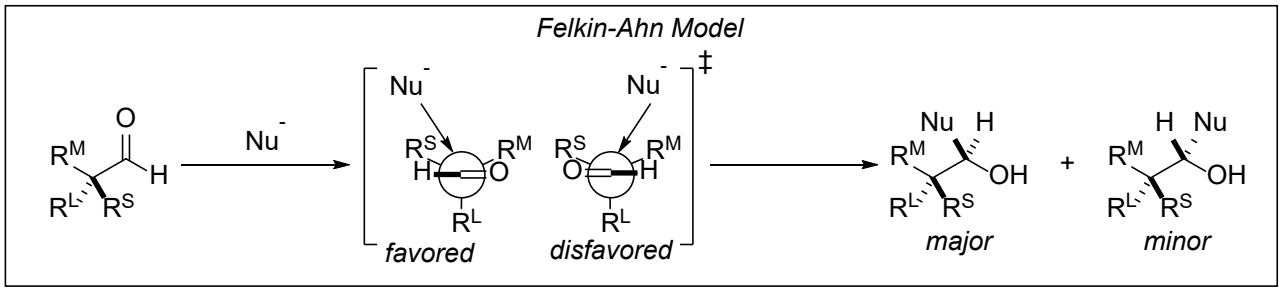

Figure 1.1.2: Felkin-Ahn stereochemical model for predicting 1,2-carbonyl addition products.

computing allowed for more advanced modeling and expansion of these findings.[18] For example in 1982, using *ab initio* methods Houk reported on the preferred angles of attack of nucleophiles, electrophiles, and radicals to double bonds,[19] building on the findings of Bürgi and Dunitz regarding the preferred angle of attack towards carbonyl compounds.[20,21] Force field models, which essentially treat molecular bonds as springs with empirically defined spring constants,[22] proved to be a valuable early application of computational chemistry, as they can provide more quantitatively accurate results while being computationally tractable.[23] This has allowed for the prediction of reaction products in more complex cases. As an example, Tareda and Yamamura were able to predict the outcome of the cope rearrangement of germacrene A using a force field model, correctly predicting that only the *cis*-elemene isomer would form (Fig. 1.1.3A).[24] Force-field models were also used to predict the selectivity of an intermolecular diels-alder reaction to generate intermediates relevant to the synthesis of the spirotetronate polyketide class of natural products(Fig

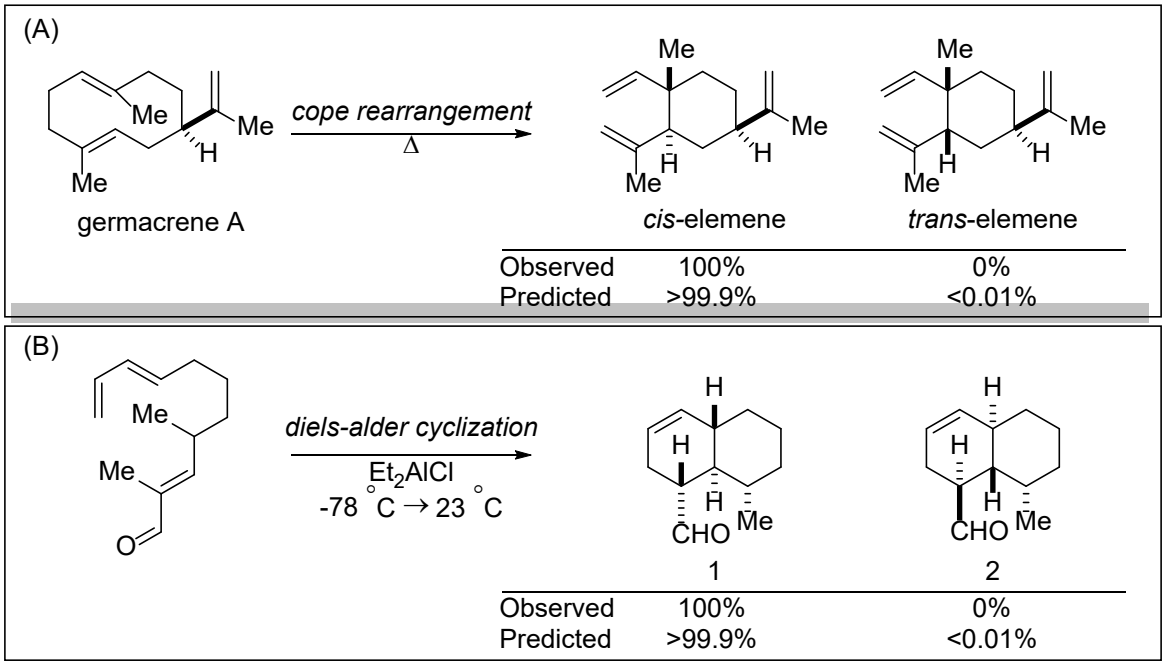

Figure 1.1.3 (A) Prediction of the major product of the cope rearrangement of germacrene A**.** (B) Prediction of the major product in an intramolecular diels-alder cyclization.

1.1.3B)[25,26]. Such models continue to find use, especially in systems with a very large number of atoms and in material chemistry.[27,28]

Force fields rely on many empirically determined parameters, and it is critical to choose the correct force field for a specific molecular system. This limits their general applicability. *Ab initio* quantum mechanical methods capable of interrogating general molecular systems became available in the 1990s.[29–33] Most prominent of these methods is Density Functional Theory (DFT), for which the 1998 Chemistry Nobel Prize was awarded to Walter Kohn and John Pople.[34–36] Usage of DFT to study chemical reactions can be divided into three somewhat overlapping categories.[37] The first and most straightforward is the direct modeling of putative transition states. The second is to make use of multivariate linear regression (MLR) to model reactions based on molecular properties derived from DFT calculations. The third method is to use DFT calculated parameters as well as other data and apply machine learning to predict novel reaction outcomes.[38–40]

Ab initio calculation of postulated transition states can be very powerful as it can directly refute or support a given mechanistic hypothesis.[41] In practice, this method requires care, both to interrogate the correct mechanistic pathways, but also ameliorate some of the inherent inaccuracies to be found in DFT,[42] including the self-interaction error of electrons,[43] non-modeling of dispersion forces,[44] and difficulty in dealing with nearly degenerate electronic states.[45] These issues are particularly noteworthy in the case of transition-metal catalyzed reactions, especially those

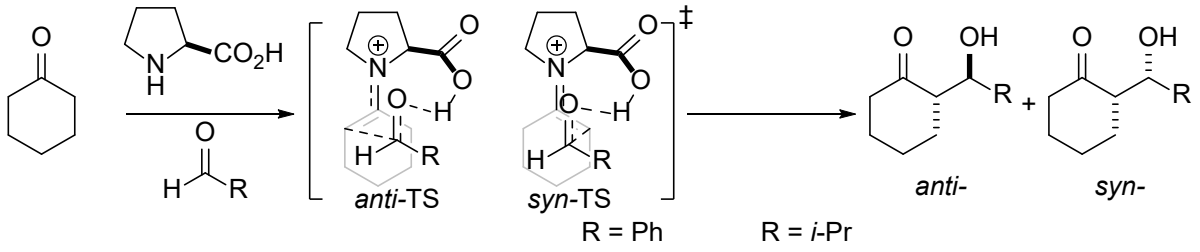

Figure 1.1.4: Houk-List model for proline-catalyzed enantioselective aldol reactions.

involving radical intermediates.[46] Perhaps because of these limitations, early successes were found among elucidating mechanisms of organocatalysts or Lewis-acid catalysts.[47] Prominent examples include the development of the Houk-List model for the prediction of stereoselectivity for intra- and intermolecular aldol reactions catalyzed by proline (Fig 1.1.4),[48,49] albeit with some ambiguity for certain substrates. Noyori reported on the *ab initio* investigation of the amino-alcohol mediated addition of dimethylzinc to benzaldehyde using Møller-Plesset perturbation theory, a non-DFT quantum chemistry method.[50,51] Because the cost of *ab initio* calculations increases very rapidly with the number of atoms and structures, it is often imperative to support such studies in tandem with mechanistic experiments that can rule out alternative pathways; the studies by Houk[52] and Noyori[53] were founded upon prior mechanistic experiments. The best use of DFT is to model reactions which cannot be otherwise disambiguated. This requisite of firm mechanistic data has spurred the development of more implicit models for use on systems for which less is known.

Multivariate linear regression (MLR) is a modeling technique for the prediction of chemical reactions. It does not seek to directly model transition states; thus it is an implicit model. MLR reduces the need for mechanistic experiments, while truncating the potential for structural insight. While MLR has recently been experiencing a renaissance,[54] the idea of correlating measurable molecular properties to reactivity is not new: Hammet pioneered the use of linear free energy relationships for gaining mechanistic insights and predicting reactivity.[55,56] As an example, Jacobsen was able to closely correlate the enantioselectivity of salen-type expoxidation catalysts with the Hammet parameter of salen backbone substituents.[57] After Hammet, other descriptors proliferated such as the steric descriptors of Taft,[58] Charton,[59] the Tolman cone angle,[60] and others,[61] as well as the electronic descriptors of Fukui,[62] electronegativity,[63,64] the Tolman electronic parameter,[60] Mayr fugacities,[65,66] and others.[67,68] MLR extends this prediction approach

by correlating many parameters at once to predict reactivity. MLR also makes use of DFT calculations to calculate other molecular parameters such as atomic charges, dipoles, molecular geometry, and others which cannot be easily measured.[54,69,70] Because there is no prerequisite for mechanistic data, MLR can used during the optimization process of methods before in-depth mechanistic studies are performed, potentially accelerating method optimization by pointing towards the most important reaction parameters. MLR has been used in good effect by Sigman to predict the enantioselectivity of chiral-phosphoric acid catalyzed nucleophilic additions to imines.[71] By analyzing over 300 molecular parameters, the enantioselectivity of enamine addition to imines was predicted for novel catalyst and substrate combinations to within 0.30 kcal•mol^{-1} ΔΔG. In another example, Jacobsen reported the remarkable prediction of the enantioselectivity of hydrogen-bond-donor catalysts in a Mannich reaction. The model was able to predict to a high degree of accuracy the selectivity of a poorly performing squaramide catalyst, and also a superior thiourea catalyst (Fig. 1.1.5).[72] While MLR approaches are more indirect than direct modeling approaches, they nevertheless can point to important factors of catalyst or substrate properties that may guide investigations into further optimization or mechanistic studies.

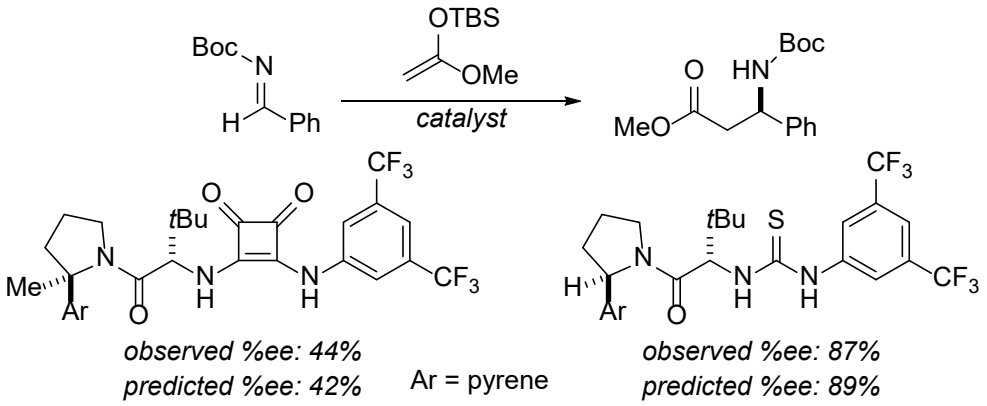

Figure 1.1.5: MLR predictions for worst and best catalyst for HBD catalyzed Mannich reaction.

In recent years, machine learning approaches have been extensively applied to tackle diverse problems in organic synthesis,[73–75] including predicting activation energies,[76] C-H activation site selectivity,[77] and regioselectivity,[78] as well as optimizing polymerization catalysts[79] among other uses.[80,81] Like MLR, machine learning also makes use of computed or measured molecular properties. However, it differs from MLR in that non-linear relationships are used with much larger data sets incorporating fewer parameters. More recently, machine learning incorporating large language models have been investigated.[82] While the large data demands of machine learning can be a drawback, trained models can quickly analyze tens of thousands of reactions.[83–85] Because machine learning models predict reactivity based on extensive correlative formulae, mechanistic interpretations are difficult and rare, though some efforts have been made to develop human-interpretable models.[86–88] More often, machine learning approaches have been applied to automated reaction development,[89,90] and ML approaches have been extensively used to optimize stereoselective transformations.[91–95] A salient recent example of this approach comes from Ao, who used ML methods to predict the selectivity of an amidase enzyme for novel amide substrates towards hydrolytic desymmetrization.[96] Specifically, the model was able to accurately

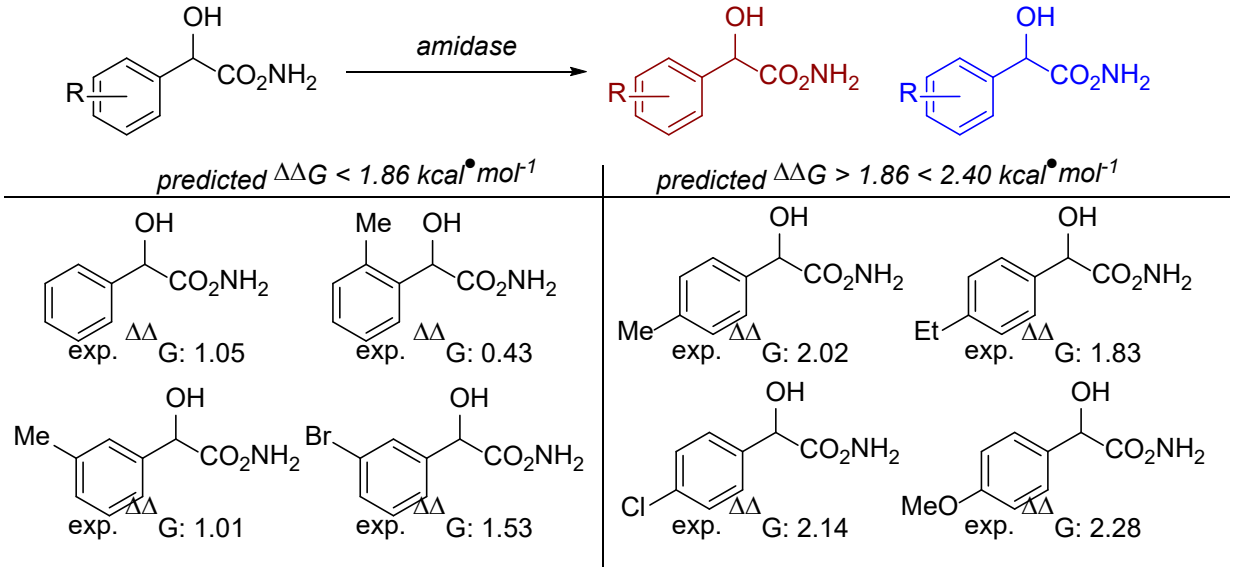

Figure 1.1.6: Machine-learning binning of substrates for amidase hydrolysis.

bind novel substrates into low and high selectivity cases high a high degree of accuracy (Fig 1.1.6), and the authors were able to determine key structural factors for further enzyme optimization.

1.2: Modeling enantioselectivity in nickel-catalyzed cross-couplings

Over the last two decades, significant progress has been realized in the asymmetric coupling of alkyl coupling partners by nickel catalysis.[97–99] Progress has not only been realized with traditional cross coupling, but also reductive[100,101] photocatalytic,[102–104] and electrochemical methods.[105–107] The success of these methods has motivated mechanistic studies which have served to greatly expand our understanding of nickel-catalyzed cross-coupling methods.[108–111] However, there are fewer studies which either seek to directly model the enantiodetermining step of these transformations or otherwise predict enantioselectivity, especially while considering observations from direct mechanistic studies.

Several stand-alone DFT studies of nickel-catalyzed cross-couplings have been reported. In 2011, Lin disclosed the computational investigation of the asymmetric alkylation of α-haloindanes by primary alkylzinc compounds by nickel catalysis, [112] a method previously disclosed by our group.[113] In this study, a Ni^{I}-Ni^{III} catalytic cycle was invoked based on calculated reaction energies. They postulated that reductive elimination was the enantio- and rate determining step and directly modeled the postulated transition state. While their model correctly anticipated the correct enantiomer of product, the ΔΔG error was more than 7 kcal•mol^{-1} and only one substrate was calculated, and therefore little can be extrapolated from these results. Similarly, Wang reported a DFT study of the doubly-diastereoselective cross-coupling secondary electrophiles and nucleophiles developed in our group.[114,115] They also argued that reductive elimination was the enantiodetermining step, and predicted a ΔΔG of 3.2 kcal•mol^{-1} higher than reported. Ren also reported a DFT study on the asymmetric synthesis of diarylkanes,[116] developed by the Reisman

group.[117] They predict a ΔΔG of 0.8 kcal•mol^{-1} for the enantiodetermining step, compared to 1.8 for the measured value. Finally, Wang performed a DFT study on our previously disclosed asymmetric coupling of olefins with tertiary electrophiles.[118,119] It can be argued that the complete reliance on DFT studies uncoupled from experimental observations reduced the utility of these reports.

DFT predictions of enantioselectivity for nickel-catalyzed asymmetric alkylation have been done as part of a more extensive mechanistic study. This approach has its benefits, as an interplay between theoretical and experimental results can significantly simplify interpretation of the DFT results.

Molander reported studies of the dual Ir/Ni photoredox mediated asymmetric coupling of benzylic trifluoroborate salts with aryl bromides,[120] modeling the racemic coupling of these coupling partners using a 2,2-bipy ligand.[121] Their calculations pointed towards a $Ni^0/Ni^{II}/Ni^{III}$ cycle in which oxidative addition of Ni^0 to the aryl bromide is followed by radical capture of the benzylic radical to form a Ni^{III} intermediate, which undergoes reductive elimination to form the product. This data indicated that reductive elimination was the enantiodetermining step due to the reversibility of the radical addition, thus operating under Curtin-Hammet conditions.[122] The

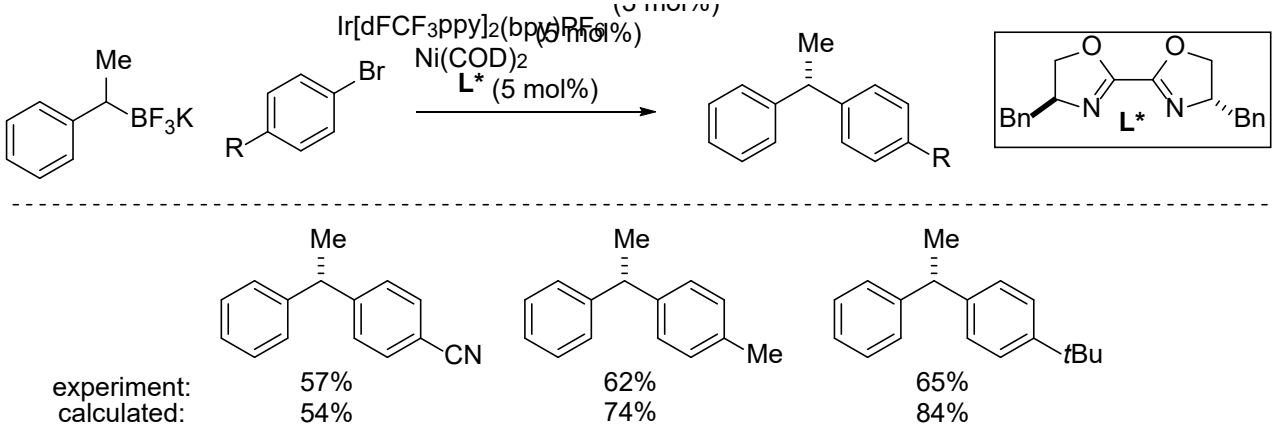

Figure 1.2.1: Predictions of asymmetric couplings of alkyltrifluoroborates by Molander.

reductive elimination barriers were calculated for the chiral Biox ligand for a variety of substrates, and reasonable agreement was found with the observed ΔΔG values (Fig. 1.2.1). In addition, further calculations were performed on the diamine catalyzed coupling of homobenzylic halides with primary alkylboronates published by our group,[123] and those calculations also indicated that reductive elimination was the enantio-determining step.

In 2019, our group published a mechanistic study of the asymmetric arylation of α-bromoketones,[124] previously developed in our group.[125] Evidence from this study was consistent

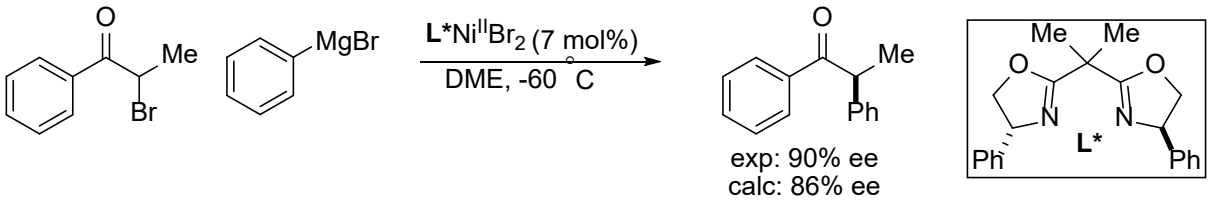

Figure 1.2.2: Enantioselectivity predictions for the arylation of α-Bromoketones published by our group.

with a Ni^{I}/Ni^{III} mechanism, similar to our previous study.[126] DFT calculations showed that radical addition to Ni^{II} was the rate- and enantio-determining step, and the calculated ΔΔG was 1.1 kcal•mol^{-1}, in good agreement with the experimental result of 1.13 kcal•mol^{-1} for a single pair of coupling partners (Fig 1.2.2). This stands in contrast to the previous Molander study, as well as the studies of Molander[120] and Lin.[112]

More implicit theoretical methods to probe asymmetric nickel-catalyzed reactions have also had success. Recently, Bahamonde reported on the asymmetric arylation of tetrahydrofuran mediated by a chiral nickel catalyst and iridium photocatalyst.[127] During the initial phases of the study, MLR both to identify the optimal catalyst, as well as determine which catalyst features were

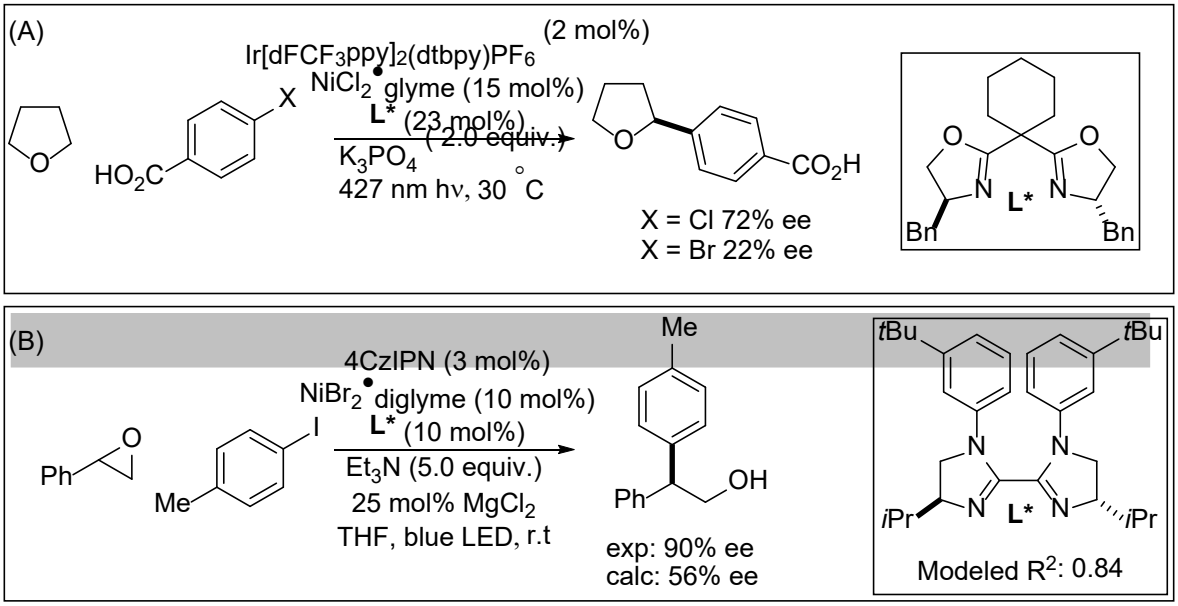

Figure 1.2.3: (A) Asymmetric α-arylation of THF by Bahamonde. (B) MLR optimized epoxide arylation developed by Doyle.

relevant to enantioselectivity, which supported further mechanistic studies which explain the strong halide effect observed. While no direct modeling of the enantiodetermining step was made, this study serves a strong example of how implicit methods can support mechanistic studies (Fig. 1.2.3A). As another example, a recent study by Doyle used MLR methods to determine the best ligand for the asymmetric arylation of epoxides via dual photoredox and nickel catalysis.[128] While the model has a relatively high R^2 of 0.84 when predicting ΔΔG, in the explicitly modeled case with a substrate, the predicted %ee was significantly lower than observed (Fig 1.2.3B). More intense modeling to discover novel reactivity has been reported using artificial intelligence (AI) driven optimization supported by high-throughput experimentation (HTE). In 2024, the Liao group reported the development of a family of asymmetric nickel-catalyzed cross couplings through an AI approach.[129] A combination of literature reported data as well as HTE-acquired data was used, and a predictive model was trained using only parameters describing the ligand and substrate served as input. The resultant model was able to predict ΔΔG values with a mean-average error of

only 0.199 kcal•mol^{-1}, and an R^2 of 0.844 when tested against literature results. The model was then used to predict the most promising ligands to accomplish the asymmetric hydroarylation of cyclic α,β-unsaturated amines in good yield and enantioselectivity with a minimum of screening. This showcases the utility of AI-driven models for the discovery of novel reactivity.

1.3: Motivation for the present study

Despite these successes in the literature for analyzing and predicting enantioselectivity in asymmetric nickel-catalyzed coupling reactions, there remains a lack of studies which

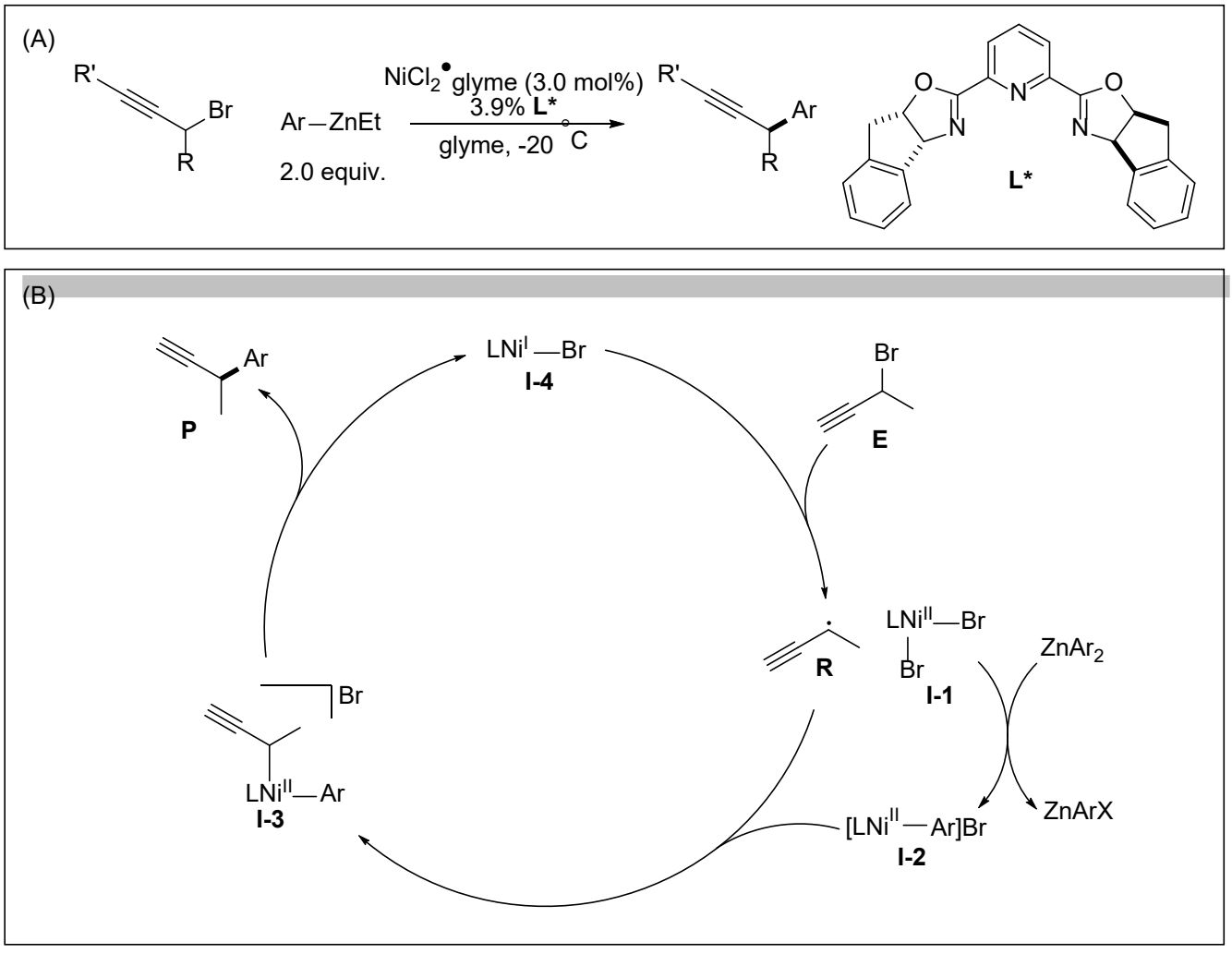

Figure 1.3.1: (A) Asymmetric alkylation of propargylic bromides reported by our group. (B) Mechanistic cycle supported by our group's later mechanistic study.

systematically study a selection of ligands and substrates to elucidate the most important factors governing the enantioselectivity from an explicit modeling approach. Therefore, our group sought to fill this gap in the literature. In 2008, we published the asymmetric nickel-catalyzed arylation of propargylic electrophiles using in-situ generated arylzinc reagents (Fig 1.3.1A).[130] Following this in 2014, our group performed a mechanistic study of this reaction, in which the catalytic cycle shown in Figure 1.3.1B was proposed. For simplicity, each step is drawn as irreversible.[126] The mechanistic study consistent with the evidence starts with the formation of chain-carrying metalloradical **I-4**, likely formed by a combination reduction-disproportionation sequence.[131] This radical can abstract a bromide atom from the electrophile **E** to generate organic radical **R** and nickel species **I-1**, which can undergo transmetalation with the arylzinc nucleophile to generate the cationic resting state **I-2**. The resting state can then capture a radical **R** to form complex **I-3**, which undergoes rapid reductive elimination to form the product **P** and regenerate metalloradical **I-4**. While this mechanistic study was extensive, it could not answer two fundamental questions about the reaction. The first is which step is the enantiodetermining step. There are two possibilities for which step is enantiodetermining:

1) Radical addition is reversible, and reductive elimination governs enantioselectivity under Curtin-Hammet conditions.
2) Radical addition is irreversible and is thus the enantiodetermining step.

The second more general inquiry was what factors of the ligand are most important for governing enantioselectivity. The present study seeks to shed light on these questions. Given that much was known about the reaction, including crystallographic characterization of the resting state, an explicit DFT approach was seen as most appropriate. The two phases of the project would be to first find a computational method that could generate results consistent with the mechanistic

study and observed enantioselectivity. After this, a selection of ligands and substrates would be synthesized and subjected to the reaction conditions, as well as modeled computationally to check for agreement of the model against diverse conditions. The degree to which the model agreed with the observed results could then be used as a measure of its validity, and in turn could be probed to learn more about which factors of the ligand and substrate govern enantioselectivity.

2. Computational results

2.1: Benchmarking with crystallographically characterized compounds

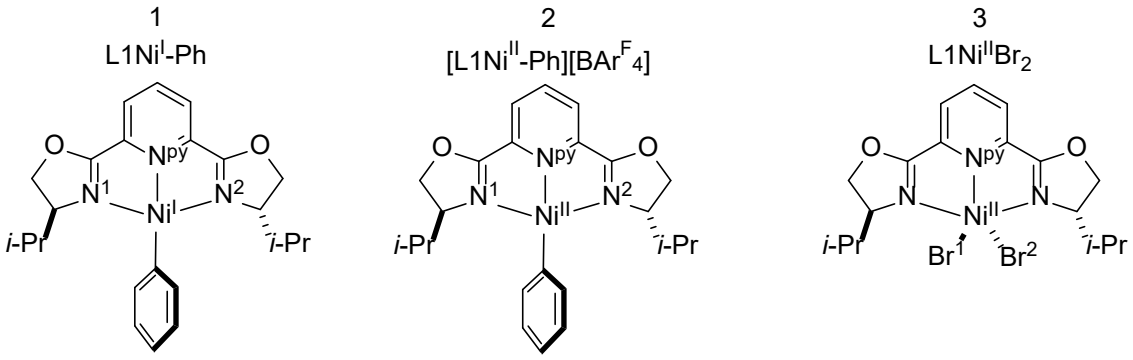

L1Ni^{I}-Ph			[L1Ni^{II}-Ph][BAr^{F}$_4$]			L1Ni^{II}Br$_2$		
Bond	Crystal (Å)	Calculated (Å)	Bond	Crystal (Å)	Calculated (Å)	Bond	Crystal (Å)	Calculated (Å)
N^1—Ni	1.906	1.910	N^1—Ni	1.900	1.930	N^1—Ni	2.135	2.160
N^2—Ni	1.934	1.940	N^2—Ni	1.892	1.920	N^2—Ni	2.133	2.180
N^{Py}—Ni	1.934	1.880	N^{Py}—Ni	1.898	1.930	N^{Py}—Ni	1.991	2.040
Ph—Ni	1.896	1.900	Ph—Ni	1.881	1.880	Br^1—Ni	2.389	2.440
						Br^2—Ni	2.421	2.450

Figure 2.1.1: Comparison between crystallographically characterized nickel species and their computed structures. Structures computed at the B3LYP/D4 -CPCM-DEF2-SVP/DEF2-QZVPPD (on Ni) level of theory.

To begin modeling the steps of the catalytic cycle, the computational methods were first benchmarked by examining how closely they came to predicting known crystallographic structures relevant to the catalysis. Figure 2.1.1 shows the comparison between the computed and crystallographic bond lengths of three nickel species.

In general, the structures were well-reproduced and in most cases the bond length deviations were less than 0.3 Å. In addition, since solid-state crystallographic structures will differ somewhat in reality from the structure of solvated species, some variation would be expected even given perfect accuracy.

2.2: Probing the enantiodetermining step

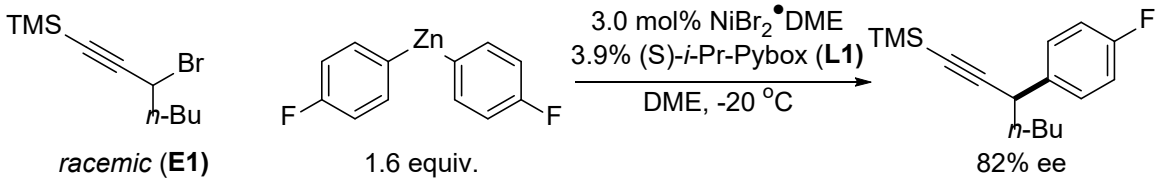

Figure 2.2.1: Reaction conditions used for modeling of the catalytic cycle.

To most closely hew to the conditions used in the in-depth mechanistic study, bis(4-fluorophenyl)zinc was chosen as the nucleophile, and (S)-*i*-Pr-Pybox was **(L1)** chosen as the ligand, along with the standard electrophile **E1**. Figure 2.2.1 shows the catalytic conditions modeled. Note that, for the (S)-ligand, the major product is the (S) product. The energetic overview of the catalytic cycle as computed is shown in Figure 2.2.2. A complete energy diagram of the

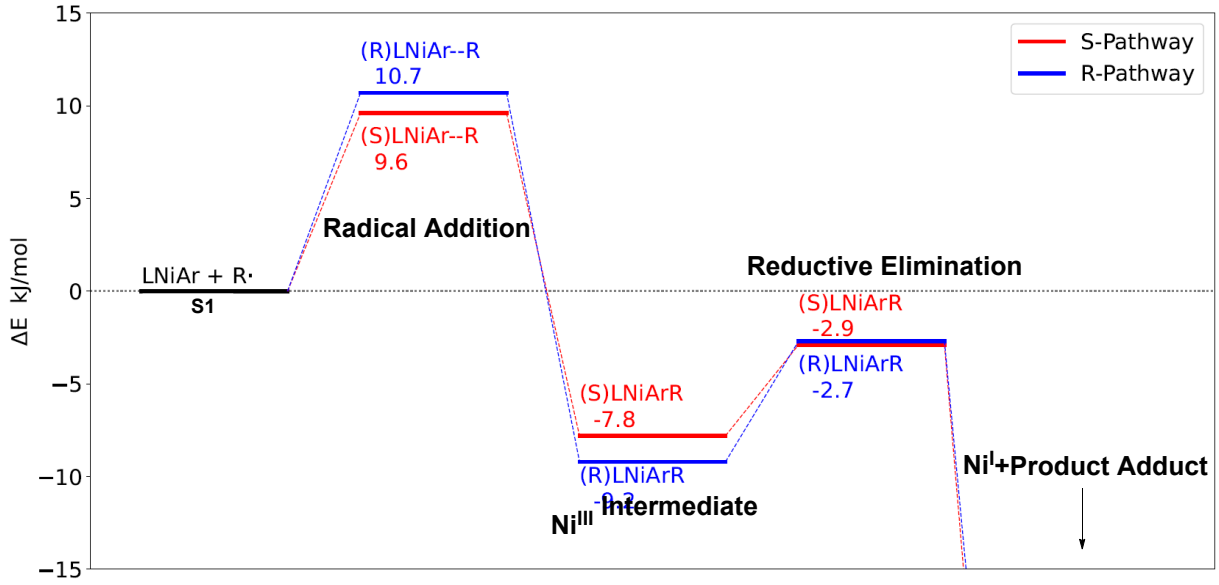

Figure 2.2.2: Calculated catalytic cycle.

catalytic cycle can be found in the appendix. The barrier to radical addition was found to be 10.7 and 10.6 kcal•mol^{-1} for the (R)-product pathway and (S)-product pathway respectively. After radical addition, the resultant Ni^{III} complex undergoes rearrangement to a pseudo octahedral geometry, where the propargyl fragment binds to the nickel center in an η^3 configuration. This

complex is computed to be energetically downhill from the starting Ni^{II} center and radical precursor. This species can undergo reductive elimination with barriers of 4.9 and 6.5 kcal•mol^{-1} for the R and S product pathways, respectively. The resultant Ni^{I} species forms an η^2 adduct with the product, which presumably can be displaced with a bromide ion to generate the Ni^{I} bromide species implicated in halogen atom abstraction step. The computed barriers to radical dissociation are 19.9 and 17.4 kcal•mol^{-1} for the R and S pathways, respectively. This indicates that radical addition is irreversible, which shows that radical addition, and not reductive elimination, is the enantio-determining step. Further, this implies that radical addition is also the rate determining step, a hypothesis which is consistent with observations. Under the reaction conditions studied, the product is formed with an enantiomeric excess of 82%, which corresponds to a $\Delta\Delta G$ between the R and S pathways of 1.2 kcal•mol^{-1} This is in reasonable agreement with the computed value of 1.1 kcal•mol^{-1}.

2.3: Geometric description of the radical-capture step

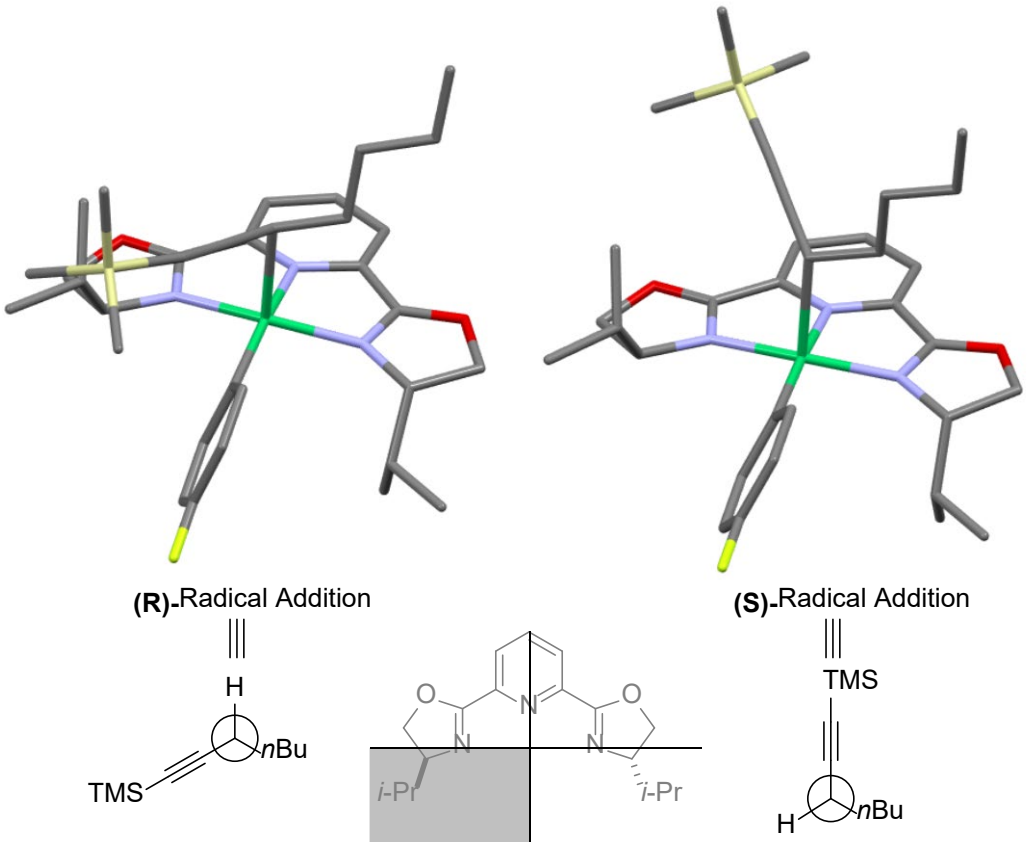

Figure 2.3.1: Calculated geometries of the radical addition transition state.

It is worth examining the geometry of the radical capture step in attempt to determine which interactions have the most impact on enantioselectivity. Figure 2.3.1 shows the configuration of the minimum energy radical addition transition states for the minor-product generating (R) radical addition (left) and the major-product generating (S)-radical addition (right). Comparing the Newman projections of each transition state looking along the forming Ni-C bond with the quadrant diagram, the (S) transition state ideally places the small hydrogen atom towards the blocked quadrant. By comparison, the (R) transition state positions the TMS-alkyne group nearby to the *i*-Pr group of the ligand, introducing a steric clash. The length of the Ni-C bond in

each transition state is very similar, with 2.309 Å for the (R) transition state, and 2.314 Å for the (S) transition state.

2.4 Geometry of the Ni^{III} intermediate

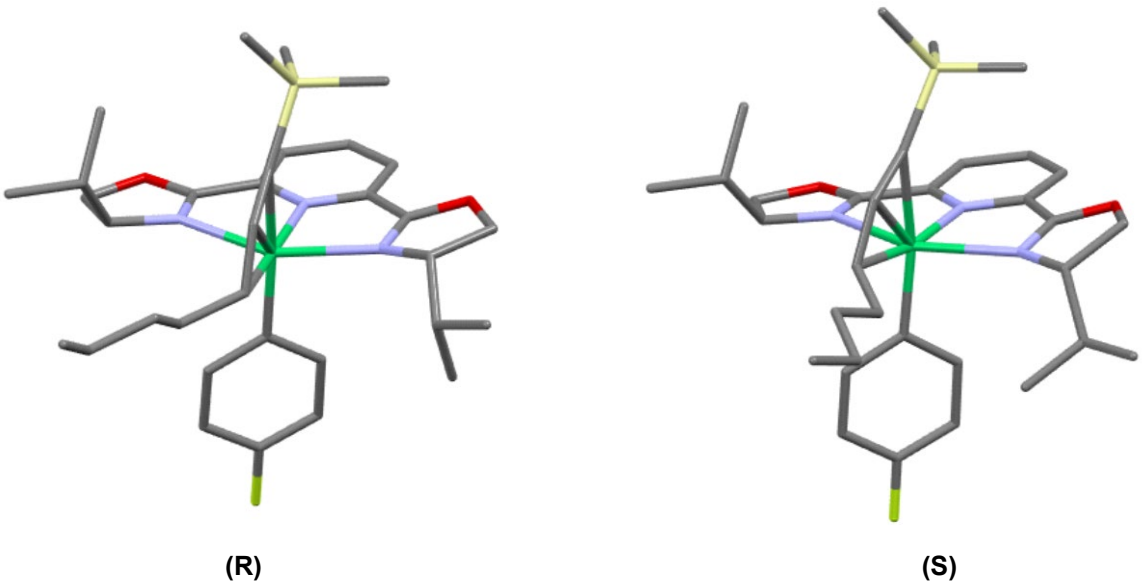

Figure 2.4.1: Calculated geometries of the Ni^{III} intermediate.

Figure 2.4.1 shows the calculated geometries of the Ni^{III} state for the (R) and (S) pathways. After radical addition, the complex rearranges from a square pyramidal geometry to a pseudooctahedral geometry. The propargyl fragment curves around the nickel center to bind in an η^3-fashion, while the aryl ring moves from an equatorial to an axial position. The energetic difference between these isomers is 1.36 kcal•mol^{-1}, and in this case the (R) isomer is more stable. This can be attributed to the orientation of the *n*-butyl group; in the (R) case it is on the opposite side of the oxazoline isopropyl group, while in the (S) case it is oriented towards it.

2.5: Geometry of the reductive elimination step

Figure 2.5.1 shows the calculated geometries of each reductive elimination step. As noted in the overall energy diagram, the (R) reductive elimination has an energy barrier of 6.50 kcal•mol^{-1}, and the (S) reductive elimination has a barrier of 4.89 kcal•mol^{-1}. Were reductive elimination the

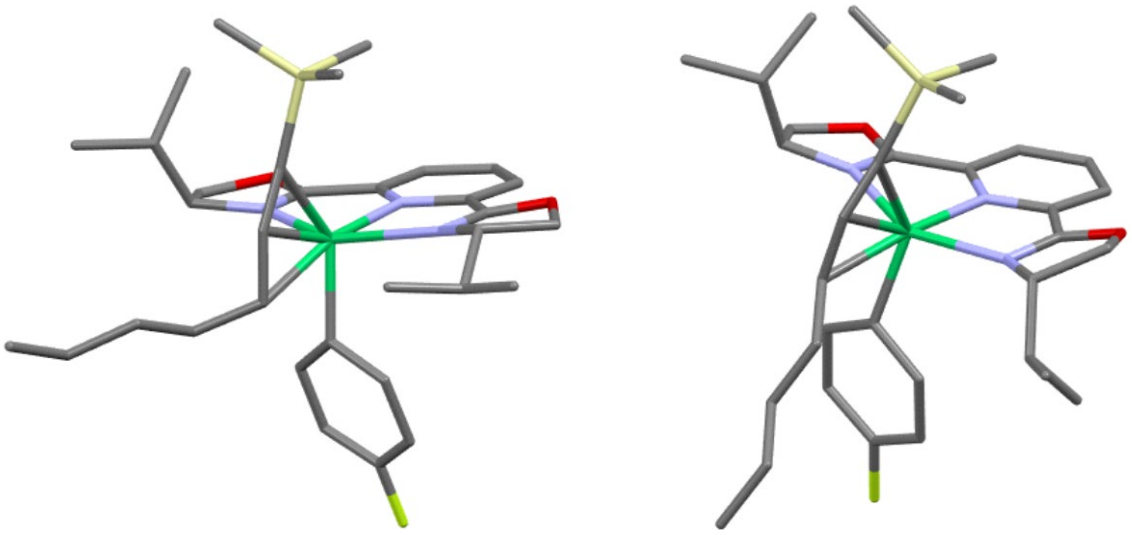

(R)-Reductive Elimination TS Geometry

Ni-C	2.099
Ni-Ar	1.995
C-Ar	2.081
C-Ni-Ar ∠	61.02°

(S)-Reductive Elimination TS Geometry

Ni-C	2.106
Ni-Ar	1.996
C-Ar	2.058
C-Ni-Ar ∠	60.17°

Figure 2.5.1: Calculated geometries of the (R) and (S) reductive elimination steps.

enantiodetermining step, the opposite orientation would be obtained. Given the lower barrier of reductive elimination compared to radical dissociation (19.9 and 17.4 kcal•mol^{-1} for (R) and (S), respectively), the radical addition step is irreversible under the reaction conditions. This is consistent with mechanistic observations that the resting state is the Ni^{II} species.

2.6: Enantioselectivity predictions of alternative substrates

To determine the applicability of the computed reaction model as well as interrogate which factors were most important for determining the enantiomeric excess of the reaction, computations were also performed which varied the electrophile and ligand used in the catalysis. The test series of ligands included those varying in steric bulk on the oxazoline ring (L1-L5), those varying in donating groups on the pyridine ring (L6-L10), and those with bis-substituted oxazoline rings (L11). For each ligand, two electrophiles were chosen, E1 with a longer *n*-butyl chain, and

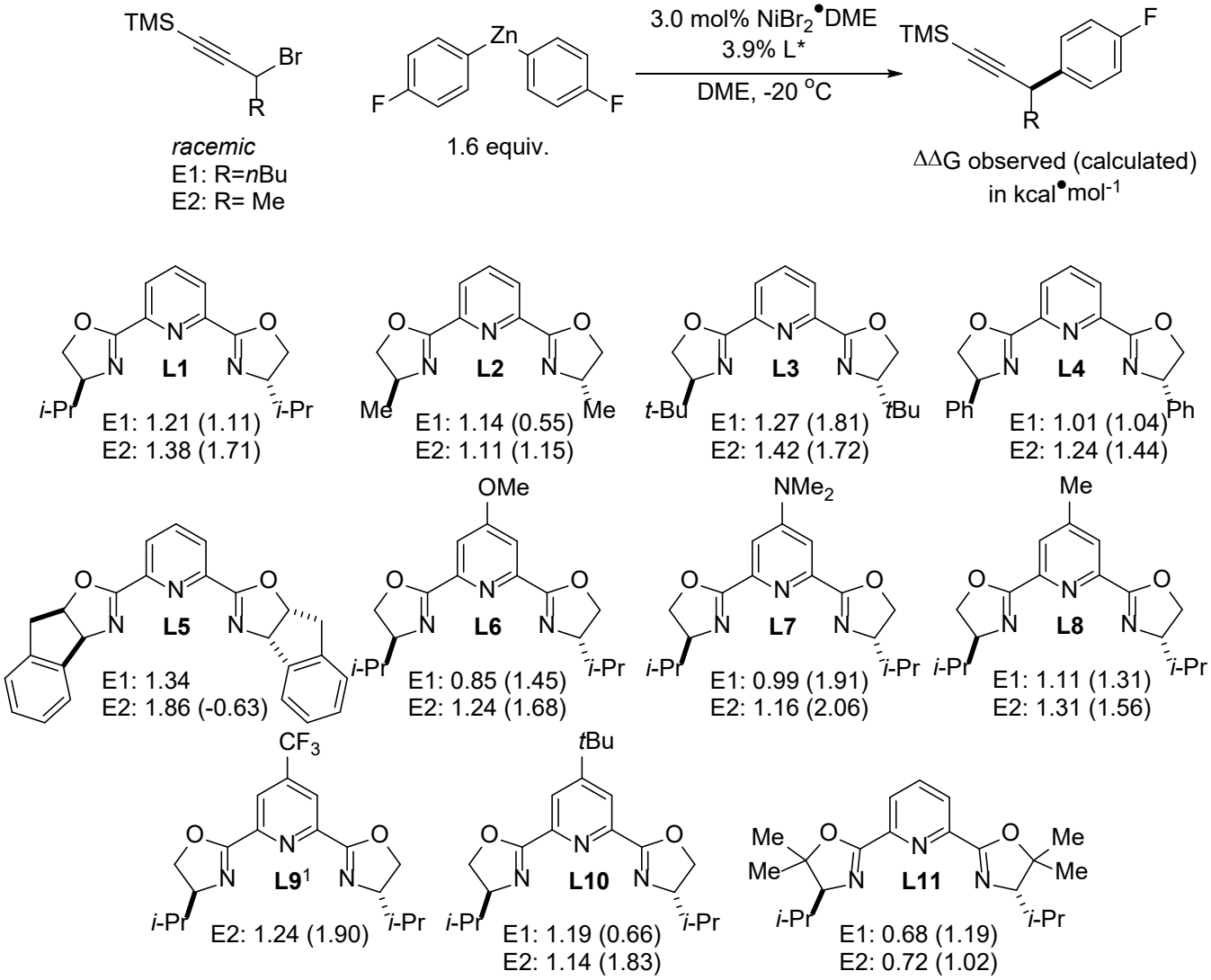

Figure 2.6.1: Enantioselectivities achieved for different electrophile and ligand combinations. [1]L9 was run using 20 mol% ligand to achieve maximum enantioselectivity. Each result is the average of two experiments.

E2 with a simple methyl substituent. In general, E2 provided higher enantioselectivities and this provided a consistent trend to compare with the predicted results. Figure 2.6.1 summarizes both the measured ΔΔG values (in kcal•mol^{-1}), as well as the predicted values based on computation in brackets. While a transition state could not be located for each collected data point, the data indicates that the present model of the catalytic system may not be correct, and as made cannot predict the enantioselectivity of the coupling reaction. For many reactions, the direction of change

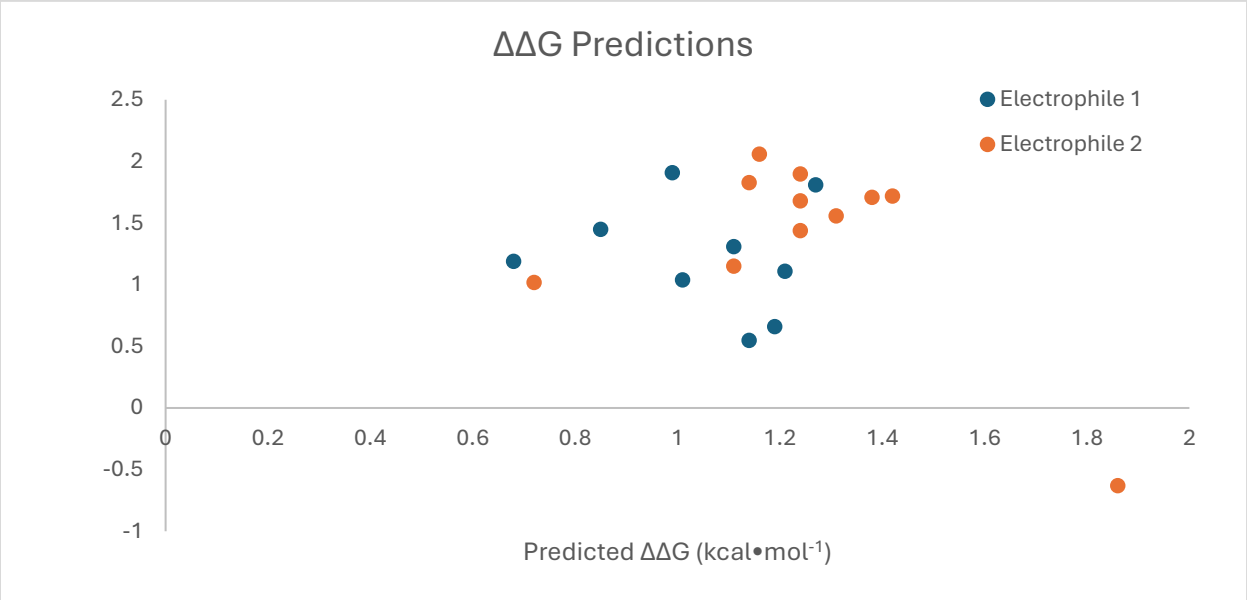

Figure 2.6.2: Plot of predicted ΔΔG values (x axis) versus the experimental values (y axis).

in enantioselectivity in moving from E1 to E2 is captured, but for many it isn't (**L3, L5, L10, L11)**, and in one case the sense of the enantioselectivity was totally reversed (**L5)**. Figure 2.4.2 summarizes these results. In certain cases, it is possible that a more thorough conformer search may improve results, such as in the case of **L10**, as the bulky *t*-butyl group on the para position may further block the major transition state, and another approach may be more favorable. It is unlikely however that such effects would impact the accuracy to this degree. Another possible explanation is that, for different ligands, the mechanism changes, and reductive elimination becomes the enantiodetermining step. However, calculations on previous iterations of computational theory showed little variation in the relative energetics of the radical capture and reductive elimination steps, rendering this possibility less likely.

Another possibility is that the C—Ar bond forming step is a concerted, inner-sphere process that does not involve a Ni^{III} intermediate. This possibility was recently studied by Diao on the same ligand system described in the current study, albeit using primary stabilized benzyl radicals and secondary unstabilized radicals.[132] Based on stereoelectronic effects, MLR analysis, photo-EPR spectroscopy, they proposed that C—Ar bond formation can occur by an inner-sphere

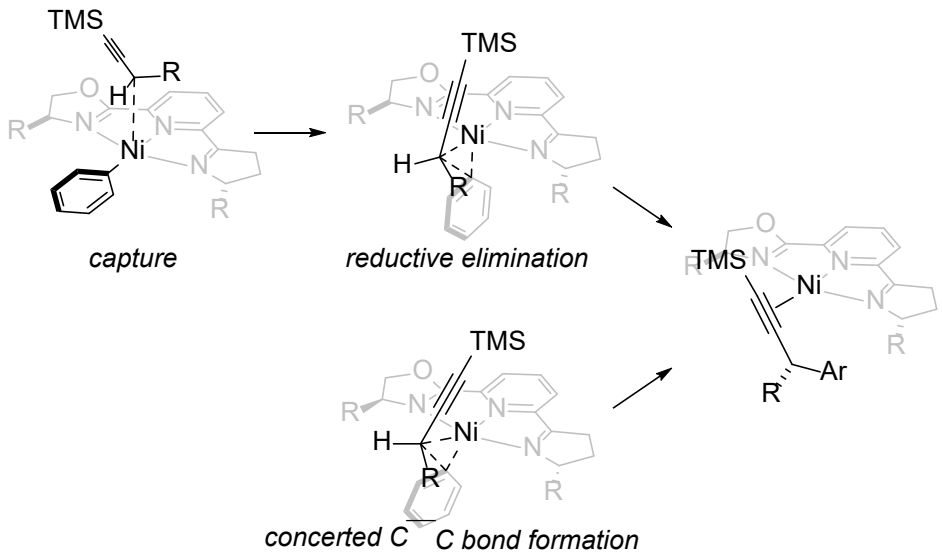

Figure 2.4.3: Computed C—C bond formation cycle (top), compared to bond formation as proposed by Diao (bottom).

concreted mechanism. A cartoon of this mechanism versus the calculated inner-sphere mechanism is shown in Figure 2.4.3. This second pathway would be consistent with our previous mechanistic study[126] and cannot be ruled out based on the calculations performed thus far. Future work should include a careful investigation of this inner-sphere pathway to determine if it would enable a better prediction of enantioselectivities.

2.7 Time course

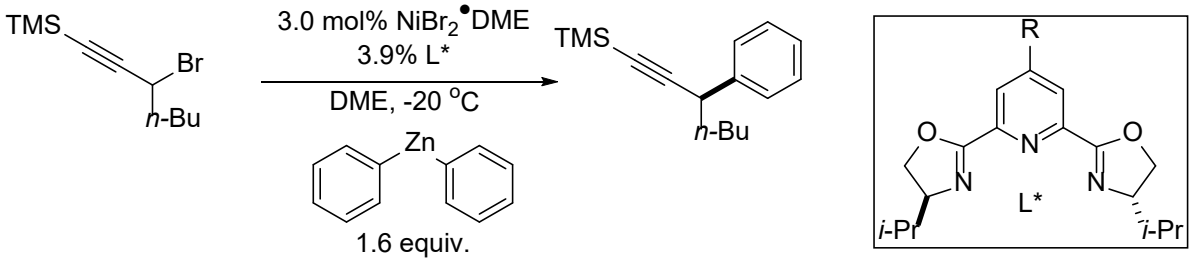

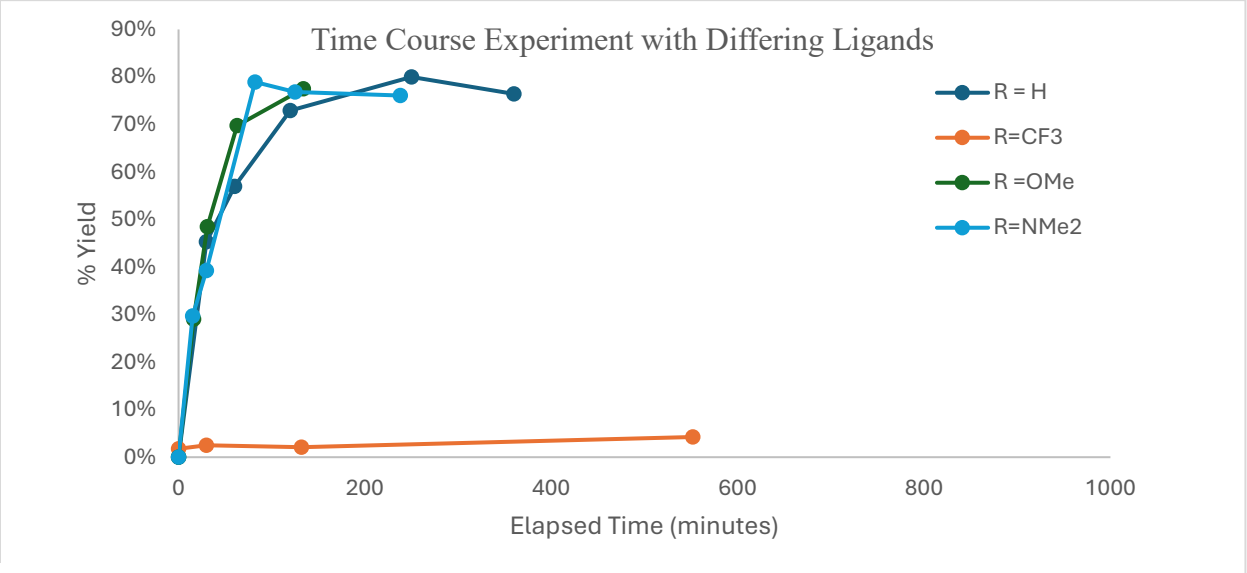

Figure 2.7.1: Time course experiment performed with different ligands. Yield estimated from GC analysis using 1,3,5-trimethoxybenzene as internal standard, and setting the maximum yield to 80%, corresponding to the maximum yield of the reaction. Yield variations are because of separate experiments used per time-point.

To gain additional insight into ligand effects on the reaction, a time course was performed with ligands varying in the electron-richness of the pyridine ring. The scheme of the reaction and the results are shown in Figure 2.7.1. There was little variation in the rate of the reaction for most ligands, except for in the case where R=CF_3 (L9), where the reaction was exceedingly slow and not complete even after 2 days.

3. Experimental procedures

3.1: General information

THF, DME, Hexanes, Et_2O, and DCM were deoxygenated and thoroughly sparged with nitrogen followed by passage through an activated alumina column in a solvent-purification system by SG Water USA LLC. DME was further dried by storage over activated 4 Å molecular sieves in a nitrogen-atmosphere glovebox. All compounds were used as purchased from commercial suppliers unless otherwise noted.

^1H, and ^{13}C NMR spectroscopic data were collected on a Bruker 400 MHz or a Varian 500 MHz spectrometer at ambient temperature; chemical shifts (δ) are reported in ppm downfield of tetramethylsilane, using the solvent resonance as the internal standard. GCMS analysis was carried out using an Agilent 8890 GC System, equipped with an FID and an Agilent 5977B Mass Spectrometer. Enantioselectivities were determined by chiral GC analysis using an Agilent Technologies 6850 GC system equipped with a chiral Supelco Beta-Dex-120 column.

3.2: Synthesis of electrophiles

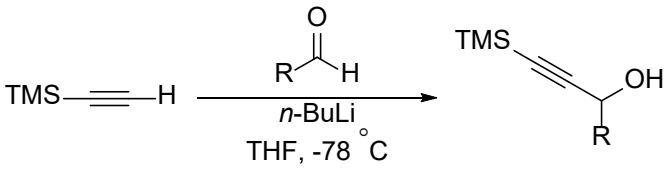

General procedure for the synthesis of propargylic alcohols. This procedure was derived from the literature.[130] To a flame dried, round bottom flask was added a magnetic stir bar and THF. The flask was capped with a rubber septum and placed under a nitrogen atmosphere through a needle attached to either a Schlenk line or nitrogen filled balloon. The flask was cooled

to -78 °C in an isopropanol-dry ice bath. To this solution, ethynyltrimethylsilane (1.0 equiv.) was added dropwise. After this, a solution of *n*-butyllithum in hexanes was added dropwise (1.05 equiv.). The solution was allowed to stir for 5 minutes, then neat aldehyde was added dropwise. The solution was allowed to gradually warm to room temperature. The reaction was then carefully quenched with a saturated ammonium chloride solution. A reaction was then concentrated under reduced pressure to remove most of the THF solvent. The resulting residue was extracted with dichloromethane (3x100 mL) using a separatory funnel. The organic solution was dried over Na_2SO_4, filtered, and concentrated to yield a clear yellow oil. The propargylic alcohol was then directly carried over to the next step without further purification.

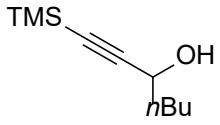

1-(trimethylsilyl)hept-1-yn-3-ol. This compound was synthesized using the general procedure from ethynyltrimethylsilane (50 mmol) and *n*-pentanal (55 mmol). The compound was isolated as a yellow oil, and directly used in the next step without further purification.

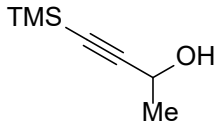

4-(trimethylsilyl)but-3-yn-2-ol. This compound was synthesized using the general procedure from ethynyltrimethylsilane (40 mmol) and acetaldehyde (48 mmol). The compound was isolated as a clear oil, and directly used in the next step without further purification.

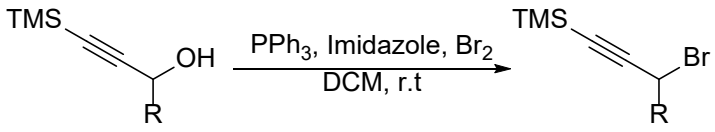

General procedure for the synthesis of propargylic bromides. This procedure was derived from the literature.[130] To a flame-dried round bottom flask was added a magnetic stir bar, triphenylphosphine (1.2 equiv.), imidazole (1.2 equiv.), and DCM. A rubber septum was added, and the solution was put under a nitrogen atmosphere using either a nitrogen balloon or a Schlenk line. To this solution bromine was added by syringe dropwise (1.2 equiv.), and left to stir for 5 minutes. The propargylic alcohol dissolved in DCM was then added by syringe, and the reaction was allowed to stir at room temperature. After consumption of the propargylic alcohol, the reaction was diluted with hexanes and passed through a silica column. The column was flushed with hexanes, and the combined organic fractions were concentrated to yield a clear oil. The crude product was purified by vacuum distillation.

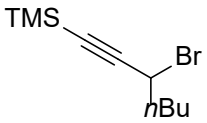

(3-bromohept-1-yn-1-yl)trimethylsilane. This compound was synthesized from 4-(trimethylsilyl)but-3-yn-2-ol (50 mmol crude) according to the general procedure. The

compound was purified by vacuum distillation (50°C, approx.. 150 mtorr) to yield a clear, colorless oil. (35% yield over 2 steps).

The NMR spectra of the compound corresponded to the literature values.[133]

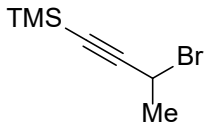

(3-bromobut-1-yn-1-yl)trimethylsilane. This compound was synthesized from **4**-(trimethylsilyl)but-3-yn-2-ol (40 mmol crude) according to the general procedure. The compound was purified by vacuum distillation (~40 °C, approx. 150 mtorr) to yield a clear, colorless oil (5.05 g, 62% yield over 2 steps).

The NMR spectra of the compound corresponded to the literature values.[133]

3.3: Synthesis of ligands

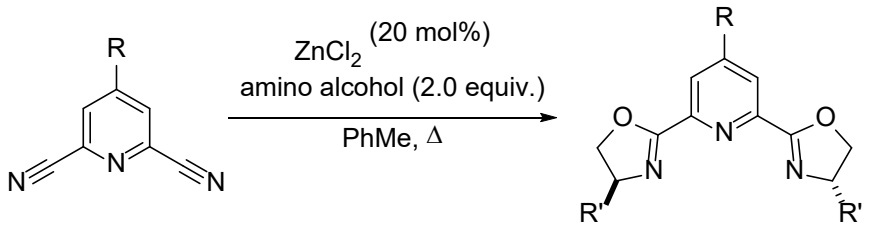

General Procedure 1: To a flame-dried round-bottom flask was added a large stir bar, zinc chloride, pyridine dinitrile, and amino alcohol. To this was added toluene to make a 0.1 M solution, and the mixture was heated at reflux until consumption of the starting material. The reaction was cooled to room temperature. The solvent was removed under reduced pressure, and the residue was directly purified with flash chromatography.

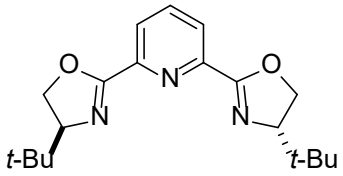

2,6-bis((S)-4-(tert-butyl)-4,5-dihydrooxazol-2-yl)pyridine. The title compound was synthesized by general procedure 1 from pyridine-2,6-dicarbonitrile (1.00 g, 7.74 mmol) and (S)-2-amino-3,3-dimethylbutan-1-ol (1.80 g, 15.48 mmol). The compound was isolated by precipitating the crude mixture in DCM/EtOAC with hexanes to yield a white colorless solid. (369 mg, 14% yield).

The NMR spectra of the compound corresponded to the literature values.[134]

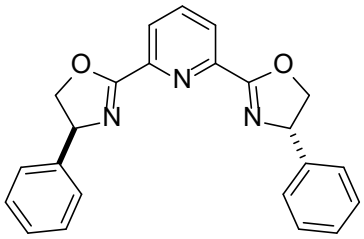

2,6-bis((S)-4-phenyl-4,5-dihydrooxazol-2-yl)pyridine. The title compound was synthesized by general procedure 1 from pyridine-2,6-dicarbonitrile (1.00 g, 7.74 mmol) and (S)-2-amino-2-phenylethan-1-ol (2.12 g, 15.48 mmol). The title compound was isolated by flash chromatography (ethyl acetate/hexanes) and was isolated as an off-white crystalline solid (748 mg, 26% yield).

The NMR spectra of the compound corresponded to the literature values.[135]

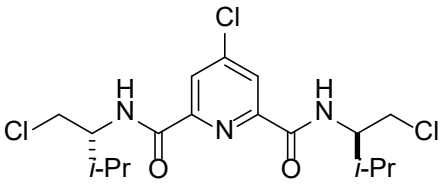

4-chloro-N2,N6-bis((R)-1-chloro-3-methylbutan-2-yl)pyridine-2,6-dicarboxamide. To a flame-dried round-bottom flask was added chelidamic acid (27 mmol, 5.0 g) and a large stir bar. To this was added thionyl chloride (50 mL, 680 mmol), and 5 drops of DMF. The mixture was refluxed overnight. Volatiles were removed by distillation, and the resultant residue was redissolved in chloroform (100 mL), and the solution was cooled to 0 °C in an ice bath. A solution of D-valinol (2.0 equiv, 5.60 g, 54 mmol) in chloroform (50 mL). The solution stirred at room-temperature overnight. The volatiles were removed under reduced pressure. To the residue was added thionyl chloride (8 mL, 11 mmol), and the mixture was refluxed overnight. Excess thionyl chloride was removed under reduced pressure, and the residue was partitioned between ethyl acetate and saturated sodium bicarbonate solution. The aqueous layer was extracted with ethyl acetate (3x50 mL), and the organic fractions were combined and dried with Na_2SO_4. The crude mixture was purified using flash chromatography (EtOAc/Hexanes) to yield the product as a white solid (2.55 g, 23% yield).

The NMR spectra of the compound corresponded to the literature values.[136]

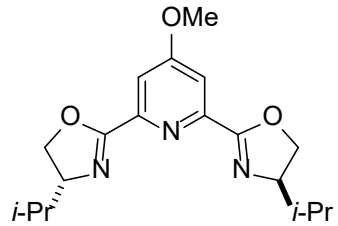

(4R,4'R)-2,2'-(4-methoxypyridine-2,6-diyl)bis(4-isopropyl-4,5-dihydrooxazole). To a 250 mL oven-dried round-bottom flask, a large stir bar and methanol (50 mL) was added. To this was carefully added small pieces of sodium metal (1.51 g, 65.6 mmol), which was allowed to stir at room temperature until all sodium was dissolved. To this solution, 4-chloro-N2,N6-bis((R)-1-chloro-3-methylbutan-2-yl)pyridine-2,6-dicarboxamide (2.55 g, 6.24 mmol) was carefully added, and the solution was refluxed overnight. The reaction was cooled to room temperature, and quenched with a saturated ammonium chloride solution (~25 mL). The aqueous later was extracted with DCM (25x3 mL), and the organic layers were combined and dried with magnesium sulfate. The solvent was removed under reduced pressure, and the residue was purified using flash chromatography on silica gel (MeOH/DCM). The title compound was isolated as a white solid (414 mg, 32% yield).

The NMR spectra of the compound corresponded to the literature values.[134]

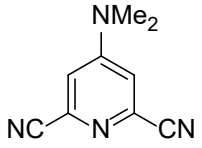

4-(dimethylamino)pyridine-2,6-dicarbonitrile. The following procedure was adapted from the literature.[137] In a nitrogen-filled glovebox, a 40 mL scintillation vial was equipped with a cross-shaped stir bar. To this was added 2,6-dichloro-N,N-dimethylpyridin-4-amine (1.0 g, 5.22 mmol),

$Zn(CN)_2$ (674 mg, 5.74 mmol), zinc (32 mg, 0.52 mmol), *rac*-2-(Di-*tert*-butylphosphino)-1,1′-binaphthyl (207 mg, 0.52 mmol) and $Pd(TFA)_2$ (86.8 mg, 0.26 mmol). DMA was then added (20 mL). The vial was capped with a PTFE septum cap and was brought out of the glovebox and heated to 95 °C overnight. The reaction was allowed to cool to room temperature and was filtered through a pad of celite. The solvent was removed under reduced pressure, and the crude material was subjected to the next step without further purification.

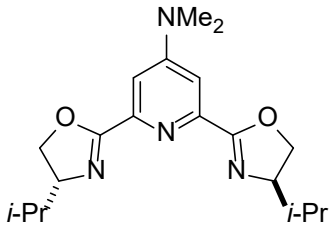

2,6-bis((R)-4-isopropyl-4,5-dihydrooxazol-2-yl)-N,N-dimethylpyridin-4-amine. The title comound was synthesized according to general procedure 1 from 4-(dimethylamino)pyridine-2,6-dicarbonitrile (899 mg, 5.22 mmol) and D-Valinol (1.08 g, 10.44 mmol). The crude reaction was purified by flash chromatography using silica deactivated with triethylamine (Acetone/DCM) to yield the title compound as a white solid (420 mg, 23% over 2 steps).

The NMR spectra of the compound corresponded to the literature values.[136]

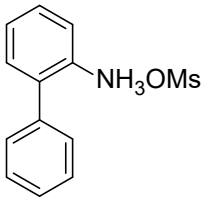

2-Ammoniumbiphenyl mesylate. The title compound was synthesized using a procedure adapted from the literature.[138] To a 100 mL round bottom flask was added a large stir bar, 2-aminobiphenyl (1.69 g, 10 mmol), and diethyl ether (30 mL). Once the amine had dissolved, a solution of methanesulfonic acid (961 mg, 10 mmol) in diethyl ether (5 mL) was added dropwise, and the mixture was stirred for 30 minutes. The reaction was then filtered, and the collected solid was washed with diethyl ether (3x10 mL). The title compound was isolated as a white solid (2.57 g, 97% yield).

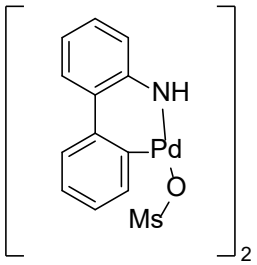

***μ*-OMs Dimer.** The title compound was synthesized using a procedure adapted from the literature.[138] A 250 mL round bottom flask was equipped with a stir bar, 2-ammonium biphenyl mesylate (2.57 g, 9.7 mmol) and $Pd(OAc)_2$ (2.19 g, 9.7 mmol). The flask was equipped with a rubber septum, and the vessel was evacuated and backfilled with nitrogen three times, and the flask was equipped with a nitrogen balloon. Anhydrous toluene (40 mL) was added by syringe through the septum. The reaction was heated to 50 °C for two hours. The solution was allowed to cool and filtered. The off-white filtrate was washed with toluene and dried to yield the product as an off-white solid (3.69 g, quantitative).

The NMR spectra of the compound corresponded to the literature values.[138]

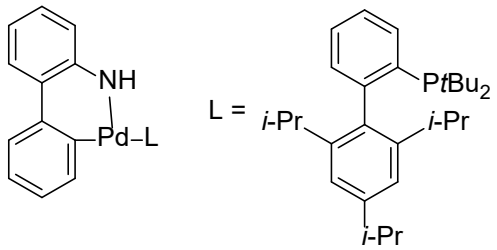

Pd-Cat-1. The title compound was synthesized using a procedure adapted from the literature.[138] A flame-dried 50 mL round bottom flask was equipped with a stir bar, μ-OMs dimer (370 mg, 0.50 mmol), and di-tert-butyl(2',4',6'-triisopropyl-[1,1'-biphenyl]-2-yl)phosphane (424 mg, 1.00 mmol). The flask was sealed with a rubber septum, evacuated and backfilled three times with nitrogen, and equipped with a nitrogen balloon. DCM was added using a syringe (10 mL), and the reaction was allowed to stir at room temperature for one hour. The solvent was removed under reduced pressure, and the residue was triturated with hexanes to yield the product as a fine yellow powder (415 mg, 50% yield).

The NMR spectra of the compound corresponded to the literature values.[138]

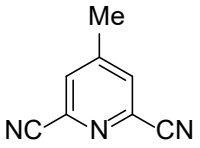

4-methylpyridine-2,6-dicarbonitrile. The title compound was synthesized with a procedure adapted from the literature.[139] To a 100 mL round bottom flask was added a stir bar, Pd-Cat-1 (159 mg, 0.2 mmol), 2,6-dichloro-4-methylpyridine (1.62 g, 10.0 mmol), and $Zn(CN)_2$ (1.55 g, 13.2 mmol). The flask was sealed with a rubber septum, evacuated and backfilled three times with nitrogen, and equipped with a nitrogen balloon. THF (10 mL) and degassed, deionized water (40 mL) was added. The reaction was heated to 40 °C and stirred overnight. The reaction was cooled to room temperature, and a saturated solution of $NaHCO_3$ was added, and ethyl acetate. The

solution was stirred for 5 minutes. The organic later was removed, and the aqueous later was extracted with ethyl acetate (3x10 mL). The organic fractions were combined and dried over $MgSO_4$. The solvent was removed under reduced pressure, and the residue was purified by flash chromatography (EtOAc/Hexanes) to yield the product as a white solid (1.13 g, 79% yield).

The NMR spectra of the compound corresponded to the literature values.[140]

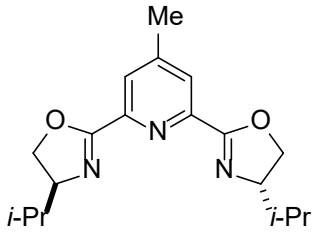

(4S,4'S)-2,2'-(4-methylpyridine-2,6-diyl)bis(4-isopropyl-4,5-dihydrooxazole). This compound was synthesized according to general proceedure 1 from 4-methylpyridine-2,6-dicarbonitrile (1.13 g, 7.89 mmol) and L-Valinol (1.63 g, 15.8 mmol). The title compound was purified by flash chromatography and was isolated as a white solid (1.33 g, 53% yield).

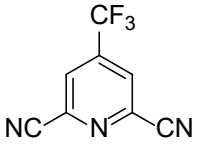

4-(trifluoromethyl)pyridine-2,6-dicarbonitrile. The title compound was synthesized according to a modified literature procedure.[137] In a nitrogen-filled glovebox, a 40 mL scintillation vial is charged with 2,6-dichloro-4-(trifluoromethyl)pyridine (1.08 g, 5.00 mmol), $Zn(CN)_2$ (646 mg, 5.5 mmol), zinc (65 mg, 1 mmol), *rac*-2-(Di-*tert*-butylphosphino)-1,1′-binaphthyl (199 mg, 0.5 mmol), and $Pd(TFA)_2$ (83 mg, 0.25 mmol). To the vial was added a cross-shaped stir-bar, followed

by 20 mL of DMA. The vial was capped with a cap with a PTFE septum, brough out of the glovebox, and heated at 95 °C overnight. The reaction was cooled to room temperature, filtered through a plug of celite, and the solvents were removed under reduced pressure. The residue was purified by flash chromatography (Ethyl acetate/hexanes) to yield the compound as a yellow solid (596 mg, 61% yield).

The NMR spectra of the compound corresponded to the literature values.[137]

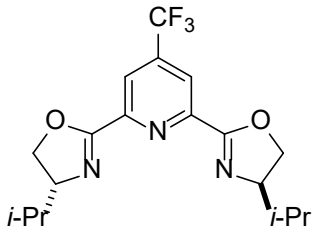

(4R,4'R)-2,2'-(4-(trifluoromethyl)pyridine-2,6-diyl)bis(4-isopropyl-4,5-dihydrooxazole). The title compound was synthesized using general procedure 1 from 4-(trifluoromethyl)pyridine-2,6-dicarbonitrile (596 mg, 3.00 mmol) and D-Valinol (619 mg, 6.00 mmol). The compound was purified using flash chromatography (Acetone/DCM), and was obtained as a white solid (634 mg, 62% yield).

The NMR spectra of the compound corresponded to the literature values.[137]

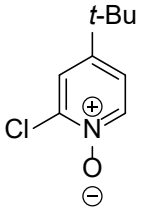

4-(tert-butyl)-2-chloropyridine 1-oxide. To a 250 mL round bottom flask was added a stir bar and 4-(tert-butyl)-2-chloropyridine (5.00 g, 29.5 mmol). Following this, glacial acetic acid was

added (42 mL), followed by aqueous hydrogen peroxide (30% in water, 33.6 mL). The reaction was stirred at 80 °C for four hours, at which time another charge of hydrogen peroxide was added (30% in water, 33.6 mL). The reaction was further stirred overnight, then allowed to cool to room temperature. The volume was reduced by solvent evaporation under reduced pressure, then was quenched by addition of Na_2CO_3. The residue was extracted with DCM (50x3 mL), and the combined organic layers were dried over $MgSO_4$, and concentrated to yield the title compound as a yellow solid, which was carried forward without further purification.

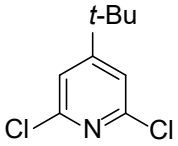

4-(tert-butyl)-2,6-dichloropyridine. To a 100 mL round bottom flask was equipped with a stir bar. To this was added 4-(tert-butyl)-2-chloropyridine 1-oxide (5.48 g, 29.5). The flask was cooled with an ice bath to 0 °C, and $POCl_3$ was slowly added (2.30 g, 15 mmol). The reaction was then heated to reflux, and left at this temperature overnight. The reaction was then cooled to room temperature, and poured over ice. The aqueous layer was extracted with dichloromethane, and the organic layers were combined and dried with $MgSO_4$. The solvent was removed under reduced pressure, and the residue was purified by flash chromatography (Ethyl acetate/hexanes) to yield the title compound as a white solid (3.13 g, 52% yield over two steps).

The NMR spectra of the compound corresponded to the literature values.[141]

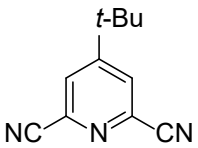

4-(tert-butyl)pyridine-2,6-dicarbonitrile. The title compound was synthesized according to a modified literature procedure.[139] To a 100 mL round bottom flask was added a stir bar, Pd-Cat-1 (264 mg, 0.33 mmol), 4-(tert-butyl)-2,6-dichloropyridine (1.70 g, 8.33 mmol), and $Zn(CN)_2$ (1.29 g, 11.0 mmol). The flask was sealed with a rubber septum, evacuated and backfilled three times with nitrogen, and equipped with a nitrogen balloon. THF (10 mL) and degassed, deionized water (40 mL) was added. The reaction was heated to 40 °C and stirred overnight. The reaction was cooled to room temperature, and a saturated solution of $NaHCO_3$ was added, and ethyl acetate. The solution was stirred for 5 minutes. The organic later was removed, and the aqueous later was extracted with ethyl acetate (3x10 mL). The organic fractions were combined and dried over $MgSO_4$. The solvent was removed under reduced pressure, and the residue was purified by flash chromatography (EtOAc/Hexanes) to yield the product as a yellow solid (1.75 g, quantitative).

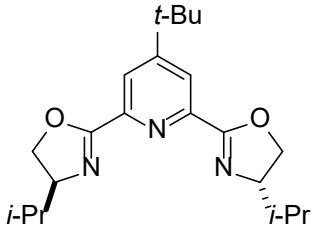

(4S,4'S)-2,2'-(4-(tert-butyl)pyridine-2,6-diyl)bis(4-isopropyl-4,5-dihydrooxazole). The title compound was synthesized from 4-(tert-butyl)pyridine-2,6-dicarbonitrile (1.52 g, 8.33 mmol) an L-Valinol (1.80 g, 17.5 mmol). The crude reaction was purified by flash chromatography (MeOH/DCM) to obtain the productas a white solid (980 mg, 33%).

The NMR spectra of the compound corresponded to the literature values.[142]

3.4: **Synthesis of the nucleophile**

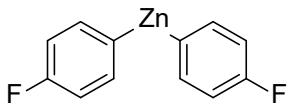

Bis(4-fluorophenyl)zinc. In a nitrogen-filled glovebox, to a 40 mL scintillation vial was added a cross-shaped magnetic stir bar, followed by zinc bromide (10 mmol, 2.25), then diethyl ether (3.0 mL). A septum cap was added, and the reaction was strongly stirred. A solution of (4-fluorophenyl)magnesium bromide in diethyl ether was added (2.0 M, 10 mL, 20 mmol). The reaction was allowed to stir overnight. A small amount of dried celite was added, followed by 1 mL of dioxane during strong stirring. The resulting cloudy solution was filtered through celite, and the filtrate was evaporated under reduced pressure. The residue was sublimed (105 °C, 100 mTorr) to yield the product as a slightly yellow microcrystalline product (1.10 g, 43% yield).

The NMR spectra of the compound corresponded to the literature values.[133]

4.1 Computational Details

4.1.1: General information

All calculations were performed using the Orca 5.0 software package,[143–149] except in certain noted cases where the ORCA 6.10 packages was used.[150] Geometry optimizations and frequency calculations were performed using the ωB97M functional[151] using the D4 dispersion correction.[152] Solvation effects were approximated using the conductor-like polarizable continuum model (CPCM),[153] using a probe radius of 2.42 Å, a dielectric coefficient of 7.2, and a refractive index of 1.38 to approximate 1,2-dimethoxyethane.[154] The basis set Def2-SVP[155] was used on all

atoms except nickel, on which DEF2-QZVPPD was used.[156] The vibrational frequencies of each species was confirmed to have no imaginary frequencies in the case of ground states, and one imaginary mode in the case of transition states.[157] Single-point calculations were performed on all geometries to refine the electronic energies using the ωB97M-V functional, and the DEF2-TZVPD basis set on all atoms except Ni, on which DEF2-QZVPPD was used. Figures of computed structure were generated using the Mercury software package.[158]

4.2 Computational Data

4.2.1: Data and Structures for comparisons with known crystal structures.

L1Ni^{I}Ph

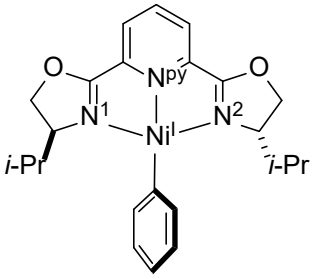

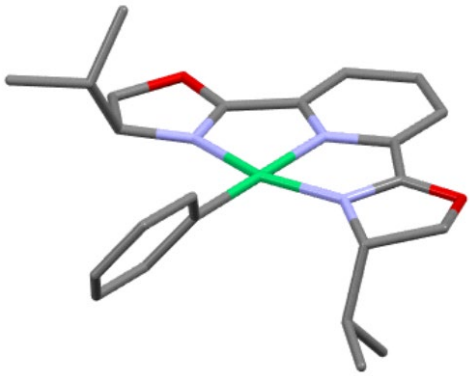

The geometry of this species was calculated using Orca 6.10.

Calculated geometry

Atom	X	Y	Z
Ni1	0	0	0
N2	-1.1051	0.1146	-1.5221
O3	-3.4249	-2.0273	0.1056
N4	-1.3937	-1.1652	0.5814
C5	1.115	-0.1025	1.5356
C6	-2.3858	-1.2796	-0.2884
N7	1.0823	1.202	-1.0711
C8	-2.2839	-0.5925	-1.526
C9	-3.1153	-0.523	-2.6669
H10	-4.0541	-1.0772	-2.6918
O11	1.2769	2.2307	-3.0484
C12	1.5054	1.0502	2.242
H13	1.1479	2.0317	1.915
C14	-3.0197	-2.6461	1.3477
H15	-2.7474	-3.6894	1.1355
H16	-3.8748	-2.6297	2.0325
C17	-2.7213	0.2517	-3.7399
H18	-3.3552	0.3131	-4.6245
C19	2.4234	1.7986	-1.0181
H20	2.5084	2.4164	-0.1154

C21	2.3434	0.9897	3.3595
H22	2.6208	1.9077	3.8838
C23	-1.8101	-1.8172	1.8231
H24	-1.0149	-2.4836	2.183
C25	0.5766	1.4628	-2.2317
C26	2.4268	2.685	-2.2828
H27	2.2731	3.7475	-2.0576
H28	3.3161	2.5706	-2.9116
C29	-0.7242	0.8653	-2.5741
C30	-1.4847	0.9784	-3.7096
H31	-1.1608	1.5923	-4.5484
C32	-3.2328	0.1707	2.5588
H33	-3.0116	0.6996	1.6208
H34	-3.3659	0.9284	3.3438
H35	-4.196	-0.3486	2.4393
C36	3.512	0.7145	-0.9648
H37	3.2789	0.1195	-0.0688
C38	2.4595	-1.4025	3.1257
H39	2.8318	-2.373	3.4633
C40	3.4772	-0.2167	-2.1746
H41	2.4968	-0.7019	-2.2844
H42	4.2283	-1.011	-2.0652
H43	3.7024	0.3174	-3.1104
C44	-2.1113	-0.7957	2.9339
H45	-1.1828	-0.2139	3.0432
C46	4.8866	1.3504	-0.7686
H47	5.171	1.9759	-1.6288
H48	5.6583	0.5763	-0.657
H49	4.9084	1.9823	0.1311
C50	1.6142	-1.3274	2.0147
H51	1.3408	-2.2573	1.5065
C52	2.8279	-0.2407	3.8063
H53	3.4856	-0.2938	4.6763
C54	-2.3861	-1.5026	4.2596
H55	-3.3006	-2.1139	4.2103
H56	-2.5236	-0.7729	5.0698
H57	-1.5531	-2.1643	4.5387

Referenced crystal structure

Atom	X	Y	Z

Ni1	0	0	0
N2	-1.1168	0.162	-1.4929
O3	-3.5902	-1.7159	0.2152
N4	-1.489	-0.9929	0.6553
C5	1.1884	-0.2011	1.4633
C6	-2.482	-1.0756	-0.2069
N7	1.1458	1.0813	-1.1226
C8	-2.3391	-0.4643	-1.4763
C9	-3.1585	-0.408	-2.6069
H10	-4.0216	-0.8056	-2.5951
O11	1.3262	2.0994	-3.1394
C12	1.4994	0.8181	2.372
H13	0.9854	1.6167	2.3525
C14	-3.1844	-2.3902	1.4421
H15	-3.0017	-3.3474	1.2725
H16	-3.8911	-2.3178	2.1308
C17	-2.6962	0.2355	-3.7465
H18	-3.2408	0.262	-4.5245
C19	2.4214	1.8454	-1.0234
H20	2.2954	2.5762	-0.351
C21	2.5305	0.7101	3.3038
H22	2.7074	1.4248	3.9046
C23	-1.9047	-1.6628	1.8944
H24	-1.2122	-2.3304	2.1702
C25	0.6418	1.3226	-2.2886
C26	2.5308	2.4912	-2.4145
H27	2.5845	3.476	-2.3376
H28	3.3393	2.1649	-2.8866
C29	-0.6843	0.7791	-2.6108
C30	-1.4301	0.8503	-3.7622
H31	-1.1058	1.295	-4.537
C32	-3.2388	0.3481	2.7012
H33	-3.0065	0.8066	1.8662
H34	-3.3058	1.0043	3.4254
H35	-4.0982	-0.1103	2.5939
C36	3.6369	1.0181	-0.605
H37	3.4734	0.6963	0.3284
C38	3.0065	-1.4743	2.4741
H39	3.5317	-2.2649	2.4884
C40	3.8327	-0.208	-1.4829
H41	2.9947	-0.7148	-1.5258
H42	4.5364	-0.7734	-1.102
H43	4.091	0.0747	-2.3841

C44	-2.1575	-0.6711	3.0372
H45	-1.3077	-0.1632	3.1822
C46	4.8969	1.904	-0.5728
H47	5.08	2.243	-1.474
H48	5.6606	1.3743	-0.2616
H49	4.7506	2.6578	0.0352
C50	1.9598	-1.3686	1.5837
H51	1.7531	-2.1121	1.0294
C52	3.2996	-0.4482	3.3467
H53	4.0144	-0.5321	3.9672
C54	-2.4561	-1.4376	4.3373
H55	-3.2415	-2.0087	4.2068
H56	-2.6325	-0.7998	5.0597
H57	-1.684	-1.9937	4.5752

L1Ni^{II}Ph[BAr$^{F}_{4}$]

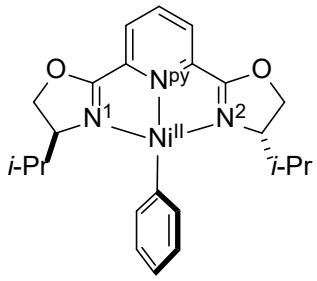

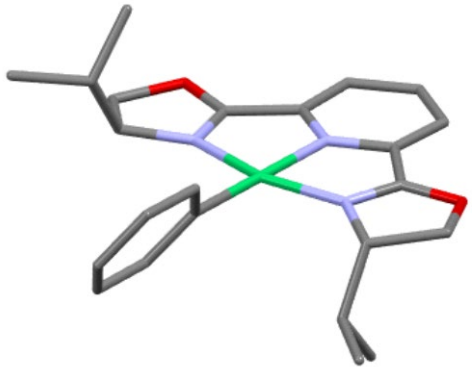

The geometry of this species was calculated using Orca 6.10.

Calculated geometry

Atom	X	Y	Z
Ni1	0	0	0
O2	-2.7273	-2.1652	1.909
O3	2.9307	2.0132	1.7687
N4	-1.5364	-1.1213	0.3328
N5	0.1065	-0.08	1.9178
N6	1.5678	1.0981	0.2528
C7	-2.5046	-1.9137	-0.444

H8	-3.0515	-1.2433	-1.118
C9	-3.4396	-2.4485	0.665
H10	-4.3968	-1.917	0.7138
H11	-3.6186	-3.5275	0.6245
C12	-1.732	-1.3775	1.5803
C13	-0.8042	-0.7871	2.5749
C14	-0.7708	-0.8765	3.9615
H15	-1.5159	-1.4537	4.5067
C16	0.2585	-0.195	4.6207
H17	0.32	-0.2417	5.708
C18	1.2107	0.5448	3.9106
H19	2.0148	1.077	4.4162
C20	1.0885	0.5733	2.5264
C21	1.9018	1.2503	1.4879
C22	3.5009	2.4034	0.4811
H23	4.4551	1.8742	0.3779
H24	3.6792	3.4828	0.5113
C25	2.4453	1.9596	-0.5574
H26	2.9101	1.3531	-1.344
C27	-1.7941	-2.9835	-1.2886
H28	-1.1083	-2.4248	-1.943
C29	-0.9656	-3.949	-0.4439
H30	-0.2054	-3.422	0.1505
H31	-0.4393	-4.6628	-1.0919
H32	-1.5934	-4.5364	0.2435
C33	-2.8039	-3.7128	-2.1727
H34	-2.2907	-4.4221	-2.836
H35	-3.3666	-3.0078	-2.8011
H36	-3.5274	-4.2875	-1.5745
C37	1.6481	3.0943	-1.2207
H38	0.8894	2.5905	-1.8382
C39	2.5539	3.902	-2.1483
H40	3.3429	4.428	-1.5894
H41	1.9715	4.662	-2.6864
H42	3.0389	3.2559	-2.894
C43	0.9267	3.9791	-0.2065
H44	0.2339	3.3998	0.4208
H45	0.3366	4.7465	-0.7255
H46	1.6325	4.5044	0.4551
C47	-0.103	0.0781	-1.8765
C48	-1.2471	0.5721	-2.5224
H49	-2.1002	0.9192	-1.9322
C50	-1.3259	0.6365	-3.9163

H51	-2.2261	1.0306	-4.3935
C52	-0.2578	0.1961	-4.6994
H53	-0.3175	0.2416	-5.7884
C54	0.8874	-0.303	-4.077
H55	1.7284	-0.6519	-4.6805
C56	0.9615	-0.3552	-2.6822
H57	1.8723	-0.746	-2.2195

Referenced crystal structure

Atom	X	Y	Z
Ni1	0	0	0
O2	-3.19011	0.391285	-2.30224
O3	3.739069	0.586127	-1.15101
N4	-1.80498	0.058345	-0.56396
N5	0.290699	0.504917	-1.80672
N6	1.892773	0.098875	0.033999
C7	-3.13921	-0.11576	0.03572
H8	-3.19208	-1.00331	0.488912
C9	-4.04611	-0.11366	-1.21367
H10	-4.36826	-1.0268	-1.416
H11	-4.828	0.479081	-1.07854
C12	-1.96018	0.364716	-1.808
C13	-0.76442	0.684129	-2.60187
C14	-0.60189	1.107278	-3.91351
H15	-1.34952	1.237237	-4.48421
C16	0.691067	1.33284	-4.35762
H17	0.832807	1.623214	-5.25115
C18	1.784846	1.144225	-3.52423
H19	2.671121	1.298864	-3.82785
C20	1.531718	0.720435	-2.22765
C21	2.421194	0.456133	-1.08117
C22	4.216706	0.352316	0.215446
H23	4.579689	1.1867	0.606936
H24	4.92375	-0.33914	0.225216
C25	2.975911	-0.12624	1.008661
H26	2.83754	0.477212	1.795248
C27	-3.42247	1.002641	1.049156
H28	-2.65083	1.026196	1.685321
C29	-3.51679	2.377153	0.405426
H30	-2.7322	2.527701	-0.16237

H31	-3.55317	3.062143	1.105498
H32	-4.32956	2.42541	-0.14064
C33	-4.66672	0.669481	1.861657
H34	-4.79961	1.353687	2.549688
H35	-4.55288	-0.20589	2.289767
H36	-5.44606	0.644783	1.26967
C37	3.01207	-1.57152	1.492914
H38	2.095747	-1.79351	1.826548
C39	3.96646	-1.72378	2.667563
H40	4.877269	-1.50802	2.379475
H41	3.937505	-2.6485	2.993617
H42	3.698779	-1.11598	3.388418
C43	3.334512	-2.55423	0.377717
H44	2.756423	-2.37629	-0.39401
H45	3.185419	-3.46931	0.694547
H46	4.27182	-2.45009	0.112442
C47	-0.29431	-0.48258	1.794371
C48	-0.77225	-1.75205	2.118002
H49	-0.96417	-2.36946	1.421628
C50	-0.97178	-2.12464	3.435517
H51	-1.28891	-2.99803	3.638899
C52	-0.7129	-1.2409	4.448828
H53	-0.85184	-1.5001	5.350961
C54	-0.25172	0.020083	4.162243
H55	-0.07943	0.635799	4.864652
C56	-0.03815	0.398608	2.834179
H57	0.28881	1.269501	2.639375

L1Ni^{II}Br$_2$

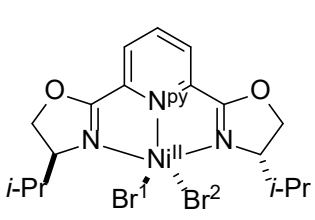

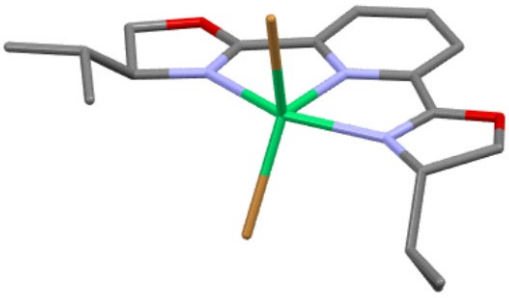

The geometry of this species was calculated using Orca 6.10

Calculated geometry

Atom	X	Y	Z
Ni1	0	0	0
Br2	0.438	1.7433	1.647
Br3	-0.2351	-2.4253	-0.2669
O4	3.1793	0.798	-2.5967
O5	-3.8214	0.7433	-1.5011
N6	2.0256	0.1116	-0.7997
N7	-0.2929	0.7093	-1.8854
N8	-2.1421	0.2706	-0.0953
C9	3.4357	0.0431	-0.3723
H10	3.6011	0.8852	0.3207
C11	4.1908	0.2731	-1.6979
H12	5.0048	1.0011	-1.635
H13	4.5624	-0.6656	-2.1328
C14	2.0215	0.5683	-1.9919
C15	0.7536	0.8872	-2.6839
C16	0.6032	1.3264	-3.9954
H17	1.4731	1.4677	-4.6343
C18	-0.6932	1.5717	-4.4512
H19	-0.8523	1.916	-5.473
C20	-1.7874	1.3745	-3.6065
H21	-2.8087	1.5534	-3.9381
C22	-1.5314	0.9359	-2.3119
C23	-2.5231	0.6451	-1.2536
C24	-4.485	0.2273	-0.3142
H25	-4.947	-0.7295	-0.5848
H26	-5.2646	0.9407	-0.0267
C27	-3.3472	0.077	0.7241
H28	-3.328	-0.9435	1.1298
C29	3.8159	-1.252	0.3473
H30	3.5519	-2.0844	-0.3265
C31	5.3243	-1.283	0.6011
H32	5.9101	-1.2384	-0.3277
H33	5.6052	-2.2074	1.1235
H34	5.6275	-0.4353	1.2347
C35	3.0479	-1.4114	1.6563
H36	3.2606	-0.5726	2.3359
H37	3.3438	-2.3408	2.1624
H38	1.9646	-1.4531	1.4913
C39	-3.3931	1.0665	1.8995

H40	-2.4559	0.9056	2.4536
C41	-3.4209	2.5229	1.4422
H42	-4.3428	2.7616	0.89
H43	-2.5597	2.7605	0.8034
H44	-3.3797	3.1936	2.3114
C45	-4.5636	0.7358	2.8237
H46	-5.5306	0.8756	2.3161
H47	-4.5581	1.3934	3.7037
H48	-4.5152	-0.3043	3.1766

Referenced crystal structure

Atom	X	Y	Z
Ni1	0	0	0
Br2	0.4338	1.7393	1.5924
Br3	-0.2151	-2.4003	-0.2258
O4	3.1741	0.7156	-2.5904
O5	-3.7978	0.9811	-1.3866
N6	1.9901	0.0911	-0.7638
N7	-0.2845	0.7453	-1.8246
N8	-2.1137	0.2986	-0.0481
C9	3.4139	0.064	-0.3245
H10	3.5974	0.9023	0.1892
C11	4.1648	0.1499	-1.661
H12	4.9558	0.7396	-1.5854
H13	4.459	-0.7463	-1.9595
C14	2.0093	0.5314	-1.9637
C15	0.7562	0.9243	-2.6363
C16	0.6243	1.4635	-3.906
H17	1.3747	1.5704	-4.4792
C18	-0.6596	1.8425	-4.309
H19	-0.7898	2.2288	-5.1671
C20	-1.7493	1.6571	-3.4593
H21	-2.6253	1.9121	-3.7233
C22	-1.5143	1.0893	-2.2204
C23	-2.4936	0.7773	-1.1671
C24	-4.4664	0.4036	-0.2136
H25	-4.9342	-0.4361	-0.4523
H26	-5.1237	1.039	0.166
C27	-3.3214	0.1298	0.7915
H28	-3.377	-0.8168	1.109

C29	3.8087	-1.1241	0.5502
H30	3.6264	-1.9708	0.0501
C31	5.312	-1.0269	0.8317
H32	5.8091	-1.1303	-0.0071
H33	5.574	-1.7355	1.4568
H34	5.5153	-0.153	1.2249
C35	3.0099	-1.1368	1.8525
H36	3.0971	-0.268	2.2977
H37	3.3549	-1.8407	2.44
H38	2.0653	-1.3092	1.6547
C39	-3.3025	1.0672	1.9946
H40	-2.4545	0.8925	2.4956
C41	-3.2988	2.5379	1.5944
H42	-4.1331	2.7516	1.1275
H43	-2.539	2.7136	1.0023
H44	-3.2229	3.0954	2.3967
C45	-4.4611	0.7526	2.9348
H46	-5.3087	0.8817	2.4616
H47	-4.424	1.3513	3.7106
H48	-4.3922	-0.1769	3.2361

4.2.2: Calculated structures for the catalytic cycle

L1Ni^{II}Ar^{+}

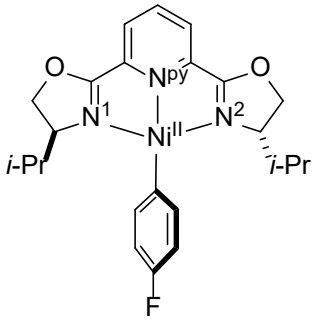

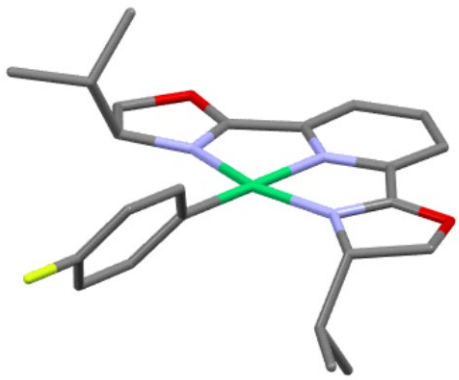

Calculated geometry

Atom	X	Y	Z
Ni1	0	0	0
O2	-3.2521	1.7194	1.4943
O3	3.6689	0.4633	1.447

N4	-1.8392	0.5401	0.2275
N5	0.2167	1.1334	1.5358
N6	1.9068	-0.1922	0.2394
C7	-3.1586	0.2025	-0.3333
H8	-3.1542	0.4222	-1.4079
C9	-4.084	1.188	0.417
H10	-4.3962	2.0392	-0.1985
H11	-4.962	0.7226	0.8757
C12	-2.0296	1.3275	1.2294
C13	-0.8562	1.7281	2.0425
C14	-0.7522	2.5584	3.1521
H15	-1.6284	3.0499	3.5716
C16	0.5227	2.7326	3.7024
H17	0.6457	3.3755	4.574
C18	1.6426	2.0969	3.1546
H19	2.6378	2.2262	3.5766
C20	1.4329	1.2885	2.0438
C21	2.3771	0.4895	1.2263
C22	4.2192	-0.4931	0.4892
H23	4.5427	-1.3709	1.0598
H24	5.0856	-0.0226	0.0138
C25	3.0471	-0.7918	-0.4746
H26	2.884	-1.8733	-0.5572
C27	-3.4802	-1.2882	-0.1397
H28	-2.6733	-1.8269	-0.6588
C29	-3.466	-1.7093	1.3281
H30	-3.6551	-2.7878	1.4144
H31	-4.2457	-1.1953	1.9108
H32	-2.4942	-1.5066	1.8009
C33	-4.7997	-1.6354	-0.8266
H34	-5.6509	-1.1203	-0.3558
H35	-4.9933	-2.7146	-0.7614
H36	-4.7812	-1.3582	-1.8903
C37	3.1878	-0.2091	-1.89
H38	2.2369	-0.4393	-2.3931
C39	4.3071	-0.9245	-2.6443
H40	5.2904	-0.7392	-2.1857
H41	4.3576	-0.5689	-3.6823
H42	4.1422	-2.0113	-2.6665
C43	3.3703	1.307	-1.8881
H44	4.3015	1.6081	-1.3844
H45	2.5317	1.8177	-1.3933
H46	3.4229	1.6833	-2.9187

C47	-0.2123	-1.1102	-1.5054
C48	0.1654	-2.4615	-1.4745
H49	0.5913	-2.8909	-0.5638
C50	0.0116	-3.2954	-2.5853
H51	0.3002	-4.3473	-2.5611
C52	-0.5223	-2.7589	-3.7489
F53	-0.6711	-3.5523	-4.8283
C54	-0.9071	-1.4278	-3.831
H55	-1.3216	-1.0443	-4.7645
C56	-0.7514	-0.6169	-2.7036
H57	-1.0612	0.4291	-2.7754

(R) Radical addition

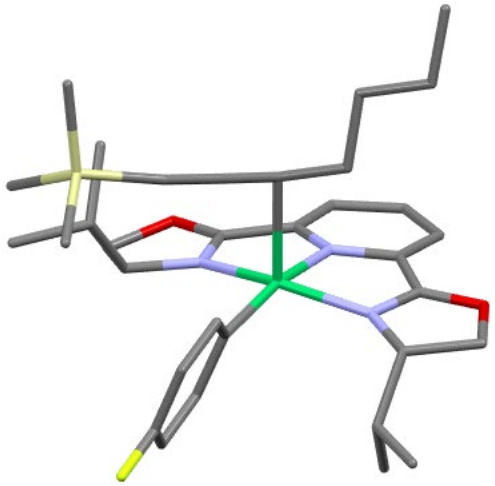

Calculated geometry

Atom	X	Y	Z
Ni1	0	0	0
O2	-3.9826	0.3983	-0.1745
O3	2.3865	0.6221	-3.1551
N4	-1.8976	-0.1002	0.4791
N5	-0.7696	0.7754	-1.5891
N6	1.5667	-0.0699	-1.1856
C7	-2.7227	-0.5948	1.5939
H8	-2.5071	-1.6646	1.7269
C9	-4.1616	-0.398	1.0438
H10	-4.6412	-1.3395	0.7435
H11	-4.83	0.1606	1.7097

C12	-2.6853	0.4256	-0.4032
C13	-2.0922	0.949	-1.6425
C14	-2.7004	1.4637	-2.7868
H15	-3.7812	1.6039	-2.8306
C16	-1.874	1.7703	-3.8774
H17	-2.3143	2.1774	-4.7899
C18	-0.4946	1.5256	-3.8237
H19	0.1542	1.7164	-4.6795
C20	0.0219	1.0027	-2.638
C21	1.374	0.5239	-2.3184
C22	3.5283	-0.0066	-2.4895
H23	4.2979	0.765	-2.3671
H24	3.9	-0.795	-3.1568
C25	2.96	-0.5326	-1.1407
H26	3.4526	-0.03	-0.2962
C27	-2.4034	0.1213	2.9203
H28	-1.3116	0.0245	3.0434
C29	-2.7607	1.61	2.9042
H30	-3.8517	1.768	2.8939
H31	-2.3373	2.1299	2.0327
H32	-2.3688	2.1044	3.8064
C33	-3.0769	-0.6129	4.084
H34	-2.7603	-1.6675	4.1281
H35	-4.1764	-0.5918	3.9911
H36	-2.8176	-0.1386	5.0433
C37	3.0696	-2.0556	-0.9257
H38	2.6356	-2.2453	0.0671
C39	4.5424	-2.4749	-0.8783
H40	5.0432	-2.3307	-1.8507
H41	4.6289	-3.5419	-0.62
H42	5.0982	-1.8974	-0.1219
C43	2.2674	-2.8591	-1.9514
H44	2.3415	-3.936	-1.7335
H45	2.6394	-2.7066	-2.979
H46	1.2004	-2.5866	-1.9302
C47	0.6359	-1.1501	1.3643
C48	1.5966	-0.8771	2.3449
H49	2.0203	0.1219	2.4449
C50	2.0616	-1.8833	3.202
H51	2.8163	-1.6782	3.965
C52	1.5536	-3.1713	3.0652
F53	2.0024	-4.1456	3.8833
C54	0.5916	-3.4805	2.1077

H55	0.2138	-4.5027	2.0285
C56	0.1356	-2.4598	1.2648
H57	-0.6126	-2.7134	0.5079
C58	0.4629	2.0248	1.0082
C59	0.4562	1.7415	2.3806
H60	-0.4725	2.4629	0.6418
C61	1.7207	2.5928	0.3881
C62	0.4113	1.4946	3.5896
Si63	0.0545	1.2179	5.3809
H64	1.6618	2.524	-0.7087
H65	2.5981	2.0025	0.6995
C66	1.9502	4.0688	0.7515
C67	0.2201	2.8665	6.2762
C68	3.188	4.6527	0.0664
H69	2.0444	4.1653	1.8474
H70	1.0576	4.6539	0.465
H71	4.0746	4.0594	0.3557
C72	3.4226	6.1265	0.3961
H73	3.0857	4.5285	-1.0276
H74	4.3198	6.5164	-0.1114
H75	3.5592	6.2754	1.4807
H76	2.5647	6.7454	0.0828
H77	-0.0223	2.7458	7.3457
H78	-0.4656	3.6167	5.8498
H79	1.2483	3.2564	6.1989
C80	1.2581	-0.0377	6.106
C81	-1.7114	0.5673	5.4938
H82	-1.8259	-0.369	4.9243
H83	-2.4284	1.3006	5.0899
H84	-1.9796	0.3655	6.5445
H85	2.3046	0.2323	5.8892
H86	1.0698	-1.0488	5.7126
H87	1.1355	-0.0785	7.2015

(S) Radical addition

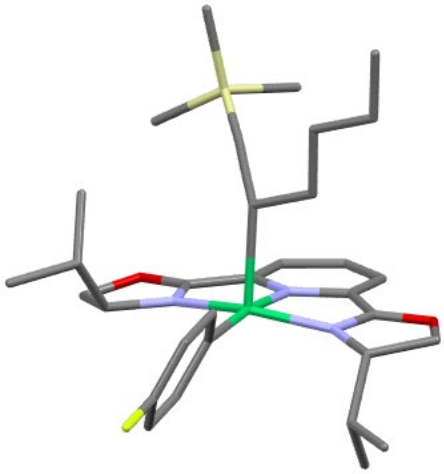

Calculated geometry

Atom	X	Y	Z
Ni1	0	0	0
O2	-3.3573	-1.3021	-1.7244
O3	1.2083	3.7909	-0.0538
N4	-1.3622	-1.2076	-0.7074
N5	-1.1771	1.2969	-0.77
N6	1.1466	1.5579	0.1148
C7	-1.6159	-2.6563	-0.8051
H8	-0.797	-3.0994	-1.3903
C9	-2.9396	-2.7019	-1.6189
H10	-2.8067	-3.076	-2.6426
H11	-3.7518	-3.2512	-1.1281
C12	-2.3718	-0.5839	-1.2261
C13	-2.33	0.8829	-1.2944
C14	-3.2267	1.7968	-1.8481
H15	-4.1655	1.4614	-2.2898
C16	-2.8751	3.1524	-1.8145
H17	-3.5577	3.8965	-2.2297
C18	-1.6504	3.5664	-1.2682
H19	-1.3564	4.6166	-1.2537
C20	-0.8084	2.5791	-0.7602
C21	0.5505	2.6609	-0.21
C22	2.4807	3.4339	0.5807
H23	2.4514	3.8282	1.6054
H24	3.2797	3.9289	0.0156
C25	2.52	1.8826	0.526

H26	2.7012	1.4672	1.528
C27	-1.6447	-3.3596	0.5664
H28	-0.7223	-3.0352	1.0755
C29	-2.8399	-2.9604	1.4356
H30	-2.7138	-3.3589	2.4545
H31	-3.7856	-3.3706	1.0438
H32	-2.9523	-1.8707	1.5134
C33	-1.5696	-4.8775	0.3708
H34	-0.6653	-5.167	-0.1885
H35	-2.4472	-5.2546	-0.1826
H36	-1.5478	-5.3919	1.3442
C37	3.5545	1.2729	-0.4435
H38	3.3895	0.1846	-0.3974
C39	4.9754	1.5558	0.0531
H40	5.1173	1.1972	1.0856
H41	5.2092	2.6338	0.0325
H42	5.7136	1.0478	-0.5868
C43	3.3454	1.7231	-1.8917
H44	3.4878	2.8106	-2.0101
H45	2.337	1.468	-2.2545
H46	4.072	1.2259	-2.553
C47	1.2808	-1.2934	0.5055
C48	1.8523	-1.4503	1.7744
H49	1.5191	-0.8439	2.619
C50	2.8697	-2.3862	2.0016
H51	3.3178	-2.5157	2.9897
C52	3.3142	-3.165	0.9375
F53	4.292	-4.0692	1.1486
C54	2.7749	-3.0361	-0.3393
H55	3.1501	-3.6624	-1.1522
C56	1.7566	-2.0974	-0.5438
H57	1.3426	-1.997	-1.5512
C58	-0.9971	0.2922	2.0674
C59	-2.3554	0.5364	1.8236
H60	-0.7658	-0.7434	2.3393
C61	-0.2362	1.3531	2.8359
C62	-3.5444	0.7682	1.5896
Si63	-5.371	0.9964	1.433
H64	-0.4145	2.3437	2.3858
H65	0.8448	1.1614	2.7725
C66	-0.6368	1.4064	4.3199
C67	-6.0353	-0.2803	0.2181
C68	0.1321	2.4745	5.1012

H69	-0.4656	0.4152	4.7775
H70	-1.7218	1.598	4.3958
H71	1.2164	2.2768	5.0145
C72	-0.2628	2.542	6.5765
H73	-0.0351	3.4586	4.6259
H74	0.3055	3.3195	7.1123
H75	-0.0753	1.5804	7.0837
H76	-1.3357	2.7722	6.6911
H77	-7.1317	-0.187	0.1388
H78	-5.8023	-1.3011	0.5628
H79	-5.6042	-0.1565	-0.7867
C80	-5.7332	2.7492	0.8451
C81	-6.1287	0.7217	3.1374
H82	-7.2246	0.8411	3.0907
H83	-5.735	1.4481	3.867
H84	-5.9087	-0.2926	3.5082
H85	-6.8234	2.915	0.8101
H86	-5.3285	2.9359	-0.1614
H87	-5.2973	3.4914	1.5338

(R)-Ni^{III}

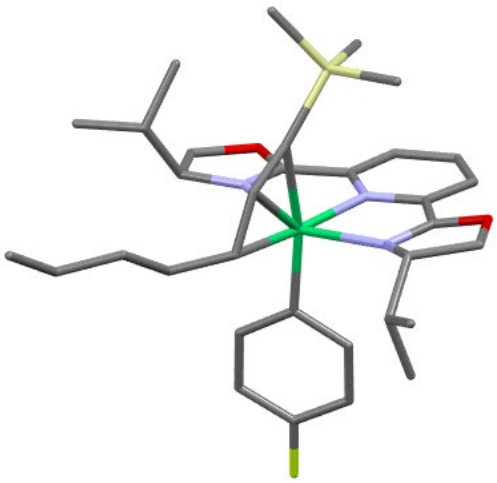

Calculated geometry

Atom	X	Y	Z
Ni1	0	0	0
O2	-2.9084	-1.9955	-2.2555

O3	3.6098	0.7377	-2.051
N4	-1.9908	-0.7128	-0.6606
N5	0.376	-0.7035	-1.8366
N6	2.1245	0.6502	-0.3711
C7	-3.3867	-0.8718	-0.223
H8	-3.3877	-1.3526	0.7648
C9	-3.9724	-1.8416	-1.2793
H10	-4.197	-2.8343	-0.8731
H11	-4.8549	-1.455	-1.8011
C12	-1.8632	-1.3494	-1.7582
C13	-0.5767	-1.3708	-2.4837
C14	-0.3455	-1.9687	-3.7182
H15	-1.1436	-2.5091	-4.2244
C16	0.9257	-1.8389	-4.2774
H17	1.1449	-2.2921	-5.2441
C18	1.9124	-1.1151	-3.6068
H19	2.908	-0.9772	-4.025
C20	1.5869	-0.5605	-2.3735
C21	2.4713	0.283	-1.5413
C22	4.2176	1.5427	-1.0048
H23	4.4749	2.5156	-1.4353
H24	5.1335	1.0325	-0.6818
C25	3.1336	1.6156	0.097
H26	2.6511	2.605	0.0872
C27	-4.1088	0.4783	-0.0879
H28	-3.5146	1.0636	0.6305
C29	-4.1517	1.2613	-1.3951
H30	-4.7198	0.7336	-2.1757
H31	-3.1402	1.4477	-1.7752
H32	-4.635	2.2357	-1.2411
C33	-5.4998	0.2731	0.5089
H34	-6.145	-0.3121	-0.164
H35	-5.9932	1.2396	0.6784
H36	-5.448	-0.2554	1.4718
C37	3.6331	1.369	1.5263
H38	2.7461	1.4574	2.1719
C39	4.6111	2.4749	1.9247
H40	5.5314	2.431	1.3222
H41	4.9045	2.3694	2.9778
H42	4.1678	3.4724	1.7934
C43	4.231	-0.0182	1.7395
H44	3.5078	-0.8086	1.5082
H45	4.5342	-0.139	2.7885

H46	5.127	-0.1807	1.1222
C47	0.3599	-1.6853	0.9088
C48	1.562	-2.3585	0.6555
H49	2.3439	-1.8898	0.0593
C50	1.8081	-3.6451	1.1436
H51	2.7485	-4.1603	0.9438
C52	0.8256	-4.2706	1.8955
F53	1.0504	-5.509	2.3743
C54	-0.3874	-3.6512	2.1595
H55	-1.145	-4.1715	2.747
C56	-0.607	-2.3655	1.6598
H57	-1.5692	-1.9032	1.8725
C58	-0.3112	0.9666	1.7565
C59	-0.5227	1.8629	0.6847
H60	0.6611	1.0851	2.2452
C61	-1.4376	0.5981	2.6928
C62	-0.5209	2.1377	-0.5292
Si63	-0.47	3.0775	-2.1521
H64	-1.0791	-0.179	3.381
H65	-2.2738	0.1621	2.1303
C66	-1.9534	1.7953	3.4941
C67	-1.7242	4.457	-1.9999
C68	-0.866	1.942	-3.5896
C69	1.2718	3.7392	-2.3497
C70	-3.0813	1.4204	4.4508
H71	-1.1207	2.2476	4.0575
H72	-2.3079	2.5703	2.7941
C73	-3.6119	2.6077	5.246
H74	-3.9015	0.9618	3.8738
H75	-2.7245	0.6384	5.1409
H76	-4.424	2.3095	5.9236
H77	-2.8178	3.0633	5.8562
H78	-4.0039	3.3892	4.5778
H79	-0.9921	2.5591	-4.4921
H80	-0.0438	1.2406	-3.7858
H81	-1.7906	1.368	-3.4462
H82	-1.7249	5.0697	-2.914
H83	-2.7367	4.0553	-1.8541
H84	-1.4851	5.1099	-1.1481
H85	1.5816	4.3316	-1.4771
H86	1.9951	2.9247	-2.4979
H87	1.3189	4.3874	-3.2378

(S)-Ni^{III}

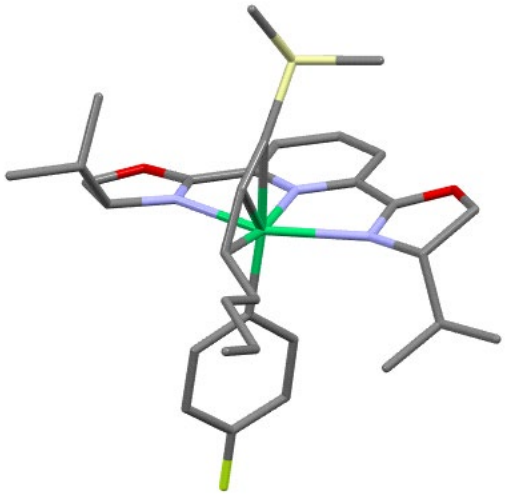

Calculated geometry

Atom	X	Y	Z
Ni1	0	0	0
O2	-2.6921	-1.4035	-2.8685
O3	4.0366	0.1419	-1.3203
N4	-1.899	-0.3356	-1.0637
N5	0.6153	-0.6625	-1.7917
N6	2.3222	0.1244	0.1322
C7	-3.3509	-0.3557	-0.8415
H8	-3.5454	-0.9474	0.0642
C9	-3.8824	-1.1041	-2.0911
H10	-4.3724	-2.0539	-1.8514
H11	-4.5481	-0.5007	-2.7191
C12	-1.672	-0.9288	-2.1679
C13	-0.2932	-1.0927	-2.6672
C14	0.0631	-1.5893	-3.9161
H15	-0.7037	-1.9404	-4.6045
C16	1.4164	-1.5984	-4.2529
H17	1.7349	-1.972	-5.2259
C18	2.3601	-1.1121	-3.3485
H19	3.4224	-1.0858	-3.5843
C20	1.9065	-0.6576	-2.1138
C21	2.765	-0.1197	-1.039
C22	4.5474	0.8382	-0.1545
H23	4.6244	1.9025	-0.4103
H24	5.5415	0.4383	0.0622

C25	3.4938	0.5498	0.9353
H26	3.2375	1.4613	1.4935
C27	-3.9255	1.0513	-0.6183
H28	-3.4217	1.4396	0.2806
C29	-3.6232	2.0046	-1.7703
H30	-4.0849	1.6725	-2.7123
H31	-2.5422	2.0977	-1.932
H32	-4.0161	3.0065	-1.5497
C33	-5.4211	0.9671	-0.3169
H34	-5.9864	0.5966	-1.1856
H35	-5.8206	1.9588	-0.0652
H36	-5.6225	0.2947	0.5294
C37	3.9498	-0.5447	1.9205
H38	4.2119	-1.4239	1.3059
C39	2.8594	-0.9494	2.9067
H40	2.6584	-0.1334	3.6155
H41	3.1853	-1.8213	3.4907
H42	1.9223	-1.2088	2.4041
C43	5.1937	-0.0936	2.6889
H44	6.0505	0.1268	2.039
H45	5.5083	-0.879	3.3895
H46	4.9739	0.8095	3.2787
C47	-0.2105	-1.7098	0.9012
C48	0.7467	-2.7017	0.6443
H49	1.6362	-2.4736	0.0557
C50	0.6194	-3.9999	1.1442
H51	1.3694	-4.7663	0.9443
C52	-0.4899	-4.3088	1.9172
F53	-0.6227	-5.5554	2.4091
C54	-1.4652	-3.363	2.1969
H55	-2.3248	-3.6389	2.8092
C56	-1.3155	-2.0723	1.6835
H57	-2.0956	-1.3466	1.9179
C58	-0.7059	0.9932	1.6053
C59	-0.4144	1.9262	0.5878
C60	0.0414	1.0204	2.9146
H61	-1.7685	0.7421	1.696
C62	-0.0034	2.2048	-0.553
Si63	0.5123	3.1423	-2.0936
C64	-0.3728	4.7885	-2.01
C65	0.015	2.1815	-3.623
C66	2.373	3.3454	-2.0355
H67	0.1138	2.841	-4.4984

H68	0.6723	1.3177	-3.7897
H69	-1.0252	1.8314	-3.5826
H70	-0.0989	5.4085	-2.8769
H71	-1.4631	4.6476	-2.0186
H72	-0.1015	5.3358	-1.0957
H73	2.6974	3.7866	-1.0821
H74	2.8889	2.3847	-2.1711
H75	2.6971	4.0117	-2.849
H76	1.0975	1.2539	2.7308
C77	-0.5463	2.0293	3.9026
H78	0.0048	0.0145	3.3557
H79	-1.6139	1.8041	4.0615
C80	0.1814	2.0277	5.244
H81	-0.5084	3.039	3.4609
C82	-0.4012	3.0194	6.2444
H83	0.1508	1.0102	5.667
H84	1.2477	2.251	5.0747
H85	-0.3536	4.0484	5.8575
H86	-1.4574	2.7949	6.4555
H87	0.142	2.9964	7.1994

(R) Reductive elimination

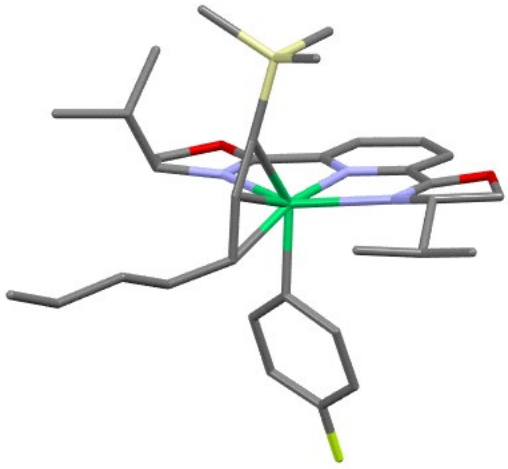

Calculated geometry

Atom	X	Y	Z
Ni1	0	0	0

O2	-3.2865	-1.8565	-1.7734
O3	3.563	-0.2975	-2.5133
N4	-2.0752	-0.5482	-0.4122
N5	0.1636	-0.9882	-1.7592
N6	2.3087	0.3845	-0.7704
C7	-3.4589	-0.3969	0.0725
H8	-3.4945	-0.627	1.1444
C9	-4.2142	-1.4849	-0.721
H10	-4.4149	-2.383	-0.1241
H11	-5.1432	-1.1431	-1.1885
C12	-2.1234	-1.3225	-1.4256
C13	-0.9163	-1.6265	-2.2145
C14	-0.8797	-2.4675	-3.3209
H15	-1.7861	-2.9676	-3.6579
C16	0.3426	-2.6378	-3.9696
H17	0.4164	-3.2905	-4.8393
C18	1.4673	-1.9612	-3.5037
H19	2.4366	-2.0567	-3.9892
C20	1.3265	-1.1397	-2.3868
C21	2.4213	-0.3254	-1.8237
C22	4.4812	0.4562	-1.6938
H23	5.0563	1.1269	-2.3388
H24	5.1587	-0.2588	-1.2035
C25	3.5656	1.1708	-0.6862
H26	3.3254	2.1855	-1.0465
C27	-3.9626	1.0411	-0.128
H28	-3.2178	1.6849	0.3663
C29	-4.0292	1.4338	-1.602
H30	-4.7367	0.8041	-2.1614
H31	-3.0467	1.3592	-2.0881
H32	-4.3742	2.4711	-1.7062
C33	-5.3048	1.2339	0.5753
H34	-6.0871	0.5991	0.1318
H35	-5.6399	2.2764	0.4892
H36	-5.235	0.9869	1.6445
C37	4.1774	1.3028	0.7085
H38	4.2942	0.2832	1.1129
C39	3.2786	2.1149	1.6327
H40	3.2045	3.1548	1.2807
H41	3.6788	2.1308	2.6555
H42	2.265	1.7079	1.6658
C43	5.5632	1.9465	0.6181
H44	6.2759	1.341	0.0418

H45	5.9849	2.0835	1.623
H46	5.4985	2.9389	0.1458
C47	0.3922	-1.4014	1.3643
C48	1.7388	-1.709	1.5976
H49	2.4999	-0.9409	1.4709
C50	2.1329	-2.9855	1.995
H51	3.1809	-3.23	2.1716
C52	1.1574	-3.9559	2.1805
F53	1.5258	-5.1887	2.5685
C54	-0.1898	-3.6801	1.9934
H55	-0.9305	-4.4613	2.1675
C56	-0.5644	-2.3975	1.593
H57	-1.6246	-2.1858	1.4656
C58	-0.0724	0.5125	2.0347
C59	-0.2383	1.6464	1.1572
H60	0.8878	0.5618	2.5537
C61	-1.2208	0.2368	2.9932
C62	-0.2916	2.2901	0.0996
Si63	-0.2519	3.5293	-1.2979
H64	-0.9488	-0.6157	3.6295
H65	-2.1125	-0.0621	2.4302
C66	-1.56	1.4467	3.8619
C67	-0.0925	2.5534	-2.8896
C68	1.2399	4.6323	-1.0349
C69	-1.8259	4.5402	-1.2401
C70	-2.6803	1.1579	4.8571
H71	-0.6579	1.776	4.4041
H72	-1.855	2.2894	3.2156
C73	-3.0493	2.3672	5.7086
H74	-3.5677	0.8069	4.3046
H75	-2.3799	0.3205	5.5077
H76	-3.8562	2.1325	6.4166
H77	-2.1855	2.7204	6.2916
H78	-3.3883	3.2052	5.0811
H79	1.292	5.3896	-1.8319
H80	1.1762	5.1557	-0.0699
H81	2.1744	4.0551	-1.0521
H82	-0.1115	3.2237	-3.7614
H83	0.8584	2.0012	-2.9019
H84	-0.9111	1.827	-2.994
H85	-2.7159	3.9085	-1.3548
H86	-1.9048	5.0793	-0.2848
H87	-1.826	5.2829	-2.0522

(S) Reductive elimination

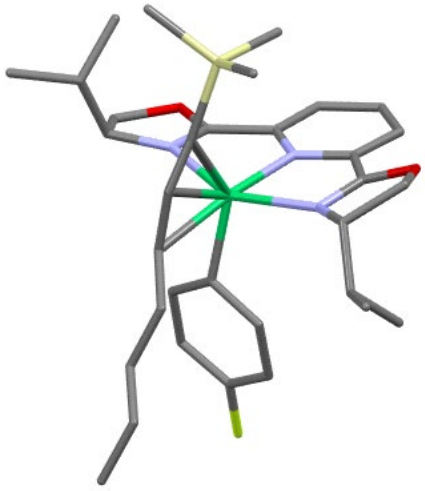

Calculated geometry

Atom	X	Y	Z
Ni1	0	0	0
O2	-3.51	-1.568	-1.6331
O3	1.3989	3.4765	-1.9259
N4	-1.9363	-1.0229	-0.1326
N5	-0.7756	0.7024	-1.7323
N6	1.3835	1.6963	-0.5574
C7	-2.8217	-1.9485	0.5911
H8	-2.2212	-2.7494	1.0432
C9	-3.7094	-2.5068	-0.5413
H10	-3.3801	-3.4937	-0.8899
H11	-4.7789	-2.539	-0.3095
C12	-2.4385	-0.8616	-1.2949
C13	-1.8643	0.123	-2.2349
C14	-2.3913	0.4888	-3.4689
H15	-3.2804	-0.0052	-3.8574
C16	-1.754	1.5144	-4.1693
H17	-2.1381	1.8325	-5.1385
C18	-0.6399	2.1481	-3.6187
H19	-0.1395	2.9716	-4.1254
C20	-0.181	1.6973	-2.3844
C21	0.9296	2.2762	-1.5996
C22	2.2215	3.8844	-0.8017

H23	1.6629	4.6477	-0.2449
H24	3.145	4.3224	-1.1933
C25	2.4212	2.5821	0.0028
H26	2.2	2.7411	1.0663
C27	-3.5721	-1.2183	1.719
H28	-2.7888	-0.7489	2.3353
C29	-4.4899	-0.1154	1.1955
H30	-4.985	0.3974	2.0311
H31	-5.2845	-0.5182	0.5501
H32	-3.9352	0.6418	0.6246
C33	-4.3312	-2.2194	2.5881
H34	-5.1272	-2.7238	2.0194
H35	-4.8075	-1.7099	3.4368
H36	-3.6609	-2.9929	2.9893
C37	3.8277	1.9715	-0.1089
H38	3.7639	0.9887	0.3818
C39	4.8336	2.811	0.6768
H40	4.9335	3.8213	0.2519
H41	5.828	2.345	0.652
H42	4.5325	2.9149	1.7289
C43	4.2761	1.7625	-1.5548
H44	4.4583	2.72	-2.0642
H45	3.5359	1.2031	-2.144
H46	5.2164	1.1951	-1.5822
C47	1.0761	-1.6277	-0.4196
C48	0.4825	-2.876	-0.6438
H49	-0.4461	-3.1423	-0.141
C50	1.0703	-3.8203	-1.484
H51	0.6123	-4.7952	-1.6544
C52	2.2749	-3.5086	-2.0996
F53	2.8522	-4.4155	-2.9055
C54	2.9026	-2.288	-1.8928
H55	3.8531	-2.0765	-2.3839
C56	2.2997	-1.3605	-1.0447
H57	2.8044	-0.4162	-0.866
C58	0.869	-1.1128	1.5626
C59	0.209	0.0881	2.021
H60	0.2591	-1.9917	1.7967
C61	2.3159	-1.2706	2.0314
C62	-0.4251	1.1507	1.9896
Si63	-1.3293	2.7705	2.1954
H64	2.3578	-0.9277	3.0771
H65	2.9629	-0.5839	1.4688

C66	2.8582	-2.6942	1.968
C67	-2.7233	2.5064	3.4168
C68	-1.9677	3.2783	0.5066
C69	-0.11	4.0358	2.8466
C70	4.2988	-2.7888	2.4618
H71	2.2149	-3.3491	2.5795
H72	2.8025	-3.0826	0.9413
C73	4.8473	-4.2106	2.4305
H74	4.932	-2.1321	1.8424
H75	4.361	-2.3873	3.4868
H76	4.8229	-4.6215	1.41
H77	5.8873	-4.252	2.7831
H78	4.2514	-4.8797	3.0694
H79	-2.6279	4.1537	0.5939
H80	-1.1344	3.5511	-0.1568
H81	-2.534	2.4646	0.0315
H82	-3.2772	3.4452	3.5683
H83	-3.4305	1.7466	3.059
H84	-2.3298	2.1806	4.3907
H85	0.3267	3.7106	3.802
H86	0.7082	4.2083	2.1331
H87	-0.6209	4.9961	3.0142

(R) Product-Catalyst Complex

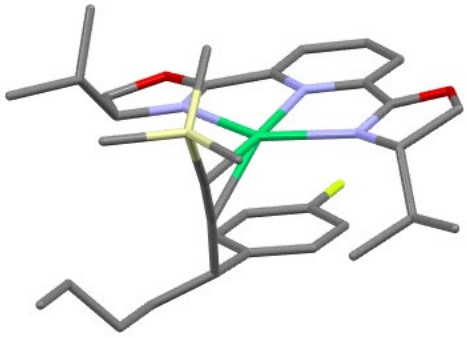

Calculated geometry

Atom	X	Y	Z
Ni1	0	0	0

O2	-3.0909	-2.7077	-0.6976
O3	3.6691	-0.9892	-1.8499
N4	-2.0044	-0.8068	-0.2144
N5	0.2798	-1.6776	-1.1303
N6	2.1855	0.0936	-0.5539
C7	-3.3582	-0.5674	0.2911
H8	-3.2923	-0.3903	1.3739
C9	-4.0802	-1.9084	0.0065
H10	-4.3582	-2.4513	0.9171
H11	-4.96	-1.8138	-0.6404
C12	-1.9841	-1.9761	-0.7196
C13	-0.731	-2.5292	-1.2788
C14	-0.5634	-3.7791	-1.8653
H15	-1.4058	-4.4616	-1.9644
C16	0.7159	-4.1213	-2.3047
H17	0.8912	-5.0942	-2.7637
C18	1.7714	-3.2204	-2.1565
H19	2.7793	-3.4584	-2.4923
C20	1.4967	-1.9978	-1.5505
C21	2.4715	-0.9162	-1.2837
C22	4.3152	0.2754	-1.5647
H23	4.3718	0.8407	-2.5034
H24	5.327	0.0597	-1.2062
C25	3.4019	0.9338	-0.5047
H26	3.1313	1.9579	-0.7998
C27	-3.9746	0.6845	-0.3466
H28	-3.2606	1.4916	-0.1214
C29	-4.1006	0.5766	-1.8639
H30	-4.844	-0.179	-2.1592
H31	-3.1417	0.3118	-2.3317
H32	-4.426	1.5361	-2.2888
C33	-5.3035	1.0307	0.3201
H34	-6.0548	0.2441	0.1502
H35	-5.7099	1.9669	-0.0867
H36	-5.1837	1.156	1.406
C37	4.045	0.9763	0.8912
H38	4.3656	-0.0549	1.1227
C39	3.0675	1.4345	1.9662
H40	2.7328	2.4644	1.7781
H41	3.5451	1.4094	2.9552
H42	2.1757	0.8035	1.9966
C43	5.2758	1.884	0.8769
H44	6.0319	1.5687	0.1452

H45	5.7563	1.8917	1.8646
H46	4.9854	2.9187	0.6383
C47	-0.1391	-1.6017	2.5451
C48	1.1405	-2.0104	2.1457
H49	1.9869	-1.3357	2.2758
C50	1.359	-3.2624	1.5769
H51	2.3514	-3.5806	1.2569
C52	0.2736	-4.111	1.4105
F53	0.4619	-5.3049	0.8222
C54	-1.0022	-3.759	1.8277
H55	-1.8268	-4.4594	1.6943
C56	-1.1985	-2.5017	2.3978
H57	-2.2041	-2.2273	2.7144
C58	-0.3376	-0.1802	3.0704
C59	-0.3856	0.7789	1.9375
H60	0.5713	0.0811	3.6368
C61	-1.526	-0.0168	4.0326
C62	-0.451	1.7267	1.1457
Si63	-0.5976	3.2839	0.1212
H64	-1.3739	-0.7437	4.8429
H65	-2.4585	-0.3092	3.5286
C66	-1.6882	1.4016	4.5967
C67	-0.7285	2.7776	-1.6795
C68	0.9389	4.319	0.3992
C69	-2.1195	4.2245	0.6789
C70	-2.7783	2.2194	3.9035
H71	-1.9241	1.3427	5.6702
H72	-0.7281	1.9408	4.534
C73	-2.8707	3.6493	4.4206
H74	-2.5965	2.2268	2.8188
H75	-3.7456	1.7091	4.0443
H76	-3.6683	4.2122	3.9157
H77	-3.0788	3.6704	5.501
H78	-1.9261	4.1905	4.2577
H79	0.8443	5.2724	-0.1426
H80	1.0789	4.5445	1.4664
H81	1.8394	3.8077	0.0324
H82	-0.7969	3.6693	-2.3204
H83	0.1585	2.2031	-1.9872
H84	-1.6169	2.1575	-1.8605
H85	-3.0358	3.6265	0.5761
H86	-2.0274	4.5327	1.7298
H87	-2.2351	5.1318	0.0666

(S) Product-Catalyst Complex

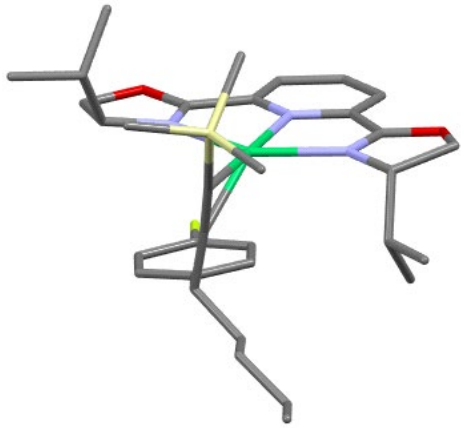

Calculated geometry

Atom	X	Y	Z
Ni1	0	0	0
O2	-2.7444	-2.8414	-1.3494
O3	3.7373	-0.0322	-1.8979
N4	-1.8302	-1.0818	-0.3032
N5	0.4732	-1.3525	-1.4805
N6	2.0134	0.5673	-0.5936
C7	-3.2272	-1.0603	0.1383
H8	-3.2507	-1.1109	1.2353
C9	-3.8021	-2.3589	-0.477
H10	-3.997	-3.137	0.2696
H11	-4.6997	-2.208	-1.0874
C12	-1.7009	-2.0554	-1.1167
C13	-0.4135	-2.2837	-1.8124
C14	-0.1007	-3.3163	-2.6902
H15	-0.8392	-4.0757	-2.9418
C16	1.1918	-3.3425	-3.2191
H17	1.4795	-4.1365	-3.9084
C18	2.1179	-2.3564	-2.871
H19	3.1298	-2.3538	-3.2729
C20	1.7015	-1.369	-1.9823
C21	2.4998	-0.2328	-1.4637
C22	4.1495	1.2367	-1.3208

H23	4.1463	1.9814	-2.1264
H24	5.1676	1.1217	-0.9349
C25	3.0809	1.5171	-0.2417
H26	2.6922	2.5389	-0.3425
C27	-3.9044	0.2499	-0.2934
H28	-3.2903	1.0452	0.1574
C29	-3.8949	0.4508	-1.8068
H30	-4.5023	-0.3083	-2.3227
H31	-2.8751	0.4085	-2.2149
H32	-4.315	1.433	-2.0635
C33	-5.3124	0.348	0.2887
H34	-5.9733	-0.4292	-0.1248
H35	-5.7629	1.3215	0.051
H36	-5.3024	0.2366	1.3825
C37	3.5373	1.3095	1.2126
H38	2.6147	1.3552	1.8128
C39	4.4542	2.4458	1.6603
H40	5.3892	2.4601	1.0796
H41	4.7256	2.3274	2.7184
H42	3.9686	3.4249	1.5428
C43	4.1884	-0.0543	1.4336
H44	3.543	-0.8778	1.098
H45	4.3958	-0.2112	2.5006
H46	5.1479	-0.1371	0.9021
C47	-0.2669	-2.0485	2.3959
C48	0.7369	-2.5499	1.5589
H49	1.668	-1.9985	1.4322
C50	0.5634	-3.7412	0.8603
H51	1.3352	-4.1315	0.196
C52	-0.636	-4.4261	1.0013
F53	-0.8268	-5.5541	0.2965
C54	-1.6406	-3.978	1.8477
H55	-2.5583	-4.5578	1.9504
C56	-1.4438	-2.7859	2.5447
H57	-2.2307	-2.4178	3.2057
C58	-0.1101	-0.6943	3.0728
C59	-0.2868	0.3983	2.0857
C60	1.222	-0.5429	3.8296
C61	-0.4753	1.4505	1.4646
Si62	-0.7711	3.1788	0.8203
C63	-0.7233	3.1196	-1.0518
C64	0.5898	4.2668	1.5102
C65	-2.4449	3.7479	1.4412

H66	0.4534	5.3065	1.1761
H67	0.5743	4.2558	2.61
H68	1.5817	3.9299	1.1792
H69	-0.8726	4.1251	-1.4722
H70	0.2446	2.7366	-1.4072
H71	-1.5152	2.4643	-1.4428
H72	-3.2543	3.1032	1.0704
H73	-2.476	3.7423	2.5406
H74	-2.6437	4.7747	1.0986
H75	-0.9285	-0.5857	3.8016
H76	2.0543	-0.6559	3.1211
C77	1.366	0.7824	4.5683
H78	1.2985	-1.3816	4.5382
C79	2.71	0.9279	5.2762
H80	1.245	1.6135	3.8549
H81	0.5472	0.888	5.2999
C82	2.8748	2.2747	5.9704
H83	2.8287	0.1116	6.0073
H84	3.518	0.7918	4.5388
H85	3.8483	2.3556	6.4738
H86	2.8023	3.1021	5.2481
H87	2.0926	2.4297	6.7287

4.2.3 Transition state structures for radical addition

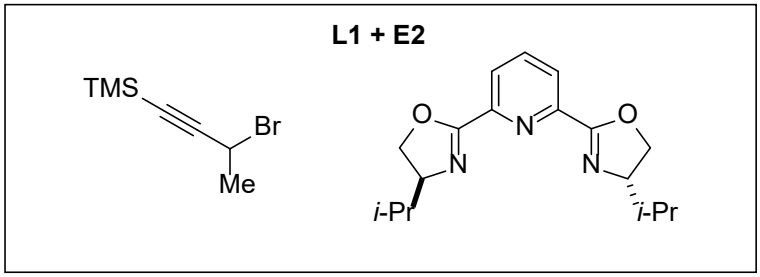

(R)-Transition State

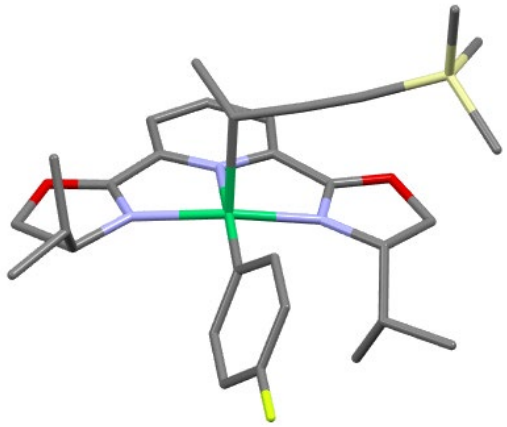

Calculated geometry

Atom	X	Y	Z
Ni1	0	0	0
O2	-3.2327	-0.9615	-2.2176
O3	1.5213	3.7219	-0.0076
N4	-1.3986	-1.0943	-0.943
N5	-1.0189	1.4173	-0.8488
N6	1.3097	1.5007	0.1364
C7	-1.6991	-2.5043	-1.2461
H8	-0.8629	-2.8923	-1.8438
C9	-2.9708	-2.3939	-2.1251
H10	-2.8293	-2.7664	-3.1448
H11	-3.8571	-2.8632	-1.6845
C12	-2.2769	-0.369	-1.5369
C13	-2.1273	1.1052	-1.511
C14	-2.8939	2.0877	-2.1259
H15	-3.8	1.8305	-2.6723
C16	-2.4418	3.4078	-2.0308
H17	-3.0166	4.2074	-2.4981
C18	-1.242	3.7117	-1.3798

H19	-0.8528	4.7279	-1.3408
C20	-0.5438	2.6574	-0.8027
C21	0.8021	2.6336	-0.1854
C22	2.826	3.265	0.4568
H23	3.0693	3.8186	1.3684
H24	3.5531	3.5167	-0.3245
C25	2.6556	1.7409	0.67
H26	2.6322	1.4994	1.742
C27	-1.8184	-3.3833	0.0056
H28	-0.88	-3.2236	0.5579
C29	-2.9792	-2.9938	0.9156
H30	-2.9317	-3.5653	1.8523
H31	-3.9544	-3.2082	0.454
H32	-2.9546	-1.9285	1.1757
C33	-1.8871	-4.8544	-0.4023
H34	-1.0129	-5.1448	-1.0024
H35	-2.7908	-5.0644	-0.9953
H36	-1.9188	-5.5004	0.4853
C37	3.7296	0.8671	0.0051
H38	3.491	-0.1662	0.2925
C39	5.1048	1.2068	0.5788
H40	5.4205	2.2257	0.3068
H41	5.8641	0.5152	0.1894
H42	5.11	1.1315	1.6758
C43	3.7002	0.9481	-1.5184
H44	2.7222	0.6432	-1.9169
H45	4.4594	0.2801	-1.9477
H46	3.9154	1.9642	-1.883
C47	1.1497	-1.3755	0.5963
C48	1.6474	-1.5577	1.8914
H49	1.2887	-0.9389	2.7155
C50	2.6318	-2.511	2.1662
H51	3.0256	-2.6552	3.1733
C52	3.1226	-3.2848	1.1237
F53	4.076	-4.2014	1.3796
C54	2.6566	-3.1408	-0.1757
H55	3.0669	-3.7669	-0.9693
C56	1.6689	-2.1854	-0.4252
H57	1.317	-2.0691	-1.4537
C58	-1.1412	0.248	1.9958
C59	-0.272	1.0814	2.7303
C60	-2.5303	0.7775	1.7373
H61	-1.064	-0.8204	2.2147

C62	0.4424	1.8497	3.3708
Si63	1.4129	3.0255	4.4311
C64	1.134	4.7521	3.7514
C65	0.7641	2.8833	6.184
C66	3.2292	2.5524	4.3817
H67	1.7502	5.4865	4.2915
H68	1.3869	4.8101	2.6832
H69	0.0791	5.0432	3.8636
H70	-0.31	3.115	6.2269
H71	0.9131	1.8665	6.5759
H72	1.2941	3.586	6.8449
H73	3.6878	2.732	3.3994
H74	3.7845	3.149	5.1212
H75	3.3636	1.49	4.6329
H76	-3.1231	0.7243	2.6651
H77	-2.5154	1.828	1.4194
H78	-3.0683	0.188	0.9858

(S)-Transition State

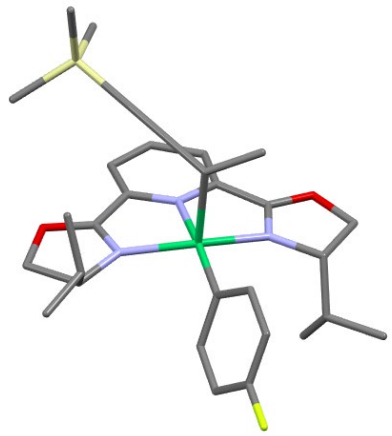

Calculated geometry

Atom	X	Y	Z
Ni1	0	0	0
O2	-3.3292	-0.7882	-2.1338
O3	1.5719	3.6995	0.1488
N4	-1.4408	-1.0148	-0.9579
N5	-1.0289	1.4824	-0.7236
N6	1.3087	1.4819	0.246
C7	-1.7923	-2.4039	-1.2971

H8	-0.9889	-2.799	-1.9338
C9	-3.0894	-2.2267	-2.1262
H10	-2.9875	-2.5456	-3.1686
H11	-3.9689	-2.7045	-1.6816
C12	-2.3339	-0.2457	-1.4671
C13	-2.1565	1.221	-1.3743
C14	-2.909	2.2425	-1.9409
H15	-3.8269	2.025	-2.4849
C16	-2.4305	3.5487	-1.799
H17	-2.9961	4.3777	-2.2245
C18	-1.2169	3.8023	-1.1526
H19	-0.808	4.8084	-1.0752
C20	-0.5304	2.7101	-0.6353
C21	0.8236	2.6361	-0.0408
C22	2.8163	3.2155	0.7375
H23	2.8705	3.612	1.7572
H24	3.6411	3.6209	0.1419
C25	2.6981	1.6717	0.6874
H26	2.8111	1.2449	1.6929
C27	-1.9004	-3.3123	-0.0654
H28	-0.9547	-3.167	0.4789
C29	-3.0515	-2.9371	0.864
H30	-2.9684	-3.4904	1.8094
H31	-4.0285	-3.192	0.4267
H32	-3.0565	-1.8657	1.1003
C33	-1.9793	-4.7737	-0.5044
H34	-1.1089	-5.0579	-1.1131
H35	-2.8863	-4.963	-1.0996
H36	-2.0147	-5.4386	0.3691
C37	3.6887	0.9604	-0.2496
H38	3.4379	-0.108	-0.1821
C39	5.1191	1.139	0.256
H40	5.4426	2.1898	0.2043
H41	5.8167	0.5525	-0.357
H42	5.2203	0.8031	1.298
C43	3.5343	1.3923	-1.7057
H44	2.5188	1.1994	-2.0803
H45	4.2343	0.8353	-2.3431
H46	3.752	2.4629	-1.8418
C47	1.1673	-1.4337	0.3854
C48	1.7375	-1.7954	1.6099
H49	1.4279	-1.3082	2.5356
C50	2.7247	-2.7817	1.6924

H51	3.1732	-3.0655	2.6454
C52	3.1423	-3.4087	0.5271
F53	4.0962	-4.3566	0.598
C54	2.6009	-3.087	-0.7099
H55	2.953	-3.6022	-1.6046
C56	1.6142	-2.1007	-0.7665
H57	1.2016	-1.8441	-1.746
C58	-0.9637	0.0878	2.0777
C59	-2.2926	0.4773	1.8036
H60	-0.8387	-0.9847	2.2508
C61	-0.13	1.0078	2.9338
C62	-3.446	0.8207	1.5542
Si63	-5.2437	1.211	1.3017
H64	-0.462	0.9472	3.9834
H65	-0.2301	2.0544	2.6185
H66	0.9316	0.7367	2.9114
C67	-5.9034	0.0848	-0.0453
C68	-6.1244	0.8759	2.9232
C69	-5.4124	3.0165	0.8226
H70	-6.9772	0.2708	-0.1992
H71	-5.3864	0.2428	-1.0014
H72	-5.7774	-0.9711	0.2368
H73	-6.0007	-0.1745	3.2248
H74	-5.7281	1.5133	3.727
H75	-7.2014	1.0796	2.823
H76	-4.9104	3.2314	-0.1308
H77	-6.4753	3.2801	0.7135
H78	-4.9772	3.6688	1.5938

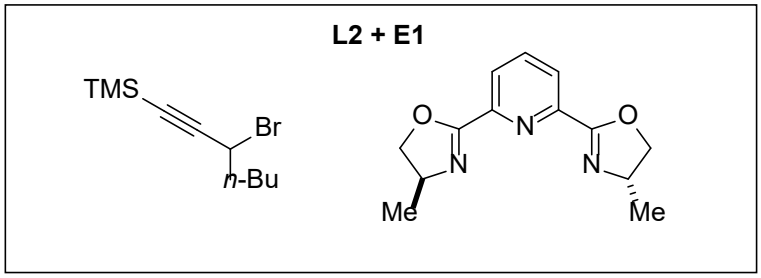

(R)-Transition State

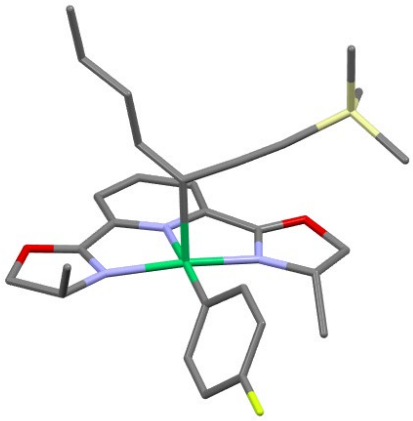

Calculated geometry

Atom	X	Y	Z
Ni1	0	0	0
O2	-3.0962	1.9448	-1.6915
O3	3.5501	-0.3983	-1.8485
N4	-1.8727	0.6117	-0.3741
N5	0.2759	0.9133	-1.6902
N6	1.7933	-0.7264	-0.5024
C7	-3.1849	0.6393	0.2972
H8	-3.5619	-0.3893	0.3625
C9	-4.0435	1.4685	-0.6898
H10	-4.8023	0.8759	-1.213
H11	-4.5091	2.347	-0.2296
C12	-1.9489	1.3679	-1.4102
C13	-0.7399	1.5675	-2.2412
C14	-0.5824	2.2591	-3.4364
H15	-1.4159	2.7948	-3.8877
C16	0.6805	2.2238	-4.0361
H17	0.8449	2.7562	-4.973

C18	1.7262	1.4886	-3.4685
H19	2.7027	1.4196	-3.9451
C20	1.4657	0.8259	-2.275
C21	2.3082	-0.1199	-1.5089
C22	3.9654	-1.4861	-0.9715
H23	4.9323	-1.2165	-0.5363
H24	4.079	-2.3822	-1.595
C25	2.8181	-1.6213	0.0571
H26	3.1144	-1.2102	1.0331
C27	-3.0825	1.2323	1.6934
H28	-2.4046	0.6308	2.3115
C29	2.3224	-3.0473	0.2271
H30	1.5073	-3.0914	0.9586
C31	-0.2906	-1.0791	1.5249
C32	0.4913	-1.068	2.6871
H33	1.2789	-0.3225	2.8158
C34	0.3091	-2.0135	3.6991
H35	0.9177	-2.0107	4.6045
C36	-0.6684	-2.9858	3.5355
F37	-0.8462	-3.9064	4.5028
C38	-1.4673	-3.0356	2.4022
H39	-2.2242	-3.8157	2.3095
C40	-1.2706	-2.0756	1.4061
H41	-1.897	-2.1276	0.512
C42	0.5735	1.9096	1.2292
C43	1.9628	1.7337	1.3665
H44	-0.0333	1.5864	2.0786
C45	0.1032	3.1544	0.5156
C46	3.1857	1.6328	1.4543
Si47	5.034	1.6457	1.6382
H48	-0.9474	3.0462	0.2156
H49	0.6917	3.3106	-0.4009
C50	0.2098	4.4035	1.3981
C51	5.4752	3.0602	2.7868
C52	-0.2994	5.658	0.6939
H53	-0.3634	4.2403	2.3255
H54	0.2768	5.8078	-0.234
H55	-1.3428	5.4935	0.3772
H56	6.5665	3.1223	2.9154
H57	5.0208	2.9171	3.778
H58	5.1221	4.0196	2.3814
C59	5.7721	1.9185	-0.0649
C60	5.5883	0.0139	2.3802

H61	5.3938	-0.8392	1.7155
H62	5.0751	-0.1735	3.3348
H63	6.6708	0.0441	2.5764
H64	5.4891	2.9093	-0.4499
H65	5.4214	1.1655	-0.7845
H66	6.8706	1.8705	-0.0219
C67	-0.2156	6.9079	1.5619
H68	1.2586	4.5453	1.7045
H69	-0.5859	7.7951	1.0295
H70	-0.8133	6.7943	2.4786
H71	0.8218	7.1097	1.8676
H72	-2.7065	2.2638	1.6547
H73	-4.0723	1.2406	2.1687
H74	3.1429	-3.6845	0.5839
H75	1.9634	-3.4466	-0.7319

(S)-Transition State

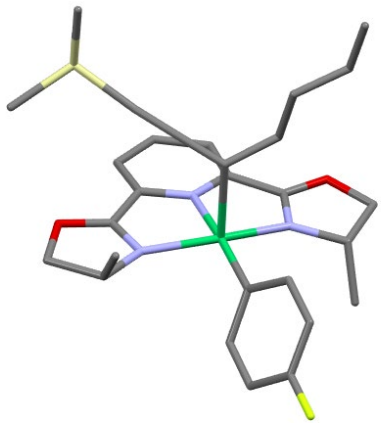

Calculated geometry

Atom	X	Y	Z
Ni1	0	0	0
O2	-3.0962	1.9448	-1.6915
O3	3.5501	-0.3983	-1.8485
N4	-1.8727	0.6117	-0.3741
N5	0.2759	0.9133	-1.6902
N6	1.7933	-0.7264	-0.5024
C7	-3.1849	0.6393	0.2972
H8	-3.5619	-0.3893	0.3625
C9	-4.0435	1.4685	-0.6898
H10	-4.8023	0.8759	-1.213

H11	-4.5091	2.347	-0.2296
C12	-1.9489	1.3679	-1.4102
C13	-0.7399	1.5675	-2.2412
C14	-0.5824	2.2591	-3.4364
H15	-1.4159	2.7948	-3.8877
C16	0.6805	2.2238	-4.0361
H17	0.8449	2.7562	-4.973
C18	1.7262	1.4886	-3.4685
H19	2.7027	1.4196	-3.9451
C20	1.4657	0.8259	-2.275
C21	2.3082	-0.1199	-1.5089
C22	3.9654	-1.4861	-0.9715
H23	4.9323	-1.2165	-0.5363
H24	4.079	-2.3822	-1.595
C25	2.8181	-1.6213	0.0571
H26	3.1144	-1.2102	1.0331
C27	-3.0825	1.2323	1.6934
H28	-2.4046	0.6308	2.3115
C29	2.3224	-3.0473	0.2271
H30	1.5073	-3.0914	0.9586
C31	-0.2906	-1.0791	1.5249
C32	0.4913	-1.068	2.6871
H33	1.2789	-0.3225	2.8158
C34	0.3091	-2.0135	3.6991
H35	0.9177	-2.0107	4.6045
C36	-0.6684	-2.9858	3.5355
F37	-0.8462	-3.9064	4.5028
C38	-1.4673	-3.0356	2.4022
H39	-2.2242	-3.8157	2.3095
C40	-1.2706	-2.0756	1.4061
H41	-1.897	-2.1276	0.512
C42	0.5735	1.9096	1.2292
C43	1.9628	1.7337	1.3665
H44	-0.0333	1.5864	2.0786
C45	0.1032	3.1544	0.5156
C46	3.1857	1.6328	1.4543
Si47	5.034	1.6457	1.6382
H48	-0.9474	3.0462	0.2156
H49	0.6917	3.3106	-0.4009
C50	0.2098	4.4035	1.3981
C51	5.4752	3.0602	2.7868
C52	-0.2994	5.658	0.6939
H53	-0.3634	4.2403	2.3255

H54	0.2768	5.8078	-0.234
H55	-1.3428	5.4935	0.3772
H56	6.5665	3.1223	2.9154
H57	5.0208	2.9171	3.778
H58	5.1221	4.0196	2.3814
C59	5.7721	1.9185	-0.0649
C60	5.5883	0.0139	2.3802
H61	5.3938	-0.8392	1.7155
H62	5.0751	-0.1735	3.3348
H63	6.6708	0.0441	2.5764
H64	5.4891	2.9093	-0.4499
H65	5.4214	1.1655	-0.7845
H66	6.8706	1.8705	-0.0219
C67	-0.2156	6.9079	1.5619
H68	1.2586	4.5453	1.7045
H69	-0.5859	7.7951	1.0295
H70	-0.8133	6.7943	2.4786
H71	0.8218	7.1097	1.8676
H72	-2.7065	2.2638	1.6547
H73	-4.0723	1.2406	2.1687
H74	3.1429	-3.6845	0.5839
H75	1.9634	-3.4466	-0.7319

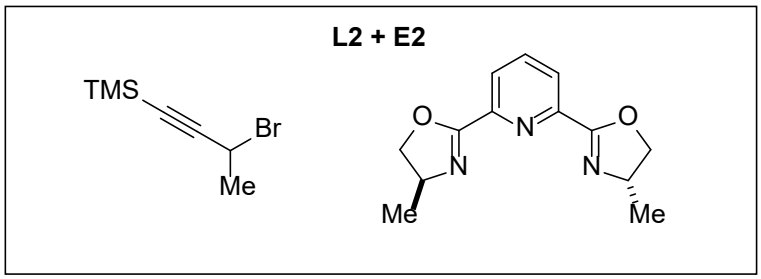

(R)-Transition State

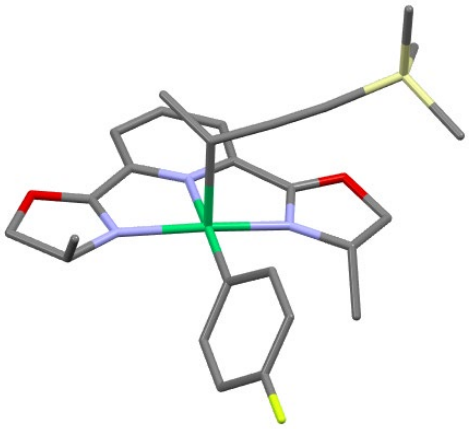

Calculated geometry

Atom	X	Y	Z
Ni1	0	0	0
O2	-3.7876	0.9755	-0.9899
O3	3.059	0.437	-2.5762
N4	-2.0089	0.0882	0.0398
N5	-0.3348	0.8718	-1.7029
N6	1.7717	-0.2728	-0.8895
C7	-3.1215	-0.2328	0.9523
H8	-3.1969	-1.3258	1.0256
C9	-4.347	0.3442	0.1997
H10	-5.056	-0.4203	-0.1358
H11	-4.8763	1.1187	0.7667
C12	-2.4935	0.7454	-0.9517
C13	-1.5792	1.2113	-2.0191
C14	-1.8642	1.8526	-3.2186
H15	-2.885	2.1295	-3.4772
C16	-0.7922	2.11	-4.079

H17	-0.9741	2.6138	-5.0283
C18	0.5047	1.6997	-3.7542
H19	1.3418	1.856	-4.4329
C20	0.6849	1.0588	-2.5342
C21	1.8867	0.3985	-1.9767
C22	3.9229	-0.4565	-1.8144
H23	4.8495	0.0813	-1.5923
H24	4.1435	-1.3206	-2.4541
C25	3.0909	-0.8388	-0.5676
H26	3.4604	-0.3177	0.3276
C27	-2.9041	0.3531	2.3375
H28	-1.9855	-0.0506	2.7806
C29	3.041	-2.3349	-0.3086
H30	2.4312	-2.5566	0.5749
C31	0.3429	-1.0466	1.536
C32	1.3266	-0.7788	2.4963
H33	1.8948	0.1531	2.4599
C34	1.6276	-1.6937	3.508
H35	2.3942	-1.4906	4.2571
C36	0.9337	-2.8956	3.5488
F37	1.221	-3.7857	4.5183
C38	-0.0479	-3.2047	2.6181
H39	-0.57	-4.1605	2.6815
C40	-0.336	-2.2711	1.619
H41	-1.1037	-2.5263	0.8841
C42	0.2764	2.0332	1.1008
C43	1.6571	2.2374	0.9053
H44	-0.004	1.5974	2.0624
C45	-0.6594	3.0773	0.5466
C46	2.8493	2.4655	0.7089
Si47	4.6243	2.9673	0.487
H48	-1.7069	2.7572	0.5854
H49	-0.4043	3.3546	-0.4846
C50	4.9026	4.5222	1.4969
H51	5.9413	4.8687	1.3849
H52	4.7171	4.3354	2.5646
H53	4.2338	5.3306	1.1673
C54	4.8977	3.3077	-1.3377
C55	5.731	1.5888	1.1164
H56	5.632	0.6633	0.5324
H57	5.4974	1.3554	2.1656
H58	6.7838	1.9053	1.0653
H59	4.2934	4.1695	-1.6577

H60	4.6137	2.4493	-1.962
H61	5.9551	3.5423	-1.532
H62	-2.8255	1.4476	2.2911
H63	-3.7488	0.0924	2.989
H64	4.0567	-2.7142	-0.1322
H65	2.6184	-2.8618	-1.1755
H66	-0.585	3.9935	1.1549
C67	-0.0739	6.5365	1.7605
H68	1.4003	4.1739	1.9031
H69	-0.4442	7.4237	1.2281
H70	-0.6716	6.4229	2.6772
H71	0.9635	6.7383	2.0662
H72	-2.5648	1.8924	1.8533
H73	-3.9306	0.8692	2.3673
H74	3.2846	-4.0559	0.7825
H75	2.1051	-3.818	-0.5333

(S)-Transition State

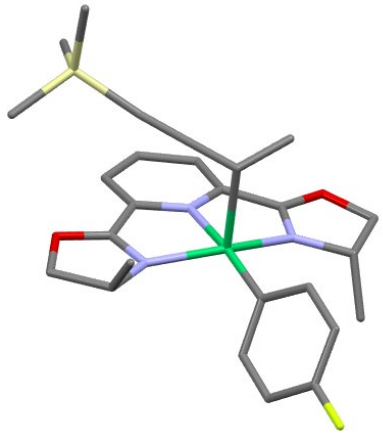

Calculated geometry

Atom	X	Y	Z
Ni1	0	0	0
O2	-3.4191	-1.1161	-1.8018
O3	1.3615	3.7802	-0.1309
N4	-1.4021	-1.1586	-0.8341
N5	-1.1154	1.3647	-0.8168
N6	1.2235	1.5626	0.1219

C7	-1.8088	-2.5751	-0.8304
H8	-1.0617	-3.1518	-1.3907
C9	-3.1509	-2.535	-1.6015
H10	-3.1018	-3.0017	-2.5915
H11	-3.99	-2.9524	-1.0339
C12	-2.3632	-0.4778	-1.346
C13	-2.2356	0.9935	-1.4248
C14	-3.0416	1.9231	-2.0715
H15	-3.9519	1.6128	-2.5819
C16	-2.6263	3.2574	-2.0539
H17	-3.2347	4.0167	-2.5452
C18	-1.4218	3.6263	-1.4454
H19	-1.0642	4.6546	-1.4591
C20	-0.6782	2.6194	-0.8426
C21	0.6773	2.665	-0.2494
C22	2.629	3.4115	0.4916
H23	2.661	3.8918	1.4758
H24	3.4345	3.802	-0.1403
C25	2.5972	1.8645	0.558
H26	2.7214	1.5175	1.5923
C27	-1.918	-3.1195	0.5848
H28	-0.9449	-3.0622	1.0885
C29	3.6205	1.1832	-0.338
H30	3.5092	0.093	-0.2879
C31	1.2337	-1.3328	0.5221
C32	1.8842	-1.4407	1.7567
H33	1.6175	-0.7822	2.5856
C34	2.8959	-2.3803	1.9715
H35	3.4043	-2.467	2.9327
C36	3.2598	-3.2193	0.9275
F37	4.2343	-4.1276	1.1255
C38	2.6452	-3.1481	-0.3147
H39	2.9592	-3.823	-1.1121
C40	1.6338	-2.2032	-0.5038
H41	1.1601	-2.1485	-1.4873
C42	-1.0218	0.1496	2.0719
C43	-2.3955	0.249	1.7676
H44	-0.6968	-0.8493	2.3711
C45	-0.3711	1.3082	2.7829
C46	-3.5904	0.3532	1.498
Si47	-5.434	0.4927	1.3126
H48	-0.635	2.269	2.3212
H49	0.7209	1.2141	2.7984

C50	-6.0591	-0.9788	0.3343
H51	-7.1575	-0.952	0.2725
H52	-5.7679	-1.9246	0.815
H53	-5.6555	-0.9706	-0.6873
C54	-5.8286	2.0996	0.429
C55	-6.1602	0.4984	3.0421
H56	-7.2568	0.58	2.9964
H57	-5.7769	1.347	3.6272
H58	-5.9075	-0.4291	3.5763
H59	-6.918	2.2523	0.3945
H60	-5.4569	2.0928	-0.6047
H61	-5.38	2.9574	0.9511
H62	-2.6525	-2.5446	1.1641
H63	-2.2333	-4.171	0.5562
H64	4.6359	1.4459	-0.0127
H65	3.4937	1.5053	-1.3813
H66	-0.7121	1.3446	3.8309
C67	-1.2946	5.964	1.9904
H68	0.1796	3.6014	2.133
H69	-1.6649	6.8512	1.458
H70	-1.8923	5.8504	2.9071
H71	-0.2572	6.1658	2.2961
H72	-3.7855	1.3199	2.0832
H73	-5.1513	0.2967	2.5972
H74	2.0639	-4.6284	1.0124
H75	0.8844	-4.3905	-0.3034

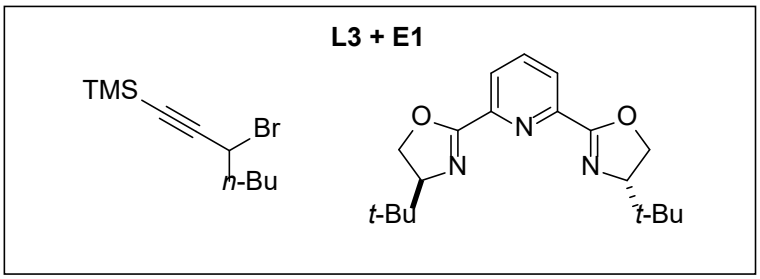

(R)-Transition State

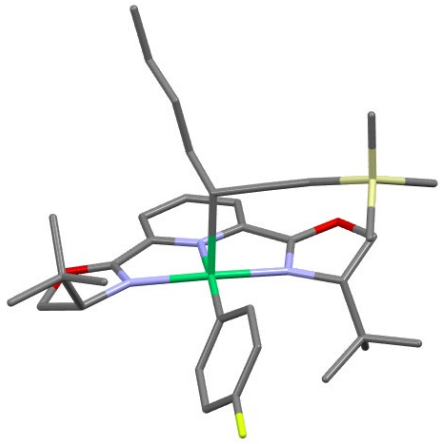

Calculated geometry

Atom	X	Y	Z
Ni1	0	0	0
O2	-4.054	0.2985	-0.3209
O3	2.3544	0.9657	-3.126
N4	-2.0084	-0.0176	0.5447
N5	-0.8181	0.7342	-1.6236
N6	1.5785	-0.0857	-1.3068
C7	-2.9283	-0.4707	1.6194
H8	-2.6556	-1.4965	1.8963
C9	-4.2954	-0.4568	0.8965
H10	-4.632	-1.457	0.5977
H11	-5.0949	0.0483	1.4441
C12	-2.7466	0.394	-0.4238
C13	-2.1342	0.8937	-1.6728
C14	-2.7595	1.4136	-2.7997
H15	-3.8411	1.5339	-2.8315
C16	-1.947	1.7647	-3.8816
H17	-2.3979	2.1831	-4.7814

C18	-0.5653	1.5619	-3.8301
H19	0.0821	1.8019	-4.672
C20	-0.0423	1.0193	-2.6624
C21	1.3453	0.6168	-2.3569
C22	3.5437	0.5887	-2.372
H23	3.9299	1.5051	-1.9138
H24	4.276	0.1866	-3.0766
C25	3.0164	-0.4181	-1.3313
H26	3.4392	-0.2159	-0.3393
C27	-2.8838	0.3928	2.9063
C28	-1.5301	0.2284	3.601
C29	3.2855	-1.9025	-1.6932
C30	2.5722	-2.8259	-0.7031
C31	0.7024	-1.0234	1.4296
C32	1.8138	-0.7559	2.2334
H33	2.3509	0.1863	2.1357
C34	2.2774	-1.6818	3.1721
H35	3.1448	-1.4742	3.8004
C36	1.6172	-2.8958	3.2955
F37	2.0607	-3.7966	4.1944
C38	0.5111	-3.207	2.5166
H39	0.0186	-4.1727	2.6387
C40	0.0625	-2.261	1.593
H41	-0.8045	-2.5196	0.979
C42	0.5696	2.1288	0.855
C43	1.9735	2.1996	0.8104
H44	0.172	1.8345	1.8291
C45	-0.2463	3.15	0.1036
C46	3.2032	2.248	0.8258
Si47	5.0157	2.2415	1.2498
H48	-1.2856	2.805	0.0183
H49	0.141	3.2765	-0.9186
C50	-0.2562	4.5105	0.8112
C51	5.419	3.9034	2.0157
C52	-1.135	5.5325	0.0961
H53	-0.613	4.3751	1.8455
H54	-0.7795	5.6503	-0.9408
H55	-2.1598	5.1327	0.0201
H56	6.4755	3.9346	2.3225
H57	4.7975	4.0877	2.904
H58	5.2466	4.7198	1.2992
C59	6.0691	1.9502	-0.2742
C60	5.2617	0.8428	2.4756

H61	4.9968	-0.1252	2.0249
H62	4.6374	0.9856	3.3699
H63	6.3137	0.7937	2.7949
H64	5.8705	2.6919	-1.0613
H65	5.9154	0.9438	-0.6894
H66	7.1303	2.033	0.0064
C67	-1.1613	6.8887	0.7911
H68	0.7757	4.8889	0.8878
H69	-1.8027	7.604	0.2577
H70	-1.5429	6.7991	1.8192
H71	-0.1524	7.3234	0.8506
C72	-3.131	1.8688	2.5803
C73	-3.9674	-0.1254	3.8644
C74	4.7982	-2.1351	-1.5848
C75	2.8001	-2.225	-3.1119
H76	-1.5089	0.8252	4.5233
H77	-1.3455	-0.8221	3.8659
H78	-0.702	0.5507	2.9639
H79	2.8449	-3.8703	-0.9102
H80	2.8478	-2.5967	0.335
H81	1.4824	-2.7371	-0.7863
H82	-3.1611	2.459	3.5065
H83	-2.3303	2.2794	1.951
H84	-4.0883	2.0233	2.0611
H85	-3.8789	0.3884	4.8314
H86	-4.9859	0.053	3.4944
H87	-3.8509	-1.2041	4.0458
H88	5.035	-3.1836	-1.813
H89	5.3699	-1.5089	-2.2842
H90	5.1546	-1.9212	-0.5664
H91	2.9876	-3.2845	-3.3355
H92	1.7178	-2.0563	-3.2138
H93	3.3173	-1.6329	-3.8796

(S)-Transition State

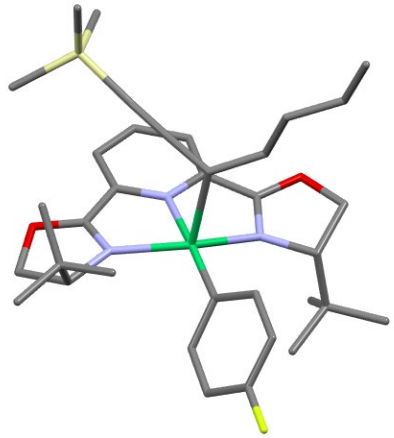

Calculated geometry

Atom	X	Y	Z
Ni1	0	0	0
O2	-3.2466	-1.2963	-2.0756
O3	1.0066	3.8889	0.0175
N4	-1.4434	-1.2851	-0.7428
N5	-1.1944	1.282	-0.8541
N6	1.1839	1.6577	-0.03
C7	-1.7402	-2.7267	-0.9409
H8	-0.8253	-3.2194	-1.2915
C9	-2.7897	-2.677	-2.0731
H10	-2.3595	-2.876	-3.0625
H11	-3.6612	-3.3174	-1.918
C12	-2.3445	-0.6307	-1.3844
C13	-2.3043	0.8468	-1.4337
C14	-3.1912	1.7275	-2.0418
H15	-4.09	1.3626	-2.5362
C16	-2.8796	3.0891	-1.9959
H17	-3.556	3.8122	-2.4517
C18	-1.6984	3.5325	-1.3944
H19	-1.4255	4.5864	-1.374
C20	-0.8626	2.5675	-0.8458
C21	0.4891	2.7133	-0.2662
C22	2.2432	3.5966	0.7347
H23	2.0463	3.7674	1.8004
H24	3.0061	4.2961	0.384
C25	2.5194	2.1167	0.4036
H26	2.8173	1.5601	1.3014
C27	-2.2217	-3.4737	0.3291

C28	-1.1521	-3.4111	1.4212
C29	3.6031	1.9005	-0.6863
C30	3.6903	0.4155	-1.0457
C31	1.2727	-1.2498	0.6323
C32	1.9261	-1.247	1.8684
H33	1.6604	-0.5215	2.6397
C34	2.94	-2.1631	2.165
H35	3.4492	-2.1638	3.1298
C36	3.3032	-3.0904	1.1993
F37	4.2809	-3.976	1.4739
C38	2.6857	-3.1298	-0.0436
H39	3.0007	-3.8708	-0.7796
C40	1.6738	-2.207	-0.3112
H41	1.2028	-2.2378	-1.2971
C42	-0.9482	0.4425	2.1357
C43	-2.3096	0.6345	1.8476
H44	-0.6734	-0.5579	2.4756
C45	-0.1802	1.5857	2.7485
C46	-3.4946	0.8444	1.5916
Si47	-5.3185	1.1232	1.3609
H48	-0.4547	2.5316	2.2574
H49	0.8965	1.4383	2.5915
C50	-0.4331	1.7161	4.2548
C51	-5.9792	-0.1114	0.1127
C52	0.3779	2.8463	4.8822
H53	-0.1825	0.7618	4.7465
H54	1.4486	2.6717	4.6839
H55	0.128	3.7928	4.3749
H56	-7.0246	0.1335	-0.1293
H57	-5.9569	-1.1299	0.5249
H58	-5.4038	-0.1136	-0.8231
C59	-5.5772	2.8846	0.7723
C60	-6.1343	0.8577	3.0279
H61	-7.2234	0.9944	2.9461
H62	-5.7539	1.5715	3.7729
H63	-5.9434	-0.1605	3.3974
H64	-6.6539	3.1032	0.7059
H65	-5.1368	3.0499	-0.2204
H66	-5.1259	3.6027	1.4725
C67	0.1476	2.9875	6.3823
H68	-1.5081	1.8815	4.4313
H69	0.7445	3.8062	6.8077
H70	-0.9101	3.1944	6.6031

H71	0.4207	2.0635	6.9136
C72	-3.5286	-2.877	0.8584
C73	-2.4314	-4.9461	-0.0534
C74	4.9496	2.3473	-0.1023
C75	3.2851	2.7047	-1.9529
H76	-1.4804	-3.9926	2.2939
H77	-0.196	-3.8227	1.0717
H78	-0.9701	-2.3822	1.7464
H79	4.5218	0.2522	-1.7456
H80	3.8622	-0.2056	-0.156
H81	2.7689	0.0642	-1.5259
H82	-3.8426	-3.4129	1.7651
H83	-3.4071	-1.8184	1.1226
H84	-4.3487	-2.9612	0.1316
H85	-2.7323	-5.5204	0.8336
H86	-3.2169	-5.0782	-0.8104
H87	-1.5028	-5.3887	-0.4429
H88	5.7489	2.1841	-0.8384
H89	4.9597	3.4141	0.1619
H90	5.1976	1.7694	0.8
H91	4.0593	2.5212	-2.7106
H92	2.322	2.403	-2.3904
H93	3.2592	3.788	-1.7697

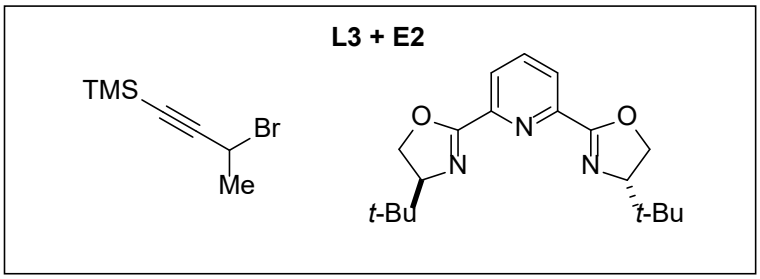

(R)-Transition State

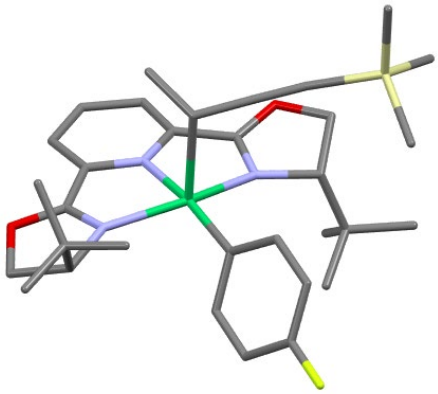

Calculated geometry

Atom	X	Y	Z
Ni1	0	0	0
O2	-4.0598	0.177	-0.3747
O3	2.3544	0.8449	-3.1648
N4	-2.0172	-0.0458	0.526
N5	-0.8212	0.6413	-1.6628
N6	1.5874	-0.1324	-1.301
C7	-2.9368	-0.4849	1.6063
H8	-2.6384	-1.4916	1.924
C9	-4.295	-0.5374	0.8685
H10	-4.5998	-1.5575	0.6049
H11	-5.1149	-0.0349	1.3876
C12	-2.7543	0.3059	-0.4663
C13	-2.1406	0.7638	-1.7309
C14	-2.7691	1.202	-2.8906
H15	-3.8532	1.2912	-2.937
C16	-1.9571	1.5092	-3.9858
H17	-2.4106	1.8629	-4.9117
C18	-0.5717	1.341	-3.9142

H19	0.0763	1.5431	-4.7655
C20	-0.0451	0.8803	-2.7134
C21	1.3478	0.5172	-2.383
C22	3.5462	0.5221	-2.3898
H23	3.9157	1.4647	-1.9723
H24	4.2884	0.1003	-3.0721
C25	3.0302	-0.4444	-1.3064
H26	3.4463	-0.1917	-0.3232
C27	-2.9305	0.4258	2.8603
C28	-1.577	0.3315	3.5685
C29	3.3225	-1.9397	-1.5995
C30	2.623	-2.8256	-0.5663
C31	0.7024	-0.9589	1.4739
C32	1.7947	-0.6536	2.2896
H33	2.3183	0.2942	2.1775
C34	2.2567	-1.5498	3.2577
H35	3.11	-1.3135	3.895
C36	1.6145	-2.7714	3.3987
F37	2.0577	-3.6442	4.3248
C38	0.5268	-3.1189	2.6095
H39	0.0479	-4.0895	2.746
C40	0.0793	-2.2025	1.6562
H41	-0.772	-2.4907	1.0334
C42	0.5312	2.1548	0.7522
C43	1.9392	2.2213	0.7345
H44	0.1128	1.92	1.7334
C45	-0.2498	3.1446	-0.0724
C46	3.1674	2.2753	0.7689
Si47	4.9784	2.2908	1.199
H48	-1.3188	2.9018	-0.0976
H49	0.1265	3.2184	-1.1011
C50	5.3715	3.9747	1.9208
H51	6.4271	4.0194	2.2287
H52	4.7472	4.1801	2.8024
H53	5.1968	4.7706	1.1821
C54	6.0367	1.9657	-0.3149
C55	5.232	0.9264	2.4612
H56	4.9702	-0.0542	2.0367
H57	4.6093	1.09	3.353
H58	6.2849	0.8904	2.7791
H59	5.8358	2.6856	-1.1216
H60	5.8899	0.948	-0.704
H61	7.0968	2.0618	-0.0343

C62	-3.2212	1.8798	2.4773
C63	-4.0047	-0.0913	3.8293
C64	4.8384	-2.1443	-1.4812
C65	2.8424	-2.3359	-3.0012
H66	-1.5837	0.9577	4.4713
H67	-1.357	-0.7027	3.868
H68	-0.7565	0.6633	2.9261
H69	2.9147	-3.8741	-0.7203
H70	2.8912	-2.54	0.4597
H71	1.5322	-2.7605	-0.6561
H72	-3.2734	2.504	3.3799
H73	-2.4299	2.2891	1.8349
H74	-4.1806	1.985	1.9495
H75	-3.9441	0.4634	4.7756
H76	-5.0251	0.0361	3.4434
H77	-3.8527	-1.1573	4.0548
H78	5.0902	-3.1993	-1.6573
H79	5.4011	-1.5456	-2.2114
H80	5.192	-1.875	-0.475
H81	3.0493	-3.4008	-3.1762
H82	1.7571	-2.1921	-3.1095
H83	3.3482	-1.77	-3.7958
H84	-0.1584	4.1467	0.3781

(S)-Transition State

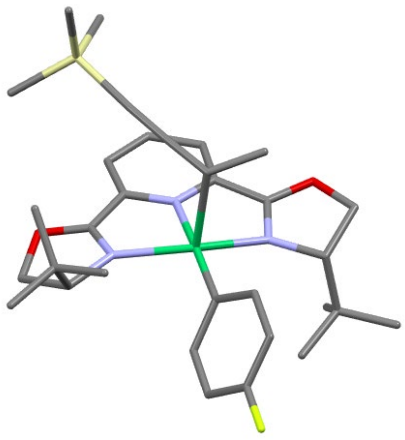

Calculated geometry

Atom	X	Y	Z
Ni1	0	0	0

O2	-3.2407	-1.3341	-2.0717
O3	1.0346	3.8847	-0.1146
N4	-1.445	-1.3017	-0.729
N5	-1.1866	1.2645	-0.895
N6	1.1942	1.652	-0.0798
C7	-1.7454	-2.746	-0.9007
H8	-0.8301	-3.2481	-1.2364
C9	-2.7878	-2.7157	-2.0399
H10	-2.3521	-2.9349	-3.0226
H11	-3.6619	-3.3511	-1.8779
C12	-2.3401	-0.6576	-1.3885
C13	-2.2939	0.8183	-1.4716
C14	-3.171	1.6852	-2.1127
H15	-4.0673	1.3101	-2.6041
C16	-2.8525	3.0458	-2.1054
H17	-3.5212	3.7586	-2.5881
C18	-1.6721	3.5001	-1.5106
H19	-1.3915	4.5521	-1.5225
C20	-0.8463	2.5474	-0.9261
C21	0.5065	2.7034	-0.3519
C22	2.274	3.6094	0.6047
H23	2.0864	3.8218	1.6643
H24	3.0396	4.2894	0.2229
C25	2.5363	2.1159	0.327
H26	2.8366	1.5897	1.2421
C27	-2.2351	-3.4671	0.3809
C28	-1.1764	-3.3709	1.4812
C29	3.6099	1.8533	-0.7635
C30	3.6845	0.3565	-1.073
C31	1.2711	-1.2338	0.665
C32	1.9401	-1.1857	1.8916
H33	1.6814	-0.4344	2.64
C34	2.9627	-2.0861	2.2058
H35	3.4851	-2.0509	3.1628
C36	3.3184	-3.0438	1.2672
F37	4.3051	-3.9138	1.5584
C38	2.6846	-3.1288	0.0349
H39	2.994	-3.8927	-0.6798
C40	1.6645	-2.2206	-0.2508
H41	1.1825	-2.2862	-1.2295
C42	-0.937	0.4972	2.1127
C43	-2.3018	0.6569	1.8082
H44	-0.6514	-0.4865	2.4892

C45	-0.2057	1.6761	2.6983
C46	-3.4876	0.8437	1.5412
Si47	-5.3096	1.1249	1.2963
H48	-0.4723	2.6151	2.1957
H49	0.882	1.5461	2.6604
C50	-5.9728	-0.1194	0.0592
H51	-7.0137	0.1337	-0.1935
H52	-5.9649	-1.1325	0.4847
H53	-5.3911	-0.1405	-0.8723
C54	-5.5535	2.8809	0.6854
C55	-6.1352	0.8833	2.9621
H56	-7.2233	1.0231	2.8731
H57	-5.7557	1.6047	3.7002
H58	-5.9499	-0.131	3.3449
H59	-6.6282	3.1048	0.6068
H60	-5.103	3.0322	-0.3051
H61	-5.1043	3.6043	1.3814
C62	-3.5511	-2.8682	0.8845
C63	-2.4318	-4.9487	0.029
C64	4.9643	2.3098	-0.2057
C65	3.2874	2.6148	-2.0551
H66	-1.5099	-3.9313	2.3656
H67	-0.2152	-3.7865	1.1512
H68	-1.0031	-2.3325	1.7808
H69	4.5097	0.1643	-1.773
H70	3.859	-0.2357	-0.1644
H71	2.7576	-0.0041	-1.535
H72	-3.8676	-3.3836	1.8022
H73	-3.4402	-1.8025	1.1227
H74	-4.3647	-2.9782	0.154
H75	-2.7417	-5.5051	0.9243
H76	-3.2066	-5.1011	-0.7353
H77	-1.4961	-5.3948	-0.3387
H78	5.756	2.1171	-0.9428
H79	4.984	3.3845	0.0237
H80	5.2163	1.7598	0.7128
H81	4.0537	2.3979	-2.8122
H82	2.3185	2.3054	-2.4737
H83	3.2718	3.7042	-1.9109
H84	-0.4826	1.7889	3.7596

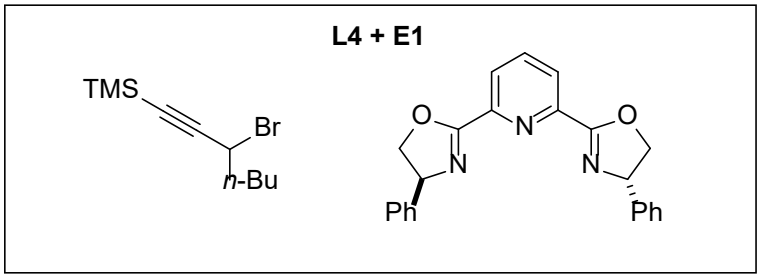

(R)-Transition State

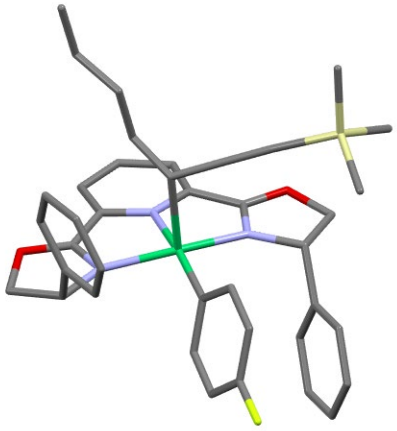

Calculated geometry

Atom	X	Y	Z
Ni1	0	0	0
O2	-3.9786	0.6009	-0.1932
O3	2.4127	0.6167	-3.1545
N4	-1.9423	-0.0776	0.4344
N5	-0.7464	0.8344	-1.5969
N6	1.5814	-0.0518	-1.1904
C7	-2.7959	-0.4505	1.5796
H8	-2.6629	-1.5189	1.7836
C9	-4.2112	-0.1694	1.0241
H10	-4.736	-1.0861	0.7316
H11	-4.8444	0.4268	1.6873
C12	-2.6878	0.512	-0.4308
C13	-2.0574	1.041	-1.662
C14	-2.6405	1.6029	-2.7914
H15	-3.7151	1.7707	-2.842
C16	-1.7952	1.9208	-3.8591
H17	-2.214	2.3643	-4.7624
C18	-0.426	1.6424	-3.7987

H19	0.2366	1.8421	-4.6394
C20	0.0591	1.0762	-2.6257
C21	1.4079	0.5522	-2.31
C22	3.5161	-0.0999	-2.5257
H23	4.3533	0.5981	-2.4342
H24	3.791	-0.9292	-3.1867
C25	2.9548	-0.5697	-1.1562
H26	3.4823	-0.0837	-0.3259
C27	0.6398	-1.1343	1.3706
C28	1.5797	-0.857	2.3673
H29	2.0134	0.1383	2.4589
C30	2.0018	-1.8406	3.2649
H31	2.7373	-1.6285	4.0424
C32	1.4783	-3.1195	3.1495
F33	1.8957	-4.0797	3.9999
C34	0.5433	-3.4413	2.1761
H35	0.1589	-4.4601	2.112
C36	0.1304	-2.4393	1.2958
H37	-0.6056	-2.7004	0.53
C38	0.3912	1.9945	1.1346
C39	1.7884	2.131	1.0465
H40	0.0309	1.5606	2.0728
C41	-0.4863	3.059	0.5265
C42	3.013	2.243	1.0071
Si43	4.8459	2.3616	1.2731
H44	-1.5251	2.7031	0.4937
H45	-0.1798	3.2667	-0.51
C46	-0.458	4.3643	1.3297
C47	5.2198	4.0708	1.9456
C48	-1.4476	5.3975	0.8002
H49	-0.6849	4.1421	2.3842
H50	-1.2256	5.6006	-0.2605
H51	-2.4613	4.9632	0.8177
H52	6.2964	4.1747	2.1487
H53	4.6738	4.2525	2.8826
H54	4.9312	4.8484	1.2232
C55	5.7599	2.0791	-0.3411
C56	5.2874	1.023	2.5115
H57	5.0243	0.0294	2.1195
H58	4.7469	1.17	3.4582
H59	6.3666	1.031	2.726
H60	5.376	2.7239	-1.145
H61	5.6829	1.031	-0.6636

H62	6.8285	2.3045	-0.2048
C63	-1.4327	6.7001	1.5912
H64	0.5632	4.7778	1.3141
H65	-2.1565	7.4245	1.1924
H66	-1.6835	6.5236	2.648
H67	-0.4383	7.17	1.5627
C68	-1.4592	1.8313	4.9855
C69	-2.2829	2.4289	4.03
C70	-2.7397	1.6881	2.9417
C71	-2.3818	0.343	2.8015
C72	-1.5659	-0.2523	3.7664
C73	-1.104	0.4891	4.8534
H74	-1.0988	2.4118	5.8362
H75	-2.5701	3.4765	4.1314
H76	-3.3756	2.1722	2.1969
H77	-1.2772	-1.2989	3.6567
H78	-0.463	0.0149	5.5981
C79	2.9346	-4.8323	-0.5065
C80	3.6307	-3.9956	0.3641
C81	3.6462	-2.6179	0.1464
C82	2.9642	-2.0674	-0.9384
C83	2.2682	-2.9109	-1.8105
C84	2.2527	-4.2873	-1.5966
H85	2.9204	-5.91	-0.3361
H86	4.1575	-4.4144	1.2229
H87	4.1805	-1.9616	0.8346
H88	1.7259	-2.4911	-2.6617
H89	1.7066	-4.938	-2.2816

(S)-Transition State

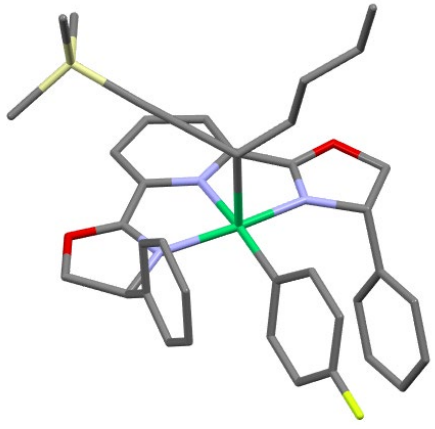

Calculated geometry

Atom	X	Y	Z
Ni1	0	0	0
O2	-3.3405	-1.2686	-1.8327
O3	1.2889	3.7907	-0.2492
N4	-1.3581	-1.204	-0.8026
N5	-1.1577	1.3175	-0.8327
N6	1.1663	1.5873	0.1001
C7	-1.6201	-2.6473	-0.9465
H8	-0.9233	-3.0348	-1.7024
C9	-3.0709	-2.6586	-1.4871
H10	-3.1987	-3.2624	-2.39
H11	-3.8062	-2.9548	-0.7293
C12	-2.3429	-0.572	-1.3333
C13	-2.2762	0.9046	-1.4168
C14	-3.1235	1.8034	-2.054
H15	-4.0368	1.4635	-2.5399
C16	-2.7465	3.1497	-2.0572
H17	-3.3869	3.8856	-2.5434
C18	-1.5429	3.5618	-1.4754
H19	-1.2177	4.6005	-1.5071
C20	-0.7594	2.5843	-0.874
C21	0.6049	2.6708	-0.3031
C22	2.591	3.4458	0.3122
H23	2.6989	3.9935	1.2541
H24	3.3562	3.7704	-0.4009
C25	2.543	1.9058	0.5052
H26	2.6724	1.6441	1.5627
C27	1.2733	-1.298	0.5092
C28	1.7719	-1.591	1.7808
H29	1.3808	-1.0872	2.6665
C30	2.7869	-2.5351	1.9655
H31	3.1785	-2.7699	2.9562
C32	3.307	-3.1807	0.8548
F33	4.2935	-4.0854	1.0229
C34	2.8451	-2.9189	-0.4273
H35	3.2835	-3.4434	-1.2772
C36	1.8279	-1.9787	-0.5855
H37	1.468	-1.7765	-1.5982
C38	-1.0101	0.1714	2.0877
C39	-2.3693	0.3882	1.798

H40	-0.7612	-0.8642	2.3319
C41	-0.2452	1.2413	2.8256
C42	-3.5542	0.5802	1.528
Si43	-5.3792	0.8251	1.289
H44	-0.4563	2.2268	2.3834
H45	0.833	1.0645	2.7124
C46	-0.5781	1.279	4.3212
C47	-5.9897	-0.4196	0.0269
C48	0.2308	2.3328	5.0719
H49	-0.3886	0.2848	4.7583
H50	1.305	2.1307	4.9264
H51	0.0458	3.3196	4.6162
H52	-7.0781	-0.3203	-0.1028
H53	-5.779	-1.447	0.3596
H54	-5.5108	-0.2753	-0.9507
C55	-5.6735	2.5825	0.7033
C56	-6.205	0.5347	2.9477
H57	-7.2948	0.6618	2.86
H58	-5.8362	1.2449	3.702
H59	-6.007	-0.4848	3.3097
H60	-6.7528	2.7711	0.5993
H61	-5.2017	2.7676	-0.2717
H62	-5.2684	3.3083	1.4235
C63	-0.0866	2.3846	6.5617
H64	-1.6556	1.4715	4.4499
H65	0.5118	3.1493	7.0763
H66	-1.1479	2.619	6.7328
H67	0.1194	1.4177	7.0445
C68	-0.9	-4.7413	2.7486
C69	-1.865	-3.7336	2.6943
C70	-2.1169	-3.0716	1.4943
C71	-1.3988	-3.4043	0.3419
C72	-0.4432	-4.42	0.3992
C73	-0.1937	-5.0883	1.5973
H74	-0.7011	-5.258	3.6889
H75	-2.4226	-3.4595	3.5913
H76	-2.8632	-2.2753	1.4615
H77	0.1237	-4.6769	-0.4971
H78	0.5605	-5.8759	1.6324
C79	5.3491	-0.378	-1.841
C80	5.3856	-0.4426	-0.4492
C81	4.4839	0.3044	0.3088
C82	3.54	1.1178	-0.3177

C83	3.5077	1.1811	-1.7148
C84	4.4076	0.4366	-2.4739
H85	6.0522	-0.9639	-2.4352
H86	6.1124	-1.0849	0.0505
H87	4.5028	0.2416	1.3982
H88	2.7695	1.8105	-2.2184
H89	4.375	0.491	-3.5633

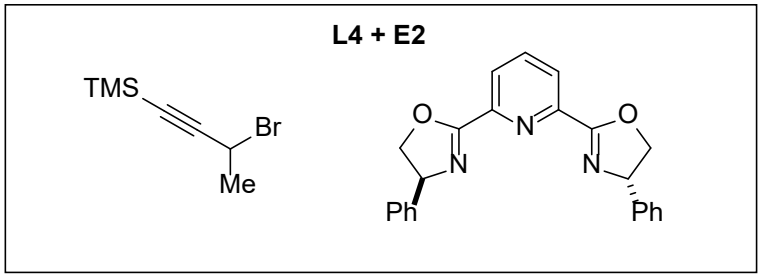

(R)-Transition State

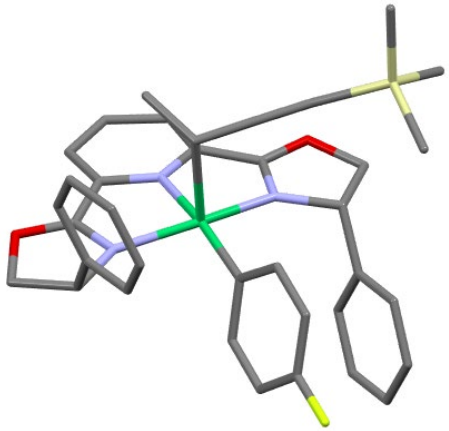

Calculated geometry

Atom	X	Y	Z
Ni1	0	0	0
O2	-3.9846	0.5757	-0.1957
O3	2.4003	0.587	-3.1725
N4	-1.9442	-0.0865	0.4358
N5	-0.7539	0.8169	-1.6043
N6	1.5771	-0.0673	-1.2003
C7	-2.7949	-0.4726	1.5781
H8	-2.6683	-1.546	1.7598
C9	-4.213	-0.1712	1.0368
H10	-4.7623	-1.0805	0.768
H11	-4.8228	0.4489	1.7002
C12	-2.6933	0.4934	-0.4324
C13	-2.0669	1.0118	-1.6705
C14	-2.6571	1.5465	-2.8095
H15	-3.7333	1.7037	-2.8609
C16	-1.8172	1.8492	-3.8858
H17	-2.2418	2.2707	-4.797

C18	-0.446	1.5813	-3.8238
H19	0.2126	1.7668	-4.6708
C20	0.0464	1.0423	-2.6411
C21	1.3981	0.5264	-2.3244
C22	3.5099	-0.1152	-2.5384
H23	4.3408	0.591	-2.4516
H24	3.7927	-0.9466	-3.1934
C25	2.9525	-0.5797	-1.1655
H26	3.4787	-0.0867	-0.3388
C27	0.6437	-1.13	1.3718
C28	1.569	-0.8535	2.3816
H29	1.9885	0.1459	2.4914
C30	1.9943	-1.8442	3.2701
H31	2.719	-1.6334	4.0579
C32	1.4883	-3.1277	3.132
F33	1.9104	-4.0944	3.9726
C34	0.5667	-3.448	2.1454
H35	0.1959	-4.4705	2.0636
C36	0.1504	-2.4396	1.2744
H37	-0.5744	-2.6994	0.4974
C38	0.3815	1.9864	1.113
C39	1.7835	2.1118	1.0414
H40	0.0096	1.5668	2.0526
C41	-0.4695	3.0603	0.4874
C42	3.0086	2.2147	1.0145
Si43	4.8408	2.323	1.2902
H44	-1.5284	2.7775	0.4622
H45	-0.1409	3.3077	-0.5308
C46	5.2269	4.0388	1.9385
H47	6.3035	4.1358	2.1452
H48	4.6783	4.24	2.87
H49	4.9491	4.8079	1.203
C50	5.7623	2.0095	-0.3143
C51	5.2642	0.9999	2.5515
H52	4.9928	0.0028	2.1744
H53	4.7213	1.1672	3.4933
H54	6.3426	1.0008	2.7706
H55	5.3936	2.6519	-1.1274
H56	5.673	0.9595	-0.6275
H57	6.8329	2.2214	-0.1723
C58	-1.407	1.7265	5.0161
C59	-2.2037	2.3612	4.0614
C60	-2.682	1.6452	2.9659

C61	-2.3673	0.2907	2.8138
C62	-1.5772	-0.3407	3.7768
C63	-1.0982	0.374	4.8742
H64	-1.0306	2.2867	5.8735
H65	-2.4528	3.4179	4.1694
H66	-3.2978	2.1557	2.2221
H67	-1.3198	-1.3944	3.6564
H68	-0.4776	-0.1285	5.6177
C69	2.96	-4.8385	-0.4906
C70	3.6478	-3.9918	0.3767
C71	3.6536	-2.6152	0.151
C72	2.9699	-2.076	-0.9384
C73	2.2817	-2.9296	-1.8069
C74	2.2761	-4.3049	-1.5851
H75	2.9537	-5.9154	-0.3142
H76	4.1756	-4.4017	1.2392
H77	4.182	-1.9511	0.8362
H78	1.7382	-2.5187	-2.6617
H79	1.7364	-4.9636	-2.2674
H80	-0.4043	3.9831	1.0874

(S)-Transition State

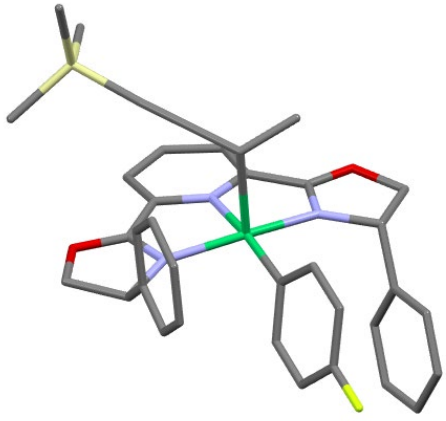

Calculated geometry

Atom	X	Y	Z
Ni1	0	0	0
O2	-3.3689	-1.2746	-1.7802
O3	1.3125	3.7782	-0.3425
N4	-1.373	-1.2084	-0.7767

N5	-1.1615	1.3131	-0.8387
N6	1.1783	1.5841	0.0572
C7	-1.645	-2.6519	-0.8987
H8	-0.9601	-3.0531	-1.6583
C9	-3.1025	-2.6617	-1.4208
H10	-3.2453	-3.276	-2.3144
H11	-3.8298	-2.9443	-0.6502
C12	-2.3611	-0.5775	-1.3024
C13	-2.2875	0.8973	-1.4064
C14	-3.1351	1.7901	-2.0515
H15	-4.0543	1.4472	-2.5238
C16	-2.7501	3.1339	-2.0814
H17	-3.3904	3.8653	-2.5745
C18	-1.5379	3.548	-1.5192
H19	-1.2057	4.5835	-1.5735
C20	-0.755	2.576	-0.908
C21	0.6182	2.6634	-0.3588
C22	2.6209	3.435	0.2049
H23	2.7459	3.9972	1.1362
H24	3.3771	3.7436	-0.5245
C25	2.5667	1.8985	0.4238
H26	2.7212	1.6517	1.4813
C27	1.2746	-1.3002	0.4969
C28	1.8003	-1.5909	1.7576
H29	1.4308	-1.083	2.6501
C30	2.8155	-2.5387	1.9215
H31	3.2291	-2.7721	2.9036
C32	3.307	-3.1899	0.801
F33	4.2937	-4.0977	0.9488
C34	2.8166	-2.9302	-0.471
H35	3.2331	-3.4591	-1.3292
C36	1.8003	-1.9861	-0.6086
H37	1.4183	-1.7848	-1.6135
C38	-0.9602	0.2027	2.0911
C39	-2.3256	0.4169	1.814
H40	-0.7156	-0.8301	2.3496
C41	-0.1991	1.2817	2.8167
C42	-3.5137	0.6069	1.5599
Si43	-5.3413	0.8585	1.3476
H44	-0.391	2.274	2.3881
H45	0.8809	1.094	2.7985
C46	-5.9827	-0.4082	0.1234
H47	-7.0725	-0.3035	0.0102

H48	-5.7738	-1.43	0.474
H49	-5.5195	-0.2877	-0.8651
C50	-5.6354	2.6046	0.7286
C51	-6.1402	0.6112	3.0262
H52	-7.2306	0.7422	2.954
H53	-5.7552	1.3372	3.7571
H54	-5.9413	-0.4004	3.4093
H55	-6.7154	2.7982	0.6421
H56	-5.1824	2.7646	-0.2596
H57	-5.2112	3.3437	1.4239
C58	-0.8928	-4.7073	2.8119
C59	-1.8551	-3.697	2.7566
C60	-2.1168	-3.0467	1.5523
C61	-1.4117	-3.3942	0.3962
C62	-0.4585	-4.4121	0.4548
C63	-0.1991	-5.0685	1.6574
H64	-0.6864	-5.2148	3.7556
H65	-2.4032	-3.4124	3.6561
H66	-2.8608	-2.2484	1.5186
H67	0.0984	-4.6804	-0.4443
H68	0.553	-5.8582	1.6933
C69	5.294	-0.4401	-1.9622
C70	5.367	-0.4848	-0.5712
C71	4.4909	0.2796	0.1996
C72	3.5364	1.0909	-0.4134
C73	3.4677	1.1343	-1.81
C74	4.3419	0.3724	-2.5817
H75	5.9768	-1.0398	-2.5662
H76	6.1021	-1.1255	-0.0815
H77	4.5386	0.2323	1.2889
H78	2.7212	1.7619	-2.3035
H79	4.2809	0.4115	-3.6706
H80	-0.5086	1.3153	3.8745

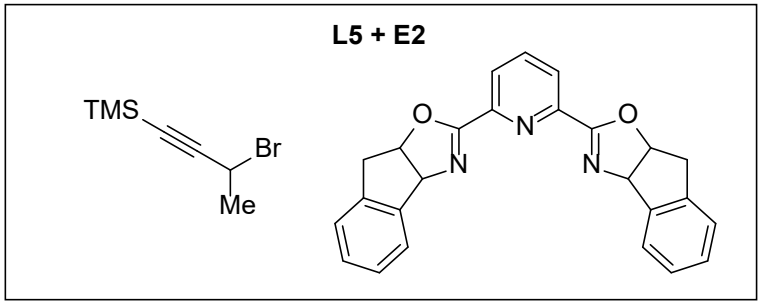

(R)-Transition State

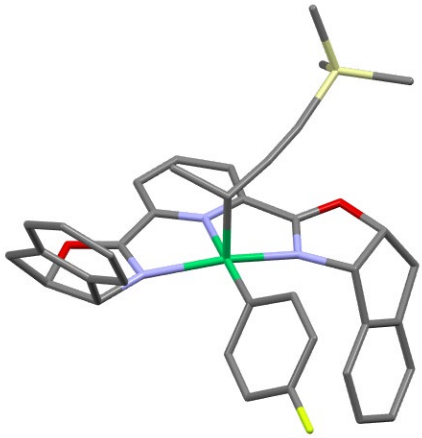

Calculated geometry

Atom	X	Y	Z
Ni1	0	0	0
O2	-2.6775	2.4729	-1.9708
O3	3.6117	-0.6704	-1.7709
N4	-1.8605	0.8722	-0.62
N5	0.5129	1.0128	-1.6434
N6	1.707	-1.0145	-0.6381
C7	-1.6746	1.725	-1.5604
C8	-0.3551	1.8378	-2.2148
C9	-0.016	2.6008	-3.3265
H10	-0.7392	3.2773	-3.7789
C11	1.272	2.4455	-3.8445
H12	1.5801	3.0274	-4.7133
C13	2.1519	1.5161	-3.2846
H14	3.1389	1.3364	-3.7068

C15	1.7124	0.804	-2.1748
C16	2.371	-0.3283	-1.4924
C17	-0.4531	-1.1375	1.4156
C18	0.3163	-1.5297	2.5124
H19	1.2258	-0.9874	2.7789
C20	-0.055	-2.6322	3.2823
H21	0.5357	-2.9569	4.1395
C22	-1.2066	-3.3316	2.9399
F23	-1.5692	-4.3908	3.6827
C24	-1.9921	-2.9684	1.8559
H25	-2.8882	-3.5424	1.6182
C26	-1.6037	-1.8632	1.0935
H27	-2.2161	-1.5887	0.2323
C28	0.6648	1.3531	1.2951
C29	2.0871	1.4581	1.0373
H30	0.4885	0.9975	2.3134
C31	-0.0108	2.7108	1.0981
C32	3.2625	1.6691	0.7723
Si33	4.9966	2.2324	0.4092
H34	-1.0882	2.6598	1.2734
H35	0.1693	3.1213	0.096
C36	5.2212	3.8985	1.2426
H37	6.233	4.2876	1.0513
H38	5.0847	3.8199	2.331
H39	4.4957	4.6303	0.8578
C40	5.2014	2.4096	-1.4475
C41	6.2203	0.9877	1.0927
H42	6.1286	0.0132	0.5928
H43	6.0718	0.8371	2.1719
H44	7.2479	1.3499	0.9371
H45	4.4654	3.1156	-1.8602
H46	5.079	1.4422	-1.9536
H47	6.2068	2.7939	-1.6779
C48	-3.2665	1.0314	-0.1912
C49	-3.8483	2.0676	-1.2006
C50	-4.403	3.2494	-0.4044
H51	-4.0113	4.1966	-0.7996
H52	-5.4979	3.2918	-0.4891
H53	-4.56	1.6467	-1.9184
H54	-3.7726	0.0589	-0.2296
C55	-3.9777	2.9762	1.0168
C56	-3.4046	1.7104	1.1536
C57	-2.9962	1.2378	2.3997

C58	-3.1418	2.0672	3.5109
C59	-3.6931	3.3457	3.3739
C60	-4.1217	3.805	2.1287
H61	-2.5543	0.2472	2.5018
H62	-2.8189	1.7182	4.4927
H63	-3.7951	3.9875	4.2505
H64	-4.563	4.7979	2.026
C65	3.9259	-1.8272	-0.9332
C66	2.5831	-2.106	-0.1951
C67	4.2598	-3.0504	-1.7904
H68	4.4744	-2.7488	-2.8247
H69	5.1586	-3.5539	-1.408
C70	2.1294	-3.4392	-0.7427
C71	3.0434	-3.9371	-1.6722
C72	2.7785	-5.1316	-2.3412
C73	1.5923	-5.8124	-2.0649
C74	0.6837	-5.3122	-1.1257
C75	0.9473	-4.118	-0.4552
H76	3.4863	-5.5271	-3.0719
H77	1.3717	-6.7455	-2.5861
H78	-0.2375	-5.8586	-0.9177
H79	0.2413	-3.7207	0.2746
H80	2.6696	-2.0928	0.8985
H81	4.7427	-1.5168	-0.2757
H82	0.4099	3.4293	1.8174

(S)-Transition State

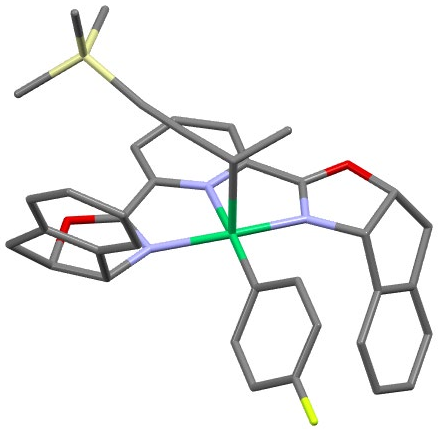

Calculated geometry

Atom	X	Y	Z
Ni1	0	0	0
O2	-3.3703	-1.1623	-1.9057
O3	1.3094	3.8131	-0.2114
N4	-1.3986	-1.1891	-0.8424
N5	-1.1152	1.3405	-0.868
N6	1.233	1.5905	0.0635
C7	-2.3482	-0.5165	-1.3897
C8	-2.2376	0.9555	-1.463
C9	-3.0667	1.8728	-2.0976
H10	-3.983	1.5499	-2.5892
C11	-2.6694	3.2128	-2.0879
H12	-3.2958	3.9639	-2.569
C13	-1.4606	3.5969	-1.4988
H14	-1.1155	4.6293	-1.5185
C15	-0.6966	2.6005	-0.9034
C16	0.6608	2.6763	-0.3201
C17	1.2086	-1.3167	0.6173
C18	1.9007	-1.2963	1.8347
H19	1.6774	-0.5378	2.5876
C20	2.9	-2.2281	2.1264
H21	3.4419	-2.212	3.0729
C22	3.2082	-3.1941	1.1781
F23	4.1715	-4.0943	1.4488
C24	2.5487	-3.2565	-0.0413
H25	2.8204	-4.0273	-0.7636
C26	1.5525	-2.3142	-0.3082
H27	1.0567	-2.357	-1.2805
C28	-1.0199	0.2847	2.075
C29	-2.3892	0.3544	1.7505
H30	-0.6824	-0.685	2.4423
C31	-0.3902	1.4976	2.7096
C32	-3.5806	0.4739	1.4726
Si33	-5.4022	0.7893	1.2879
H34	-0.6683	2.4236	2.1892
H35	0.703	1.4226	2.7397
C36	-6.127	-0.3393	-0.0187
H37	-7.1857	-0.0857	-0.1803
H38	-6.0749	-1.3876	0.3073
H39	-5.5976	-0.2488	-0.9767
C40	-5.6102	2.5891	0.7996
C41	-6.1916	0.4417	2.9531
H42	-7.2788	0.6056	2.9056

H43	-5.7782	1.0976	3.7329
H44	-6.0143	-0.602	3.2521
H45	-6.6781	2.8418	0.7171
H46	-5.1366	2.7944	-0.1712
H47	-5.1577	3.2549	1.5489
C48	-1.8231	-2.5985	-0.855
C49	-3.0634	-2.5916	-1.7903
C50	-4.1897	-3.3263	-1.0744
H51	-5.1531	-2.8252	-1.2275
H52	-4.2845	-4.3426	-1.484
C53	2.6002	3.5047	0.4097
C54	2.5942	1.9485	0.4931
C55	3.7554	3.9273	-0.4983
H56	3.4072	4.6352	-1.2627
H57	4.5335	4.4389	0.0851
H58	-2.8704	-2.9467	-2.8086
H59	-1.0095	-3.2381	-1.2149
H60	2.7773	1.5627	1.5035
H61	2.5971	4.007	1.3823
C62	-3.7347	-3.3733	0.364
C63	-2.383	-3.0417	0.4791
C64	-1.7262	-3.1072	1.7048
C65	-2.4575	-3.4703	2.8357
C66	-3.8199	-3.7694	2.7324
C67	-4.4651	-3.734	1.495
H68	-0.6633	-2.8741	1.7768
H69	-1.9635	-3.5199	3.8073
H70	-4.3812	-4.0463	3.6262
H71	-5.5231	-3.9897	1.4146
C72	3.6597	1.5219	-0.4945
C73	4.2734	2.6328	-1.0765
C74	5.2694	2.4609	-2.0374
C75	5.6421	1.1669	-2.4018
C76	5.0359	0.0569	-1.8043
C77	4.0408	0.2269	-0.8422
H78	5.7532	3.3254	-2.4954
H79	6.4187	1.0195	-3.1541
H80	5.3446	-0.9499	-2.0901
H81	3.5719	-0.6364	-0.3735
H82	-0.7398	1.5929	3.751

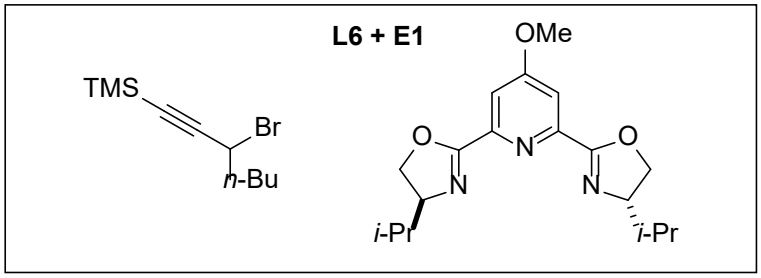

(R)-Transition State

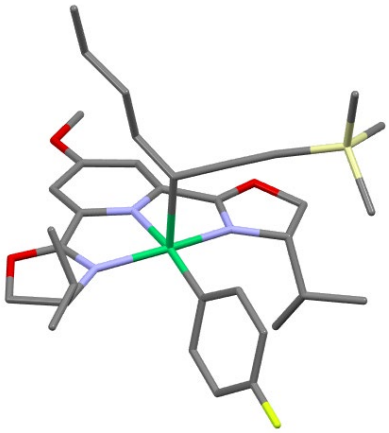

Calculated geometry

Atom	X	Y	Z
Ni1	0	0	0
O2	-4.0046	0.4291	-0.2784
O3	2.3852	0.5892	-3.2044
N4	-1.9496	-0.0836	0.4366
N5	-0.753	0.7852	-1.6136
N6	1.6006	-0.0648	-1.2134
C7	-2.8144	-0.5766	1.5196
H8	-2.6211	-1.65	1.6438
C9	-4.2303	-0.3479	0.9368
H10	-4.7279	-1.2772	0.6375
H11	-4.896	0.2315	1.5843
C12	-2.7028	0.4405	-0.4623
C13	-2.0733	0.9599	-1.6988
C14	-2.6696	1.4488	-2.8401
H15	-3.7467	1.5852	-2.9193
C16	-1.8345	1.7462	-3.943
C17	-0.4505	1.4906	-3.8625
H18	0.2257	1.6439	-4.6998

C19	0.0316	0.994	-2.6613
C20	1.3947	0.5085	-2.3429
C21	3.5211	-0.0718	-2.5748
H22	4.3358	0.6568	-2.5185
H23	3.8176	-0.9016	-3.2265
C24	2.9958	-0.5233	-1.1881
H25	3.5098	0.0229	-0.3864
C26	-2.5161	0.1167	2.8561
H27	-1.4324	-0.0105	3.0072
C28	-2.8325	1.6103	2.8394
H29	-3.9159	1.7967	2.802
H30	-2.3734	2.1206	1.9828
H31	-2.4523	2.0899	3.7514
C32	-3.2423	-0.6033	3.9909
H33	-2.9569	-1.6639	4.0379
H34	-4.3346	-0.5508	3.8632
H35	-3.0015	-0.1428	4.9585
C36	3.1152	-2.0265	-0.8958
H37	2.7301	-2.1594	0.1252
C38	4.5847	-2.4456	-0.9022
H39	5.0271	-2.3659	-1.9069
H40	4.6866	-3.4914	-0.5822
H41	5.1815	-1.8239	-0.2194
C42	2.2666	-2.8795	-1.8341
H43	2.3534	-3.941	-1.5649
H44	2.587	-2.7807	-2.8828
H45	1.2037	-2.6062	-1.7739
C46	0.6159	-1.1377	1.3827
C47	1.5557	-0.8933	2.39
H48	1.9828	0.1007	2.5183
C49	1.9962	-1.9116	3.2404
H50	2.7332	-1.7247	4.0229
C51	1.4858	-3.191	3.0741
F52	1.9117	-4.1788	3.8858
C53	0.5443	-3.4795	2.0959
H54	0.1626	-4.4966	1.9961
C55	0.115	-2.4443	1.2623
H56	-0.622	-2.6823	0.4896
C57	0.4565	2.0184	1.059
C58	1.8618	2.0865	1.0704
H59	0.0147	1.6629	1.9951
C60	-0.3162	3.0894	0.3292
C61	3.0905	2.1315	1.1121

Si62	4.9171	2.0684	1.4382
H63	-1.3519	2.7598	0.168
H64	0.1218	3.261	-0.6657
C65	-0.3558	4.4111	1.1046
C66	5.375	3.562	2.4739
C67	-1.1881	5.4779	0.3993
H68	0.6729	4.7754	1.2564
H69	-0.768	4.2258	2.1102
H70	-0.7711	5.6535	-0.606
C71	-1.2542	6.7918	1.1688
H72	-2.2074	5.0888	0.2387
H73	-1.8582	7.5414	0.6387
H74	-0.2498	7.2155	1.3174
H75	-1.7007	6.6456	2.1638
H76	6.4481	3.5426	2.7175
H77	4.809	3.5739	3.4166
H78	5.1633	4.4963	1.9338
C79	5.8592	2.0817	-0.184
C80	5.2369	0.4728	2.3732
H81	4.8947	-0.3991	1.7967
H82	4.7068	0.4711	3.3371
H83	6.3123	0.351	2.5727
H84	5.5563	2.9273	-0.8186
H85	5.7043	1.1508	-0.7474
H86	6.9377	2.1738	0.0149
O87	-2.4413	2.2249	-5.0185
C88	-1.6777	2.5158	-6.1875
H89	-2.3885	2.8985	-6.925
H90	-0.917	3.28	-5.9757
H91	-1.198	1.6063	-6.5752

(S)-Transition State

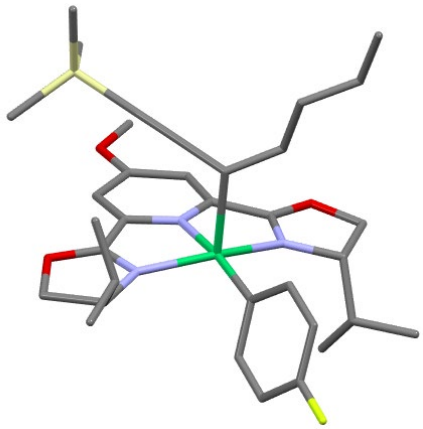

Calculated geometry

Atom	X	Y	Z
Ni1	0	0	0
O2	-3.2744	-1.3347	-1.9449
O3	1.1749	3.844	-0.2679
N4	-1.3507	-1.2421	-0.8091
N5	-1.1713	1.2835	-0.8583
N6	1.1489	1.6342	0.0692
C7	-1.5837	-2.6878	-0.9539
H8	-0.7384	-3.1061	-1.5163
C9	-2.872	-2.7309	-1.8138
H10	-2.7049	-3.1165	-2.8253
H11	-3.7023	-3.2721	-1.3486
C12	-2.322	-0.6255	-1.3791
C13	-2.2856	0.8527	-1.4486
C14	-3.1526	1.7196	-2.0756
H15	-4.0578	1.3767	-2.5736
C16	-2.8283	3.0955	-2.0636
C17	-1.6199	3.5299	-1.4833
H18	-1.3014	4.5692	-1.496
C19	-0.8184	2.5597	-0.9017
C20	0.5424	2.6932	-0.3302
C21	2.4621	3.5599	0.3579
H22	2.465	4.054	1.3358
H23	3.2408	3.996	-0.2766
C24	2.5146	2.0155	0.4551
H25	2.6916	1.7021	1.4925
C26	-1.6527	-3.4105	0.3981
H27	-0.7362	-3.1088	0.9284
C28	-2.8553	-2.9948	1.2414
H29	-2.7599	-3.3965	2.2595
H30	-3.7973	-3.3853	0.8278
H31	-2.9467	-1.9039	1.3194
C32	-1.6041	-4.9222	0.1829
H33	-0.6975	-5.2203	-0.363
H34	-2.4764	-5.2723	-0.3909
H35	-1.6103	-5.4508	1.1457
C36	3.5588	1.3278	-0.4399
H37	3.4167	0.2495	-0.2747
C38	4.9708	1.6932	0.0144
H39	5.1219	1.4612	1.0784

H40	5.182	2.7632	-0.1333
H41	5.7164	1.1306	-0.5635
C42	3.3401	1.6132	-1.9237
H43	3.4465	2.6841	-2.1559
H44	2.3441	1.2882	-2.2568
H45	4.0835	1.0751	-2.5274
C46	1.2814	-1.2912	0.5257
C47	1.8256	-1.5428	1.7895
H48	1.4663	-1.0069	2.6694
C49	2.8422	-2.4846	1.9755
H50	3.2657	-2.6838	2.9608
C51	3.3184	-3.1807	0.8741
F52	4.296	-4.0916	1.0455
C53	2.8115	-2.9655	-0.4001
H54	3.2108	-3.5308	-1.2433
C55	1.7947	-2.022	-0.559
H56	1.404	-1.8559	-1.5671
C57	-0.9631	0.2251	2.088
C58	-2.3032	0.5476	1.7995
H59	-0.7925	-0.8262	2.3388
C60	-0.1315	1.2357	2.84
C61	-3.4681	0.8345	1.529
Si62	-5.2777	1.1352	1.2464
H63	-0.3253	2.2441	2.4449
H64	0.9354	1.0327	2.6779
C65	-0.4058	1.2187	4.3473
C66	-5.908	-0.1887	0.0765
C67	0.4662	2.2116	5.1105
H68	-0.2323	0.2006	4.7338
H69	-1.4706	1.4385	4.5273
H70	1.5264	1.9872	4.907
C71	0.2163	2.198	6.614
H72	0.2911	3.2244	4.7116
H73	0.8583	2.9204	7.1372
H74	0.4161	1.2033	7.0397
H75	-0.8293	2.4511	6.8445
H76	-6.9866	-0.0571	-0.0981
H77	-5.7519	-1.1886	0.508
H78	-5.3978	-0.1583	-0.8957
C79	-5.5261	2.8552	0.5385
C80	-6.1318	0.995	2.9105
H81	-7.2163	1.1458	2.7988
H82	-5.7512	1.7504	3.6135

H83	-5.9668	0.0013	3.3518
H84	-6.6024	3.079	0.4825
H85	-5.1112	2.9591	-0.4728
H86	-5.0562	3.613	1.1827
O87	-3.7133	3.9028	-2.6324
C88	-3.4625	5.3064	-2.6644
H89	-4.3255	5.7566	-3.1624
H90	-3.3719	5.7077	-1.6456
H91	-2.5505	5.5252	-3.237

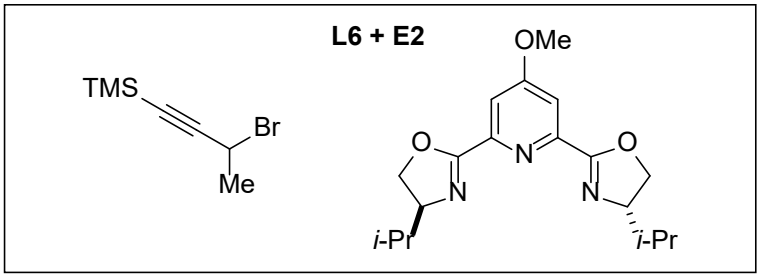

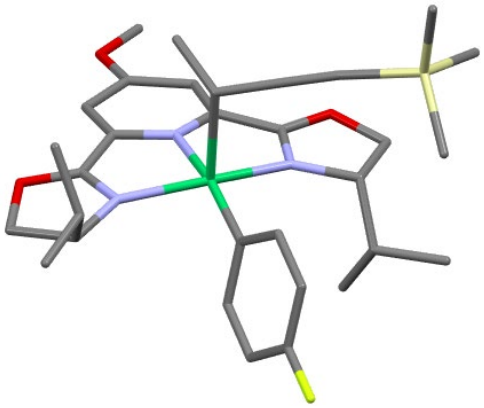

(R)-Transition State

Calculated geometry

Atom	X	Y	Z
Ni1	0	0	0
O2	-4.0163	0.3114	-0.3078
O3	2.3716	0.5585	-3.2261
N4	-1.9519	-0.1238	0.4311
N5	-0.7679	0.7365	-1.6329
N6	1.6041	-0.0647	-1.2185
C7	-2.8088	-0.6355	1.5116
H8	-2.5881	-1.7036	1.6374
C9	-4.2283	-0.4444	0.9229
H10	-4.7098	-1.3881	0.6432
H11	-4.9045	0.1366	1.5582
C12	-2.7139	0.3618	-0.4814
C13	-2.0928	0.8694	-1.7267
C14	-2.7012	1.2959	-2.8867
H15	-3.7819	1.3944	-2.9722

C16	-1.8742	1.5707	-4.0013
C17	-0.4838	1.3574	-3.9101
H18	0.1883	1.4919	-4.7538
C19	0.0106	0.9232	-2.6898
C20	1.3844	0.4772	-2.3606
C21	3.525	-0.0541	-2.5799
H22	4.3157	0.7014	-2.5335
H23	3.8513	-0.8857	-3.2148
C24	3.0081	-0.4954	-1.1869
H25	3.5112	0.0719	-0.3934
C26	-2.5341	0.0648	2.849
H27	-1.4498	-0.0438	3.0098
C28	-2.8741	1.5529	2.826
H29	-3.9596	1.7221	2.7686
H30	-2.407	2.07	1.9775
H31	-2.5188	2.0382	3.745
C32	-3.2581	-0.6658	3.9785
H33	-2.9577	-1.7221	4.0275
H34	-4.3501	-0.6293	3.8431
H35	-3.031	-0.2022	4.9479
C36	3.1559	-1.9914	-0.8717
H37	2.7721	-2.1159	0.1511
C38	4.6332	-2.3828	-0.8714
H39	5.0738	-2.3117	-1.8775
H40	4.7547	-3.4211	-0.5342
H41	5.2186	-1.7389	-0.1995
C42	2.3252	-2.8744	-1.7982
H43	2.4324	-3.9302	-1.5143
H44	2.645	-2.7837	-2.8479
H45	1.2571	-2.6214	-1.7432
C46	0.6259	-1.1117	1.3993
C47	1.5264	-0.8433	2.4353
H48	1.9206	0.162	2.5794
C49	1.9682	-1.8513	3.2974
H50	2.6749	-1.6458	4.1028
C51	1.4992	-3.144	3.1134
F52	1.9272	-4.1213	3.9365
C53	0.5966	-3.4562	2.1062
H54	0.2462	-4.4831	1.9932
C55	0.1648	-2.4312	1.2615
H56	-0.5421	-2.6875	0.4668
C57	0.4285	2.0277	1.0159
C58	1.8363	2.092	1.0557

H59	-0.031	1.6994	1.9529
C60	-0.3144	3.0896	0.246
C61	3.0631	2.1375	1.1229
Si62	4.8852	2.0723	1.4734
H63	-1.3821	2.8567	0.1526
H64	0.1033	3.2348	-0.7588
C65	5.3338	3.5646	2.515
H66	6.4034	3.5415	2.7733
H67	4.7551	3.5784	3.4499
H68	5.133	4.4998	1.9722
C69	5.8455	2.0846	-0.1384
C70	5.1909	0.4761	2.4119
H71	4.8511	-0.3946	1.8323
H72	4.651	0.4763	3.3703
H73	6.2638	0.3507	2.6222
H74	5.5559	2.9353	-0.7724
H75	5.6891	1.1575	-0.7077
H76	6.9225	2.1673	0.0724
O77	-2.4935	1.9832	-5.0967
C78	-1.7391	2.2277	-6.2823
H79	-2.4602	2.5514	-7.0378
H80	-0.997	3.0207	-6.1155
H81	-1.2379	1.3099	-6.62
H82	-0.2414	4.0543	0.7751

(S)-Transition State

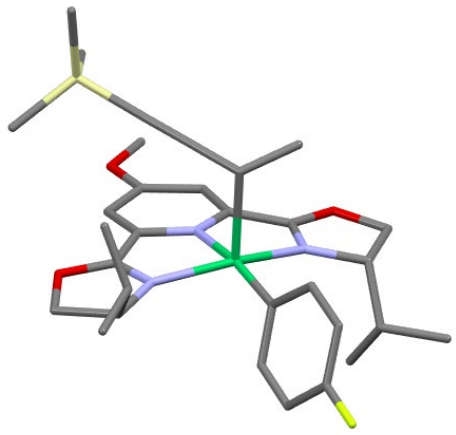

Calculated geometry

Atom	X	Y	Z

Ni1	0	0	0
O2	-3.32	-1.3037	-1.8934
O3	1.2099	3.8325	-0.314
N4	-1.376	-1.232	-0.791
N5	-1.1766	1.2945	-0.8375
N6	1.1664	1.6259	0.0424
C7	-1.6222	-2.6753	-0.9407
H8	-0.7951	-3.0934	-1.53
C9	-2.934	-2.7044	-1.7652
H10	-2.8009	-3.0985	-2.7784
H11	-3.7588	-3.2308	-1.2738
C12	-2.3518	-0.6051	-1.3415
C13	-2.3042	0.8728	-1.4088
C14	-3.1743	1.7466	-2.0217
H15	-4.0908	1.4108	-2.5037
C16	-2.838	3.1196	-2.0171
C17	-1.6144	3.5435	-1.4613
H18	-1.2858	4.5794	-1.4835
C19	-0.8117	2.5669	-0.892
C20	0.5628	2.6888	-0.351
C21	2.5126	3.5376	0.2736
H22	2.5567	4.0479	1.2419
H23	3.276	3.951	-0.3941
C24	2.545	1.9938	0.3941
H25	2.7385	1.6935	1.4324
C26	-1.6575	-3.4108	0.4057
H27	-0.7229	-3.1223	0.9112
C28	-2.8305	-2.9938	1.289
H29	-2.7076	-3.4061	2.2998
H30	-3.7877	-3.3731	0.9007
H31	-2.9108	-1.903	1.3793
C32	-1.6287	-4.9207	0.1744
H33	-0.7419	-5.2213	-0.4018
H34	-2.5211	-5.2577	-0.3758
H35	-1.6102	-5.4587	1.1318
C36	3.5613	1.2779	-0.5114
H37	3.4163	0.2048	-0.3184
C38	4.9875	1.6418	-0.1024
H39	5.1642	1.4354	0.9629
H40	5.2047	2.7055	-0.2832
H41	5.7128	1.0574	-0.6845
C42	3.306	1.5306	-1.9953
H43	3.4096	2.5956	-2.2544

H44	2.3007	1.202	-2.2952
H45	4.0319	0.9761	-2.6053
C46	1.2855	-1.3002	0.4862
C47	1.8713	-1.5584	1.7294
H48	1.5399	-1.0289	2.6239
C49	2.8963	-2.4984	1.8742
H50	3.3536	-2.703	2.8432
C51	3.3374	-3.1851	0.7524
F52	4.3232	-4.0934	0.8841
C53	2.7869	-2.9632	-0.5025
H54	3.159	-3.5217	-1.3626
C55	1.7627	-2.0219	-0.6206
H56	1.3385	-1.8491	-1.6139
C57	-0.9032	0.2311	2.1006
C58	-2.252	0.5482	1.8321
H59	-0.7301	-0.8178	2.3569
C60	-0.0784	1.2509	2.8445
C61	-3.4221	0.832	1.5849
Si62	-5.2359	1.1414	1.3396
H63	-0.2398	2.2635	2.4532
H64	0.9928	1.0246	2.7938
C65	-5.899	-0.1735	0.1778
H66	-6.9818	-0.0388	0.0341
H67	-5.733	-1.1767	0.5978
H68	-5.4158	-0.1367	-0.8078
C69	-5.4894	2.8657	0.6437
C70	-6.0568	0.9994	3.0202
H71	-7.1425	1.156	2.9314
H72	-5.6582	1.7502	3.7181
H73	-5.8879	0.0032	3.4547
H74	-6.5656	3.0945	0.6081
H75	-5.0922	2.9725	-0.3745
H76	-5.0049	3.6189	1.2825
O77	-3.7266	3.934	-2.5697
C78	-3.4632	5.335	-2.6103
H79	-4.3317	5.7923	-3.092
H80	-3.3485	5.7378	-1.5945
H81	-2.5608	5.5437	-3.2015
H82	-0.3617	1.2595	3.9101

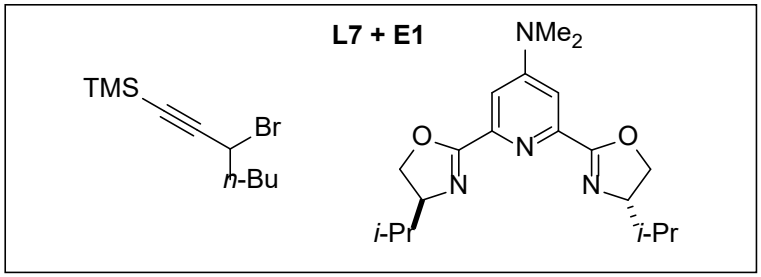

(R)-Transition State

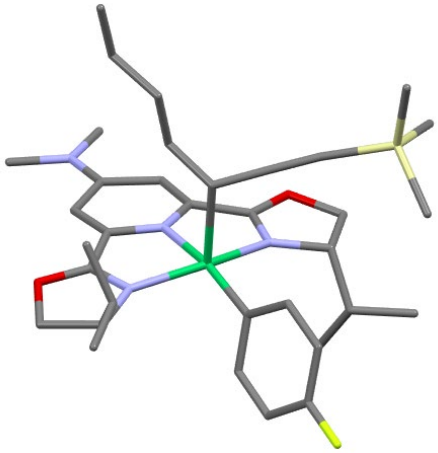

Calculated geometry

Atom	X	Y	Z
Ni1	0	0	0
O2	-4.0028	0.4546	-0.2419
O3	2.3586	0.5767	-3.2264
N4	-1.945	-0.067	0.4576
N5	-0.7593	0.796	-1.5937
N6	1.5886	-0.0679	-1.2273
C7	-2.8029	-0.5485	1.5504
H8	-2.6161	-1.6225	1.6795
C9	-4.2223	-0.3132	0.9792
H10	-4.7294	-1.241	0.691
H11	-4.8779	0.2743	1.6298
C12	-2.7016	0.4577	-0.4387
C13	-2.0779	0.9704	-1.6811
C14	-2.6926	1.4511	-2.814
H15	-3.7736	1.5553	-2.8325
C16	-1.8789	1.7628	-3.9488
C17	-0.4798	1.483	-3.8524
H18	0.1942	1.6142	-4.6939
C19	0.0105	0.9971	-2.6614

C20	1.3734	0.5041	-2.3566
C21	3.4978	-0.0822	-2.603
H22	4.3114	0.648	-2.5484
H23	3.7946	-0.9102	-3.257
C24	2.9798	-0.5373	-1.215
H25	3.5052	-0.001	-0.4142
C26	-2.4885	0.1502	2.8804
H27	-1.4045	0.0154	3.0231
C28	-2.7932	1.6461	2.8572
H29	-3.8755	1.8407	2.8288
H30	-2.3383	2.1471	1.993
H31	-2.4008	2.1287	3.7625
C32	-3.2108	-0.5568	4.0257
H33	-2.9338	-1.6194	4.0769
H34	-4.3038	-0.4963	3.9065
H35	-2.9587	-0.0925	4.9885
C36	3.0888	-2.0434	-0.9334
H37	2.7066	-2.1804	0.0881
C38	4.5546	-2.4747	-0.9489
H39	4.9939	-2.3909	-1.9547
H40	4.6495	-3.5237	-0.6371
H41	5.1591	-1.8629	-0.2639
C42	2.2293	-2.8829	-1.8741
H43	2.3087	-3.9472	-1.6137
H44	2.5456	-2.7784	-2.9236
H45	1.1689	-2.6014	-1.807
C46	0.6189	-1.1511	1.3735
C47	1.572	-0.921	2.3723
H48	2.0109	0.0683	2.4987
C49	2.0115	-1.9458	3.2157
H50	2.759	-1.7685	3.9905
C51	1.4864	-3.2195	3.0518
F52	1.9111	-4.2143	3.8564
C53	0.5313	-3.4954	2.0833
H54	0.1379	-4.5082	1.9852
C55	0.104	-2.4532	1.2573
H56	-0.6441	-2.6818	0.4923
C57	0.4867	2.0199	1.0641
C58	1.8923	2.0724	1.0697
H59	0.0442	1.6623	1.9989
C60	-0.278	3.0997	0.3392
C61	3.1217	2.1048	1.1068
Si62	4.949	2.0159	1.4181

H63	-1.3169	2.7795	0.1801
H64	0.1577	3.2671	-0.6574
C65	-0.3001	4.4202	1.1173
C66	5.4356	3.4951	2.4619
C67	-1.1211	5.4995	0.418
H68	0.7333	4.7721	1.2674
H69	-0.7114	4.2376	2.1238
H70	-0.7041	5.6744	-0.5874
C71	-1.1699	6.811	1.1933
H72	-2.1453	5.1234	0.2579
H73	-1.7657	7.5703	0.6678
H74	-0.1601	7.2217	1.3417
H75	-1.6161	6.6657	2.1885
H76	6.5104	3.4601	2.6963
H77	4.8778	3.5067	3.4095
H78	5.2314	4.4365	1.9312
C79	5.8794	2.0307	-0.2111
C80	5.2581	0.4097	2.3388
H81	4.9001	-0.4539	1.7594
H82	4.7367	0.4075	3.3074
H83	6.3337	0.2736	2.5277
H84	5.5851	2.8876	-0.8345
H85	5.7052	1.1085	-0.7831
H86	6.9607	2.1037	-0.0195
N87	-2.4158	2.263	-5.0759
C88	-1.5722	2.528	-6.2326
H89	-2.1851	2.9573	-7.0296
H90	-0.7749	3.2446	-5.9873
H91	-1.1077	1.6056	-6.6125
C92	-3.8502	2.4979	-5.1608
H93	-4.081	2.9437	-6.1319
H94	-4.419	1.5606	-5.0663
H95	-4.1863	3.1909	-4.3761

(S)-Transition State

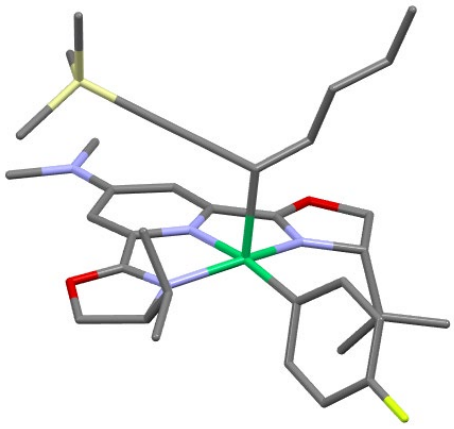

Calculated geometry

Atom	X	Y	Z
Ni1	0	0	0
O2	-3.2354	-1.3835	-1.9766
O3	1.1454	3.8524	-0.3104
N4	-1.3344	-1.2627	-0.8059
N5	-1.174	1.2582	-0.8751
N6	1.1291	1.6493	0.0661
C7	-1.5547	-2.7111	-0.9364
H8	-0.6978	-3.1305	-1.4805
C9	-2.8291	-2.7746	-1.8154
H10	-2.6444	-3.1775	-2.8171
H11	-3.6637	-3.3124	-1.3539
C12	-2.2974	-0.6588	-1.4036
C13	-2.267	0.8186	-1.494
C14	-3.1239	1.6561	-2.1698
H15	-3.986	1.2412	-2.6836
C16	-2.8356	3.0556	-2.1832
C17	-1.6188	3.4865	-1.5691
H18	-1.2891	4.5208	-1.6047
C19	-0.8325	2.5424	-0.9478
C20	0.5187	2.6965	-0.3604
C21	2.4222	3.5886	0.3425
H22	2.4009	4.0909	1.3162
H23	3.2092	4.0277	-0.2797
C24	2.489	2.0466	0.4551
H25	2.6655	1.745	1.496
C26	-1.6389	-3.4189	0.4226
H27	-0.7305	-3.1074	0.9613

C28	-2.8539	-2.9981	1.2452
H29	-2.7731	-3.3918	2.2677
H30	-3.7895	-3.3925	0.8209
H31	-2.9466	-1.9067	1.3132
C32	-1.5818	-4.9327	0.2256
H33	-0.668	-5.2334	-0.3068
H34	-2.4462	-5.293	-0.3539
H35	-1.5967	-5.4505	1.1942
C36	3.5435	1.3611	-0.4297
H37	3.4069	0.2828	-0.2603
C38	4.9505	1.7375	0.0311
H39	5.0968	1.511	1.097
H40	5.1556	2.8083	-0.1197
H41	5.7033	1.1774	-0.5399
C42	3.3326	1.6379	-1.9164
H43	3.4349	2.7082	-2.1532
H44	2.3402	1.3063	-2.2538
H45	4.0822	1.1006	-2.513
C46	1.2927	-1.2799	0.5377
C47	1.832	-1.5248	1.8055
H48	1.4656	-0.9866	2.6812
C49	2.8516	-2.4613	2.0028
H50	3.2699	-2.6538	2.9918
C51	3.3374	-3.1611	0.9082
F52	4.3178	-4.0676	1.0899
C53	2.8372	-2.9539	-0.3699
H54	3.2438	-3.5216	-1.2081
C55	1.8174	-2.0151	-0.5392
H56	1.4323	-1.8562	-1.5507
C57	-0.9741	0.2265	2.0983
C58	-2.3118	0.5428	1.7983
H59	-0.7957	-0.8235	2.3481
C60	-0.1455	1.2452	2.8416
C61	-3.4751	0.8282	1.5189
Si62	-5.2693	1.1585	1.1909
H63	-0.3451	2.2498	2.44
H64	0.9217	1.0464	2.6769
C65	-0.4141	1.2371	4.35
C66	-5.8847	-0.1097	-0.0472
C67	0.4542	2.2411	5.1029
H68	-0.2326	0.2231	4.7434
H69	-1.4796	1.4515	4.5327
H70	1.5152	2.0225	4.8967

C71	0.2106	2.2369	6.6075
H72	0.2707	3.2499	4.6975
H73	0.8495	2.9676	7.1228
H74	0.4193	1.2468	7.0397
H75	-0.8359	2.4841	6.8405
H76	-6.9551	0.0482	-0.2488
H77	-5.7602	-1.1271	0.3526
H78	-5.3448	-0.0559	-1.0018
C79	-5.4581	2.9095	0.5429
C80	-6.1886	0.9686	2.8152
H81	-7.2655	1.1436	2.6696
H82	-5.8225	1.688	3.5621
H83	-6.0578	-0.0449	3.2218
H84	-6.5196	3.1304	0.3534
H85	-4.9069	3.0644	-0.3941
H86	-5.0858	3.6364	1.2797
N87	-3.6708	3.9316	-2.7732
C88	-3.342	5.3493	-2.799
H89	-4.1648	5.8966	-3.2664
H90	-3.2033	5.7409	-1.7813
H91	-2.425	5.5424	-3.3763
C92	-4.8616	3.456	-3.4634
H93	-5.4212	4.3164	-3.8397
H94	-4.6027	2.8098	-4.3158
H95	-5.5169	2.892	-2.7843

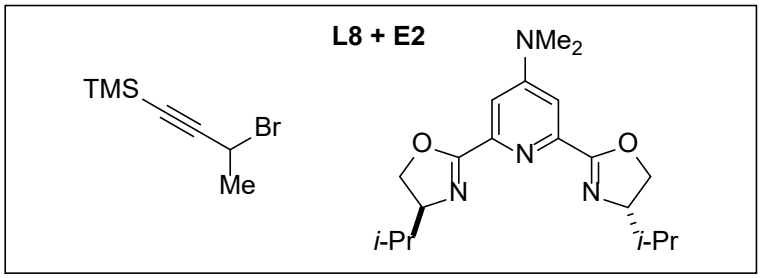

(R)-Transition State

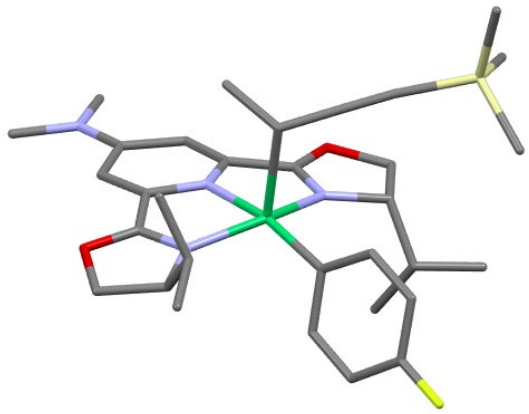

Calculated geometry

Atom	X	Y	Z
Ni1	0	0	0
O2	-4.01	0.4216	-0.2356
O3	2.3358	0.5883	-3.2454
N4	-1.9472	-0.0826	0.4622
N5	-0.7702	0.8057	-1.5867
N6	1.5818	-0.0658	-1.2433
C7	-2.801	-0.5948	1.544
H8	-2.6075	-1.6709	1.6448
C9	-4.2234	-0.354	0.9815
H10	-4.734	-1.2789	0.6906
H11	-4.8742	0.2304	1.6399
C12	-2.7085	0.4427	-0.4294
C13	-2.091	0.9661	-1.6703
C14	-2.716	1.4304	-2.8046
H15	-3.7983	1.5208	-2.8191
C16	-1.9117	1.7387	-3.9467
C17	-0.5102	1.4702	-3.8554
H18	0.1576	1.5945	-4.7029
C19	-0.0093	1	-2.6625

C20	1.3572	0.5103	-2.3685
C21	3.4852	-0.0577	-2.627
H22	4.2854	0.6866	-2.5621
H23	3.7983	-0.8728	-3.2894
C24	2.9728	-0.5357	-1.2447
H25	3.502	-0.0133	-0.4374
C26	-2.4888	0.0688	2.892
H27	-1.4062	-0.0749	3.036
C28	-2.785	1.5664	2.9052
H29	-3.8657	1.7684	2.866
H30	-2.3137	2.0876	2.0616
H31	-2.4038	2.0212	3.8294
C32	-3.2203	-0.6636	4.0155
H33	-2.9519	-1.7294	4.0386
H34	-4.3124	-0.5912	3.8951
H35	-2.9675	-0.2279	4.9916
C36	3.0813	-2.0461	-0.9868
H37	2.6971	-2.1986	0.0318
C38	4.5473	-2.4768	-1.0061
H39	4.9886	-2.3768	-2.0095
H40	4.6419	-3.5305	-0.7108
H41	5.15	-1.8756	-0.3103
C42	2.224	-2.8709	-1.9423
H43	2.3028	-3.9392	-1.6984
H44	2.5431	-2.7499	-2.9892
H45	1.1635	-2.5907	-1.8735
C46	0.6204	-1.1771	1.35
C47	1.559	-0.9744	2.3676
H48	1.9894	0.0128	2.5332
C49	1.9949	-2.0251	3.1807
H50	2.7316	-1.8697	3.9703
C51	1.4806	-3.2957	2.9667
F52	1.9026	-4.315	3.7414
C53	0.5385	-3.5443	1.9783
H54	0.1527	-4.5555	1.8409
C55	0.1143	-2.4771	1.1833
H56	-0.6235	-2.684	0.4022
C57	0.5042	1.9899	1.0696
C58	1.9134	2.0152	1.092
H59	0.0476	1.6462	2.0024
C60	-0.2188	3.0918	0.338
C61	3.142	2.0284	1.1408
Si62	4.9671	1.9146	1.4568

H63	-1.2928	2.8881	0.2504
H64	0.1903	3.2503	-0.6683
C65	5.4689	3.3762	2.5182
H66	6.5421	3.3247	2.7564
H67	4.9074	3.3849	3.4637
H68	5.2791	4.3258	1.9969
C69	5.9011	1.9368	-0.1706
C70	5.2555	0.2945	2.3597
H71	4.8903	-0.5579	1.7683
H72	4.7301	0.2861	3.3261
H73	6.3288	0.1444	2.5512
H74	5.618	2.8041	-0.7847
H75	5.7173	1.0232	-0.7535
H76	6.9828	1.995	0.0237
N77	-2.4593	2.2219	-5.076
C78	-1.6252	2.4784	-6.2416
H79	-2.2463	2.8944	-7.0393
H80	-0.8309	3.2028	-6.0102
H81	-1.1574	1.5545	-6.6138
C82	-3.8966	2.44	-5.1564
H83	-4.1367	2.876	-6.1297
H84	-4.4545	1.4972	-5.0522
H85	-4.2369	3.1351	-4.3754
H86	-0.1139	4.0404	0.8904

(S)-Transition State

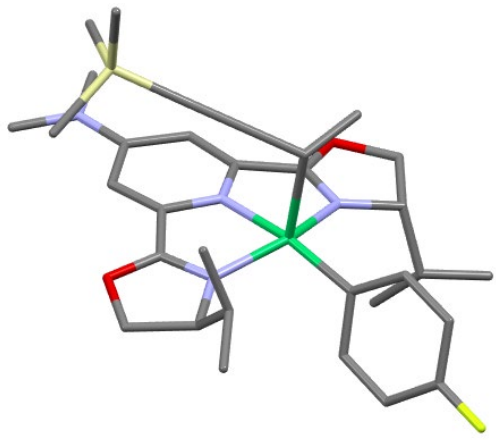

Calculated geometry

Atom	X	Y	Z

Ni1	0	0	0
O2	-3.2398	-1.3471	-2.0005
O3	1.1703	3.849	-0.2996
N4	-1.3402	-1.2505	-0.8252
N5	-1.17	1.273	-0.863
N6	1.1393	1.6455	0.0745
C7	-1.5627	-2.6961	-0.9823
H8	-0.7114	-3.1036	-1.5443
C9	-2.8462	-2.7426	-1.8493
H10	-2.6765	-3.1439	-2.8542
H11	-3.6818	-3.2733	-1.3809
C12	-2.3	-0.6345	-1.4153
C13	-2.2638	0.8437	-1.4879
C14	-3.1157	1.6904	-2.1584
H15	-3.9789	1.2833	-2.6767
C16	-2.8204	3.0885	-2.1612
C17	-1.6	3.5078	-1.5462
H18	-1.2627	4.5398	-1.5774
C19	-0.82	2.5552	-0.9298
C20	0.5345	2.6979	-0.3469
C21	2.4516	3.5743	0.3396
H22	2.4472	4.0802	1.3115
H23	3.2355	4.0036	-0.2934
C24	2.5048	2.0316	0.4556
H25	2.6836	1.73	1.4961
C26	-1.6314	-3.4333	0.3616
H27	-0.7152	-3.1359	0.895
C28	-2.8341	-3.0277	1.2096
H29	-2.7405	-3.444	2.222
H30	-3.7765	-3.4105	0.7897
H31	-2.9228	-1.9378	1.302
C32	-1.581	-4.9426	0.1307
H33	-0.6756	-5.2338	-0.4208
H34	-2.4544	-5.2882	-0.4444
H35	-1.5838	-5.4814	1.0879
C36	3.5488	1.336	-0.4342
H37	3.409	0.2593	-0.2578
C38	4.9617	1.7079	0.0116
H39	5.1164	1.4887	1.0778
H40	5.172	2.7762	-0.1495
H41	5.7061	1.1389	-0.5617
C42	3.3259	1.6049	-1.9206
H43	3.429	2.6735	-2.1647

H44	2.3299	1.2741	-2.2476
H45	4.069	1.062	-2.5204
C46	1.2924	-1.2898	0.5091
C47	1.8482	-1.5549	1.7653
H48	1.4921	-1.0322	2.6544
C49	2.8721	-2.4927	1.9326
H50	3.3041	-2.7014	2.9123
C51	3.3445	-3.1724	0.8195
F52	4.3288	-4.0799	0.9724
C53	2.8271	-2.9442	-0.4482
H54	3.2234	-3.4966	-1.3014
C55	1.8036	-2.0048	-0.5876
H56	1.4053	-1.8284	-1.5911
C57	-0.9511	0.2077	2.097
C58	-2.2943	0.5129	1.7956
H59	-0.7691	-0.8416	2.3451
C60	-0.1478	1.232	2.8568
C61	-3.4597	0.7909	1.5211
Si62	-5.2554	1.122	1.2007
H63	-0.3125	2.2441	2.4656
H64	0.9261	1.016	2.8205
C65	-5.8738	-0.1307	-0.0516
H66	-6.9456	0.0279	-0.2453
H67	-5.7454	-1.1534	0.3333
H68	-5.339	-0.0625	-1.0081
C69	-5.4462	2.8805	0.5736
C70	-6.1711	0.9122	2.8245
H71	-7.2485	1.0874	2.6833
H72	-5.8043	1.6233	3.579
H73	-6.0382	-0.1058	3.2191
H74	-6.5078	3.1031	0.3872
H75	-4.8953	3.0461	-0.3617
H76	-5.0738	3.5992	1.3185
N77	-3.6515	3.9731	-2.7438
C78	-3.3144	5.3891	-2.7614
H79	-4.1354	5.9443	-3.2229
H80	-3.1705	5.7732	-1.7416
H81	-2.398	5.5804	-3.3401
C82	-4.8463	3.5089	-3.4348
H83	-5.4025	4.375	-3.8031
H84	-4.5929	2.868	-4.2927
H85	-5.5028	2.9431	-2.7583
H86	-0.4463	1.2347	3.9184

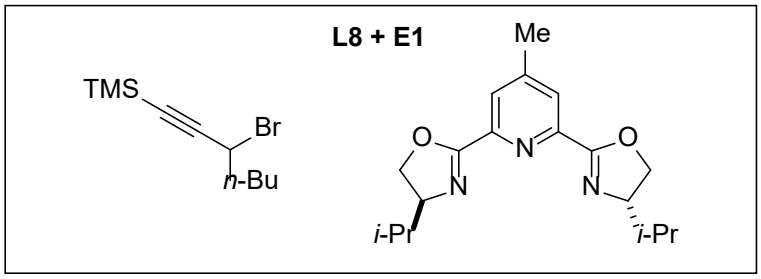

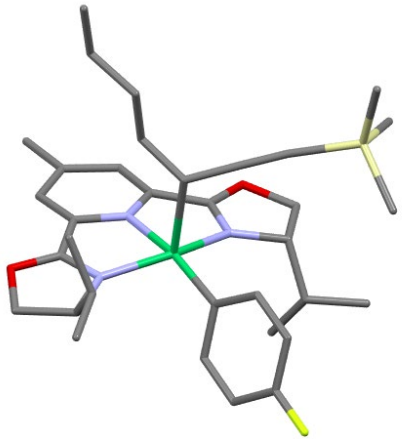

(R)-Transition State

Calculated geometry

Atom	X	Y	Z
Ni1	0	0	0
O2	-4.0037	0.444	-0.2207
O3	2.3437	0.5675	-3.2355
N4	-1.9414	-0.0774	0.4665
N5	-0.7753	0.7824	-1.6072
N6	1.5804	-0.0808	-1.2347
C7	-2.7932	-0.5613	1.564
H8	-2.6038	-1.6351	1.6901
C9	-4.2159	-0.3277	1.0002
H10	-4.7223	-1.2556	0.7112
H11	-4.8696	0.2571	1.655
C12	-2.7045	0.4479	-0.4234
C13	-2.0916	0.9603	-1.6705
C14	-2.6997	1.4503	-2.8152
H15	-3.7807	1.5816	-2.8535

C16	-1.8931	1.7431	-3.9301
C17	-0.5149	1.4831	-3.8536
H18	0.1355	1.6421	-4.713
C19	0.0006	0.9869	-2.664
C20	1.3634	0.4937	-2.362
C21	3.4817	-0.1042	-2.6218
H22	4.3052	0.6152	-2.5802
H23	3.7588	-0.939	-3.2758
C24	2.9733	-0.5467	-1.2261
H25	3.5012	0.0005	-0.4342
C26	-2.4734	0.1362	2.8933
H27	-1.3884	0.0043	3.0305
C28	-2.7829	1.6311	2.8747
H29	-3.8659	1.8225	2.8519
H30	-2.3337	2.1359	2.0096
H31	-2.3876	2.1128	3.7792
C32	-3.1881	-0.5756	4.0405
H33	-2.9072	-1.6373	4.0885
H34	-4.2817	-0.5186	3.9266
H35	-2.933	-0.1121	5.0029
C36	3.0897	-2.0492	-0.929
H37	2.7204	-2.176	0.0986
C38	4.5567	-2.476	-0.9572
H39	4.9831	-2.4038	-1.9693
H40	4.6585	-3.5208	-0.6335
H41	5.1678	-1.854	-0.2873
C42	2.222	-2.902	-1.85
H43	2.3077	-3.9628	-1.5776
H44	2.5259	-2.8093	-2.9041
H45	1.1616	-2.623	-1.7742
C46	0.6308	-1.1335	1.3779
C47	1.5872	-0.8886	2.3689
H48	2.0218	0.1037	2.4849
C49	2.0346	-1.9049	3.2181
H50	2.7845	-1.7181	3.9882
C51	1.5141	-3.1821	3.0666
F52	1.9463	-4.1677	3.8774
C53	0.5563	-3.4704	2.1044
H54	0.1672	-4.4857	2.016
C55	0.1202	-2.4374	1.2716
H56	-0.6299	-2.6749	0.5117
C57	0.4776	2.0146	1.0403
C58	1.8838	2.0793	1.0299

H59	0.0506	1.6689	1.9869
C60	-0.3011	3.0883	0.3201
C61	3.1129	2.1214	1.0519
Si62	4.9444	2.0547	1.3491
H63	-1.3418	2.7651	0.1789
H64	0.1204	3.2536	-0.6829
C65	-0.3183	4.4133	1.0904
C66	5.421	3.549	2.3753
C67	-1.1544	5.483	0.394
H68	0.7155	4.7709	1.2233
H69	-0.7149	4.2354	2.1035
H70	-0.7528	5.651	-0.6188
C71	-1.1983	6.8008	1.1585
H72	-2.179	5.1006	0.2521
H73	-1.8058	7.5522	0.635
H74	-0.1886	7.2179	1.2882
H75	-1.6291	6.6622	2.1614
H76	6.4975	3.5278	2.6028
H77	4.8692	3.5636	3.3264
H78	5.2031	4.4829	1.8368
C79	5.8608	2.0637	-0.2878
C80	5.2753	0.4603	2.2822
H81	4.9221	-0.4121	1.7132
H82	4.7606	0.4619	3.2544
H83	6.3534	0.3364	2.4648
H84	5.5498	2.9093	-0.9185
H85	5.695	1.1326	-0.8477
H86	6.9425	2.1536	-0.1059
C87	-2.5028	2.3029	-5.1806
H88	-1.8548	2.1397	-6.0492
H89	-3.4862	1.8561	-5.3722
H90	-2.6497	3.3871	-5.0643

(S)-Transition State

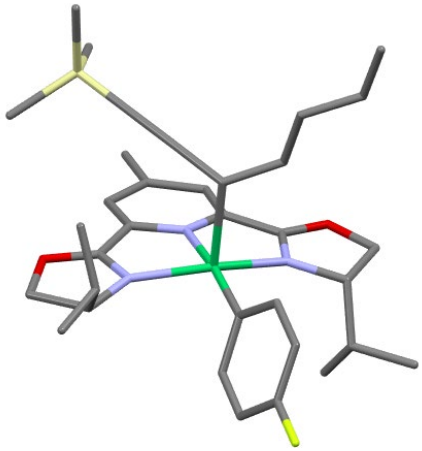

Calculated geometry

Atom	X	Y	Z
Ni1	0	0	0
O2	-3.2687	-1.3387	-1.9461
O3	1.2475	3.8064	-0.3703
N4	-1.3624	-1.2478	-0.7804
N5	-1.1539	1.2783	-0.8942
N6	1.1736	1.6085	0.0284
C7	-1.601	-2.6938	-0.9186
H8	-0.7734	-3.1072	-1.5112
C9	-2.9161	-2.7383	-1.7374
H10	-2.7998	-3.1963	-2.725
H11	-3.7512	-3.2125	-1.2106
C12	-2.3166	-0.6304	-1.3781
C13	-2.2562	0.8443	-1.492
C14	-3.0844	1.7103	-2.1907
H15	-3.9761	1.3362	-2.6928
C16	-2.7327	3.0692	-2.2551
C17	-1.5346	3.4885	-1.6502
H18	-1.201	4.5233	-1.7216
C19	-0.7643	2.5444	-0.9883
C20	0.5912	2.6681	-0.406
C21	2.5187	3.5147	0.2843
H22	2.5101	4.0256	1.2535
H23	3.3154	3.9285	-0.3425
C24	2.5457	1.9722	0.4098
H25	2.7168	1.6745	1.4527
C26	-1.6217	-3.4284	0.4281
H27	-0.6825	-3.139	0.9238

C28	-2.7848	-3.0139	1.3252
H29	-2.6463	-3.4226	2.3355
H30	-3.7456	-3.3981	0.9511
H31	-2.8683	-1.9232	1.412
C32	-1.593	-4.9382	0.1955
H33	-0.7122	-5.2373	-0.3905
H34	-2.491	-5.2764	-0.345
H35	-1.5632	-5.4767	1.1524
C36	3.579	1.2517	-0.4723
H37	3.4189	0.1789	-0.2896
C38	4.9965	1.6002	-0.022
H39	5.1421	1.3832	1.046
H40	5.227	2.6636	-0.1873
H41	5.7328	1.0148	-0.5891
C42	3.3669	1.5162	-1.961
H43	3.4883	2.5816	-2.2103
H44	2.3672	1.1993	-2.2909
H45	4.1038	0.9582	-2.5545
C46	1.276	-1.2803	0.5586
C47	1.8475	-1.4604	1.8224
H48	1.5057	-0.8766	2.6786
C49	2.8721	-2.3871	2.0373
H50	3.3179	-2.5307	3.0225
C51	3.328	-3.1402	0.9651
F52	4.3134	-4.0367	1.1643
C53	2.7933	-2.9962	-0.3077
H54	3.1778	-3.6045	-1.1276
C55	1.7693	-2.066	-0.4961
H56	1.359	-1.9537	-1.5036
C57	-0.9647	0.2816	2.0795
C58	-2.3132	0.5552	1.7815
H59	-0.7654	-0.7537	2.3718
C60	-0.1604	1.3437	2.7887
C61	-3.4868	0.7953	1.5034
Si62	-5.3047	1.0305	1.2132
H63	-0.3717	2.3284	2.3455
H64	0.9117	1.1555	2.6449
C65	-0.4469	1.3913	4.2932
C66	-5.8938	-0.3625	0.1043
C67	0.3996	2.4355	5.0155
H68	-0.2569	0.396	4.7277
H69	-1.5172	1.5984	4.455
H70	1.4657	2.2218	4.8313

C71	0.1366	2.4877	6.5158
H72	0.2094	3.425	4.568
H73	0.7607	3.2456	7.0097
H74	0.3507	1.5179	6.9894
H75	-0.9154	2.7319	6.7257
H76	-6.9753	-0.2722	-0.0784
H77	-5.7074	-1.3382	0.5772
H78	-5.3786	-0.3533	-0.866
C79	-5.5882	2.7017	0.4104
C80	-6.1567	0.9533	2.882
H81	-7.2441	1.0743	2.7625
H82	-5.794	1.7508	3.5467
H83	-5.9706	-0.0135	3.3719
H84	-6.6673	2.8947	0.3134
H85	-5.1466	2.7455	-0.5942
H86	-5.1498	3.5091	1.0151
C87	-3.6119	4.0558	-2.964
H88	-3.0163	4.8356	-3.4537
H89	-4.2468	3.5616	-3.7084
H90	-4.2702	4.5503	-2.2336

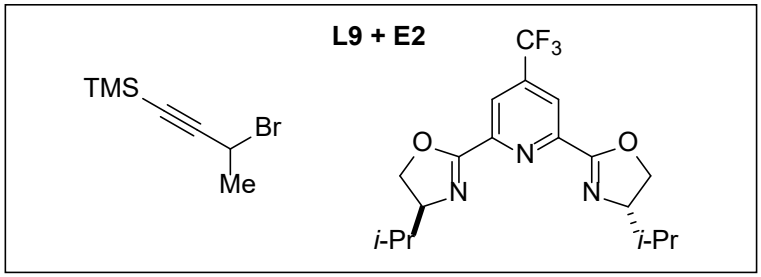

(R)-Transition State

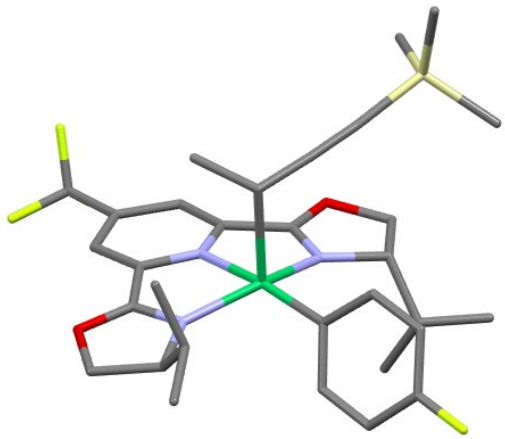

Calculated geometry

Atom	X	Y	Z
Ni1	0	0	0
O2	-3.9378	0.6308	-0.6371
O3	2.7163	0.5584	-2.911
N4	-1.9941	-0.0118	0.2673
N5	-0.5664	0.8703	-1.6442
N6	1.6625	-0.1868	-1.0851
C7	-2.9959	-0.5722	1.1915
H8	-2.9093	-1.666	1.1369
C9	-4.3327	-0.1153	0.5541
H10	-4.9647	-0.9459	0.2239
H11	-4.9178	0.561	1.1863
C12	-2.6256	0.5893	-0.6753
C13	-1.8548	1.1319	-1.8194
C14	-2.3118	1.7328	-2.9865
H15	-3.3694	1.9423	-3.136
C16	-1.3573	2.028	-3.9615
C17	-1.7735	2.7167	-5.2459
C18	-0.0105	1.6911	-3.7903
H19	0.7306	1.8677	-4.5688

C20	0.341	1.0896	-2.5898
C21	1.6279	0.484	-2.1768
C22	3.7136	-0.2615	-2.2302
H23	4.5926	0.3654	-2.0535
H24	3.9818	-1.0771	-2.9114
C25	3.0127	-0.7406	-0.9338
H26	3.4654	-0.2702	-0.0504
C27	-2.7694	-0.1625	2.6523
H28	-1.7278	-0.4436	2.8698
C29	-2.9199	1.3362	2.8955
H30	-3.9632	1.6679	2.7884
H31	-2.3046	1.9266	2.2056
H32	-2.6042	1.5852	3.9176
C33	-3.6838	-0.9795	3.5644
H34	-3.5224	-2.0586	3.4305
H35	-4.7452	-0.7673	3.3621
H36	-3.495	-0.7363	4.6186
C37	3.0056	-2.2617	-0.7182
H38	2.4952	-2.4212	0.2417
C39	4.4385	-2.7735	-0.578
H40	5.0074	-2.6543	-1.5129
H41	4.4409	-3.843	-0.328
H42	4.9772	-2.2389	0.2175
C43	2.2244	-3.0091	-1.7955
H44	2.2117	-4.0852	-1.5758
H45	2.6736	-2.8855	-2.7929
H46	1.1811	-2.6661	-1.8465
C47	0.5316	-1.1	1.4387
C48	1.5329	-0.8352	2.3795
H49	2.0227	0.1392	2.409
C50	1.9537	-1.811	3.287
H51	2.7355	-1.6119	4.0213
C52	1.3628	-3.0661	3.2414
F53	1.7677	-4.0127	4.1095
C54	0.3655	-3.3722	2.3259
H55	-0.0738	-4.3706	2.3192
C56	-0.0426	-2.3801	1.4316
H57	-0.8181	-2.6329	0.7038
C58	0.4219	2.0083	1.0521
C59	1.8152	2.1521	0.8836
H60	0.1079	1.6082	2.0202
C61	-0.4504	3.0899	0.4638
C62	3.0208	2.3219	0.7143

Si63	4.8308	2.7061	0.5435
H64	-1.5082	2.8038	0.4352
H65	-0.1309	3.3695	-0.5484
C66	5.2543	4.0125	1.8195
H67	6.3173	4.2881	1.7449
H68	5.0676	3.6411	2.8377
H69	4.6527	4.9205	1.6685
C70	5.1127	3.3542	-1.1945
C71	5.8253	1.1471	0.8685
H72	5.6977	0.3903	0.0822
H73	5.5387	0.694	1.8289
H74	6.8958	1.3975	0.9173
H75	4.5841	4.3079	-1.3394
H76	4.748	2.6489	-1.9548
H77	6.1846	3.5274	-1.3731
F78	-1.1699	2.1605	-6.2997
F79	-3.0921	2.647	-5.4363
F80	-1.4288	4.0079	-5.215
H81	-0.3854	3.9952	1.0894

(S)-Transition State

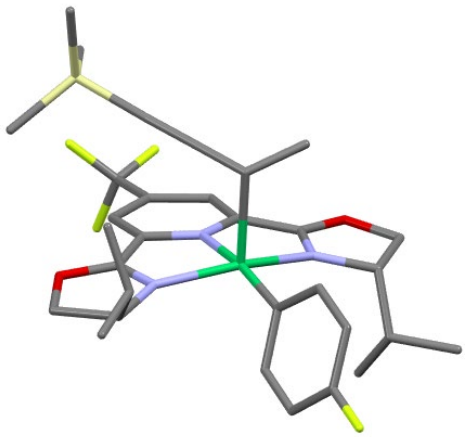

Calculated geometry

Atom	X	Y	Z
Ni1	0	0	0
O2	-3.3275	-1.275	-1.8927
O3	1.2529	3.8131	-0.3072
N4	-1.3829	-1.223	-0.7886
N5	-1.1774	1.3115	-0.8293

N6	1.1821	1.6054	0.0398
C7	-1.6285	-2.6647	-0.9658
H8	-0.8195	-3.0583	-1.596
C9	-2.9676	-2.6818	-1.7462
H10	-2.8803	-3.1017	-2.7535
H11	-3.7864	-3.1762	-1.2129
C12	-2.357	-0.5889	-1.3325
C13	-2.2973	0.8886	-1.4037
C14	-3.1454	1.7742	-2.0532
H15	-4.0593	1.4263	-2.5336
C16	-2.7635	3.1194	-2.0774
C17	-3.6431	4.1072	-2.8166
C18	-1.5637	3.5456	-1.5056
H19	-1.2397	4.5836	-1.5539
C20	-0.7789	2.5744	-0.8941
C21	0.5935	2.6784	-0.3481
C22	2.5518	3.4994	0.2816
H23	2.5985	4.0035	1.253
H24	3.3204	3.9086	-0.3824
C25	2.5665	1.9545	0.3927
H26	2.7564	1.6455	1.429
C27	-1.6102	-3.4422	0.3567
H28	-0.6585	-3.1657	0.8358
C29	-2.7499	-3.0621	1.2979
H30	-2.5831	-3.5041	2.2897
H31	-3.7192	-3.4373	0.937
H32	-2.8346	-1.9755	1.4237
C33	-1.5836	-4.9436	0.0742
H34	-0.7175	-5.2207	-0.5436
H35	-2.4945	-5.267	-0.4533
H36	-1.5276	-5.5122	1.0123
C37	3.5741	1.2326	-0.5181
H38	3.4206	0.1602	-0.3293
C39	5.004	1.5818	-0.1093
H40	5.1799	1.369	0.9549
H41	5.2314	2.644	-0.2861
H42	5.7226	0.9925	-0.6948
C43	3.3184	1.4942	-2.0004
H44	3.4287	2.5596	-2.2549
H45	2.3107	1.1734	-2.3008
H46	4.0398	0.9376	-2.6137
C47	1.2875	-1.296	0.4758
C48	1.9035	-1.5186	1.7106

H49	1.5894	-0.9703	2.5998
C50	2.9409	-2.4453	1.8503
H51	3.4239	-2.6238	2.8119
C52	3.3616	-3.1521	0.733
F53	4.359	-4.0473	0.8604
C54	2.7794	-2.9632	-0.5131
H55	3.1372	-3.5362	-1.3695
C56	1.7435	-2.0345	-0.6277
H57	1.2963	-1.8847	-1.6142
C58	-0.8948	0.2196	2.0936
C59	-2.2571	0.4836	1.8352
H60	-0.6854	-0.8199	2.3611
C61	-0.1031	1.2737	2.8256
C62	-3.4413	0.7135	1.6004
Si63	-5.2764	0.9293	1.4038
H64	-0.2949	2.2765	2.4229
H65	0.9745	1.0792	2.7816
C66	-5.8879	-0.3592	0.1859
H67	-6.9813	-0.2885	0.0819
H68	-5.6439	-1.372	0.5395
H69	-5.4404	-0.2322	-0.809
C70	-5.6227	2.6682	0.7956
C71	-6.0515	0.6552	3.0891
H72	-7.1453	0.7615	3.0284
H73	-5.676	1.3864	3.8197
H74	-5.8255	-0.3535	3.4647
H75	-6.7088	2.8392	0.7464
H76	-5.2111	2.8435	-0.207
H77	-5.1922	3.4142	1.4795
F78	-3.3268	5.3678	-2.5203
F79	-3.5166	3.9488	-4.1379
F80	-4.9322	3.9178	-2.51
H81	-0.3908	1.2854	3.8899

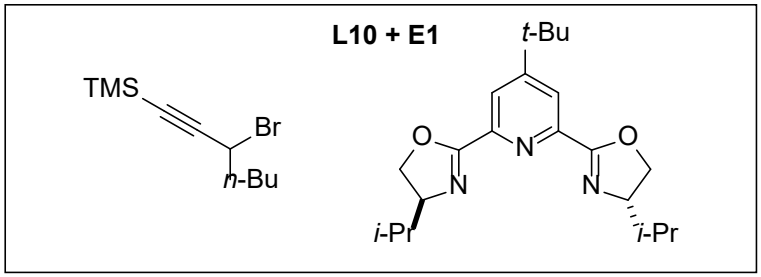

(R)-Transition State

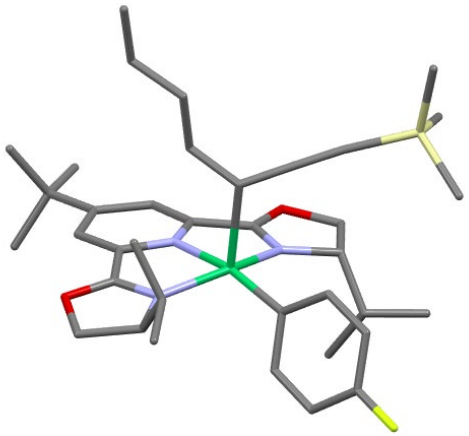

Calculated geometry

Atom	X	Y	Z
Ni1	0	0	0
O2	-3.9994	0.4721	-0.2472
O3	2.3697	0.5824	-3.2133
N4	-1.9456	-0.0664	0.4523
N5	-0.758	0.7977	-1.606
N6	1.5891	-0.0765	-1.2228
C7	-2.8082	-0.5495	1.5414
H8	-2.6285	-1.6256	1.6625
C9	-4.2255	-0.3011	0.9701
H10	-4.7388	-1.2234	0.6756
H11	-4.8775	0.2878	1.623
C12	-2.6988	0.4678	-0.4411
C13	-2.0736	0.9788	-1.682
C14	-2.6696	1.4657	-2.8319
H15	-3.7504	1.5947	-2.8616
C16	-1.8603	1.7553	-3.9491
C17	-0.4843	1.4952	-3.8539
H18	0.1899	1.6473	-4.6928
C19	0.0213	0.9998	-2.6578
C20	1.382	0.505	-2.3485

C21	3.5071	-0.0783	-2.5863
H22	4.3153	0.6563	-2.5157
H23	3.8143	-0.8966	-3.2474
C24	2.9785	-0.5515	-1.2082
H25	3.5011	-0.0291	-0.3964
C26	-2.4911	0.1373	2.8769
H27	-1.4083	-0.0058	3.0208
C28	-2.7861	1.6353	2.8648
H29	-3.867	1.8372	2.8365
H30	-2.3269	2.1405	2.0052
H31	-2.3918	2.1081	3.7743
C32	-3.2204	-0.574	4.0151
H33	-2.9505	-1.6387	4.0586
H34	-4.3127	-0.5052	3.8943
H35	-2.9671	-0.1187	4.9819
C36	3.0776	-2.0622	-0.9476
H37	2.6845	-2.2122	0.0679
C38	4.5417	-2.4995	-0.9538
H39	4.9929	-2.4007	-1.9528
H40	4.6283	-3.554	-0.6587
H41	5.1406	-1.902	-0.2514
C42	2.2245	-2.8837	-1.9097
H43	2.2965	-3.952	-1.664
H44	2.5529	-2.7655	-2.954
H45	1.1646	-2.5987	-1.8501
C46	0.6128	-1.1587	1.3648
C47	1.5693	-0.9409	2.3619
H48	2.0121	0.0452	2.4973
C49	2.0065	-1.9773	3.1921
H50	2.7569	-1.8119	3.9666
C51	1.4755	-3.2469	3.0151
F52	1.8984	-4.2521	3.8067
C53	0.5163	-3.5084	2.0466
H54	0.1185	-4.5184	1.9383
C55	0.0905	-2.4558	1.2333
H56	-0.6603	-2.6721	0.4676
C57	0.4899	1.9994	1.0643
C58	1.8966	2.0497	1.0721
H59	0.0476	1.6507	2.0028
C60	-0.2692	3.0853	0.3416
C61	3.1257	2.0782	1.1125
Si62	4.9521	1.9886	1.4343
H63	-1.3113	2.7738	0.1859

H64	0.1657	3.2522	-0.6555
C65	-0.2813	4.4057	1.1201
C66	5.4312	3.4703	2.4775
C67	-1.1024	5.4874	0.4244
H68	0.7544	4.7532	1.2639
H69	-0.6878	4.2248	2.1288
H70	-0.6933	5.6569	-0.5852
C71	-1.1376	6.8012	1.1961
H72	-2.1299	5.1161	0.2744
H73	-1.7348	7.5616	0.6738
H74	-0.1246	7.2076	1.3338
H75	-1.5752	6.6611	2.1959
H76	6.5043	3.4357	2.7192
H77	4.867	3.4841	3.4213
H78	5.2306	4.4104	1.9431
C79	5.891	1.9981	-0.1898
C80	5.2535	0.3839	2.3595
H81	4.9002	-0.4804	1.7782
H82	4.7251	0.3826	3.3242
H83	6.3277	0.248	2.5564
H84	5.5965	2.8495	-0.8206
H85	5.7246	1.071	-0.7565
H86	6.9709	2.0771	0.0074
C87	-2.5067	2.2939	-5.2249
C88	-1.4712	2.5549	-6.3224
C89	-3.523	1.2564	-5.7351
C90	-3.2249	3.6133	-4.8909
H91	-1.9795	2.9525	-7.2106
H92	-0.7204	3.2933	-6.0082
H93	-0.9515	1.6341	-6.6218
H94	-3.9895	1.6232	-6.6598
H95	-3.0302	0.2991	-5.9562
H96	-4.3242	1.0721	-5.0069
H97	-3.6933	4.0164	-5.7992
H98	-4.0154	3.4726	-4.1413
H99	-2.5161	4.3613	-4.5087

(S)-Transition State

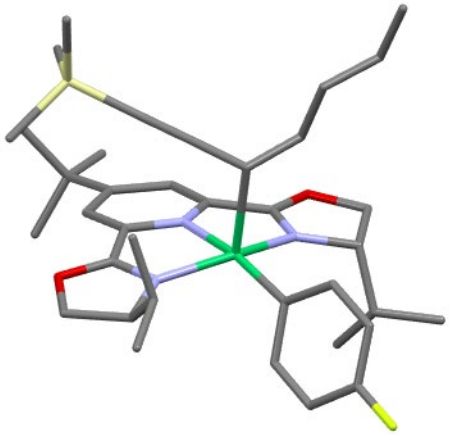

Calculated geometry

Atom	X	Y	Z
Ni1	0	0	0
O2	-3.2826	-1.2798	-1.9652
O3	1.2367	3.8212	-0.2916
N4	-1.377	-1.2214	-0.7964
N5	-1.181	1.3112	-0.821
N6	1.1662	1.6168	0.0728
C7	-1.5983	-2.6618	-1.0064
H8	-0.7873	-3.0226	-1.6545
C9	-2.9429	-2.6848	-1.7754
H10	-2.8733	-3.1425	-2.7671
H11	-3.7634	-3.1472	-1.2156
C12	-2.3354	-0.5875	-1.3696
C13	-2.2728	0.8894	-1.451
C14	-3.0578	1.7563	-2.1933
H15	-3.9303	1.371	-2.7187
C16	-2.672	3.1079	-2.2999
C17	-1.4981	3.512	-1.6449
H18	-1.1173	4.5273	-1.7194
C19	-0.773	2.5672	-0.9288
C20	0.5802	2.683	-0.3398
C21	2.5087	3.5206	0.3561
H22	2.4962	4.0059	1.3385
H23	3.3038	3.955	-0.2587
C24	2.5437	1.976	0.4422
H25	2.734	1.6534	1.4742
C26	-1.5511	-3.4776	0.2912
H27	-0.5947	-3.2048	0.763

C28	-2.6783	-3.1382	1.2624
H29	-2.4899	-3.6076	2.2377
H30	-3.65	-3.5126	0.9071
H31	-2.771	-2.0566	1.4204
C32	-1.5138	-4.9696	-0.0363
H33	-0.6566	-5.2187	-0.6782
H34	-2.431	-5.2871	-0.5566
H35	-1.4342	-5.5657	0.8828
C36	3.5668	1.2847	-0.475
H37	3.4158	0.2067	-0.3201
C38	4.9893	1.6275	-0.0363
H39	5.1519	1.38	1.0226
H40	5.2129	2.6963	-0.1738
H41	5.7193	1.062	-0.6311
C42	3.3306	1.5886	-1.9524
H43	3.444	2.6609	-2.1746
H44	2.3271	1.2765	-2.2752
H45	4.06	1.0497	-2.5722
C46	1.3193	-1.2883	0.4233
C47	1.9646	-1.5182	1.643
H48	1.649	-0.9978	2.5488
C49	3.0357	-2.4105	1.7482
H50	3.5406	-2.5907	2.6982
C51	3.4635	-3.0784	0.6099
F52	4.4975	-3.9368	0.7021
C53	2.852	-2.8873	-0.6215
H54	3.2149	-3.4304	-1.4952
C55	1.7824	-1.9933	-0.6998
H56	1.3145	-1.8398	-1.6762
C57	-0.8728	0.1384	2.1481
C58	-2.2326	0.3921	1.8994
H59	-0.6359	-0.9069	2.367
C60	-0.0606	1.1794	2.8766
C61	-3.4215	0.6048	1.6666
Si62	-5.2468	0.8214	1.4162
H63	-0.3103	2.1808	2.4951
H64	1.0076	1.0221	2.6776
C65	-0.2807	1.1389	4.3928
C66	-5.8203	-0.4439	0.156
C67	0.5784	2.1579	5.1358
H68	-0.0538	0.1251	4.7624
H69	-1.3463	1.3148	4.6124
H70	1.6382	1.9815	4.8876

C71	0.3895	2.1129	6.6476
H72	0.3451	3.1677	4.7597
H73	1.0199	2.8556	7.1563
H74	0.6496	1.1223	7.0497
H75	-0.656	2.3162	6.9231
H76	-6.911	-0.3765	0.0251
H77	-5.5794	-1.4638	0.4907
H78	-5.347	-0.2878	-0.8229
C79	-5.543	2.5668	0.8042
C80	-6.0893	0.5301	3.0659
H81	-7.1791	0.6465	2.9645
H82	-5.7367	1.2469	3.8217
H83	-5.8866	-0.4861	3.4346
H84	-6.614	2.7402	0.6208
H85	-5.004	2.7416	-0.1365
H86	-5.1959	3.3065	1.5404
C87	-3.4812	4.0571	-3.1859
C88	-2.8924	5.4709	-3.1915
C89	-3.46	3.505	-4.6235
C90	-4.9301	4.124	-2.6766
H91	-3.5117	6.1169	-3.8276
H92	-2.8763	5.9101	-2.1843
H93	-1.871	5.4876	-3.5964
H94	-4.0098	4.1873	-5.2863
H95	-2.4299	3.4193	-4.9975
H96	-3.9353	2.5171	-4.6916
H97	-5.5206	4.7709	-3.3398
H98	-5.4085	3.1354	-2.6611
H99	-4.973	4.545	-1.6629

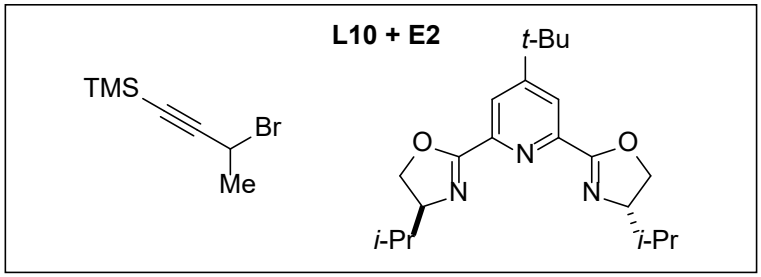

(R)-Transition State

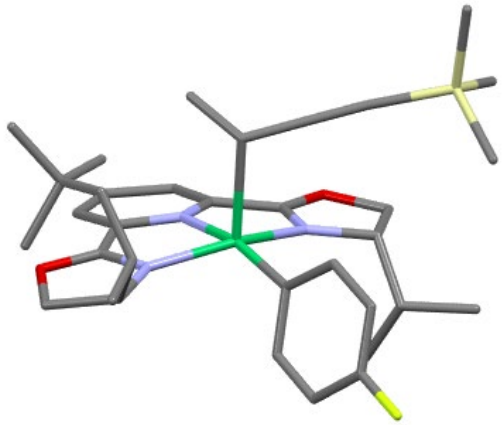

Calculated geometry

Atom	X	Y	Z
Ni1	0	0	0
O2	-4.0059	0.4487	-0.2345
O3	2.3477	0.6163	-3.2273
N4	-1.9471	-0.079	0.4587
N5	-0.7689	0.8183	-1.5939
N6	1.582	-0.0648	-1.2386
C7	-2.8055	-0.5957	1.5356
H8	-2.621	-1.6744	1.6235
C9	-4.226	-0.3368	0.9759
H10	-4.7452	-1.2539	0.6757
H11	-4.8712	0.2477	1.6395
C12	-2.7052	0.4609	-0.4267
C13	-2.0867	0.9868	-1.6647
C14	-2.694	1.4605	-2.8144
H15	-3.7763	1.5762	-2.8391
C16	-1.8947	1.7487	-3.939
C17	-0.5159	1.5018	-3.8495
H18	0.1517	1.6509	-4.6942
C19	0.0013	1.0191	-2.6532

C20	1.3659	0.5274	-2.3567
C21	3.4966	-0.0301	-2.6059
H22	4.2862	0.7228	-2.5151
H23	3.8279	-0.8274	-3.2806
C24	2.9712	-0.5406	-1.2401
H25	3.4962	-0.0416	-0.4157
C26	-2.4883	0.0496	2.8912
H27	-1.4071	-0.1052	3.0347
C28	-2.7719	1.5494	2.9224
H29	-3.8508	1.7608	2.8855
H30	-2.2961	2.0777	2.0858
H31	-2.3873	1.9892	3.8525
C32	-3.2272	-0.69	4.0051
H33	-2.9684	-1.7583	4.0155
H34	-4.3185	-0.6063	3.8847
H35	-2.9714	-0.2684	4.9865
C36	3.0679	-2.0578	-1.0198
H37	2.6681	-2.2343	-0.011
C38	4.5319	-2.4952	-1.0278
H39	4.9901	-2.369	-2.0206
H40	4.6167	-3.5574	-0.761
H41	5.1257	-1.917	-0.3053
C42	2.2209	-2.8527	-2.0092
H43	2.2919	-3.9275	-1.7933
H44	2.5555	-2.705	-3.0477
H45	1.1604	-2.57	-1.9481
C46	0.6132	-1.1942	1.333
C47	1.5577	-1.012	2.3479
H48	1.9942	-0.0303	2.5279
C49	1.991	-2.0797	3.1397
H50	2.7326	-1.9425	3.9281
C51	1.4684	-3.3435	2.9056
F52	1.8884	-4.3782	3.6595
C53	0.5197	-3.5696	1.918
H54	0.1276	-4.576	1.7648
C55	0.097	-2.4867	1.1442
H56	-0.6456	-2.6749	0.3631
C57	0.5138	1.9626	1.0832
C58	1.924	1.9842	1.1109
H59	0.0551	1.6206	2.0157
C60	-0.2002	3.0774	0.3612
C61	3.152	1.9935	1.1668
Si62	4.9758	1.8658	1.4917

H63	-1.2763	2.8852	0.2723
H64	0.2116	3.2444	-0.6428
C65	5.4796	3.3202	2.5613
H66	6.5511	3.2613	2.8056
H67	4.9127	3.3287	3.5036
H68	5.2987	4.2729	2.0425
C69	5.9181	1.8871	-0.1307
C70	5.2474	0.2399	2.3888
H71	4.8827	-0.6076	1.7901
H72	4.7144	0.2293	3.351
H73	6.3183	0.0833	2.5878
H74	5.6401	2.7548	-0.7466
H75	5.7371	0.9733	-0.7143
H76	6.9987	1.9439	0.0701
C77	-2.5548	2.2628	-5.218
C78	-1.527	2.5362	-6.3197
C79	-3.5486	1.1977	-5.7161
C80	-3.3022	3.5687	-4.8961
H81	-2.0448	2.9178	-7.2094
H82	-0.7898	3.291	-6.012
H83	-0.9903	1.6236	-6.6143
H84	-4.026	1.5455	-6.6426
H85	-3.0345	0.25	-5.9303
H86	-4.343	1.0015	-4.9836
H87	-3.7812	3.9514	-5.8078
H88	-4.0883	3.4182	-4.1439
H89	-2.6101	4.3369	-4.5234
H90	-0.0873	4.0194	0.9232

(S)-Transition State

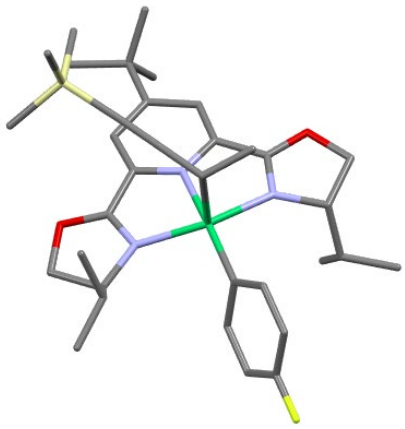

Calculated geometry

Atom	X	Y	Z
Ni1	0	0	0
O2	-3.3072	-1.279	-1.9283
O3	1.273	3.8039	-0.3662
N4	-1.3869	-1.2259	-0.7832
N5	-1.165	1.3021	-0.8495
N6	1.1849	1.6061	0.031
C7	-1.6326	-2.6669	-0.9591
H8	-0.8252	-3.0599	-1.5924
C9	-2.9735	-2.6852	-1.7356
H10	-2.8986	-3.1428	-2.7272
H11	-3.7991	-3.1454	-1.1819
C12	-2.3443	-0.5895	-1.3553
C13	-2.2712	0.8864	-1.4484
C14	-3.0904	1.7625	-2.1492
H15	-3.9816	1.379	-2.6395
C16	-2.7224	3.1152	-2.2297
C17	-1.5164	3.5123	-1.6192
H18	-1.1515	4.5357	-1.689
C19	-0.7603	2.5635	-0.9516
C20	0.6042	2.6723	-0.3888
C21	2.5568	3.4979	0.2553
H22	2.58	4.0094	1.2239
H23	3.3416	3.9025	-0.3924
C24	2.5696	1.9549	0.3805
H25	2.7625	1.6551	1.419
C26	-1.6089	-3.4483	0.3605
H27	-0.6513	-3.1796	0.8323
C28	-2.7372	-3.0628	1.3132
H29	-2.5653	-3.5098	2.3019
H30	-3.7127	-3.4288	0.9595
H31	-2.8116	-1.9759	1.4424
C32	-1.5954	-4.949	0.0739
H33	-0.7381	-5.2304	-0.5544
H34	-2.5143	-5.2649	-0.4445
H35	-1.5328	-5.5211	1.0095
C36	3.5744	1.2248	-0.527
H37	3.4149	0.1538	-0.3353

C38	5.0062	1.5672	-0.1197
H39	5.1811	1.3567	0.9452
H40	5.2393	2.6277	-0.2995
H41	5.7219	0.9725	-0.7033
C42	3.3208	1.483	-2.0104
H43	3.4373	2.5471	-2.268
H44	2.3113	1.1672	-2.3101
H45	4.039	0.9203	-2.6221
C46	1.2898	-1.2972	0.4773
C47	1.9144	-1.513	1.7096
H48	1.6059	-0.958	2.5969
C49	2.9527	-2.4387	1.8509
H50	3.4411	-2.6102	2.8112
C51	3.3674	-3.1536	0.7366
F52	4.3661	-4.0482	0.8649
C53	2.7782	-2.9734	-0.5073
H54	3.1312	-3.5524	-1.3617
C55	1.7417	-2.0453	-0.6223
H56	1.2894	-1.9028	-1.6076
C57	-0.8875	0.2285	2.1102
C58	-2.2479	0.4877	1.8448
H59	-0.6719	-0.8088	2.3806
C60	-0.0927	1.2913	2.8251
C61	-3.4314	0.7136	1.602
Si62	-5.2545	0.9524	1.3522
H63	-0.2845	2.2881	2.4079
H64	0.9845	1.0949	2.7786
C65	-5.8608	-0.3689	0.1676
H66	-6.9489	-0.2802	0.0283
H67	-5.6482	-1.3729	0.5638
H68	-5.38	-0.2844	-0.8165
C69	-5.5379	2.6673	0.65
C70	-6.0853	0.7692	3.0233
H71	-7.1743	0.8957	2.9258
H72	-5.7146	1.5235	3.7326
H73	-5.8924	-0.2265	3.4486
H74	-6.6129	2.8503	0.5022
H75	-5.0374	2.7785	-0.3213
H76	-5.1478	3.4416	1.3265
C77	-3.5465	4.1435	-3.0051
H78	-0.3754	1.3188	3.8905
C79	-3.8826	5.323	-2.0762
C80	-2.7019	4.6388	-4.1939

C81	-4.8502	3.5432	-3.54
H82	-4.4773	6.0644	-2.6273
H83	-4.469	4.9896	-1.2091
H84	-2.9797	5.8284	-1.7085
H85	-3.2783	5.3733	-4.7733
H86	-1.774	5.125	-3.8635
H87	-2.4366	3.807	-4.8615
H88	-5.4173	4.3228	-4.0654
H89	-4.6639	2.7307	-4.2558
H90	-5.4846	3.1563	-2.7304

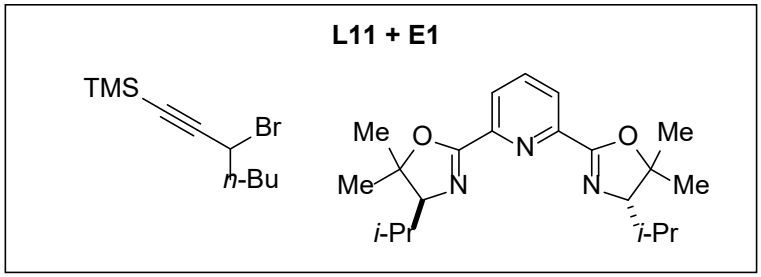

(R)-Transition State

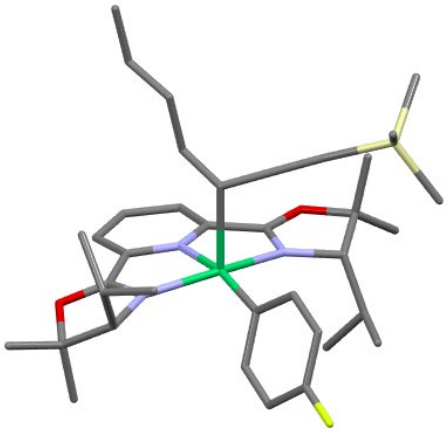

Calculated geometry

Atom	X	Y	Z
Ni1	0	0	0
O2	-4.0433	0.3498	-0.1561
O3	2.1554	0.4465	-3.4237
N4	-1.9563	0.0551	0.6026
N5	-0.8637	0.6671	-1.6318
N6	1.5464	-0.1821	-1.3587
C7	-2.817	-0.3176	1.7462
H8	-2.4872	-1.2894	2.1325
C9	-4.1991	-0.5062	1.0516
C10	-4.3469	-1.9325	0.5402
C11	-5.435	-0.0494	1.7936
C12	-2.7458	0.44	-0.3373
C13	-2.1783	0.8594	-1.6362
C14	-2.8422	1.3048	-2.7723
H15	-3.9209	1.4523	-2.7646
C16	-2.0742	1.5376	-3.917
C17	-0.701	1.2813	-3.9151
H18	-0.0904	1.4134	-4.8068
C19	-0.1365	0.8236	-2.7297

C20	1.2444	0.36	-2.4843
C21	3.4307	0.0454	-2.7827
C22	4.1558	1.3351	-2.4382
C23	4.1968	-0.7698	-3.8033
C24	2.9293	-0.6857	-1.4882
H25	3.5123	-0.3219	-0.6336
C26	-2.7565	0.6986	2.9002
H27	-3.6279	0.4647	3.53
C28	-1.5168	0.489	3.7683
H29	-0.5935	0.6955	3.2137
H30	-1.4521	-0.547	4.1297
H31	-1.5445	1.1552	4.6414
C32	-2.874	2.1518	2.4391
H33	-3.7252	2.3168	1.7652
H34	-1.9684	2.4728	1.9091
H35	-3.0001	2.8158	3.3046
C36	3.0005	-2.2298	-1.5195
H37	3.9196	-2.4646	-2.0734
C38	1.8242	-2.861	-2.2649
H39	0.8918	-2.7456	-1.6933
H40	1.9973	-3.936	-2.4084
H41	1.6658	-2.4144	-3.2573
C42	3.1752	-2.8447	-0.1323
H43	3.3518	-3.926	-0.2212
H44	2.289	-2.6977	0.4936
H45	4.0362	-2.4053	0.3903
C46	0.6333	-1.0275	1.4605
C47	1.6697	-0.7841	2.3669
H48	2.2266	0.1507	2.3291
C49	2.0314	-1.7261	3.3332
H50	2.8396	-1.5377	4.0416
C51	1.3465	-2.932	3.3836
F52	1.6934	-3.8468	4.31
C53	0.311	-3.2196	2.5057
H54	-0.205	-4.1783	2.5727
C55	-0.0377	-2.2576	1.5551
H56	-0.8531	-2.4954	0.8658
C57	0.6519	2.1122	0.8005
C58	2.0552	2.0932	0.8665
H59	0.1567	1.891	1.7493
C60	-0.0285	3.129	-0.0812
C61	3.2807	2.0772	0.9733
Si62	5.0859	2.012	1.4094

H63	-1.093	2.8776	-0.1825
H64	0.408	3.1112	-1.0914
C65	0.0739	4.551	0.484
C66	5.212	2.4331	3.2329
C67	-0.6725	5.572	-0.3697
H68	1.1355	4.8339	0.5666
H69	-0.329	4.5614	1.5102
H70	-0.2756	5.5406	-1.3977
C71	-0.5793	6.9916	0.1773
H72	-1.7304	5.2705	-0.4459
H73	-1.1283	7.7049	-0.4531
H74	0.4668	7.328	0.2301
H75	-0.997	7.0527	1.1934
H76	6.2628	2.4085	3.5596
H77	4.6486	1.7092	3.84
H78	4.8126	3.4373	3.4363
C79	6.0181	3.2616	0.3704
C80	5.7133	0.2662	1.1224
H81	5.7341	-0.0021	0.057
H82	5.0808	-0.4634	1.6493
H83	6.7384	0.1731	1.5123
H84	5.6349	4.2772	0.5473
H85	5.9304	3.0439	-0.7032
H86	7.0863	3.2494	0.6346
H87	-2.5558	1.8954	-4.827
H88	-4.4772	-2.6117	1.3929
H89	-5.2235	-2.0165	-0.1147
H90	-3.4526	-2.2485	-0.0152
H91	-5.5638	-0.6582	2.6975
H92	-5.3837	1.0046	2.0843
H93	-6.3173	-0.1958	1.1572
H94	5.1269	1.0945	-1.9867
H95	4.3302	1.9288	-3.3447
H96	3.579	1.9299	-1.7185
H97	5.1539	-1.0982	-3.379
H98	3.6356	-1.6504	-4.1346
H99	4.4106	-0.142	-4.6781

(S)-Transition State

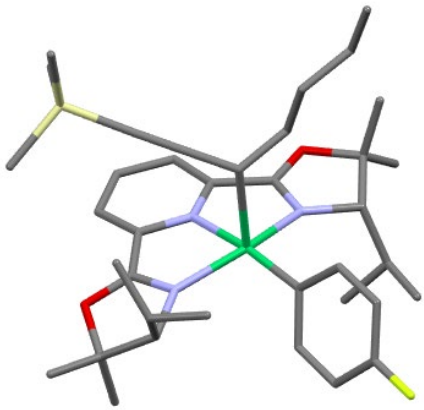

Calculated geometry

Atom	X	Y	Z
Ni1	0	0	0
O2	-3.2094	-1.4503	-2.0029
O3	1.0227	3.8965	-0.4348
N4	-1.3932	-1.3246	-0.6975
N5	-1.2259	1.2283	-0.8802
N6	1.1609	1.6893	-0.0717
C7	-1.634	-2.7775	-0.8477
H8	-0.6936	-3.2568	-1.1453
C9	-2.6053	-2.8084	-2.0674
C10	-1.8181	-2.8569	-3.37
C11	-3.7266	-3.8233	-2.0619
C12	-2.3358	-0.7275	-1.3378
C13	-2.332	0.7485	-1.4349
C14	-3.2282	1.583	-2.091
H15	-4.1219	1.1794	-2.5639
C16	-2.9278	2.9475	-2.1304
C17	-1.7438	3.4336	-1.5698
H18	-1.4712	4.4861	-1.6268
C19	-0.9	2.5112	-0.9621
C20	0.472	2.7084	-0.447
C21	2.3557	3.7301	0.1938
C22	2.2427	4.269	1.6099
C23	3.3216	4.5479	-0.6394
C24	2.533	2.1684	0.1955
H25	2.8219	1.8582	1.2087
C26	-2.1229	-3.4618	0.4404

H27	-2.4863	-4.4472	0.1102
C28	-0.9803	-3.7171	1.4215
H29	-1.3365	-4.3193	2.2686
H30	-0.5782	-2.7778	1.8201
H31	-0.1483	-4.2538	0.9447
C32	-3.2708	-2.7241	1.126
H33	-4.0795	-2.457	0.4343
H34	-2.9195	-1.793	1.5859
H35	-3.7027	-3.3479	1.9205
C36	3.5738	1.6005	-0.7999
H37	4.3429	2.3778	-0.897
C38	2.9894	1.3473	-2.1895
H39	2.4576	2.225	-2.5852
H40	2.2808	0.5066	-2.1724
H41	3.7905	1.0967	-2.8976
C42	4.2911	0.3669	-0.254
H43	3.6082	-0.4789	-0.1264
H44	4.7554	0.5795	0.7197
H45	5.0883	0.0577	-0.9448
C46	1.2774	-1.2625	0.5923
C47	1.8801	-1.3799	1.849
H48	1.5945	-0.7207	2.6703
C49	2.8633	-2.3398	2.1025
H50	3.3333	-2.4353	3.0823
C51	3.2485	-3.1892	1.0749
F52	4.1968	-4.1165	1.3112
C53	2.6827	-3.1091	-0.1897
H54	3.0136	-3.7909	-0.9743
C55	1.6994	-2.1439	-0.4152
H56	1.2658	-2.0813	-1.4171
C57	-0.9429	0.3712	2.123
C58	-2.2871	0.6769	1.8529
H59	-0.7478	-0.667	2.4041
C60	-0.0895	1.4239	2.7825
C61	-3.4599	0.9589	1.6103
Si62	-5.2751	1.2908	1.3986
H63	-0.3694	2.4145	2.3951
H64	0.9669	1.2685	2.5247
C65	-0.2251	1.4134	4.3088
C66	-5.9973	-0.0181	0.2646
C67	0.652	2.4656	4.981
H68	0.0428	0.4125	4.686
H69	-1.2804	1.5732	4.5832

H70	1.6996	2.3076	4.6754
C71	0.5501	2.4474	6.5017
H72	0.3746	3.4623	4.6
H73	1.1898	3.2149	6.9592
H74	0.8563	1.4715	6.9073
H75	-0.4829	2.6322	6.8321
H76	-7.052	0.2133	0.0515
H77	-5.9576	-1.0075	0.7423
H78	-5.4624	-0.0817	-0.6931
C79	-5.5023	3.0088	0.6826
C80	-6.0617	1.1832	3.0976
H81	-7.1464	1.3567	3.0284
H82	-5.6369	1.9361	3.7774
H83	-5.9006	0.1897	3.5408
H84	-6.5741	3.2541	0.6341
H85	-5.0922	3.0844	-0.3334
H86	-5.0077	3.7642	1.3105
H87	-3.6108	3.6358	-2.6284
H88	-1.3572	-3.8475	-3.4781
H89	-2.4819	-2.682	-4.2262
H90	-1.0171	-2.1041	-3.3773
H91	-3.3029	-4.8348	-2.1004
H92	-4.3625	-3.7423	-1.1752
H93	-4.3491	-3.6821	-2.9548
H94	3.2155	4.176	2.1109
H95	1.9527	5.3275	1.5973
H96	1.5038	3.7026	2.189
H97	4.3328	4.4853	-0.2186
H98	3.3489	4.2135	-1.6826
H99	3.0096	5.6001	-0.6176

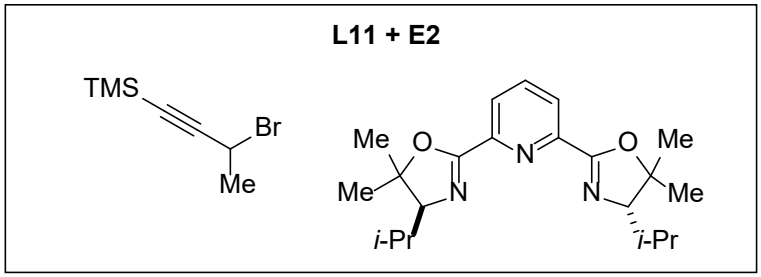

(R)-Transition State

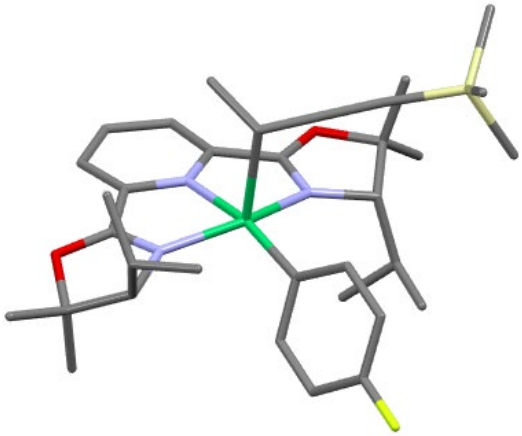

Calculated geometry

Atom	X	Y	Z
Ni1	0	0	0
O2	-4.0471	0.3248	-0.1479
O3	2.1368	0.483	-3.433
N4	-1.9584	0.0295	0.6054
N5	-0.8698	0.6953	-1.617
N6	1.5385	-0.1738	-1.3738
C7	-2.8166	-0.3826	1.737
H8	-2.4774	-1.3614	2.097
C9	-4.1957	-0.5663	1.0352
C10	-4.3274	-1.9793	0.4838
C11	-5.4374	-0.1442	1.7879
C12	-2.7501	0.4316	-0.325
C13	-2.1856	0.8806	-1.6156
C14	-2.8555	1.3334	-2.7453
H15	-3.9352	1.4737	-2.7327
C16	-2.0931	1.5799	-3.8907
C17	-0.7192	1.3273	-3.8967
H18	-0.1132	1.466	-4.7905
C19	-0.1482	0.8617	-2.7175

C20	1.2324	0.3888	-2.4879
C21	3.4129	0.0555	-2.8113
C22	4.1604	1.3296	-2.4567
C23	4.1549	-0.757	-3.8517
C24	2.9165	-0.6856	-1.5205
H25	3.5087	-0.3337	-0.6673
C26	-2.7669	0.6022	2.918
H27	-3.6343	0.3409	3.5425
C28	-1.5223	0.3856	3.7773
H29	-0.6045	0.6283	3.2283
H30	-1.4376	-0.6606	4.1035
H31	-1.5605	1.0217	4.6722
C32	-2.9008	2.0655	2.4957
H33	-3.7566	2.2397	1.8299
H34	-1.9999	2.408	1.9705
H35	-3.0297	2.7054	3.3788
C36	2.9774	-2.2302	-1.5653
H37	3.8812	-2.4675	-2.1426
C38	1.7803	-2.8489	-2.2874
H39	0.8618	-2.7324	-1.694
H40	1.9437	-3.9238	-2.4429
H41	1.6023	-2.3937	-3.2727
C42	3.1822	-2.854	-0.1862
H43	3.337	-3.938	-0.2836
H44	2.318	-2.6935	0.4664
H45	4.0663	-2.4318	0.3112
C46	0.6359	-1.0547	1.4397
C47	1.658	-0.8278	2.3661
H48	2.2073	0.1122	2.3625
C49	2.0149	-1.7939	3.3105
H50	2.8122	-1.6188	4.0344
C51	1.3388	-3.0057	3.3191
F52	1.681	-3.943	4.2244
C53	0.3166	-3.2767	2.4205
H54	-0.1929	-4.2406	2.4546
C55	-0.0267	-2.2918	1.4918
H56	-0.8315	-2.5167	0.7858
C57	0.6508	2.0861	0.8179
C58	2.0565	2.0467	0.8824
H59	0.1542	1.8629	1.7652
C60	-0.003	3.1304	-0.0488
C61	3.2812	2.0194	0.9863
Si62	5.0871	1.9431	1.4186

H63	-1.0877	2.9848	-0.1152
H64	0.418	3.1472	-1.0628
C65	5.216	2.3383	3.2477
H66	6.267	2.3082	3.5731
H67	4.6523	1.6066	3.8452
H68	4.8178	3.3399	3.4654
C69	6.0209	3.2054	0.3961
C70	5.7115	0.2011	1.1044
H71	5.7287	-0.0508	0.035
H72	5.0793	-0.5353	1.622
H73	6.7375	0.1009	1.4899
H74	5.641	4.2196	0.5876
H75	5.9311	3.0028	-0.6802
H76	7.0895	3.1865	0.6585
H77	-2.5798	1.943	-4.7959
H78	-4.4511	-2.6835	1.3171
H79	-5.2024	-2.0545	-0.1742
H80	-3.4293	-2.2699	-0.0792
H81	-5.5604	-0.7797	2.6741
H82	-5.3982	0.9016	2.1084
H83	-6.3173	-0.2824	1.1465
H84	5.1327	1.0684	-2.0192
H85	4.3335	1.9344	-3.356
H86	3.5998	1.9215	-1.7218
H87	5.1123	-1.1047	-3.4439
H88	3.5765	-1.6251	-4.1866
H89	4.3666	-0.1212	-4.7211
H90	0.1636	4.1292	0.3878

(S)-Transition State

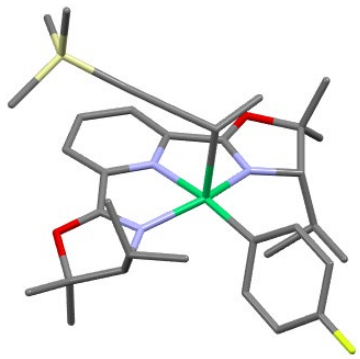

Calculated geometry

Atom	X	Y	Z
Ni1	0	0	0
O2	-3.2289	-1.4089	-2.0098
O3	1.049	3.8929	-0.433
N4	-1.4033	-1.3127	-0.7149
N5	-1.2258	1.2443	-0.8614
N6	1.1732	1.6844	-0.0723
C7	-1.6488	-2.7619	-0.8911
H8	-0.7119	-3.2365	-1.2073
C9	-2.6314	-2.768	-2.1025
C10	-1.8563	-2.7976	-3.4129
C11	-3.757	-3.7781	-2.1041
C12	-2.3476	-0.7011	-1.3386
C13	-2.3374	0.776	-1.4151
C14	-3.2324	1.6217	-2.0584
H15	-4.1308	1.2274	-2.5304
C16	-2.9246	2.9848	-2.0873
C17	-1.7332	3.4583	-1.5319
H18	-1.4532	4.5091	-1.5834
C19	-0.8915	2.5254	-0.9371
C20	0.4879	2.7096	-0.437
C21	2.3926	3.7146	0.1685
C22	2.3153	4.2612	1.5839
C23	3.3489	4.5184	-0.6892
C24	2.5536	2.1506	0.1742
H25	2.8522	1.8411	1.1847
C26	-2.1255	-3.472	0.3874
H27	-2.4939	-4.4498	0.0408
C28	-0.9731	-3.7487	1.3512
H29	-1.3212	-4.3684	2.1892
H30	-0.5668	-2.8179	1.7653
H31	-0.1463	-4.2758	0.8549
C32	-3.2644	-2.7468	1.1006
H33	-4.0782	-2.4606	0.4228
H34	-2.9052	-1.8279	1.5785
H35	-3.6913	-3.3876	1.8842
C36	3.5755	1.5687	-0.8334
H37	4.3438	2.3432	-0.9546
C38	2.9661	1.2999	-2.2092
H39	2.4285	2.1738	-2.6056

H40	2.2571	0.4605	-2.1702
H41	3.7543	1.0401	-2.9285
C42	4.3018	0.3415	-0.2849
H43	3.6201	-0.5004	-0.1288
H44	4.7886	0.5681	0.6745
H45	5.0825	0.0193	-0.9885
C46	1.2772	-1.2765	0.5592
C47	1.8922	-1.4259	1.8061
H48	1.6171	-0.7857	2.6457
C49	2.8745	-2.395	2.0257
H50	3.3548	-2.5158	2.9977
C51	3.2457	-3.2207	0.9738
F52	4.1926	-4.1568	1.1779
C53	2.6673	-3.1078	-0.2827
H54	2.9874	-3.7714	-1.0871
C55	1.6855	-2.134	-0.4743
H56	1.2417	-2.0456	-1.4698
C57	-0.9113	0.3515	2.1254
C58	-2.2629	0.6438	1.8603
H59	-0.7102	-0.6846	2.4079
C60	-0.0806	1.4153	2.7918
C61	-3.4393	0.9166	1.6288
Si62	-5.2572	1.2461	1.4339
H63	-0.3191	2.4105	2.3966
H64	0.994	1.2366	2.6695
C65	-5.9862	-0.0361	0.2741
H66	-7.0421	0.2015	0.074
H67	-5.9449	-1.0365	0.7281
H68	-5.4587	-0.0782	-0.6887
C69	-5.4908	2.9799	0.7589
C70	-6.0339	1.0964	3.1342
H71	-7.1198	1.2661	3.0749
H72	-5.6089	1.8355	3.8288
H73	-5.8657	0.0937	3.5536
H74	-6.5633	3.2237	0.7187
H75	-5.0831	3.0803	-0.2559
H76	-4.9966	3.7217	1.4031
H77	-3.6067	3.6816	-2.5744
H78	-1.4006	-3.7881	-3.5421
H79	-2.527	-2.6052	-4.2598
H80	-1.0522	-2.0481	-3.4146
H81	-3.3383	-4.7907	-2.1648
H82	-4.3841	-3.7103	-1.21

H83	-4.3874	-3.6184	-2.9884
H84	3.297	4.1583	2.0651
H85	2.0384	5.3231	1.5723
H86	1.5806	3.7057	2.1794
H87	4.3684	4.4483	-0.2901
H88	3.3504	4.1781	-1.731
H89	3.0476	5.5737	-0.6668
H90	-0.2907	1.4307	3.8742

5. References

(1) Markownikoff, W. I. Ueber Die Abhängigkeit Der Verschiedenen Vertretbarkeit Des Radicalwasserstoffs in Den Isomeren Buttersäuren. *Justus Liebigs Ann. Chem.* **1870**, *153* (2), 228–259. https://doi.org/10.1002/jlac.18701530204.

(2) Saytzeff, A. Zur Kenntniss Der Reihenfolge Der Analgerung Und Ausscheidung Der Jodwasserstoffelemente in Organischen Verbindungen. *Justus Liebigs Ann. Chem.* **1875**, *179* (3), 296–301. https://doi.org/10.1002/jlac.18751790304.

(3) XIV. Researches into the Molecular Constitution of the Organic Bases. *Philos. Trans. R. Soc. Lond.* **1851**, *141*, 357–398. https://doi.org/10.1098/rstl.1851.0017.

(4) Walden, P. Ueber Die Gegenseitige Umwandlung Optischer Antipoden. *Berichte Dtsch. Chem. Ges.* **1896**, *29* (1), 133–138. https://doi.org/10.1002/cber.18960290127.

(5) Schrödinger, E. An Undulatory Theory of the Mechanics of Atoms and Molecules. *Phys. Rev.* **1926**, *28* (6), 1049–1070. https://doi.org/10.1103/PhysRev.28.1049.

(6) Hartree, D. R. The Wave Mechanics of an Atom with a Non-Coulomb Central Field. Part II. Some Results and Discussion. *Math. Proc. Camb. Philos. Soc.* **1928**, *24* (1), 111–132. https://doi.org/10.1017/S0305004100011920.

(7) Hückel, E. Theory of Free Radicals of Organic Chemistry. *Trans Faraday Soc* **1934**, *30* (0), 40–52. https://doi.org/10.1039/TF9343000040.

(8) Woodward, R. B.; Hoffmann, R. Stereochemistry of Electrocyclic Reactions. *J. Am. Chem. Soc.* **1965**, *87* (2), 395–397. https://doi.org/10.1021/ja01080a054.

(9) Stockdale, T. P.; Lam, N. Y. S.; Anketell, M. J.; Paterson, I. The Stereocontrolled Total Synthesis of Polyketide Natural Products: A Thirty-Year Journey. *Bull. Chem. Soc. Jpn.* **2021**, *94* (2), 713–731. https://doi.org/10.1246/bcsj.20200309.

(10) Cram, D. J.; Elhafez, F. A. A. Studies in Stereochemistry. X. The Rule of "Steric Control of Asymmetric Induction" in the Syntheses of Acyclic Systems. *J. Am. Chem. Soc.* **1952**, *74* (23), 5828–5835. https://doi.org/10.1021/ja01143a007.

(11) Chérest, M.; Felkin, H.; Prudent, N. Torsional Strain Involving Partial Bonds. The Stereochemistry of the Lithium Aluminium Hydride Reduction of Some Simple Open-Chain Ketones. *Tetrahedron Lett.* **1968**, *9* (18), 2199–2204. https://doi.org/10.1016/S0040-4039(00)89719-1.

(12) Nguyen Trong Anh, .; Eisenstein, O.; Lefour, J. M.; Tran Huu Dau, M. E. Orbital Factors and Asymmetric Induction. *J. Am. Chem. Soc.* **1973**, *95* (18), 6146–6147. https://doi.org/10.1021/ja00799a068.

(13) Prelog, V. Untersuchungen Über Asymmetrische Synthesen I. Über Den Sterischen Verlauf Der Reaktion von α-Ketosäure-estern Optisch Aktiver Alkohole Mit *Grignard* 'schen Verbindungen. *Helv. Chim. Acta* **1953**, *36* (1), 308–319. https://doi.org/10.1002/hlca.19530360140.

(14) Zimmerman, H. E.; Traxler, M. D. The Stereochemistry of the Ivanov and Reformatsky Reactions. I. *J. Am. Chem. Soc.* **1957**, *79* (8), 1920–1923. https://doi.org/10.1021/ja01565a041.

(15) Leitereg, T. J.; Cram, D. J. Studies in Stereochemistry. XXXVII. Open-Chain Models for 1,3-Asymmetric Induction in Stereospecific Addition Polymerization. *J. Am. Chem. Soc.* **1968**, *90* (15), 4011–4018. https://doi.org/10.1021/ja01017a018.

(16) Reetz, M. T.; Jung, A. 1,3-Asymmetric Induction in Addition Reactions of Chiral .Beta.-Alkoxy Aldehydes: Efficient Chelation Control via Lewis Acidic Titanium Reagents. *J. Am. Chem. Soc.* **1983**, *105* (14), 4833–4835. https://doi.org/10.1021/ja00352a051.
(17) Reetz, M. T.; Kesseler, K.; Jung, A. Concerning the Role of Lewis Acids in Chelation Controlled Addition to Chiral Alkoxy Aldehydes. *Tetrahedron Lett.* **1984**, *25* (7), 729–732. https://doi.org/10.1016/S0040-4039(01)80011-3.
(18) Houk, K. N.; Paddon-Row, M. N.; Rondan, N. G.; Wu, Y.-D.; Brown, F. K.; Spellmeyer, D. C.; Metz, J. T.; Li, Y.; Loncharich, R. J. Theory and Modeling of Stereoselective Organic Reactions. *Science* **1986**, *231* (4742), 1108–1117. https://doi.org/10.1126/science.3945819.
(19) Paddon-Row, M. N.; Rondan, N. G.; Houk, K. N. Staggered Models for Asymmetric Induction: Attack Trajectories and Conformations of Allylic Bonds from Ab Initio Transition Structures of Addition Reactions. *J. Am. Chem. Soc.* **1982**, *104* (25), 7162–7166. https://doi.org/10.1021/ja00389a045.
(20) B:urgi, H. B.; Dunitz, J. D.; Lehn, J. M.; Wipff, G. Stereochemistry of Reaction Paths at Carbonyl Centres. *Tetrahedron* **1974**, *30* (12), 1563–1572. https://doi.org/10.1016/S0040-4020(01)90678-7.
(21) Burgi, H. B.; Dunitz, J. D.; Shefter, Eli. Geometrical Reaction Coordinates. II. Nucleophilic Addition to a Carbonyl Group. *J. Am. Chem. Soc.* **1973**, *95* (15), 5065–5067. https://doi.org/10.1021/ja00796a058.
(22) Chipot, C. Recent Advances in Simulation Software and Force Fields: Their Importance in Theoretical and Computational Chemistry and Biophysics. *J. Phys. Chem. B* **2024**, *128* (49), 12023–12026. https://doi.org/10.1021/acs.jpcb.4c06231.
(23) Eksterowicz, J. E.; Houk, K. N. Transition-State Modeling with Empirical Force Fields. *Chem. Rev.* **1993**, *93* (7), 2439–2461. https://doi.org/10.1021/cr00023a006.
(24) Terada, Y.; Yamamura, S. Stereochemical Studies on Germacrenes: An Application of Molecular Mechanics Calculations. *Tetrahedron Lett.* **1979**, *20* (35), 3303–3306. https://doi.org/10.1016/S0040-4039(01)95391-2.
(25) Marshall, J. A.; Grote, J.; Audia, J. E. Acyclic Stereocontrol in Catalyzed Intramolecular Diels-Alder Cyclizations Leading to Octahydronaphthalenecarboxaldehydes. *J. Am. Chem. Soc.* **1987**, *109* (4), 1186–1194. https://doi.org/10.1021/ja00238a030.
(26) Lacoske, M. H.; Theodorakis, E. A. Spirotetronate Polyketides as Leads in Drug Discovery. *J. Nat. Prod.* **2015**, *78* (3), 562–575. https://doi.org/10.1021/np500757w.
(27) Lewis-Atwell, T.; Townsend, P. A.; Grayson, M. N. Comparisons of Different Force Fields in Conformational Analysis and Searching of Organic Molecules: A Review. *Tetrahedron* **2021**, *79*, 131865. https://doi.org/10.1016/j.tet.2020.131865.
(28) Odinokov, A.; Yakubovich, A.; Son, W.-J.; Jung, Y.; Choi, H. Exploiting the Quantum Mechanically Derived Force Field for Functional Materials Simulations. *Npj Comput. Mater.* **2021**, *7* (1), 155. https://doi.org/10.1038/s41524-021-00628-z.
(29) Becke, A. D. Density-Functional Exchange-Energy Approximation with Correct Asymptotic Behavior. *Phys. Rev. A* **1988**, *38* (6), 3098–3100. https://doi.org/10.1103/PhysRevA.38.3098.
(30) Vosko, S. H.; Wilk, L.; Nusair, M. Accurate Spin-Dependent Electron Liquid Correlation Energies for Local Spin Density Calculations: A Critical Analysis. *Can. J. Phys.* **1980**, *58* (8), 1200–1211. https://doi.org/10.1139/p80-159.

(31) Lee, C.; Yang, W.; Parr, R. G. Development of the Colle-Salvetti Correlation-Energy Formula into a Functional of the Electron Density. *Phys. Rev. B* **1988**, *37* (2), 785–789. https://doi.org/10.1103/PhysRevB.37.785.
(32) Becke, A. D. Density-Functional Thermochemistry. III. The Role of Exact Exchange. *J. Chem. Phys.* **1993**, *98* (7), 5648–5652. https://doi.org/10.1063/1.464913.
(33) Stephens, P. J.; Devlin, F. J.; Chabalowski, C. F.; Frisch, M. J. Ab Initio Calculation of Vibrational Absorption and Circular Dichroism Spectra Using Density Functional Force Fields. *J. Phys. Chem.* **1994**, *98* (45), 11623–11627. https://doi.org/10.1021/j100096a001.
(34) John A. Pople. Quantum Mechanical Models; 1998.
(35) Walter Kohn. Electronic Structure of Matter - Wave Functions and Density Functionals; 1999.
(36) Kohn, W.; Sham, L. J. Self-Consistent Equations Including Exchange and Correlation Effects. *Phys. Rev.* **1965**, *140* (4A), A1133–A1138. https://doi.org/10.1103/PhysRev.140.A1133.
(37) Pinus, S.; Genzling, J.; Burai-Patrascu, M.; Moitessier, N. Computational Methods for Asymmetric Catalysis. *Nat. Catal.* **2024**, *7* (12), 1272–1287. https://doi.org/10.1038/s41929-024-01258-6.
(38) Keith, J. A.; Vassilev-Galindo, V.; Cheng, B.; Chmiela, S.; Gastegger, M.; Müller, K.-R.; Tkatchenko, A. Combining Machine Learning and Computational Chemistry for Predictive Insights Into Chemical Systems. *Chem. Rev.* **2021**, *121* (16), 9816–9872. https://doi.org/10.1021/acs.chemrev.1c00107.
(39) Reid, J. P.; Sigman, M. S. Comparing Quantitative Prediction Methods for the Discovery of Small-Molecule Chiral Catalysts. *Nat. Rev. Chem.* **2018**, *2* (10), 290–305. https://doi.org/10.1038/s41570-018-0040-8.
(40) Williams, W. L.; Zeng, L.; Gensch, T.; Sigman, M. S.; Doyle, A. G.; Anslyn, E. V. The Evolution of Data-Driven Modeling in Organic Chemistry. *ACS Cent. Sci.* **2021**, *7* (10), 1622–1637. https://doi.org/10.1021/acscentsci.1c00535.
(41) Ahn, S.; Hong, M.; Sundararajan, M.; Ess, D. H.; Baik, M.-H. Design and Optimization of Catalysts Based on Mechanistic Insights Derived from Quantum Chemical Reaction Modeling. *Chem. Rev.* **2019**, *119* (11), 6509–6560. https://doi.org/10.1021/acs.chemrev.9b00073.
(42) Kruse, H.; Goerigk, L.; Grimme, S. Why the Standard B3LYP/6-31G* Model Chemistry Should Not Be Used in DFT Calculations of Molecular Thermochemistry: Understanding and Correcting the Problem. *J. Org. Chem.* **2012**, *77* (23), 10824–10834. https://doi.org/10.1021/jo302156p.
(43) Bao, J. L.; Gagliardi, L.; Truhlar, D. G. Self-Interaction Error in Density Functional Theory: An Appraisal. *J. Phys. Chem. Lett.* **2018**, *9* (9), 2353–2358. https://doi.org/10.1021/acs.jpclett.8b00242.
(44) Caldeweyher, E.; Mewes, J.-M.; Ehlert, S.; Grimme, S. Extension and Evaluation of the D4 London-Dispersion Model for Periodic Systems. *Phys. Chem. Chem. Phys.* **2020**, *22* (16), 8499–8512. https://doi.org/10.1039/D0CP00502A.
(45) Savin, A. On Degeneracy, near-Degeneracy and Density Functional Theory. In *Theoretical and Computational Chemistry*; Elsevier, 1996; Vol. 4, pp 327–357. https://doi.org/10.1016/S1380-7323(96)80091-4.

(46) Lledós, A. Computational Organometallic Catalysis: Where We Are, Where We Are Going. *Eur. J. Inorg. Chem.* **2021**, *2021* (26), 2547–2555. https://doi.org/10.1002/ejic.202100330.
(47) Brown, J. M.; Deeth, R. J. Is Enantioselectivity Predictable in Asymmetric Catalysis? *Angew. Chem. Int. Ed.* **2009**, *48* (25), 4476–4479. https://doi.org/10.1002/anie.200900697.
(48) Bahmanyar, S.; Houk, K. N. The Origin of Stereoselectivity in Proline-Catalyzed Intramolecular Aldol Reactions. *J. Am. Chem. Soc.* **2001**, *123* (51), 12911–12912. https://doi.org/10.1021/ja011714s.
(49) Bahmanyar, S.; Houk, K. N.; Martin, H. J.; List, B. Quantum Mechanical Predictions of the Stereoselectivities of Proline-Catalyzed Asymmetric Intermolecular Aldol Reactions. *J. Am. Chem. Soc.* **2003**, *125* (9), 2475–2479. https://doi.org/10.1021/ja028812d.
(50) Yamakawa, M.; Noyori, R. An Ab Initio Molecular Orbital Study on the Amino Alcohol-Promoted Reaction of Dialkylzincs and Aldehydes. *J. Am. Chem. Soc.* **1995**, *117* (23), 6327–6335. https://doi.org/10.1021/ja00128a023.
(51) Fink, R. F. Why Does MP2 Work? *J. Chem. Phys.* **2016**, *145* (18), 184101. https://doi.org/10.1063/1.4966689.
(52) List, B. Asymmetric Aminocatalysis. *Synlett* **2001**, *2001* (11), 1675–1686. https://doi.org/10.1055/s-2001-18074.
(53) Kitamura, M.; Okada, S.; Suga, S.; Noyori, R. Enantioselective Addition of Dialkylzincs to Aldehydes Promoted by Chiral Amino Alcohols. Mechanism and Nonlinear Effect. *J. Am. Chem. Soc.* **1989**, *111* (11), 4028–4036. https://doi.org/10.1021/ja00193a040.
(54) Santiago, C. B.; Guo, J.-Y.; Sigman, M. S. Predictive and Mechanistic Multivariate Linear Regression Models for Reaction Development. *Chem. Sci.* **2018**, *9* (9), 2398–2412. https://doi.org/10.1039/C7SC04679K.
(55) Hammett, L. P. Some Relations between Reaction Rates and Equilibrium Constants. *Chem. Rev.* **1935**, *17* (1), 125–136. https://doi.org/10.1021/cr60056a010.
(56) Hammett, L. P. The Effect of Structure upon the Reactions of Organic Compounds. Benzene Derivatives. *J. Am. Chem. Soc.* **1937**, *59* (1), 96–103. https://doi.org/10.1021/ja01280a022.
(57) Jacobsen, E. N.; Zhang, W.; Guler, M. L. Electronic Tuning of Asymmetric Catalysts. *J. Am. Chem. Soc.* **1991**, *113* (17), 6703–6704. https://doi.org/10.1021/ja00017a069.
(58) Taft, R. W. Linear Free Energy Relationships from Rates of Esterification and Hydrolysis of Aliphatic and Ortho-Substituted Benzoate Esters. *J. Am. Chem. Soc.* **1952**, *74* (11), 2729–2732. https://doi.org/10.1021/ja01131a010.
(59) Charton, M. Steric Effects. I. Esterification and Acid-Catalyzed Hydrolysis of Esters. *J. Am. Chem. Soc.* **1975**, *97* (6), 1552–1556. https://doi.org/10.1021/ja00839a047.
(60) Tolman, C. A. Steric Effects of Phosphorus Ligands in Organometallic Chemistry and Homogeneous Catalysis. *Chem. Rev.* **1977**, *77* (3), 313–348. https://doi.org/10.1021/cr60307a002.
(61) Fujita, Toshio.; Iwasa, Junkichi.; Hansch, Corwin. A New Substituent Constant, π, Derived from Partition Coefficients. *J. Am. Chem. Soc.* **1964**, *86* (23), 5175–5180. https://doi.org/10.1021/ja01077a028.
(62) Fukui, K.; Yonezawa, T.; Shingu, H. A Molecular Orbital Theory of Reactivity in Aromatic Hydrocarbons. *J. Chem. Phys.* **1952**, *20* (4), 722–725. https://doi.org/10.1063/1.1700523.

(63) Pauling, L. THE NATURE OF THE CHEMICAL BOND. IV. THE ENERGY OF SINGLE BONDS AND THE RELATIVE ELECTRONEGATIVITY OF ATOMS. *J. Am. Chem. Soc.* **1932**, *54* (9), 3570–3582. https://doi.org/10.1021/ja01348a011.
(64) Mulliken, R. S. A New Electroaffinity Scale; Together with Data on Valence States and on Valence Ionization Potentials and Electron Affinities. *J. Chem. Phys.* **1934**, *2* (11), 782–793. https://doi.org/10.1063/1.1749394.
(65) Mayr, H.; Ofial, A. R. Philicities, Fugalities, and Equilibrium Constants. *Acc. Chem. Res.* **2016**, *49* (5), 952–965. https://doi.org/10.1021/acs.accounts.6b00071.
(66) Mayr, H.; Ofial, A. R. Do General Nucleophilicity Scales Exist? *J. Phys. Org. Chem.* **2008**, *21* (7–8), 584–595. https://doi.org/10.1002/poc.1325.
(67) Jones, R. N.; Forbes, W. F.; Mueller, W. A. THE INFRARED CARBONYL STRETCHING BANDS OF RING SUBSTITUTED ACETOPHENONES. *Can. J. Chem.* **1957**, *35* (5), 504–514. https://doi.org/10.1139/v57-071.
(68) McDANIEL, D. H.; Brown, H. C. An Extended Table of Hammett Substitutent Constants Based on the Ionization of Substituted Benzoic Acids. *J. Org. Chem.* **1958**, *23* (3), 420–427. https://doi.org/10.1021/jo01097a026.
(69) Sigman, M. S.; Harper, K. C.; Bess, E. N.; Milo, A. The Development of Multidimensional Analysis Tools for Asymmetric Catalysis and Beyond. *Acc. Chem. Res.* **2016**, *49* (6), 1292–1301. https://doi.org/10.1021/acs.accounts.6b00194.
(70) Haas, B. C.; Kalyani, D.; Sigman, M. S. Applying Statistical Modeling Strategies to Sparse Datasets in Synthetic Chemistry. *Sci. Adv.* **2025**, *11* (1), eadt3013. https://doi.org/10.1126/sciadv.adt3013.
(71) Reid, J. P.; Sigman, M. S. Holistic Prediction of Enantioselectivity in Asymmetric Catalysis. *Nature* **2019**, *571* (7765), 343–348. https://doi.org/10.1038/s41586-019-1384-z.
(72) Samha, M. H.; Wahlman, J. L. H.; Read, J. A.; Werth, J.; Jacobsen, E. N.; Sigman, M. S. Exploring Structure–Function Relationships of Aryl Pyrrolidine-Based Hydrogen-Bond Donors in Asymmetric Catalysis Using Data-Driven Techniques. *ACS Catal.* **2022**, *12* (24), 14836–14845. https://doi.org/10.1021/acscatal.2c04824.
(73) Sandfort, F.; Strieth-Kalthoff, F.; Kühnemund, M.; Beecks, C.; Glorius, F. A Structure-Based Platform for Predicting Chemical Reactivity. *Chem* **2020**, *6* (6), 1379–1390. https://doi.org/10.1016/j.chempr.2020.02.017.
(74) Zahrt, A. F.; Henle, J. J.; Rose, B. T.; Wang, Y.; Darrow, W. T.; Denmark, S. E. Prediction of Higher-Selectivity Catalysts by Computer-Driven Workflow and Machine Learning. *Science* **2019**, *363* (6424), eaau5631. https://doi.org/10.1126/science.aau5631.
(75) Bender, A.; Schneider, N.; Segler, M.; Patrick Walters, W.; Engkvist, O.; Rodrigues, T. Evaluation Guidelines for Machine Learning Tools in the Chemical Sciences. *Nat. Rev. Chem.* **2022**, *6* (6), 428–442. https://doi.org/10.1038/s41570-022-00391-9.
(76) Jorner, K.; Brinck, T.; Norrby, P.-O.; Buttar, D. Machine Learning Meets Mechanistic Modelling for Accurate Prediction of Experimental Activation Energies. *Chem. Sci.* **2021**, *12* (3), 1163–1175. https://doi.org/10.1039/D0SC04896H.
(77) Chen, X.; Zhang, Z.-J.; Hong, X.; Ackermann, L. Integrating a Multitask Graph Neural Network with DFT Calculations for Site-Selectivity Prediction of Arenes and Mechanistic Knowledge Generation. *Nat. Synth.* **2025**, *4* (7), 877–887. https://doi.org/10.1038/s44160-025-00770-2.
(78) Schleinitz, J.; Carretero-Cerdán, A.; Gurajapu, A.; Harnik, Y.; Lee, G.; Pandey, A.; Milo, A.; Reisman, S. E. Designing Target-Specific Data Sets for Regioselectivity Predictions on

Complex Substrates. *J. Am. Chem. Soc.* **2025**, *147* (9), 7476–7484. https://doi.org/10.1021/jacs.4c15902.

(79) Kim, Y.; Kim, Y.; Kim, H.; Kang, S.; Kim, J.; Lee, K.; Jeong, W.; Lee, W. J.; Ryu, H.; Kim, K.; Kim, W. Y. Machine-Learning-Based Design of Metallocene Catalysts for Controlled Olefin Copolymerization. *Chem. – Eur. J.* **2025**, *31* (32), e202500316. https://doi.org/10.1002/chem.202500316.

(80) Garrison, A. G.; Heras-Domingo, J.; Kitchin, J. R.; Dos Passos Gomes, G.; Ulissi, Z. W.; Blau, S. M. Applying Large Graph Neural Networks to Predict Transition Metal Complex Energies Using the tmQM_wB97MV Data Set. *J. Chem. Inf. Model.* **2023**, *63* (24), 7642–7654. https://doi.org/10.1021/acs.jcim.3c01226.

(81) Li, S.-W.; Xu, L.-C.; Zhang, C.; Zhang, S.-Q.; Hong, X. Reaction Performance Prediction with an Extrapolative and Interpretable Graph Model Based on Chemical Knowledge. *Nat. Commun.* **2023**, *14* (1), 3569. https://doi.org/10.1038/s41467-023-39283-x.

(82) Su, Y.; Wang, X.; Ye, Y.; Xie, Y.; Xu, Y.; Jiang, Y.; Wang, C. Automation and Machine Learning Augmented by Large Language Models in a Catalysis Study. *Chem. Sci.* **2024**, *15* (31), 12200–12233. https://doi.org/10.1039/D3SC07012C.

(83) Zahrt, A. F.; Henle, J. J.; Rose, B. T.; Wang, Y.; Darrow, W. T.; Denmark, S. E. Prediction of Higher-Selectivity Catalysts by Computer-Driven Workflow and Machine Learning. *Science* **2019**, *363* (6424), eaau5631. https://doi.org/10.1126/science.aau5631.

(84) Fooshee, D.; Mood, A.; Gutman, E.; Tavakoli, M.; Urban, G.; Liu, F.; Huynh, N.; Van Vranken, D.; Baldi, P. Deep Learning for Chemical Reaction Prediction. *Mol. Syst. Des. Eng.* **2018**, *3* (3), 442–452. https://doi.org/10.1039/C7ME00107J.

(85) Li, B.; Su, S.; Zhu, C.; Lin, J.; Hu, X.; Su, L.; Yu, Z.; Liao, K.; Chen, H. A Deep Learning Framework for Accurate Reaction Prediction and Its Application on High-Throughput Experimentation Data. *J. Cheminformatics* **2023**, *15* (1), 72. https://doi.org/10.1186/s13321-023-00732-w.

(86) Aguilar-Bejarano, E.; Özcan, E.; Rit, R. K.; Li, H.; Lam, H. W.; Moore, J. C.; Woodward, S.; Figueredo, G. Homogeneous Catalyst Graph Neural Network: A Human-Interpretable Graph Neural Network Tool for Ligand Optimization in Asymmetric Catalysis. *iScience* **2025**, *28* (3), 111881. https://doi.org/10.1016/j.isci.2025.111881.

(87) Aouichaoui, A. R. N.; Fan, F.; Mansouri, S. S.; Abildskov, J.; Sin, G. Combining Group-Contribution Concept and Graph Neural Networks Toward Interpretable Molecular Property Models. *J. Chem. Inf. Model.* **2023**, *63* (3), 725–744. https://doi.org/10.1021/acs.jcim.2c01091.

(88) Kotobi, A.; Singh, K.; Höche, D.; Bari, S.; Meißner, R. H.; Bande, A. Integrating Explainability into Graph Neural Network Models for the Prediction of X-Ray Absorption Spectra. *J. Am. Chem. Soc.* **2023**, *145* (41), 22584–22598. https://doi.org/10.1021/jacs.3c07513.

(89) Kalikadien, A. V.; Mirza, A.; Hossaini, A. N.; Sreenithya, A.; Pidko, E. A. Paving the Road towards Automated Homogeneous Catalyst Design. *ChemPlusChem* **2024**, *89* (7), e202300702. https://doi.org/10.1002/cplu.202300702.

(90) Ekeli, J. B.; Foscato, M.; Blanco, C. O.; Occhipinti, G.; Fogg, D. E.; Jensen, V. R. Enabling Automation of de Novo Catalyst Design: An Experimentally Validated, Multifactor Design Metric for Olefin Metathesis. *ACS Catal.* **2024**, *14* (22), 16731–16747. https://doi.org/10.1021/acscatal.4c06212.

(91) Li, J.; Reid, J. P. Connecting the Complexity of Stereoselective Synthesis to the Evolution of Predictive Tools. *Chem. Sci.* **2025**, *16* (9), 3832–3851. https://doi.org/10.1039/D4SC07461K.
(92) Betinol, I. O.; Demchenko, A.; Reid, J. P. Evaluating Predictive Accuracy in Asymmetric Catalysis: A Machine Learning Perspective on Local Reaction Space. *ACS Catal.* **2025**, *15* (8), 6067–6077. https://doi.org/10.1021/acscatal.5c01051.
(93) Xu, L.-C.; Frey, J.; Hou, X.; Zhang, S.-Q.; Li, Y.-Y.; Oliveira, J. C. A.; Li, S.-W.; Ackermann, L.; Hong, X. Enantioselectivity Prediction of Pallada-Electrocatalysed C–H Activation Using Transition State Knowledge in Machine Learning. *Nat. Synth.* **2023**, *2* (4), 321–330. https://doi.org/10.1038/s44160-022-00233-y.
(94) Betinol, I. O.; Kuang, Y.; Lai, J.; Yousofi, C.; Reid, J. P. Machine Learning Enables a Top-Down Approach to Mechanistic Elucidation in Asymmetric Catalysis. *ACS Catal.* **2025**, *15* (11), 8799–8810. https://doi.org/10.1021/acscatal.5c02264.
(95) Kim, D.; Choi, G.; Kim, H. One-Pot Multisubstrate Screening for Asymmetric Catalysis Enabled by^{19} F NMR-Based Simultaneous Chiral Analysis. *J. Am. Chem. Soc.* **2025**, *147* (23), 19770–19776. https://doi.org/10.1021/jacs.5c03446.
(96) Li, Z.-L.; Pei, S.; Chen, Z.; Huang, T.-Y.; Wang, X.-D.; Shen, L.; Chen, X.; Wang, Q.-Q.; Wang, D.-X.; Ao, Y.-F. Machine Learning-Assisted Amidase-Catalytic Enantioselectivity Prediction and Rational Design of Variants for Improving Enantioselectivity. *Nat. Commun.* **2024**, *15* (1), 8778. https://doi.org/10.1038/s41467-024-53048-0.
(97) Fu, G. C. Transition-Metal Catalysis of Nucleophilic Substitution Reactions: A Radical Alternative to S $_N$ 1 and S $_N$ 2 Processes. *ACS Cent. Sci.* **2017**, *3* (7), 692–700. https://doi.org/10.1021/acscentsci.7b00212.
(98) Yin, H.; Fu, G. C. Mechanistic Investigation of Enantioconvergent Kumada Reactions of Racemic α-Bromoketones Catalyzed by a Nickel/Bis(Oxazoline) Complex. *J. Am. Chem. Soc.* **2019**, *141* (38), 15433–15440. https://doi.org/10.1021/jacs.9b08185.
(99) Cherney, A. H.; Kadunce, N. T.; Reisman, S. E. Enantioselective and Enantiospecific Transition-Metal-Catalyzed Cross-Coupling Reactions of Organometallic Reagents To Construct C–C Bonds. *Chem. Rev.* **2015**, *115* (17), 9587–9652. https://doi.org/10.1021/acs.chemrev.5b00162.
(100) Poremba, K. E.; Dibrell, S. E.; Reisman, S. E. Nickel-Catalyzed Enantioselective Reductive Cross-Coupling Reactions. *ACS Catal.* **2020**, *10* (15), 8237–8246. https://doi.org/10.1021/acscatal.0c01842.
(101) Jin, Y.; Wang, C. Nickel-Catalyzed Asymmetric Cross-Electrophile Coupling Reactions. *Synlett* **2020**, *31* (19), 1843–1850. https://doi.org/10.1055/s-0040-1707216.
(102) Li, Z.; Li, C.; Ding, Y.; Huo, H. Photoinduced Nickel-Catalyzed Enantioselective Coupling Reactions. *Coord. Chem. Rev.* **2022**, *460*, 214479. https://doi.org/10.1016/j.ccr.2022.214479.
(103) Lipp, A.; Badir, S. O.; Molander, G. A. Stereoinduction in Metallaphotoredox Catalysis. *Angew. Chem. Int. Ed.* **2021**, *60* (4), 1714–1726. https://doi.org/10.1002/anie.202007668.
(104) Xu, W.; Xu, T. Dual Nickel- and Photoredox-Catalyzed Asymmetric Reductive Cross-Couplings: Just a Change of the Reduction System? *Acc. Chem. Res.* **2024**, *57* (14), 1997–2011. https://doi.org/10.1021/acs.accounts.4c00309.
(105) Li, M.; Peters, J. C. Electrochemical Nickel-Catalyzed Asymmetric Hydrogenation of C═C Bonds Facilitated by a Proton-Coupled Electron Transfer Mediator. *ACS Catal.* **2025**, *15* (16), 13720–13726. https://doi.org/10.1021/acscatal.5c04130.

(106) Liu, D.; Liu, Z.-R.; Wang, Z.-H.; Ma, C.; Herbert, S.; Schirok, H.; Mei, T.-S. Paired Electrolysis-Enabled Nickel-Catalyzed Enantioselective Reductive Cross-Coupling between α-Chloroesters and Aryl Bromides. *Nat. Commun.* **2022**, *13* (1), 7318. https://doi.org/10.1038/s41467-022-35073-z.
(107) Zhang, Q.; Liang, K.; Guo, C. Enantioselective Nickel-Catalyzed Electrochemical Radical Allylation. *Angew. Chem. Int. Ed.* **2022**, *61* (38), e202210632. https://doi.org/10.1002/anie.202210632.
(108) Diccianni, J.; Lin, Q.; Diao, T. Mechanisms of Nickel-Catalyzed Coupling Reactions and Applications in Alkene Functionalization. *Acc. Chem. Res.* **2020**, *53* (4), 906–919. https://doi.org/10.1021/acs.accounts.0c00032.
(109) Diccianni, J. B.; Diao, T. Mechanisms of Nickel-Catalyzed Cross-Coupling Reactions. *Trends Chem.* **2019**, *1* (9), 830–844. https://doi.org/10.1016/j.trechm.2019.08.004.
(110) Dawson, G. A.; Spielvogel, E. H.; Diao, T. Nickel-Catalyzed Radical Mechanisms: Informing Cross-Coupling for Synthesizing Non-Canonical Biomolecules. *Acc. Chem. Res.* **2023**, *56* (24), 3640–3653. https://doi.org/10.1021/acs.accounts.3c00588.
(111) Nebra, N. High-Valent NiIII and NiIV Species Relevant to C–C and C–Heteroatom Cross-Coupling Reactions: State of the Art. *Molecules* **2020**, *25* (5), 1141. https://doi.org/10.3390/molecules25051141.
(112) Lin, X.; Sun, J.; Xi, Y.; Lin, D. How Racemic Secondary Alkyl Electrophiles Proceed to Enantioselective Products in Negishi Cross-Coupling Reactions. *Organometallics* **2011**, *30* (12), 3284–3292. https://doi.org/10.1021/om1012049.
(113) Arp, F. O.; Fu, G. C. Catalytic Enantioselective Negishi Reactions of Racemic Secondary Benzylic Halides. *J. Am. Chem. Soc.* **2005**, *127* (30), 10482–10483. https://doi.org/10.1021/ja053751f.
(114) Zhang, C.; Lu, Y.; Zhao, R.; Chen, X.-Y.; Wang, Z.-X. How Does the Nickel Catalyst Control the Doubly Enantioconvergent Coupling of Racemic Alkyl Nucleophiles and Electrophiles? The Rebound Mechanism. *Org. Chem. Front.* **2020**, *7* (21), 3411–3419. https://doi.org/10.1039/D0QO00903B.
(115) Huo, H.; Gorsline, B. J.; Fu, G. C. Catalyst-Controlled Doubly Enantioconvergent Coupling of Racemic Alkyl Nucleophiles and Electrophiles. *Science* **2020**, *367* (6477), 559–564. https://doi.org/10.1126/science.aaz3855.
(116) Ren, Q.; Zhang, D.; Zheng, L. DFT Studies on the Mechanisms of Enantioselective Ni-Catalyzed Reductive Coupling Reactions to Form 1,1-Diarylalkanes. *J. Organomet. Chem.* **2021**, *952*, 122042. https://doi.org/10.1016/j.jorganchem.2021.122042.
(117) Poremba, K. E.; Kadunce, N. T.; Suzuki, N.; Cherney, A. H.; Reisman, S. E. Nickel-Catalyzed Asymmetric Reductive Cross-Coupling To Access 1,1-Diarylalkanes. *J. Am. Chem. Soc.* **2017**, *139* (16), 5684–5687. https://doi.org/10.1021/jacs.7b01705.
(118) Zhang, C.-S.; Zhang, B.-B.; Zhong, L.; Chen, X.-Y.; Wang, Z.-X. DFT Insight into Asymmetric Alkyl–Alkyl Bond Formation *via* Nickel-Catalysed Enantioconvergent Reductive Coupling of Racemic Electrophiles with Olefins. *Chem. Sci.* **2022**, *13* (13), 3728–3739. https://doi.org/10.1039/D1SC05605K.
(119) Wang, Z.; Yin, H.; Fu, G. C. Catalytic Enantioconvergent Coupling of Secondary and Tertiary Electrophiles with Olefins. *Nature* **2018**, *563* (7731), 379–383. https://doi.org/10.1038/s41586-018-0669-y.
(120) Gutierrez, O.; Tellis, J. C.; Primer, D. N.; Molander, G. A.; Kozlowski, M. C. Nickel-Catalyzed Cross-Coupling of Photoredox-Generated Radicals: Uncovering a General

Manifold for Stereoconvergence in Nickel-Catalyzed Cross-Couplings. *J. Am. Chem. Soc.* **2015**, *137* (15), 4896–4899. https://doi.org/10.1021/ja513079r.
(121) Tellis, J. C.; Primer, D. N.; Molander, G. A. Single-Electron Transmetalation in Organoboron Cross-Coupling by Photoredox/Nickel Dual Catalysis. *Science* **2014**, *345* (6195), 433–436. https://doi.org/10.1126/science.1253647.
(122) Seeman, J. I. Effect of Conformational Change on Reactivity in Organic Chemistry. Evaluations, Applications, and Extensions of Curtin-Hammett Winstein-Holness Kinetics. *Chem. Rev.* **1983**, *83* (2), 83–134. https://doi.org/10.1021/cr00054a001.
(123) Saito, B.; Fu, G. C. Enantioselective Alkyl−Alkyl Suzuki Cross-Couplings of Unactivated Homobenzylic Halides. *J. Am. Chem. Soc.* **2008**, *130* (21), 6694–6695. https://doi.org/10.1021/ja8013677.
(124) Yin, H.; Fu, G. C. Mechanistic Investigation of Enantioconvergent Kumada Reactions of Racemic α-Bromoketones Catalyzed by a Nickel/Bis(Oxazoline) Complex. *J. Am. Chem. Soc.* **2019**, *141* (38), 15433–15440. https://doi.org/10.1021/jacs.9b08185.
(125) Lou, S.; Fu, G. C. Nickel/Bis(Oxazoline)-Catalyzed Asymmetric Kumada Reactions of Alkyl Electrophiles: Cross-Couplings of Racemic α-Bromoketones. *J. Am. Chem. Soc.* **2010**, *132* (4), 1264–1266. https://doi.org/10.1021/ja909689t.
(126) Schley, N. D.; Fu, G. C. Nickel-Catalyzed Negishi Arylations of Propargylic Bromides: A Mechanistic Investigation. *J. Am. Chem. Soc.* **2014**, *136* (47), 16588–16593. https://doi.org/10.1021/ja508718m.
(127) McManus, B. D.; Hung, L. C.; Taylor, O. R.; Nguyen, P. Q.; Cedeño, A. L.; Arriola, K.; Bradley, R. D.; Saucedo, P. J.; Hannan, R. J.; Luna, Y. A.; Farias, P.; Bahamonde, A. Mechanistic Interrogation of Photochemical Nickel-Catalyzed Tetrahydrofuran Arylation Leveraging Enantioinduction Data. *J. Am. Chem. Soc.* **2024**, *146* (46), 32135–32146. https://doi.org/10.1021/jacs.4c13485.
(128) Lau, S. H.; Borden, M. A.; Steiman, T. J.; Wang, L. S.; Parasram, M.; Doyle, A. G. Ni/Photoredox-Catalyzed Enantioselective Cross-Electrophile Coupling of Styrene Oxides with Aryl Iodides. *J. Am. Chem. Soc.* **2021**, *143* (38), 15873–15881. https://doi.org/10.1021/jacs.1c08105.
(129) Gao, Y.; Hu, K.; Rao, J.; Zhu, Q.; Liao, K. Artificial Intelligence-Driven Development of Nickel-Catalyzed Enantioselective Cross-Coupling Reactions. *ACS Catal.* **2024**, *14* (24), 18457–18468. https://doi.org/10.1021/acscatal.4c04277.
(130) Smith, S. W.; Fu, G. C. Nickel-Catalyzed Asymmetric Cross-Couplings of Racemic Propargylic Halides with Arylzinc Reagents. *J. Am. Chem. Soc.* **2008**, *130* (38), 12645–12647. https://doi.org/10.1021/ja805165y.
(131) Day, C. S. Advances in Understanding Comproportionation and Disproportionation in Nickel Catalysis. *Pure Appl. Chem.* **2024**, *96* (3), 437–446. https://doi.org/10.1515/pac-2024-0106.
(132) Spielvogel, E. H.; Yuan, J.; Hoffmann, N. M.; Diao, T. Nickel-Mediated Radical Capture: Evidence for a Concerted Inner-Sphere Mechanism. *J. Am. Chem. Soc.* **2025**, *147* (23), 19632–19642. https://doi.org/10.1021/jacs.5c01554.
(133) Schley, N. D.; Fu, G. C. Nickel-Catalyzed Negishi Arylations of Propargylic Bromides: A Mechanistic Investigation. *J. Am. Chem. Soc.* **2014**, *136* (47), 16588–16593. https://doi.org/10.1021/ja508718m.
(134) Konowalchuk, D. J.; Hall, D. G. Divergent Synthesis of 1,2,3,4-Tetrasubstituted Cyclobutenes from a Common Scaffold: Enantioselective Desymmetrization by Dual-

Catalyzed Photoredox Cross-Coupling. *Angew. Chem. Int. Ed.* **2023**, *62* (49), e202313503. https://doi.org/10.1002/anie.202313503.
(135) Schaus, S. E.; Jacobsen, E. N. Asymmetric Ring Opening of Meso Epoxides with TMSCN Catalyzed by (Pybox)Lanthanide Complexes. *Org. Lett.* **2000**, *2* (7), 1001–1004. https://doi.org/10.1021/ol005721h.
(136) Nishiyama, H.; Yamaguchi, S.; Kondo, M.; Itoh, K. Electronic Substituent Effect of Nitrogen Ligands in Catalytic Asymmetric Hydrosilylation of Ketones: Chiral 4-Substituted Bis(Oxazolinyl)Pyridines. *J. Org. Chem.* **1992**, *57* (15), 4306–4309. https://doi.org/10.1021/jo00041a049.
(137) Poh, J.; Makai, S.; von Keutz, T.; Tran, D. N.; Battilocchio, C.; Pasau, P.; Ley, S. V. Rapid Asymmetric Synthesis of Disubstituted Allenes by Coupling of Flow-Generated Diazo Compounds and Propargylated Amines. *Angew. Chem. Int. Ed.* **2017**, *56* (7), 1864–1868. https://doi.org/10.1002/anie.201611067.
(138) Bruno, N. C.; Tudge, M. T.; Buchwald, S. L. Design and Preparation of New Palladium Precatalysts for C–C and C–N Cross-Coupling Reactions. *Chem Sci* **2013**, *4* (3), 916–920. https://doi.org/10.1039/C2SC20903A.
(139) Cohen, D. T.; Buchwald, S. L. Mild Palladium-Catalyzed Cyanation of (Hetero)Aryl Halides and Triflates in Aqueous Media. *Org. Lett.* **2015**, *17* (2), 202–205. https://doi.org/10.1021/ol5032359.
(140) Roblou, E.; Sasaki, I.; Pezet, F.; Aït-Haddou, H.; Vincendeau, S. Synthesis of Dicyanopyridines. *Synth. Commun.* **2004**, *34* (20), 3743–3749. https://doi.org/10.1081/SCC-200032468.
(141) Pintus, A.; Rocchigiani, L.; Fernandez-Cestau, J.; Budzelaar, P. H. M.; Bochmann, M. Stereo- and Regioselective Alkyne Hydrometallation with Gold(III) Hydrides. *Angew. Chem. Int. Ed.* **2016**, *55* (40), 12321–12324. https://doi.org/10.1002/anie.201607522.
(142) Janabel, J.; Kumar, D.; Kanale, V. V.; Liu, M.; Uyeda, C. Catalytic Asymmetric Synthesis of Axially Chiral Methylenecyclopropanes. *J. Am. Chem. Soc.* **2025**, *147* (26), 23270–23276. https://doi.org/10.1021/jacs.5c07968.
(143) Neese, F. Software Update: The ORCA Program System—Version 5.0. *WIREs Comput. Mol. Sci.* **2022**, *12* (5), e1606. https://doi.org/10.1002/wcms.1606.
(144) Lehtola, S.; Steigemann, C.; Oliveira, M. J. T.; Marques, M. A. L. Recent Developments in Libxc — A Comprehensive Library of Functionals for Density Functional Theory. *SoftwareX* **2018**, *7*, 1–5. https://doi.org/10.1016/j.softx.2017.11.002.
(145) Helmich-Paris, B.; De Souza, B.; Neese, F.; Izsák, R. An Improved Chain of Spheres for Exchange Algorithm. *J. Chem. Phys.* **2021**, *155* (10), 104109. https://doi.org/10.1063/5.0058766.
(146) Neese, F. An Improvement of the Resolution of the Identity Approximation for the Formation of the Coulomb Matrix. *J. Comput. Chem.* **2003**, *24* (14), 1740–1747. https://doi.org/10.1002/jcc.10318.
(147) Bykov, D.; Petrenko, T.; Izsák, R.; Kossmann, S.; Becker, U.; Valeev, E.; Neese, F. Efficient Implementation of the Analytic Second Derivatives of Hartree–Fock and Hybrid DFT Energies: A Detailed Analysis of Different Approximations. *Mol. Phys.* **2015**, *113* (13–14), 1961–1977. https://doi.org/10.1080/00268976.2015.1025114.
(148) Neese, F.; Wennmohs, F.; Hansen, A.; Becker, U. Efficient, Approximate and Parallel Hartree–Fock and Hybrid DFT Calculations. A 'Chain-of-Spheres' Algorithm for the

Hartree–Fock Exchange. *Chem. Phys.* **2009**, *356* (1–3), 98–109. https://doi.org/10.1016/j.chemphys.2008.10.036.
(149) Neese, F. The SHARK Integral Generation and Digestion System. *J. Comput. Chem.* **2023**, *44* (3), 381–396. https://doi.org/10.1002/jcc.26942.
(150) Neese, F. Software Update: The ORCA Program System—Version 6.0. *WIREs Comput. Mol. Sci.* **2025**, *15* (2), e70019. https://doi.org/10.1002/wcms.70019.
(151) Mardirossian, N.; Head-Gordon, M. ω B97M-V: A Combinatorially Optimized, Range-Separated Hybrid, Meta-GGA Density Functional with VV10 Nonlocal Correlation. *J. Chem. Phys.* **2016**, *144* (21), 214110. https://doi.org/10.1063/1.4952647.
(152) Caldeweyher, E.; Bannwarth, C.; Grimme, S. Extension of the D3 Dispersion Coefficient Model. *J. Chem. Phys.* **2017**, *147* (3), 034112. https://doi.org/10.1063/1.4993215.
(153) Garcia-Ratés, M.; Neese, F. Efficient Implementation of the Analytical Second Derivatives of Hartree–Fock and Hybrid DFT Energies within the Framework of the Conductor-like Polarizable Continuum Model. *J. Comput. Chem.* **2019**, *40* (20), 1816–1828. https://doi.org/10.1002/jcc.25833.
(154) 1,2-Dimethoxyethane. *The Merck Index - Encyclopedia of Chemicals, Drugs and Biologicals*; Merck and Co., Inc., 1989; p 509.
(155) Weigend, F.; Ahlrichs, R. Balanced Basis Sets of Split Valence, Triple Zeta Valence and Quadruple Zeta Valence Quality for H to Rn: Design and Assessment of Accuracy. *Phys. Chem. Chem. Phys.* **2005**, *7* (18), 3297. https://doi.org/10.1039/b508541a.
(156) Rappoport, D.; Furche, F. Property-Optimized Gaussian Basis Sets for Molecular Response Calculations. *J. Chem. Phys.* **2010**, *133* (13), 134105. https://doi.org/10.1063/1.3484283.
(157) Heidrich, D.; Quapp, W. Saddle Points of Index 2 on Potential Energy Surfaces and Their Role in Theoretical Reactivity Investigations. *Theor. Chim. Acta* **1986**, *70* (2), 89–98. https://doi.org/10.1007/BF00532206.
(158) Macrae, C. F.; Sovago, I.; Cottrell, S. J.; Galek, P. T. A.; McCabe, P.; Pidcock, E.; Platings, M.; Shields, G. P.; Stevens, J. S.; Towler, M.; Wood, P. A. *Mercury 4.0* : From Visualization to Analysis, Design and Prediction. *J. Appl. Crystallogr.* **2020**, *53* (1), 226–235. https://doi.org/10.1107/S1600576719014092.

CHAPTER TWO

[This section has been temporarily redacted.]

CHAPTER THREE

During the course of my thesis work I contributed to diverse projects pioneered by my coworkers. My contributions to these works are collected here.

1. Enantio- and diastereoselective allenylation of alkyl electrophiles.

1.1 Background

Stereochemically rich compounds are common in both natural products and pharmaceutical compounds of interest. In recent years, this has motivated the development of metal-catalyzed reactions to accomplish stereoselective and stereospecific couplings.[1,2] Our group has been particularly interested in nickel-catalyzed asymmetric constructions of C—C bonds between alkyl coupling partners.[3,4] When a racemic nucleophile and electrophile are used, there is the possibility of accomplishing controlling both chiral centers at once, swiftly adding synthetic complexity. These so-called doubly enantioconvergent couplings have been of interest in recent years, with examples published using nickel,[5–9] cobalt,[10,11] copper,[12–14], and iridium,[15] and others.[16,17] Our group has made inroads into this motif as well first in 2017, when we reported the diastereoselective coupling of α-zincated pyrrolidines with secondary cyclic electrophiles.[18] This was followed in 2020 by our report of the doubly enantioconvergent coupling of acyclic coupling partners, specifically secondary propargylic bromides and β-zincated amides.[19] At the start of this project, it was noted that there had not yet been a report of a coupling reaction that simultaneously controlled axial and point chirality simultaneously . Therefore, we sought to fill this gap by exploring the hydroalkylation of enynes with secondary electrophiles via nickel hydride catalysis[20] to generate synthetically valuable chiral allenes.[21–24] After a period of optimization, a suitable

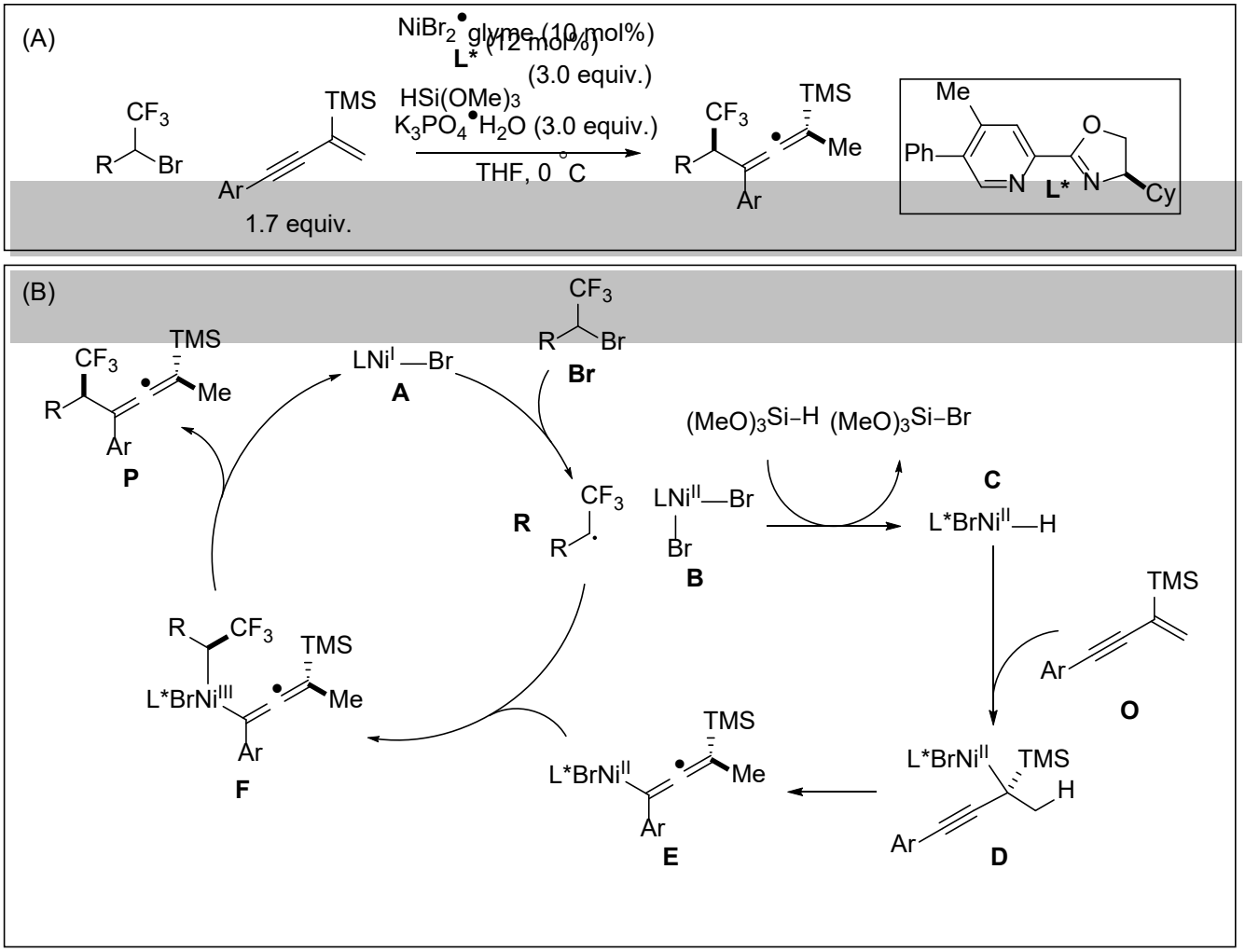

Figure 1.1.1: (A) Reported enantio- and diastereoselective hydroalkylation of enynes. (B) Proposed catalytic cycle consistent with observations.

reaction condition was found using a chiral pyridine-oxazoline ligand to coupling α-trifluoromethyl bromides with enynes (Fig 1.1.1A)[20]. A proposed mechanistic cycle for this process which is consistent with mechanistic experiments and is analogous to previously studied mechanisms is shown in Figure 3.1.1.1B[25,26]. In the cycle, metalloradical **A** would undergo halogen atom abstraction with the alkyl halide **Br** to generate organoradical **R** and nickel species **B**. This species can undergo transmetalation with the silane reductant to form nickel hydride **C**, which can then undergo hydroalkylation with the enyne substrate **O** to form propargylic nickel intermediate **D**. This intermediate can rearrange to the more thermodynamically stable allenyl species **E.** This

species can then capture the radical **R** to form intermediate **F**, which undergoes rapid reductive elimination to form the product **P** and regenerate metalloradical **A**.

In performing calculations on this system, there were two key questions that we hoped to shed light on. The first is the nature of the rearrangement step from species **D** to **E**. The second was to rationalize the differing reactivity of different electrophiles. Specifically, it was observed that alkyl iodides as well as unfluorinated secondary bromides displayed worse reactivity, and secondary unactivated alkyl iodides were completely unreactive, which is an unexpected result in light of the lower BDE of the C—I bond.

1.2: Calculations of Ni^{II} hydride species

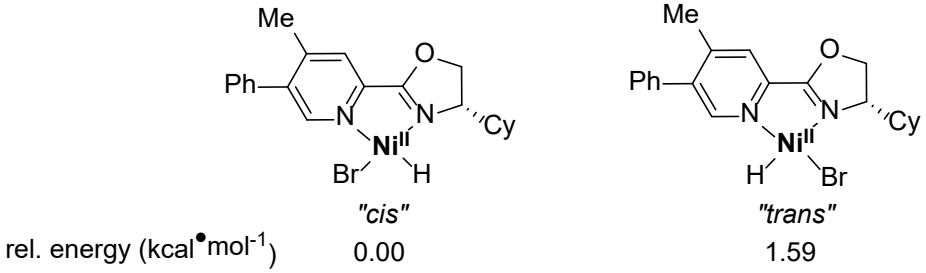

Figure 1.2.1: Calculated relative energies of nickel hydride isomers.

As a start to investigating the possible geometries of the nickel-alkyl intermediates, the putative Ni^{II} hydride species was calculated. Given the symmetry of the ligand, two possible low spin square planar isomers are possible. In the first, the hydrogen atom lies trans to the oxazoline fragment, and in the other it is trans. Figure 1.2.1 shows the geometry of these species, and their calculated energy differences. The *cis* geometry was found to be the most stable. However, the trans isomer is close enough in energy that it cannot be ruled out as a relevant species, given that interconversion may occur, and the trans isomer may be more reactive with the enyne.

1.3: Calculations of L*NiBr—propargyl species

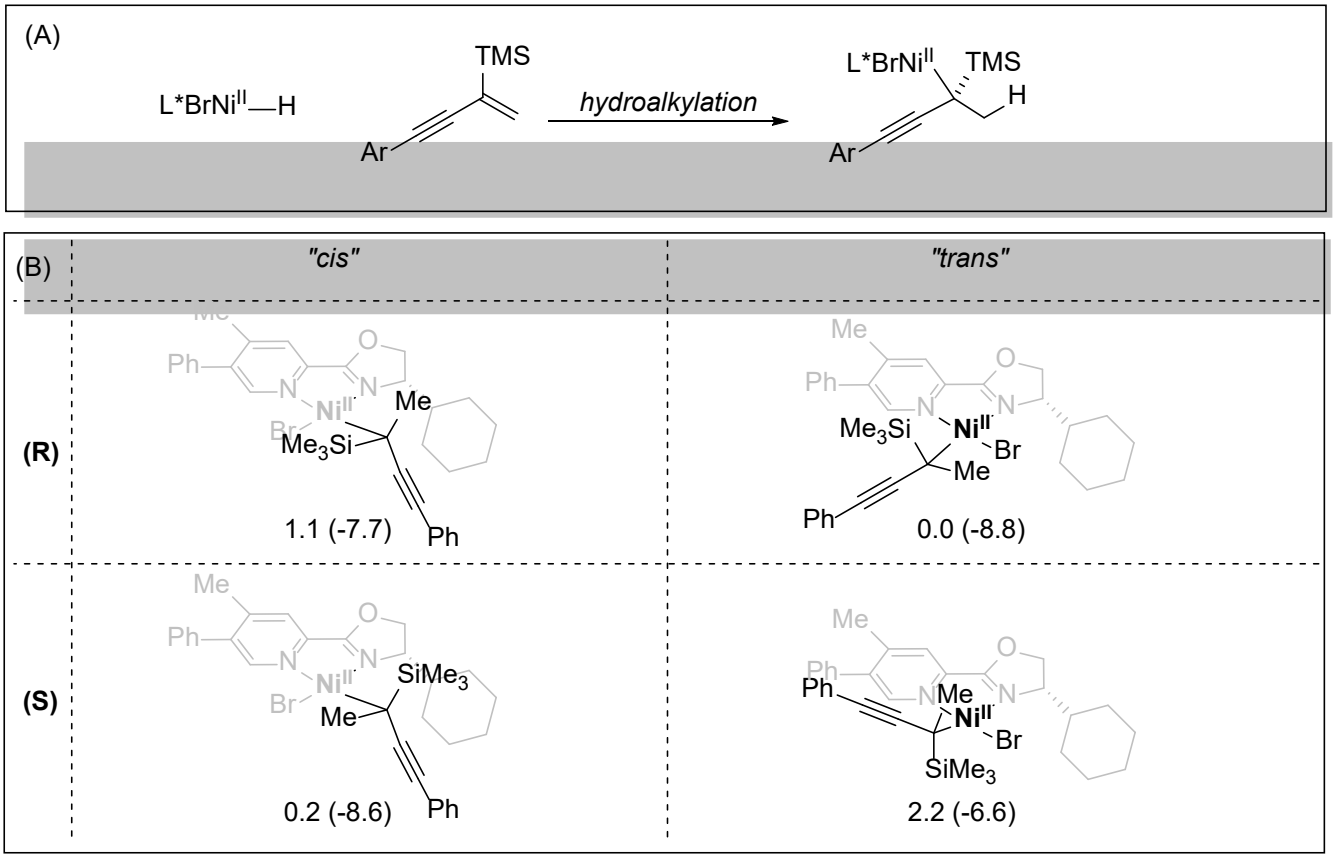

Figure 1.3.1: (A) Modeled hydroalkylation reaction. (B) Lowest-energy isomers for Ni^{II} propargyl species. Numbers are relative energy in kcal•mol^{-1}. The bracketed values are energies relative to the starting materials.

We next moved to interrogate the possible geometries of the Ni^{II} species after hydroalkylation with the enyne, a reaction shown in Figure 1.3.1A. Because we could not assume the geometry of the Ni^{II}—H species, complexes resulting from reaction of both the cis and trans isomers of the Ni^{II} hydride species were considered. An extensive geometric search was performed to find the lowest energy conformation of each diastereomeric complex. The result of this search is shown in Figure 1.3.1B, showing the four lowest energy isomers. It should be noted that the diastereomer with the R configuration on the propargyl group corresponds to the stereochemistry of the major project. Overall, the reaction is downhill for each isomer. This is consistent with the mechanistic data which shows that hydroalkylation is an irreversible process under the reaction

conditions. While we can note that, on average, the R conformers are more stable than the S conformers, the difference is not very great. Efforts were made to locate transition states for the hydroalkylation step, but they were not successful. With the present data, no concrete conclusions can be reached about the probable geometry of the Ni^{II}—propargyl species.

1.4 Calculations of L*NiBr—allenyl species

We next turned our attention to the next step in the putative catalytic cycle: the rearrangement of the Ni^{II}-propargyl species to a Ni^{II}-allenyl species (Fig 1.4.1A). As before, an extensive geometry search was undertaken. Figure 1.4.1B shows the results. In this case, the relative energy of the diastereomers is very close, and no determination can be made about how

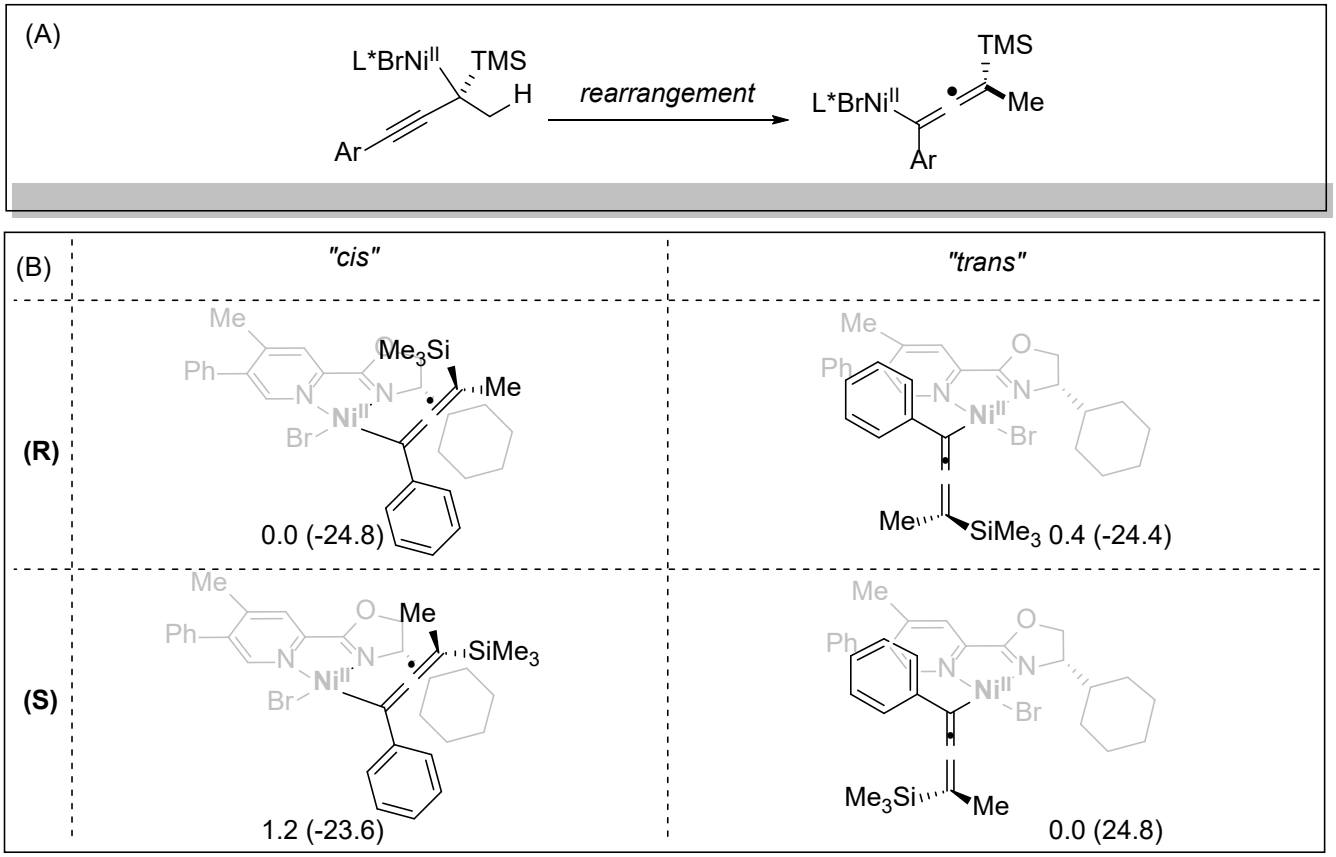

Figure 1.4.1: (A) Modeled rearrangement. (B) Lowest-energy isomers for Ni^{II} allenyl species. Numbers are relative energy in kcal•mol^{-1}. The bracketed values are energies relative to the starting materials.

the relative energies of these structures effect the ultimate diastereoselectivity. What can be said is that the Ni^{II}-allenyl species is significantly downhill from the Ni^{II}-propargyl species, and therefore this step is likely irreversible. It also cannot be ruled out that these species may interconvert. Unfortunately, reasonable transition states for this rearrangement reaction were not located. The bond dissociation energy for dissociation of the allenyl fragment was calculated to be 10 kcal•mol^{-1}. This places within the realm of possibility that under the reaction conditions, rearrangement of the allenyl species can take place by dissociation and reassociation of the allenyl radical. By extension, this could also be a reasonable pathway for isomerization of the propargyl species to the allenyl species. It should be noted that using α-bromo lactams as electrophiles results in the opposite sense of allene axial chirality. This is consistent with an interconverting Ni^{II}-allenyl species, where one diastereomer preferentially can capture the alkyl radical and undergo reductive elimination to the product. This would mean that radical capture would be both the enantio- and diastereo- determining step.

1.5: Estimation of bond dissociation energies

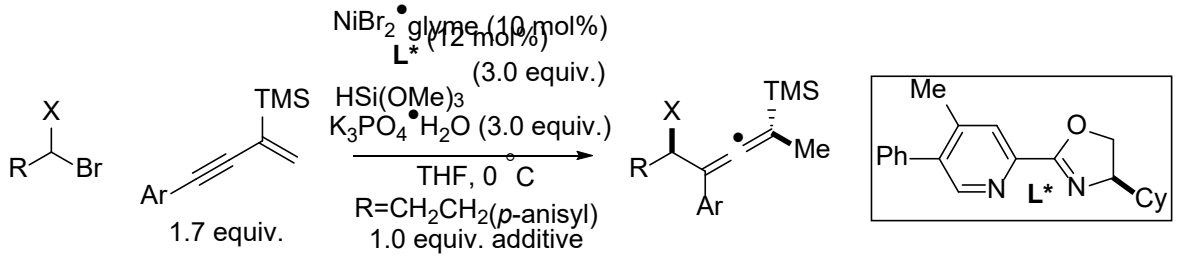

entry	X	additive	yield (%)	ee (%)	dr	additive recovery (%)
1	X = CF_3	--	65%	92%	90:10	--
2	X = CF_2H	--	55%	71%	85:15	--
3	X = Me	--	No T.M	--	--	--
4	X = CF_3	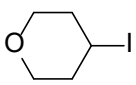	40%	88%	90:10	87%

Figure 1.5.1: Results of catalysis using different electrophiles and with a secondary alkyl iodide as an additive. No T.M = no target molecule detected.

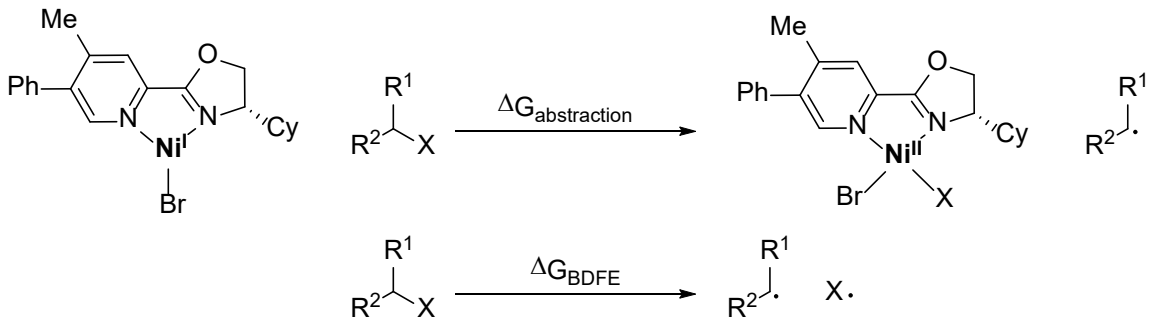

Substrate	$\Delta G_{abstraction}$	ΔG_{BDFE}
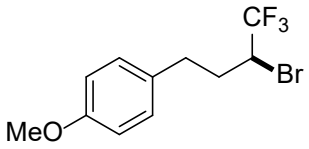	-5.44	57.16
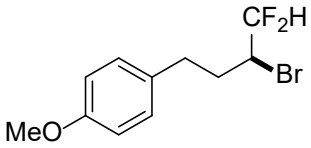	-3.84	58.78
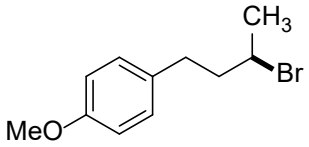	-2.67	59.93
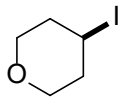	-2.26	44.89

Figure 3.1.5.2: Free energies of halogen atom abstraction by $LNi^{I}Br$ and bond energy BDFE values calculated. All values are in kcal•mol^{-1}

During our investigation, some unexpected reactivity was discovered regarding the identity and tolerance of the electrophile. These findings are summarized in Figure 3.1.5.1. Entries 1, 2, and 3 show the necessity of an α-fluorinated substituent on the catalysis. While changing the α-trilfuoromethyl group for an α-difluoromethyl group results in somewhat worse results, replacement of this group by methyl completely shuts down. This may be explained by a weakening of the C—Br bond as a result of an electronegative α-group. However, it was also noted that secondary unactivated alkyl iodides were tolerated in this reaction. These results encouraged us to calculate both the BDE energies of bond homolysis of the relevant carbon-halogen bonds,

but also calculate the favorability of halogen atom abstraction by the putative Ni^{I}—Br complex implicated in the catalysis. Figure 3.1.5.2 shows the results of these calculations. For each of the bromide substrates, halogen atom abstraction is favorable for each one, but it is most favorable for the α-trifluoromethyl substrate, and barely exergonic for the unfluorinated case. This effect can mostly be explained by the weakening of the C—Br bond as fluorination increases. Interestingly, the abstraction of an iodine atom from the tetrahydropyran substrate is the least exergonic, even though the C—I bond was calculated to be the weakest. This disparity can be attributed to the greater affinity of the nickel catalyst for bromine over iodine.

1.6: Computation details

1.6.1 General methods

All molecular structure images were generated using the Mercury software package.[27]

Calculation method A: All calculations were performed using the Orca 5.0.3 software package. [28–31] Geometry optimizations were performed using the B3LYP functional, utilizing the D4 dispersion correction. [32–34] The def2-SVP basis set was used for all atoms except nickel where applicable, with which def2-QZVPPD was used.[35,36] The RIJCOSX approximation was used with the def2/J auxiliary basis set in all calculations.[37] Frequency calculations were performed to ensure that all molecular geometries were energy minima by confirming the absence of imaginary vibrational modes.[38] Solvent was modeling using the CPCM solvation model with THF as a solvent.[33,39] All thermochemical values were corrected to 273.15 K.

Calculation method B: All calculations were performed using the Orca 5.0.3 software package.[28–31] Geometry optimizations were performed using the B3LYP functional, utilizing the D4 dispersion correction.[32–34] The def2-TZVP basis set was used for all atoms except nickel where

applicable, with which def2-QZVPPD was used.[35,36] The RIJCOSX approximation was used with the def2/J auxiliary basis set in all calculations.[37] Refinements to the electronic energy were calculated by single point calculations on optimized geometries using the MO62X functional using the def2-QZVPPD basis set.[40] This functional was chosen on the basis of its previous success in predicting the thermochemistry of bond-breaking reactions.[41] Frequency calculations were performed to ensure that all molecular geometries were energy minima by confirming the absence of imaginary vibrational modes.[38]

1.6.2 Geometry of calculated species

These geometries were calculated using calculation method A.

L*NiBr—H, cis

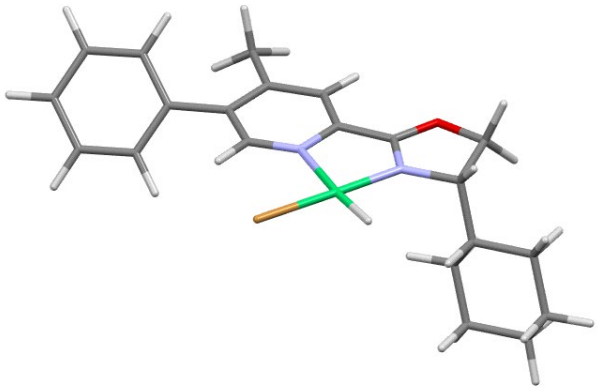

Calculated geometry

Atom	X	Y	Z
Ni1	0	0	0
O2	1.0014	3.8116	-0.2485
N3	0.9739	1.6043	0.1242
N4	-1.4156	1.234	-0.7883
C5	2.3521	1.9863	0.4721
H6	2.5683	1.65	1.497
C7	2.2753	3.5346	0.413
H8	2.2341	3.9976	1.4089
H9	3.0681	4.0066	-0.1801
C10	0.3547	2.6571	-0.2915

C11	-1.0029	2.5217	-0.81
C12	-1.79	3.5574	-1.2886
H13	-1.3965	4.5753	-1.2935
C14	-3.077	3.2831	-1.7799
C15	-3.5086	1.9377	-1.7565
C16	-2.6303	0.9594	-1.2506
H17	1.1019	-0.753	0.5848
H18	-2.9287	-0.0911	-1.2071
C19	-3.9144	4.4058	-2.3247
Br20	-1.2088	-1.9807	-0.1022
C21	3.1506	1.6943	-1.9545
C22	3.368	1.329	-0.4783
C23	4.8095	1.6277	-0.0374
C24	5.8326	0.9402	-0.9488
C25	5.6138	1.3124	-2.4194
C26	4.1785	1.0051	-2.86
H27	3.2368	2.7888	-2.0855
H28	2.1301	1.4159	-2.2652
H29	3.2047	0.241	-0.3765
H30	4.9518	1.3085	1.0094
H31	4.9847	2.7196	-0.0601
H32	6.8562	1.2024	-0.632
H33	5.7384	-0.1554	-0.8343
H34	5.8116	2.3925	-2.5539
H35	6.3352	0.779	-3.0613
H36	4.0138	-0.0876	-2.8256
H37	4.0224	1.3131	-3.9076
C38	-7.3218	0.5817	-3.2063
C39	-7.2596	1.641	-2.2947
C40	-6.0246	2.0951	-1.8273
C41	-4.8311	1.4919	-2.2616
C42	-4.9054	0.4201	-3.1697
C43	-6.1409	-0.0277	-3.6421
H44	-8.2893	0.2305	-3.5745
H45	-8.1789	2.1147	-1.9408
H46	-5.9895	2.9088	-1.1005
H47	-3.9855	-0.0546	-3.5202
H48	-6.1804	-0.8551	-4.3552
H49	-4.5265	4.0775	-3.1768
H50	-4.6067	4.7867	-1.5556
H51	-3.2776	5.2449	-2.639

L*NiBr—H, trans

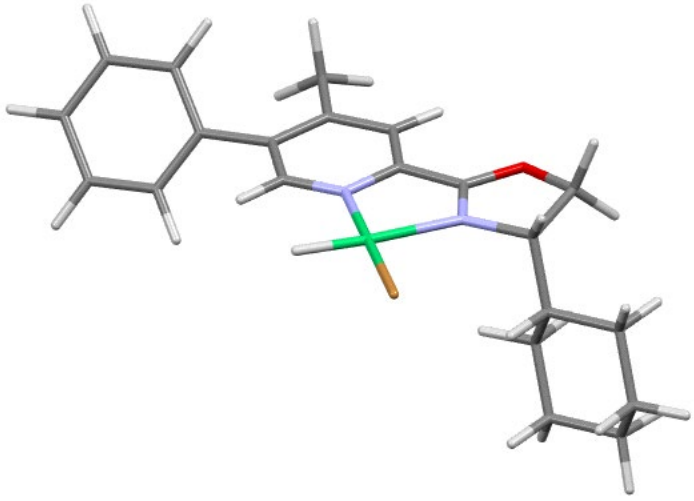

Calculated geometry

Atom	X	Y	Z
Ni1	0	0	0
O2	1.0083	3.8467	-0.4759
N3	1.087	1.6575	0.0054
N4	-1.3395	1.153	-0.7533
C5	2.4586	2.1132	0.275
H6	2.7342	1.8315	1.3022
C7	2.3171	3.6537	0.1465
H8	2.2953	4.1647	1.1196
H9	3.0667	4.126	-0.5003
C10	0.4143	2.6613	-0.431
C11	-0.9623	2.4517	-0.8714
C12	-1.804	3.4354	-1.3629
H13	-1.4355	4.4592	-1.4463
C14	-3.1095	3.1083	-1.763
C15	-3.5055	1.7583	-1.6342
C16	-2.5788	0.8284	-1.1288
H17	3.3548	0.3679	-0.5184
Br18	1.5763	-1.3978	0.9805
H19	-2.8587	-0.2183	-1.0125
C20	-4.0038	4.1782	-2.3221
H21	-0.9101	-1.1415	-0.0559
C22	5.9187	1.1407	-1.2443
C23	4.9059	1.8383	-0.329
C24	3.4626	1.4529	-0.6875
C25	3.166	1.7262	-2.1691

C26	4.1817	1.0247	-3.0792
C27	5.6208	1.4134	-2.7229
H28	5.878	0.0512	-1.0613
H29	6.9425	1.464	-0.9909
H30	5.0325	2.9334	-0.421
H31	5.1063	1.5864	0.7266
H32	2.1456	1.3907	-2.4178
H33	3.2012	2.8139	-2.3657
H34	4.0642	-0.0694	-2.9722
H35	3.9686	1.2617	-4.1353
H36	5.7674	2.4902	-2.9302
H37	6.3354	0.8702	-3.3643
C38	-7.3778	0.2519	-2.7373
C39	-6.2172	-0.3557	-3.2266
C40	-4.9616	0.1407	-2.869
C41	-4.8484	1.2587	-2.0235
C42	-6.0212	1.8605	-1.5348
C43	-7.2755	1.3586	-1.8878
H44	-8.3605	-0.1376	-3.0153
H45	-6.2881	-1.2199	-3.8921
H46	-4.0583	-0.333	-3.2618
H47	-5.9533	2.712	-0.855
H48	-8.1778	1.8321	-1.4924
H49	-4.6615	3.7846	-3.1099
H50	-4.6535	4.5955	-1.5348
H51	-3.4061	5.0059	-2.7295

L*NiBr—propargyl, (R), cis

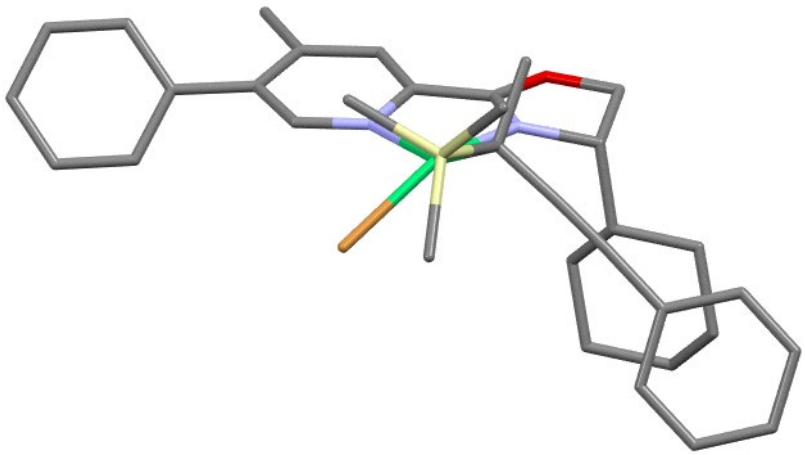

Calculated geometry

Atom	X	Y	Z
Ni1	0	0	0
O2	-1.759	0.8286	-3.4914
N3	-1.2608	0.6626	-1.3115
N4	0.9546	-0.6347	-1.7089
C5	-2.2994	1.7124	-1.3691
H6	-3.0776	1.514	-0.6208
C7	-2.8438	1.5211	-2.7996
H8	-3.7283	0.8677	-2.8362
H9	-3.0461	2.4528	-3.3405
C10	-0.9835	0.3445	-2.5306
C11	0.203	-0.4513	-2.8161
C12	0.5608	-0.9416	-4.0629
H13	-0.0769	-0.7367	-4.9244
C14	1.7464	-1.6795	-4.2068
C15	2.5205	-1.8949	-3.0436
C16	2.0735	-1.343	-1.8277
Br17	2.0159	0.1114	1.2211
H18	2.6516	-1.4749	-0.911
C19	-1.3245	-0.1145	1.4937
C20	-1.7321	1.2004	1.8711
Si21	-0.7267	-1.0017	3.1063
C22	-2.4708	-0.9657	0.8928

C23	-2.0506	2.323	2.2466
H24	-3.2804	-1.1288	1.6237
H25	-2.9291	-0.5015	0.0102
H26	-2.1024	-1.958	0.587
C27	-2.9038	6.3509	3.2973
C28	-3.9359	5.4978	2.8882
C29	-3.6662	4.1703	2.5566
C30	-2.348	3.6649	2.6215
C31	-1.3162	4.5351	3.0433
C32	-1.595	5.8608	3.3757
H33	-3.119	7.3911	3.5548
H34	-4.9617	5.8717	2.8266
H35	-4.474	3.5084	2.2365
H36	-0.2929	4.1567	3.0981
H37	-0.7825	6.519	3.6956
C38	2.1469	-2.1765	-5.5675
C39	0.1664	-2.6236	2.7243
C40	0.2456	0.1065	4.285
C41	-2.2967	-1.4675	4.0765
H42	0.2641	-3.2235	3.6452
H43	-0.4104	-3.219	1.9968
H44	1.1694	-2.4491	2.3102
H45	0.4258	-0.4427	5.2254
H46	1.2111	0.4247	3.8717
H47	-0.345	1.005	4.5281
H48	-2.0115	-1.8287	5.0797
H49	-2.9555	-0.5929	4.2096
H50	-2.8797	-2.2644	3.5878
C51	-0.5774	3.5177	-2.054
C52	-1.687	3.0967	-1.0783
C53	-2.7858	4.1683	-1.0001
C54	-2.2125	5.541	-0.6333
C55	-1.0934	5.9579	-1.5935
C56	-0.0005	4.8861	-1.6696
H57	-0.9767	3.5732	-3.0832
H58	0.2294	2.7664	-2.0636
H59	-1.2332	3.0119	-0.0785
H60	-3.5463	3.8654	-0.2625
H61	-3.3009	4.2407	-1.9763
H62	-3.0174	6.2953	-0.6274
H63	-1.8156	5.4994	0.3952
H64	-1.5171	6.1144	-2.6035
H65	-0.6614	6.9241	-1.2818

H66	0.4955	4.8022	-0.6851
H67	0.7802	5.1818	-2.3907
C68	6.2375	-4.0536	-2.9477
C69	6.141	-2.7832	-2.3709
C70	4.932	-2.0854	-2.41
C71	3.8019	-2.6434	-3.0353
C72	3.9091	-3.9231	-3.6081
C73	5.117	-4.6223	-3.5622
H74	7.1833	-4.6006	-2.9162
H75	7.0117	-2.3307	-1.8893
H76	4.8661	-1.0896	-1.9646
H77	3.0364	-4.387	-4.0712
H78	5.1812	-5.6197	-4.0048
H79	3.2381	-2.1591	-5.6996
H80	1.8185	-3.2185	-5.7174
H81	1.6783	-1.5675	-6.3537

L*NiBr—propargyl, (R), trans

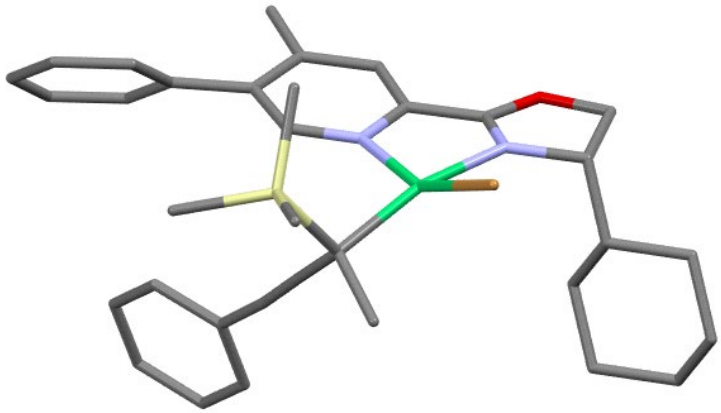

Calculated geometry

Atom	X	Y	Z
Ni1	0	0	0
O2	-0.7196	0.7406	-3.8823
N3	-0.9477	0.2279	-1.7121
N4	1.5967	0.0978	-1.2262
C5	-2.3189	0.5547	-2.1301

H6	-2.9844	-0.2785	-1.8641
C7	-2.1641	0.6696	-3.6685
H8	-2.5318	-0.2188	-4.2018
H9	-2.6109	1.5717	-4.1043
C10	-0.1721	0.4191	-2.7167
C11	1.2655	0.2871	-2.5272
C12	2.1953	0.2993	-3.5554
H13	1.8512	0.4465	-4.5803
C14	3.5544	0.0914	-3.2783
C15	3.9038	-0.1313	-1.9284
C16	2.8833	-0.1199	-0.9606
Br17	-1.9089	-1.0503	0.9529
H18	3.1499	-0.2667	0.0801
C19	0.9218	0.3213	1.7535
C20	1.923	1.2987	1.4554
Si21	1.6563	-1.338	2.388
C22	-0.0705	0.9657	2.7577
C23	2.7736	2.1491	1.2205
H24	0.4657	1.3252	3.6547
H25	-0.5731	1.8396	2.3095
H26	-0.8484	0.266	3.0794
C27	5.9094	4.8018	0.1319
C28	4.6247	5.3006	0.3802
C29	3.5897	4.4387	0.7434
C30	3.8208	3.0496	0.8698
C31	5.1249	2.5608	0.6233
C32	6.1523	3.4286	0.255
H33	6.7168	5.4803	-0.1556
H34	4.4271	6.372	0.2871
H35	2.5873	4.8303	0.9317
H36	5.3203	1.492	0.722
H37	7.1505	3.0275	0.0621
C38	4.5458	0.076	-4.4067
C39	0.6525	-1.9543	3.8648
C40	1.652	-2.7185	1.091
C41	3.4451	-1.0674	2.9536
H42	1.0766	-2.9045	4.2317
H43	0.6648	-1.2323	4.6972
H44	-0.3955	-2.1326	3.5782
H45	2.0622	-3.6394	1.54
H46	0.6243	-2.9263	0.756
H47	2.2578	-2.4818	0.2038
H48	3.8597	-1.9977	3.3782

H49	4.1003	-0.7544	2.125
H50	3.4946	-0.2845	3.7287
C51	-2.8185	1.8189	-1.4072
C52	-1.9392	3.0551	-1.647
C53	-2.4677	4.2714	-0.8771
C54	-3.9332	4.5617	-1.2193
C55	-4.8129	3.3291	-0.9821
C56	-4.2882	2.1085	-1.747
H57	-2.7662	1.5756	-0.3316
H58	-1.9164	3.2962	-2.7259
H59	-0.8997	2.8449	-1.3454
H60	-1.8404	5.1536	-1.0889
H61	-2.3791	4.0753	0.2074
H62	-4.3037	5.4164	-0.6283
H63	-4.0048	4.8597	-2.2823
H64	-4.8283	3.0972	0.0987
H65	-5.8562	3.538	-1.2735
H66	-4.3879	2.2939	-2.8328
H67	-4.9035	1.2205	-1.5216
H68	5.3556	-0.6449	-4.2256
H69	4.0466	-0.172	-5.3542
H70	5.0138	1.0669	-4.5304
C71	7.8744	-0.8037	-0.4273
C72	7.6391	0.2304	-1.3392
C73	6.3572	0.4394	-1.8507
C74	5.2872	-0.3823	-1.4563
C75	5.5345	-1.4189	-0.5379
C76	6.8177	-1.6291	-0.0294
H77	8.8785	-0.9652	-0.0269
H78	8.4566	0.8871	-1.6473
H79	6.1813	1.2743	-2.53
H80	4.7169	-2.0727	-0.2267
H81	6.9917	-2.442	0.6801

L*NiBr—propargyl, (S), cis

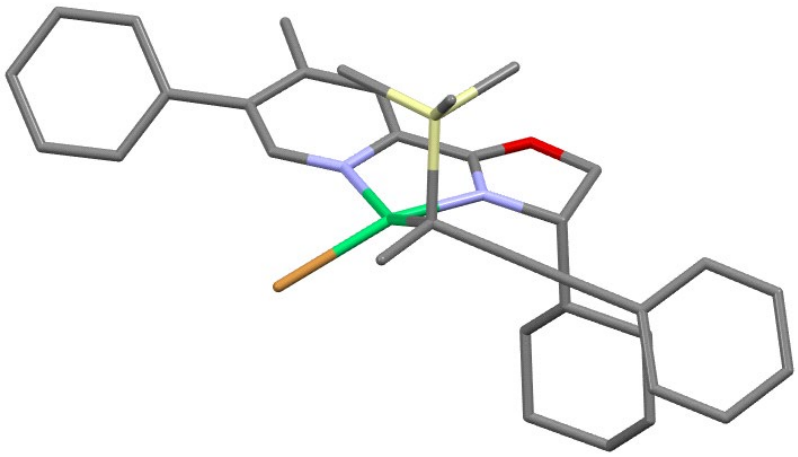

Calculated geometry

Atom	X	Y	Z
Ni1	0	0	0
O2	-1.9084	1.4205	-3.2141
N3	-1.207	1.0485	-1.1131
N4	0.4591	-0.8319	-1.8231
C5	-1.9213	2.3419	-1.0354
H6	-2.6547	2.3099	-0.2235
C7	-2.63	2.3959	-2.4054
H8	-3.6793	2.0703	-2.3539
H9	-2.5675	3.3651	-2.9142
C10	-1.1959	0.704	-2.3565
C11	-0.3616	-0.4013	-2.803
C12	-0.3748	-0.9485	-4.0776
H13	-1.0483	-0.5378	-4.8317
C14	0.4862	-2.0123	-4.387
C15	1.3325	-2.4791	-3.3553
C16	1.274	-1.8465	-2.0997
Br17	2.0912	-0.6433	0.89
H18	1.9202	-2.1721	-1.2828
C19	-0.9986	0.1308	1.7285
C20	-1.6303	1.3889	1.9666
Si21	-2.334	-1.2021	1.3369
C22	-0.2355	-0.2745	3.0137

C23	-2.1882	2.4382	2.2645
H24	0.1726	-1.2923	2.9471
H25	0.6064	0.4037	3.215
H26	-0.9115	-0.2327	3.8854
C27	-4.0729	6.1933	2.8908
C28	-4.7792	5.1396	2.2984
C29	-4.169	3.8995	2.1106
C30	-2.8289	3.688	2.5084
C31	-2.1317	4.7566	3.1154
C32	-2.7494	5.9933	3.3011
H33	-4.5526	7.1648	3.0348
H34	-5.8147	5.2864	1.9795
H35	-4.7197	3.0795	1.6439
H36	-1.0956	4.6061	3.4266
H37	-2.1919	6.8108	3.7662
C38	0.4914	-2.5814	-5.7779
C39	-3.2259	-1.6121	2.9582
C40	-3.6549	-0.6157	0.1178
C41	-1.5335	-2.7875	0.683
H42	-4.0571	-2.3122	2.7678
H43	-2.5497	-2.0793	3.6917
H44	-3.6458	-0.6999	3.4142
H45	-4.5231	-1.2936	0.1764
H46	-4.0044	0.3989	0.3676
H47	-3.2988	-0.6125	-0.922
H48	-2.2731	-3.606	0.675
H49	-1.1582	-2.6594	-0.3442
H50	-0.6877	-3.0982	1.3171
C51	0.2194	3.5885	-1.7687
C52	-0.9299	3.4872	-0.7536
C53	-1.658	4.8356	-0.6285
C54	-0.689	5.9571	-0.2408
C55	0.4745	6.0583	-1.2332
C56	1.1919	4.7126	-1.3892
H57	-0.1875	3.7875	-2.7775
H58	0.7653	2.6329	-1.827
H59	-0.4867	3.2548	0.2295
H60	-2.4706	4.7604	0.1085
H61	-2.1293	5.0902	-1.5959
H62	-1.2287	6.9172	-0.1779
H63	-0.2935	5.7543	0.771
H64	0.0831	6.376	-2.2179
H65	1.1872	6.8374	-0.9131

H66	1.6838	4.4504	-0.4344
H67	1.9931	4.7889	-2.1436
H68	1.5012	-2.8885	-6.0852
H69	-0.152	-3.4748	-5.839
H70	0.1032	-1.846	-6.4969
C71	4.1858	-5.666	-3.7873
C72	4.5731	-4.4368	-3.2443
C73	3.6421	-3.4045	-3.1113
C74	2.3103	-3.5819	-3.5288
C75	1.9308	-4.8231	-4.0696
C76	2.8614	-5.8567	-4.1952
H77	4.9138	-6.4748	-3.89
H78	5.606	-4.2788	-2.9235
H79	3.9531	-2.4436	-2.6938
H80	0.8955	-4.991	-4.3721
H81	2.5484	-6.8185	-4.6096

L*NiBr—propargyl, (S), trans

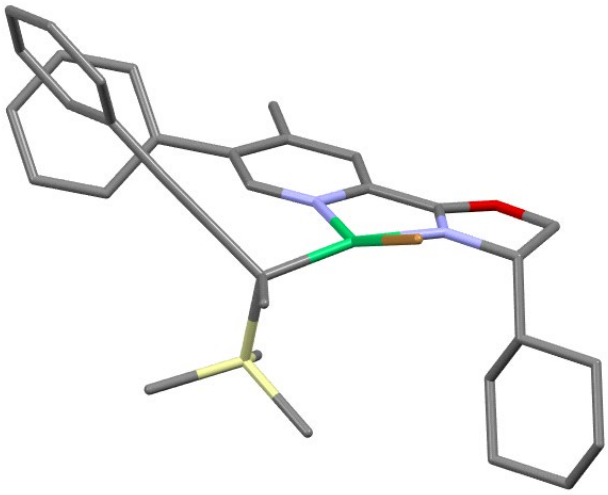

Calculated geometry

Atom	X	Y	Z
Ni1	0	0	0
O2	-1.8469	-0.1441	-3.5769
N3	-1.3545	0.2081	-1.419
N4	0.9524	-0.9894	-1.5037

C5	-2.5666	1.0149	-1.6286
H6	-3.3158	0.7373	-0.8745
C7	-3.0099	0.5626	-3.0432
H8	-3.8461	-0.1508	-3.0207
H9	-3.2453	1.3845	-3.7306
C10	-1.0328	-0.3186	-2.543
C11	0.22	-1.0513	-2.6439
C12	0.6256	-1.734	-3.7804
H13	-0.0171	-1.7244	-4.662
C14	1.8499	-2.4176	-3.7891
C15	2.6145	-2.3595	-2.6074
C16	2.1182	-1.6349	-1.511
Br17	-1.6892	0.3686	1.6044
H18	2.6997	-1.5935	-0.5933
C19	1.5504	0.2537	1.2527
C20	2.235	-0.9849	1.4636
Si21	2.5555	1.6312	0.3485
C22	1.2376	0.8212	2.6667
C23	2.7906	-2.0383	1.7564
H24	0.6292	1.7322	2.626
H25	0.6922	0.0871	3.2762
H26	2.1762	1.0581	3.2004
C27	4.6135	-5.7784	2.6329
C28	4.9548	-5.0849	1.4659
C29	4.3645	-3.855	1.1762
C30	3.4092	-3.29	2.0516
C31	3.0745	-4	3.2279
C32	3.6723	-5.2281	3.5115
H33	5.0783	-6.7419	2.8579
H34	5.6888	-5.5024	0.7718
H35	4.6381	-3.3191	0.2681
H36	2.3381	-3.5752	3.9141
H37	3.4	-5.7621	4.4261
C38	2.3024	-3.1471	-5.0209
C39	4.2737	1.7223	1.1398
C40	2.8326	1.4901	-1.5195
C41	1.6399	3.2672	0.6111
H42	4.861	2.547	0.7017
H43	4.2132	1.8866	2.2277
H44	4.8253	0.7824	0.9696
H45	3.4035	2.3837	-1.8245
H46	3.4207	0.6074	-1.8082
H47	1.892	1.4814	-2.0896

H48	2.0941	4.056	-0.0115
H49	0.5815	3.174	0.3184
H50	1.6731	3.6013	1.6597
C51	-1.1944	3.0345	-2.4472
C52	-2.2587	2.5153	-1.4691
C53	-3.5451	3.3512	-1.5505
C54	-3.2639	4.8438	-1.344
C55	-2.2075	5.3568	-2.3285
C56	-0.9212	4.529	-2.2386
H57	-1.532	2.8755	-3.488
H58	-0.2597	2.4637	-2.3253
H59	-1.8552	2.6221	-0.4471
H60	-4.2699	2.9896	-0.8011
H61	-4.0174	3.2079	-2.5404
H62	-4.1983	5.4216	-1.4441
H63	-2.9042	5.0033	-0.3107
H64	-2.6092	5.2947	-3.3574
H65	-1.9921	6.4222	-2.1393
H66	-0.4647	4.6748	-1.2432
H67	-0.1816	4.8826	-2.9767
H68	3.3882	-3.0516	-5.1666
H69	2.0816	-4.2244	-4.9383
H70	1.7818	-2.7688	-5.912
C71	6.4452	-4.2292	-2.0733
C72	6.3066	-2.8472	-1.9113
C73	5.0617	-2.2415	-2.0981
C74	3.9418	-3.0093	-2.4603
C75	4.0916	-4.396	-2.6263
C76	5.3343	-5.0015	-2.4292
H77	7.4171	-4.705	-1.9194
H78	7.1693	-2.2371	-1.6322
H79	4.9562	-1.1622	-1.965
H80	3.2243	-5.0078	-2.8846
H81	5.4338	-6.0835	-2.5466

L*NiBr—allenyl, (R), cis

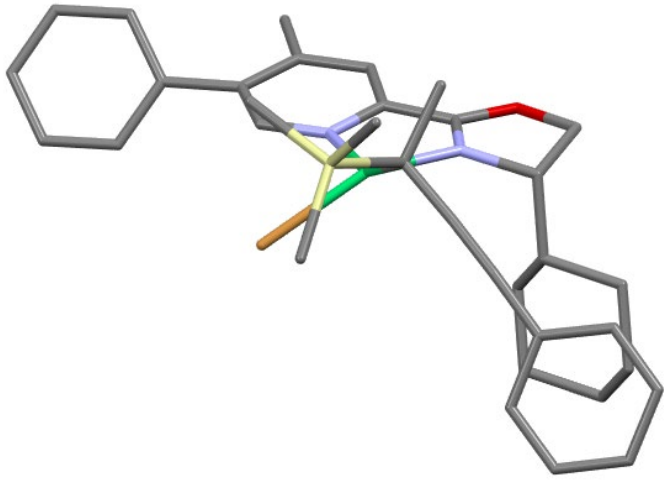

Calculated geometry

Atom	X	Y	Z
Ni1	0	0	0
O2	1.3471	3.6874	-0.6143
N3	1.1321	1.5425	-0.0008
N4	-1.1686	1.2093	-1.1493
C5	2.4615	1.9171	0.5172
H6	2.5005	1.6836	1.5897
C7	2.4716	3.4491	0.2875
H8	2.2803	4.0216	1.2064
H9	3.3778	3.8273	-0.2006
C10	0.6482	2.5624	-0.6232
C11	-0.632	2.4398	-1.3094
C12	-1.2471	3.4443	-2.04
H13	-0.7722	4.4241	-2.1112
C14	-2.4785	3.1956	-2.6673
C15	-3.0324	1.9047	-2.5151
C16	-2.3348	0.9608	-1.7373
Br17	-1.4961	-1.8105	-0.0275
H18	-2.7336	-0.0452	-1.5908
C19	0.8862	-0.4832	3.6609
C20	1.1076	-0.7231	2.3805
Si21	-0.4006	-1.5815	4.5161
C22	1.5682	0.6347	4.4305
C23	1.2068	-0.9942	1.1037
C24	4.1046	-3.6499	-0.6592
C25	4.1227	-3.396	0.7194

C26	3.1744	-2.5503	1.2931
C27	2.1792	-1.9282	0.5081
C28	2.1731	-2.1987	-0.8742
C29	3.1216	-3.0476	-1.4503
H30	4.8501	-4.3106	-1.1094
H31	4.8853	-3.8612	1.3507
H32	3.2008	-2.3497	2.3675
H33	1.4153	-1.7248	-1.5015
H34	3.0942	-3.2358	-2.5272
C35	-0.4257	-3.284	3.7084
C36	-2.1009	-0.7706	4.3465
C37	0.0452	-1.7312	6.3478
C38	-3.1533	4.2973	-3.4347
H39	2.1372	0.2404	5.2902
H40	2.264	1.2061	3.7958
H41	0.8277	1.3421	4.8455
H42	-1.1676	-3.9376	4.1976
H43	-0.6898	-3.1991	2.6421
H44	0.5615	-3.7698	3.7799
H45	-2.8765	-1.3517	4.8744
H46	-2.0977	0.2508	4.7627
H47	-2.3853	-0.7071	3.283
H48	-0.6866	-2.3672	6.8743
H49	1.0432	-2.1826	6.4782
H50	0.0515	-0.7449	6.8411
C51	3.6189	1.3274	-1.707
C52	3.5849	1.1374	-0.1842
C53	4.951	1.4399	0.4487
C54	6.0564	0.5919	-0.1911
C55	6.0964	0.78	-1.7117
C56	4.7317	0.4855	-2.3441
H57	3.7866	2.3925	-1.9529
H58	2.6449	1.0493	-2.1428
H59	3.3733	0.0767	0.0062
H60	4.9048	1.2527	1.5355
H61	5.1971	2.511	0.3226
H62	7.0335	0.8441	0.2546
H63	5.8695	-0.4733	0.0383
H64	6.3869	1.8228	-1.9405
H65	6.8719	0.1338	-2.1571
H66	4.4919	-0.5838	-2.2074
H67	4.7647	0.6655	-3.432
C68	-6.7648	0.6262	-4.2232

C69	-6.5029	0.4264	-2.864
C70	-5.2914	0.8498	-2.3136
C71	-4.3258	1.4889	-3.1126
C72	-4.598	1.6817	-4.4786
C73	-5.8072	1.2515	-5.0287
H74	-7.7121	0.2928	-4.6548
H75	-7.2458	-0.0608	-2.2272
H76	-5.0962	0.6974	-1.2491
H77	-3.8496	2.1479	-5.122
H78	-5.9997	1.4007	-6.0943
H79	-4.2475	4.2411	-3.3465
H80	-2.8121	5.2799	-3.0787
H81	-2.91	4.2327	-4.5084

L*NiBr—allenyl, (R), trans

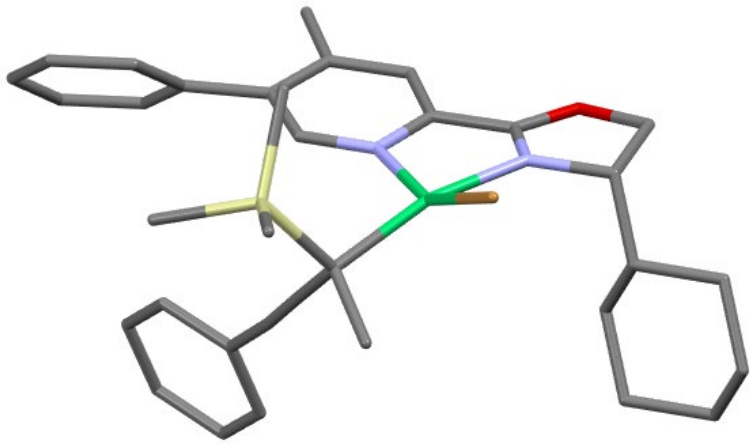

Calculated geometry

Atom	X	Y	Z
Ni1	0	0	0
O2	1.2832	3.753	-0.5477
N3	1.1249	1.6066	0.0766
N4	-1.1863	1.2044	-0.996
C5	2.5166	1.9485	0.3986
H6	2.7142	1.7088	1.4534
C7	2.5289	3.483	0.1706

H8	2.497	4.0546	1.1089
H9	3.3569	3.8433	-0.4525
C10	0.5808	2.6303	-0.4774
C11	-0.7567	2.4897	-1.0435
C12	-1.527	3.519	-1.5608
H13	-1.1289	4.535	-1.5578
C14	-2.8196	3.2579	-2.0457
C15	-3.2631	1.9172	-2.0044
C16	-2.3947	0.9405	-1.4863
Br17	1.264	-1.2037	1.5725
H18	-2.7025	-0.1018	-1.4746
C19	0.0322	-2.826	-2.337
C20	-0.6032	-2.19	-1.3678
Si21	1.2576	-4.1823	-1.8414
C22	-0.127	-2.4517	-3.8012
C23	-1.1049	-1.5182	-0.3633
C24	-4.9599	-2.0555	1.4688
C25	-4.561	-2.8827	0.4095
C26	-3.3019	-2.7298	-0.1685
C27	-2.4018	-1.7442	0.2925
C28	-2.8143	-0.9295	1.3656
C29	-4.0771	-1.0814	1.9453
H30	-5.9496	-2.1725	1.9182
H31	-5.242	-3.6492	0.0288
H32	-3.0025	-3.3685	-1.0038
H33	-2.1313	-0.1624	1.7381
H34	-4.3731	-0.4323	2.7741
C35	0.8059	-4.8736	-0.1489
C36	2.9923	-3.429	-1.7922
C37	1.2111	-5.5523	-3.1443
C38	-3.6655	4.3945	-2.545
H39	-0.5184	-3.2977	-4.3926
H40	-0.8097	-1.597	-3.933
H41	0.8469	-2.1829	-4.2485
H42	1.5087	-5.6706	0.1471
H43	0.8436	-4.0775	0.6113
H44	-0.2122	-5.297	-0.1546
H45	3.7524	-4.1886	-1.5416
H46	3.2597	-2.989	-2.7673
H47	3.0386	-2.6316	-1.0326
H48	1.9211	-6.3569	-2.8877
H49	0.2044	-5.9974	-3.2162
H50	1.4841	-5.1667	-4.1407

C51	3.2709	1.317	-1.9806
C52	3.4844	1.1255	-0.4717
C53	4.9466	1.3839	-0.0802
C54	5.9071	0.5113	-0.8967
C55	5.6949	0.7005	-2.4029
C56	4.2353	0.4451	-2.7939
H57	3.4284	2.3777	-2.251
H58	2.2302	1.0708	-2.2491
H59	3.2573	0.0719	-0.2342
H60	5.0812	1.1968	0.999
H61	5.1943	2.4486	-0.2494
H62	6.951	0.7392	-0.6224
H63	5.7373	-0.5498	-0.6372
H64	5.9701	1.7354	-2.681
H65	6.3662	0.034	-2.9706
H66	3.9921	-0.6176	-2.6159
H67	4.0881	0.625	-3.8722
H68	-4.7259	4.2495	-2.2933
H69	-3.3208	5.3481	-2.1207
H70	-3.6009	4.4784	-3.6427
C71	-7.1463	0.4963	-3.18
C72	-6.5816	0.1027	-1.9622
C73	-5.3238	0.577	-1.5871
C74	-4.6112	1.4597	-2.4223
C75	-5.1865	1.8457	-3.6456
C76	-6.4433	1.3655	-4.0208
H77	-8.1309	0.1244	-3.475
H78	-7.1215	-0.5766	-1.2977
H79	-4.8962	0.2689	-0.63
H80	-4.6388	2.5029	-4.3228
H81	-6.873	1.6681	-4.9793

L*NiBr—allenyl, (S), cis

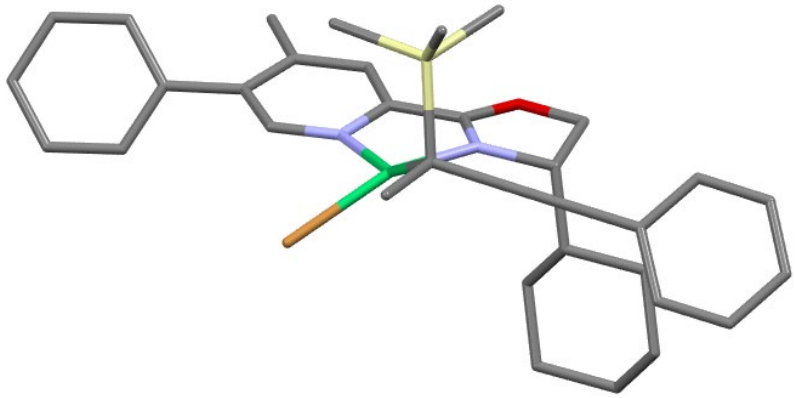

Calculated geometry

Atom	X	Y	Z
Ni1	0	0	0
O2	1.4719	3.6015	-0.7919
N3	1.2315	1.445	-0.2359
N4	-1.2631	1.3055	-0.922
C5	2.6815	1.6831	-0.1064
H6	3.0225	1.3209	0.8706
C7	2.7461	3.2247	-0.1803
H8	2.7852	3.6982	0.8115
H9	3.5506	3.618	-0.8125
C10	0.6989	2.5307	-0.6837
C11	-0.7021	2.5252	-1.0853
C12	-1.3961	3.6153	-1.5863
H13	-0.8923	4.5796	-1.6709
C14	-2.7406	3.4718	-1.9654
C15	-3.3229	2.1936	-1.8119
C16	-2.5362	1.1567	-1.2742
Br17	-1.5306	-1.7822	0.0439
H18	-2.9518	0.1567	-1.1339
C19	0.6511	-0.5947	3.6578
C20	0.9902	-0.7669	2.3904
C21	-0.3021	-1.5528	4.359
Si22	1.3366	0.8659	4.6381
C23	1.225	-0.9552	1.1179

C24	4.4876	-3.2067	-0.5536
C25	4.6316	-2.5669	0.6838
C26	3.5692	-1.848	1.2336
C27	2.3337	-1.7475	0.5607
C28	2.2044	-2.3978	-0.6832
C29	3.2657	-3.1216	-1.2304
H30	5.3222	-3.7635	-0.9874
H31	5.5833	-2.6219	1.2201
H32	3.691	-1.3378	2.1926
H33	1.2555	-2.3249	-1.2182
H34	3.1403	-3.6175	-2.197
H35	-0.6312	-2.3626	3.6896
H36	-1.2003	-1.0229	4.7219
H37	0.171	-2.0103	5.2459
C38	-3.4945	4.6649	-2.4818
C39	2.4349	0.2211	6.0362
C40	2.3315	2.001	3.5104
C41	-0.1104	1.827	5.3869
H42	2.8205	1.0521	6.6514
H43	1.8741	-0.4584	6.6996
H44	3.2977	-0.3351	5.6328
H45	2.7167	2.8666	4.0747
H46	3.1909	1.47	3.0708
H47	1.7019	2.3791	2.6895
H48	0.2518	2.6915	5.969
H49	-0.7824	2.2036	4.5973
H50	-0.7049	1.1905	6.0632
C51	3.4686	0.9438	-1.2032
C52	3.1004	1.3602	-2.6347
C53	3.8939	0.5441	-3.663
C54	5.4041	0.66	-3.4285
C55	5.7768	0.2577	-1.9973
C56	4.9813	1.0596	-0.9612
H57	3.2043	-0.1171	-1.0968
H58	3.3136	2.4342	-2.7866
H59	2.0196	1.2221	-2.8047
H60	3.6365	0.8709	-4.6847
H61	3.5945	-0.5173	-3.5861
H62	5.9537	0.0387	-4.1561
H63	5.7189	1.7055	-3.6071
H64	5.5652	-0.8167	-1.8539
H65	6.8589	0.3916	-1.8288
H66	5.2879	2.1215	-1.0098

H67	5.2186	0.708	0.0571
H68	-4.5489	4.6424	-2.172
H69	-3.0326	5.5964	-2.1244
H70	-3.4803	4.6908	-3.5842
C71	-7.3812	1.21	-2.8342
C72	-6.8642	0.8679	-1.5805
C73	-5.5474	1.1963	-1.2516
C74	-4.7291	1.8812	-2.1684
C75	-5.2581	2.2172	-3.4271
C76	-6.5728	1.882	-3.757
H77	-8.4112	0.951	-3.0929
H78	-7.489	0.3434	-0.8531
H79	-5.1522	0.9324	-0.2674
H80	-4.6302	2.7216	-4.1638
H81	-6.9659	2.1425	-4.7431

L*NiBr—allenyl, (S), trans

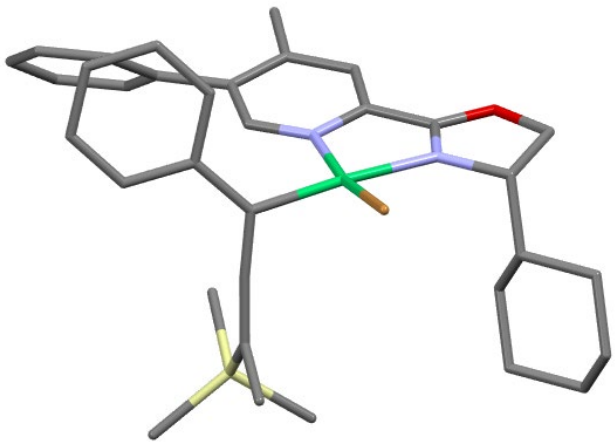

Calculated geometry

Atom	X	Y	Z
Ni1	0	0	0
O2	1.2467	3.7557	-0.6195
N3	1.1302	1.6079	0.0117
N4	-1.2569	1.2144	-0.8851
C5	2.5383	1.9539	0.2498

H6	2.7995	1.7128	1.2904
C7	2.5324	3.4888	0.0245
H8	2.553	4.0585	0.9644
H9	3.3215	3.8529	-0.6449
C10	0.5518	2.6317	-0.5069
C11	-0.8191	2.4939	-0.9855
C12	-1.6088	3.5199	-1.4793
H13	-1.2021	4.5317	-1.5214
C14	-2.9277	3.2608	-1.8898
C15	-3.3795	1.9268	-1.7918
C16	-2.4953	0.9553	-1.2933
Br17	1.3759	-1.226	1.4593
H18	-2.8155	-0.0804	-1.2384
C19	-0.0557	-2.8178	-2.3482
C20	-0.6397	-2.1968	-1.3373
C21	0.9287	-3.9571	-2.1319
Si22	-0.4021	-2.2291	-4.11
C23	-1.1139	-1.5212	-0.3227
C24	-4.8999	-2.0701	1.6454
C25	-4.5724	-2.8388	0.5199
C26	-3.3355	-2.6832	-0.1041
C27	-2.3877	-1.7533	0.3762
C28	-2.7296	-0.9952	1.5136
C29	-3.9694	-1.1505	2.1397
H30	-5.8719	-2.189	2.1313
H31	-5.2918	-3.5609	0.1234
H32	-3.0922	-3.2749	-0.9907
H33	-2.0095	-0.2697	1.8993
H34	-4.2102	-0.5466	3.019
H35	1.067	-4.1784	-1.0622
H36	1.9165	-3.7106	-2.5599
H37	0.591	-4.8803	-2.6345
C38	-1.0491	-3.6789	-5.137
C39	-1.6606	-0.8255	-4.1029
C40	1.2193	-1.6093	-4.8613
C41	-1.2234	-3.3723	-6.1826
H42	-0.328	-4.5131	-5.1456
H43	-2.0012	-4.0574	-4.7287
H44	-1.9202	-0.5414	-5.1365
H45	-2.5885	-1.1138	-3.5837
H46	-1.25	0.0635	-3.5996
H47	1.07	-1.267	-5.8996
H48	1.6166	-0.7644	-4.2754

H49	1.9856	-2.4021	-4.8734
H50	-3.7878	4.3921	-2.376
C51	3.151	1.3228	-2.1707
C52	3.4595	1.1391	-0.6773
C53	4.9395	1.4192	-0.3762
C54	5.8628	0.5627	-1.2504
C55	5.5546	0.7469	-2.7404
C56	4.0784	0.465	-3.0399
H57	3.2739	2.385	-2.4528
H58	2.1003	1.058	-2.3746
H59	3.2613	0.0835	-0.4235
H60	5.1429	1.2345	0.6926
H61	5.1605	2.4875	-0.5591
H62	6.9174	0.8093	-1.0411
H63	5.7283	-0.5011	-0.9813
H64	5.7924	1.7864	-3.0348
H65	6.2014	0.0926	-3.3492
H66	3.8643	-0.602	-2.8461
H67	3.8607	0.6371	-4.1072
H68	-4.8376	4.2581	-2.0781
H69	-3.421	5.3517	-1.9849
H70	-3.7677	4.4541	-3.477
C71	-7.2956	0.4725	-2.8027
C72	-6.6907	0.1091	-1.595
C73	-5.4238	0.5967	-1.2711
C74	-4.7426	1.4632	-2.148
C75	-5.3578	1.8184	-3.3613
C76	-6.6237	1.3249	-3.6852
H77	-8.2871	0.0896	-3.0577
H78	-7.2056	-0.5578	-0.8988
H79	-4.9635	0.3098	-0.3227
H80	-4.8338	2.4607	-4.0709
H81	-7.0846	1.6031	-4.6365

L*Ni^{I}—Br

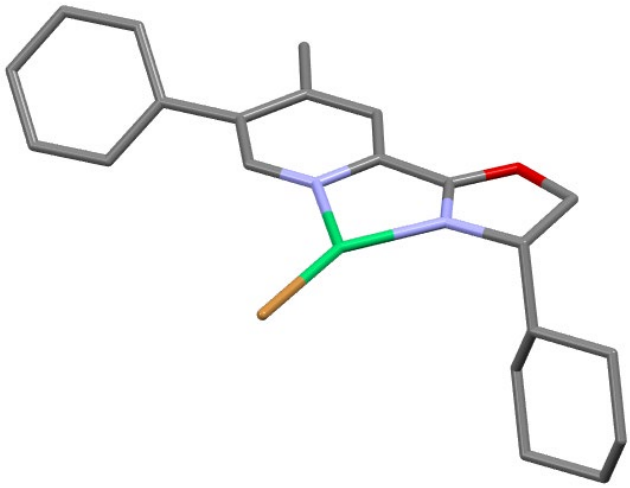

Calculated geometry

Atom	X	Y	Z
Ni1	0	0	0
O2	-3.0017	2.1138	1.6307
N3	-1.7935	0.7798	0.2876
N4	0.4796	1.269	1.5016
C5	-3.1745	0.5576	-0.164
H6	-3.2413	0.8031	-1.2357
C7	-3.9735	1.591	0.6775
H8	-4.341	2.4368	0.0797
H9	-4.8056	1.1607	1.2495
C10	-1.8241	1.6069	1.2719
C11	-0.5891	1.949	1.9775
C12	-0.4962	2.858	3.022
H13	-1.3967	3.3618	3.3772
C14	0.7477	3.111	3.6211
C15	0.8332	4.0747	4.7719
C16	1.8678	2.413	3.1133
C17	1.6658	1.5018	2.06
H18	-2.8518	-1.4935	-0.593
Br19	1.245	-1.5457	-1.1915
H20	2.512	0.9467	1.647
H21	1.5842	3.7583	5.5098
H22	1.1243	5.0797	4.4238

H23	-0.1428	4.1686	5.2692
C24	5.8819	2.8388	4.5945
C25	5.1415	3.974	4.248
C26	3.8327	3.8438	3.7792
C27	3.2443	2.5738	3.6451
C28	4.0007	1.4385	3.9878
C29	5.3075	1.5706	4.4628
H30	6.9053	2.9426	4.9642
H31	5.5871	4.968	4.3379
H32	3.272	4.7353	3.4921
H33	3.5541	0.4453	3.8955
H34	5.8782	0.6783	4.7327
C35	-5.3658	-2.6608	-0.4531
C36	-4.9768	-1.1826	-0.5708
C37	-3.5789	-0.9169	0.0089
C38	-3.4754	-1.4157	1.458
C39	-3.8651	-2.8946	1.5696
C40	-5.2616	-3.155	0.9941
H41	-4.6926	-3.2623	-1.0911
H42	-6.3869	-2.8147	-0.8411
H43	-5.7219	-0.5703	-0.0291
H44	-5.011	-0.8588	-1.6253
H45	-2.4501	-1.2661	1.8344
H46	-4.1436	-0.8194	2.1064
H47	-3.1254	-3.504	1.0184
H48	-3.8156	-3.2186	2.6228
H49	-6.0127	-2.6283	1.6123
H50	-5.5062	-4.2293	1.0505

trimethyl(4-phenylbut-1-en-3-yn-2-yl)silane

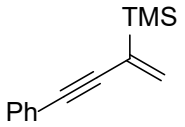

Calculated geometry

Atom	X	Y	Z
C1	0	0	0
C2	-1.0938	0.1429	0.9048
Si3	1.3574	-1.2288	0.5433
C4	0.0655	0.6978	-1.1559

C5	-1.9842	0.2011	1.7401
C6	-5.0881	0.4524	4.6263
C7	-5.3957	0.1928	3.2857
C8	-4.3798	0.112	2.3328
C9	-3.031	0.2896	2.7103
C10	-2.7315	0.5491	4.0654
C11	-3.7541	0.6302	5.011
H12	-5.8865	0.5152	5.37
H13	-6.4355	0.0519	2.9797
H14	-4.6192	-0.0907	1.2866
H15	-1.6902	0.6856	4.3653
H16	-3.5079	0.8327	6.0566
C17	2.018	-0.6587	2.2139
C18	2.7275	-1.2542	-0.7476
C19	0.5595	-2.9287	0.7078
H20	-0.7178	1.4045	-1.4523
H21	0.9084	0.5802	-1.8429
H22	2.7738	-1.3652	2.5963
H23	2.4884	0.3353	2.1353
H24	1.2045	-0.5953	2.9552
H25	3.5158	-1.963	-0.4431
H26	2.3484	-1.5724	-1.7325
H27	3.1928	-0.2614	-0.861
H28	1.2937	-3.6697	1.0665
H29	-0.276	-2.9021	1.4261
H30	0.1688	-3.2779	-0.2622

trimethyl(4-phenylbut-1-en-3-yn-2-yl)silyl radical

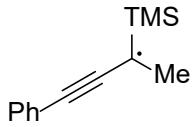

Calculated geometry

Atom	X	Y	Z
C1	0	0	0
C2	-1.0081	0.3926	0.835
Si3	1.7906	0.0943	0.608
C4	-0.2974	-0.5131	-1.3892
C5	-1.8955	0.7642	1.6231
C6	-4.8818	2.0264	4.3478

C7	-5.2439	1.5426	3.083
C8	-4.2681	1.1261	2.1812
C9	-2.893	1.185	2.529
C10	-2.5422	1.6781	3.8136
C11	-3.528	2.0912	4.7058
H12	-5.6518	2.3519	5.0519
H13	-6.2986	1.4906	2.7998
H14	-4.5505	0.7489	1.1958
H15	-1.4872	1.7288	4.092
H16	-3.2412	2.4682	5.6911
C17	1.8628	1.11	2.1919
C18	2.8386	0.8858	-0.7488
C19	2.4	-1.6661	0.9257
H20	-1.3644	-0.745	-1.5302
H21	-0.0106	0.2375	-2.1496
H22	0.2912	-1.4192	-1.616
H23	2.8986	1.1695	2.566
H24	1.5003	2.1369	2.0208
H25	1.2394	0.6571	2.9802
H26	3.8947	0.9467	-0.4356
H27	2.7952	0.2952	-1.6788
H28	2.4896	1.9069	-0.9754
H29	3.458	-1.6601	1.239
H30	1.8092	-2.1499	1.721
H31	2.3187	-2.2834	0.0157

3.1.6.3 Geometries of calculated species for BDE estimation

These geometries were calculated using calculation method B.

4-iodotetrahydro-2H-pyran

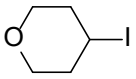

Calculated geometry

Atom	X	Y	Z
O1	0	0	0
C2	-1.3522	0.006	-0.4251
C3	-2.2913	0.5058	0.6774

C4	-2.0974	-0.3513	1.9163
C5	-0.6352	-0.4001	2.3242
C6	0.2021	-0.8443	1.1205
H7	-1.6475	-1.0054	-0.7429
H8	-1.4004	0.6617	-1.2947
H9	-3.3251	0.4671	0.3292
H10	-2.0534	1.5476	0.9031
I11	-3.3464	0.3682	3.5679
H12	-2.484	-1.3565	1.7523
H13	-0.3032	0.5902	2.6436
H14	-0.481	-1.0887	3.157
H15	-0.0428	-1.8834	0.8531
H16	1.2655	-0.7969	1.3559

4-iodotetrahydro-2H-pyran radical

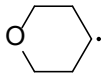

Calculated geometry

Atom	X	Y	Z
O1	0	0	0
C2	-1.3252	-0.0784	-0.5021
C3	-2.356	0.267	0.5799
C4	-2.0893	-0.5107	1.8205
C5	-0.6726	-0.6541	2.2537
C6	0.2325	-0.9302	1.0465
H7	-1.5153	-1.0908	-0.8866
H8	-1.3784	0.6224	-1.3358
H9	-3.3668	0.0907	0.2028
H10	-2.2788	1.3482	0.7816
H11	-2.8997	-0.8004	2.4762
H12	-0.3213	0.2768	2.7286
H13	-0.5564	-1.4474	2.9968
H14	0.059	-1.9516	0.6782
H15	1.2855	-0.8342	1.3128

1-(3-bromo-4,4,4-trifluorobutyl)-4-methoxybenzene

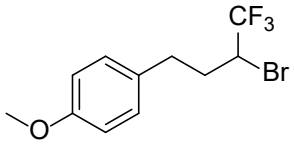

Calculated geometry

Atom	X	Y	Z
C1	0	0	0
C2	0.3821	-1.1747	0.6427
C3	-0.5343	-2.2221	0.7596
C4	-1.81	-2.087	0.2451
C5	-2.2162	-0.9146	-0.3989
C6	-1.2908	0.1154	-0.5109
H7	0.6892	0.8239	-0.1125
O8	1.6127	-1.3975	1.1797
H9	-0.2216	-3.1323	1.2543
H10	-2.5063	-2.9126	0.3416
C11	-3.625	-0.7604	-0.9091
H12	-1.5742	1.0348	-1.0104
C13	2.5807	-0.3664	1.0942
H14	3.4716	-0.749	1.587
H15	2.8181	-0.1259	0.0533
H16	2.2451	0.5406	1.6064
C17	-4.5926	-0.3518	0.2083
H18	-3.6523	-0.0142	-1.7045
H19	-3.9659	-1.7033	-1.3482
C20	-6.0416	-0.2593	-0.2433
H21	-4.5457	-1.0966	1.0077
H22	-4.2827	0.5996	0.6436
C23	-7.0126	-0.1003	0.9204
Br24	-6.3144	1.2283	-1.5061
H25	-6.3477	-1.1493	-0.7901
F26	-6.7606	0.9893	1.6617
F27	-8.2904	-0.0387	0.5168
F28	-6.9087	-1.1755	1.7363

1-(3-bromo-4,4,4-trifluorobutyl)-4-methoxybenzene radical

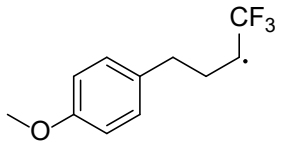

Calculated geometry

Atom	X	Y	Z
C1	0	0	0

C2	0.6137	-1.2441	0.1263
C3	-0.1279	-2.4025	-0.1147
C4	-1.4602	-2.3106	-0.4729
C5	-2.0956	-1.0727	-0.6047
C6	-1.3426	0.07	-0.3618
H7	0.5496	0.9133	0.1739
O8	1.9171	-1.4313	0.4713
H9	0.3635	-3.362	-0.0205
H10	-2.0189	-3.2205	-0.6618
C11	-3.5568	-0.9821	-0.9487
H12	-1.8065	1.045	-0.4599
C13	2.7177	-0.2887	0.7183
H14	3.707	-0.6637	0.9704
H15	2.7876	0.3497	-0.1678
H16	2.329	0.2986	1.556
C17	-4.4546	-1.0388	0.3229
H18	-3.7637	-0.0521	-1.4802
H19	-3.8393	-1.801	-1.6148
C20	-5.9001	-0.9645	0.0108
H21	-4.2387	-1.9749	0.8462
H22	-4.1656	-0.2251	0.991
C23	-6.6325	0.3172	0.0724
Br24	-6.431	-1.799	-0.4266
H25	-6.1518	1.2299	-0.8213
F26	-7.9441	0.1646	-0.1938
F27	-6.5342	0.9121	1.2872

1-(3-bromo-4,4-difluorobutyl)-4-methoxybenzene

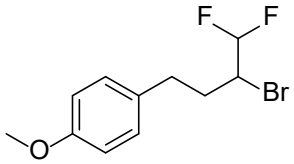

Calculated geometry

Atom	X	Y	Z
C1	0	0	0
C2	0.4165	-1.1847	0.6021

C3	-0.4697	-2.2604	0.6854
C4	-1.7506	-2.1436	0.1781
C5	-2.1907	-0.9628	-0.426
C6	-1.2942	0.0959	-0.505
H7	0.6655	0.8464	-0.0854
O8	1.6552	-1.3901	1.1291
H9	-0.1307	-3.1774	1.1491
H10	-2.4247	-2.9901	0.2495
C11	-3.6049	-0.825	-0.9248
H12	-1.6048	1.0233	-0.9727
C13	2.5896	-0.3265	1.0818
H14	3.4932	-0.6984	1.5595
H15	2.8177	-0.0395	0.0506
H16	2.2261	0.5498	1.6274
C17	-4.5581	-0.3685	0.1859
H18	-3.6398	-0.1092	-1.748
H19	-3.9526	-1.7829	-1.324
C20	-6.0068	-0.2608	-0.2528
H21	-4.5251	-1.0923	1.0062
H22	-4.2268	0.5858	0.597
C23	-6.9789	-0.0308	0.8919
Br24	-6.2778	1.2052	-1.5568
H25	-6.3317	-1.1534	-0.7851
F26	-6.5902	1.0152	1.6714
H27	-8.0028	0.1478	0.5612
F28	-6.9787	-1.1491	1.6887

1-(3-bromo-4,4-difluorobutyl)-4-methoxybenzene radical

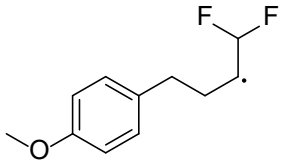

Calculated geometry

Atom	X	Y	Z
C1	0	0	0
C2	0.6087	-1.2418	0.1646

C3	-0.1341	-2.404	-0.052
C4	-1.4632	-2.3177	-0.424
C5	-2.0943	-1.0822	-0.5934
C6	-1.3394	0.0642	-0.3746
H7	0.5506	0.9162	0.1547
O8	1.9093	-1.4232	0.5259
H9	0.3533	-3.3621	0.0724
H10	-2.0234	-3.2307	-0.5927
C11	-3.5532	-0.9951	-0.9486
H12	-1.8007	1.0372	-0.5006
C13	2.7083	-0.2761	0.7545
H14	3.6938	-0.6456	1.0286
H15	2.7905	0.3402	-0.1462
H16	2.3099	0.3328	1.5721
C17	-4.4606	-1.0335	0.3137
H18	-3.755	-0.0708	-1.4922
H19	-3.8303	-1.8217	-1.608
C20	-5.9035	-0.9436	-0.0151
H21	-4.2561	-1.9677	0.8472
H22	-4.1721	-0.2172	0.9783
C23	-6.6557	0.3123	0.1603
H24	-6.4096	-1.7689	-0.4999
F25	-6.0758	1.3406	-0.5674
H26	-7.7033	0.2543	-0.1374
F27	-6.6178	0.7353	1.4734

1-(3-bromobutyl)-4-methoxybenzene

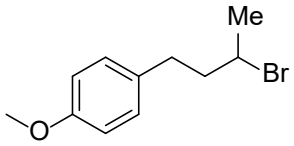

Calculated geometry

Atom	X	Y	Z
C1	0	0	0
C2	0.4315	-1.1945	0.5713
C3	-0.4425	-2.2815	0.6294
C4	-1.7254	-2.1669	0.1253
C5	-2.1803	-0.9775	-0.4502
C6	-1.2956	0.0931	-0.5019
H7	0.6556	0.8559	-0.0655

O8	1.6748	-1.3992	1.0897
H9	-0.092	-3.2063	1.0687
H10	-2.3886	-3.0235	0.174
C11	-3.5933	-0.844	-0.9531
H12	-1.6173	1.0276	-0.9476
C13	2.6017	-0.3292	1.0503
H14	3.5137	-0.7037	1.5098
H15	2.8148	-0.0217	0.0217
H16	2.2401	0.535	1.6163
C17	-4.56	-0.4006	0.1503
H18	-3.6297	-0.1227	-1.771
H19	-3.9337	-1.8007	-1.3612
C20	-6.0132	-0.2858	-0.273
H21	-4.525	-1.1335	0.9655
H22	-4.2276	0.5494	0.5771
C23	-6.9587	-0.0045	0.8767
Br24	-6.2183	1.1687	-1.6355
H25	-6.3248	-1.1714	-0.825
H26	-6.686	0.9181	1.391
H27	-7.9894	0.0823	0.5355
H28	-6.9022	-0.8267	1.5967

1-(3-bromobutyl)-4-methoxybenzene radical

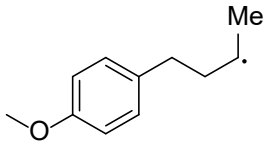

Calculated geometry

Atom	X	Y	Z
C1	0	0	0
C2	0.4728	-1.2018	0.52
C3	-0.3761	-2.3089	0.5677
C4	-1.6749	-2.2072	0.1036
C5	-2.1725	-1.0105	-0.4207
C6	-1.3119	0.0797	-0.4619
H7	0.6349	0.8721	-0.056
O8	1.7353	-1.3956	0.9964
H9	0.0062	-3.239	0.9678
H10	-2.3186	-3.0789	0.1443
C11	-3.6026	-0.8976	-0.8764
H12	-1.6655	1.0211	-0.8674
C13	2.6358	-0.3034	0.9693

H14	3.5684	-0.6711	1.3916
H15	2.8141	0.0438	-0.0533
H16	2.2699	0.5327	1.5737
C17	-4.5717	-0.5727	0.2714
H18	-3.688	-0.121	-1.641
H19	-3.9162	-1.8346	-1.3465
C20	-5.994	-0.4811	-0.15
H21	-4.4521	-1.3398	1.0558
H22	-4.2613	0.3638	0.7536
C23	-7.0314	0.0744	0.757
H24	-6.3047	-1.0105	-1.0441
H25	-6.7106	1.0236	1.2011
H26	-7.9785	0.2431	0.242
H27	-7.2408	-0.5993	1.6035

2: Copper-catalyzed C-N coupling

2.1: Background

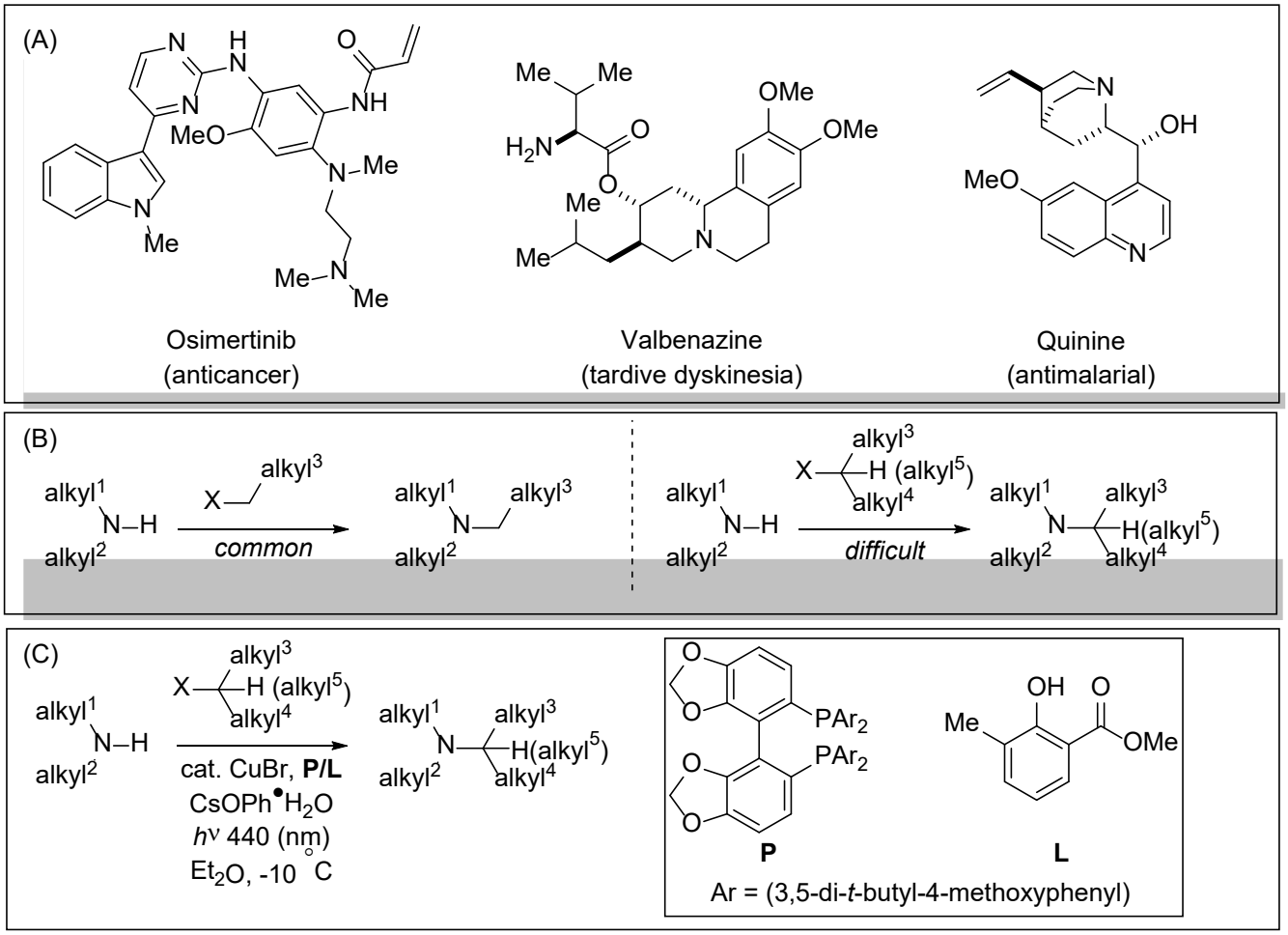

Figure 2.1.1: (A) Representative alkaloids of pharmaceutical interest. (B) Difficulty of nucleophilic substitution of secondary amines by secondary or tertiary electrophiles. (C) Developed photocatalytic method for general synthesis of alkyl C-N bonds.

Tertiary amines are a widespread motif in pharmaceuticals[42–44] as well as natural products, especially well represented in the rich chemistry of alkaloids (Fig 2.1.1A)[45–47]. The coupling of secondary amines with primary electrophiles is an elemental and widely used method for the synthesis of tertiary alkylamines[48]. However, attempted substitution of secondary or tertiary electrophiles often results in elimination products and poor yields. Reductive amination reactions and ameliorate some of these difficulties[49], general solutions do not exist (Fig 2.1.1B). In recent

years, progress has been reported in the coupling of amine nucleophiles with unactivated electrophiles[20,50–55]. However, at the start of this project the only example published of the coupling of333333 alkylamines with unactivated secondary alkyl halides was limited to primary amines nuleophiles[56]. It should be noted that since publication of this work, further progress has been made in this area[54,57,58]. To address this gap in the literature, our group sought to accomplish the general coupling of secondary amines with secondary and tertiary unactivated alkyl bromides. Leveraging a dual-ligand methodology strategy previously used in our group,[55] we discovered that copper under the influence of light and in the presence of a base, a phosphine photocatalyst **P** and secondary salicylate ligand **L,** the desired coupling could be achieved with a broad scope and under mild conditions (Fig 2.1.1C)[54]. In developing this reaction, certain mechanistic questions arose which were of interest. Specifically, we were interested to understand the difference in photoactivity between Cu^{I} species in solution, and we wanted to explore how the secondary ligand promotes the C—N coupling step.

2.2: Computational investigations of the photocatalyst

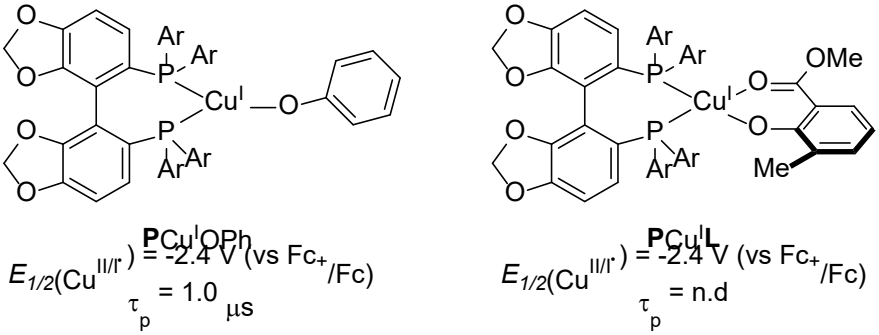

Figure 2.2.1: Cu^{I} species observed during the catalytic reaction.

Experiments showed that two Cu^{I} species were dominant during the course of the reaction. Specifically, the phenoxide complex **P**Cu^{I}OPh and the salicyclate complex **P**Cu^{I}**L** were present and theoretically could act as photocatalysts (Fig. 2.2.1). Stern-Volmer quenching experiments as well as luminescence decay measurements demonstrated that only **P**Cu^{I}OPh was quenched by the

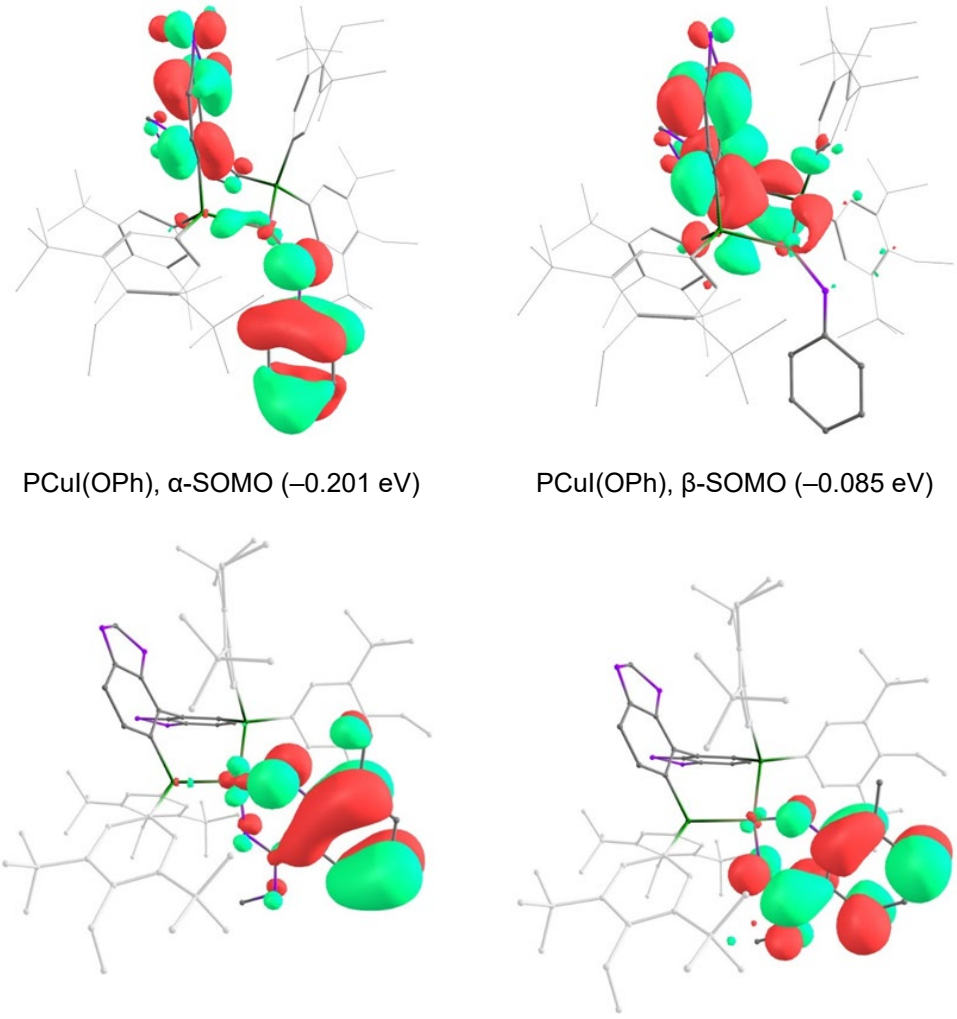

Figure 2.1.3: Excited SOMOs of **P**Cu^{I}OPh (top) and **P**Cu^{I}**L** (bottom).

electrophile, and it displayed a phosphorescence decay time on the order of τ_p = 1.0 μs, while the salicyclate complex showed no phosphorescence. Measurements indicated that the excited state reduction potential of each complex were similar. Therefore, the difference in reactivity was likely due to the differences in their excited state lifetimes, or their differing efficiency in undergoing intersystem crossing. To probe this difference, we turned to TD-DFT analysis to model the excited state of each complex. Figure 2.1.3 shows the predicted SOMOs of the triplet state for each complex. In the case of the **L**Cu^{I}OPh complex, the orbitals of the α and β SOMOs are widely distributed in space. This reduced overlap tends to increase the lifetime of the excited state. In

addition, the geometry of each complex likely plays a role. It has been reported that 4-coordinate Cu^{I} complexes can undergo rapid non-radiative decay via flattening of their tetrahedral geometry[59]. Given that **P**Cu^{I}OPh is Y shaped while **P**Cu^{I}**L** is tetrahedral, this relaxation pathway likely also plays a role in their divergent photoactivity. Figure 2.1.4 shows the geometric overlap between the excited triplet state and ground singlet state for the core region of each complex. The small change in geometry of the **P**Cu^{I}OPh complex limits non-radiative pathways for the excited state, increasing the lifetime. In contrat, **P**Cu^{I}**L** shows a flattening of the tetrahedral geometry around the Cu atom in the excited state, opening up a pathway for relaxation via geometric distortion of the Cu geometry.

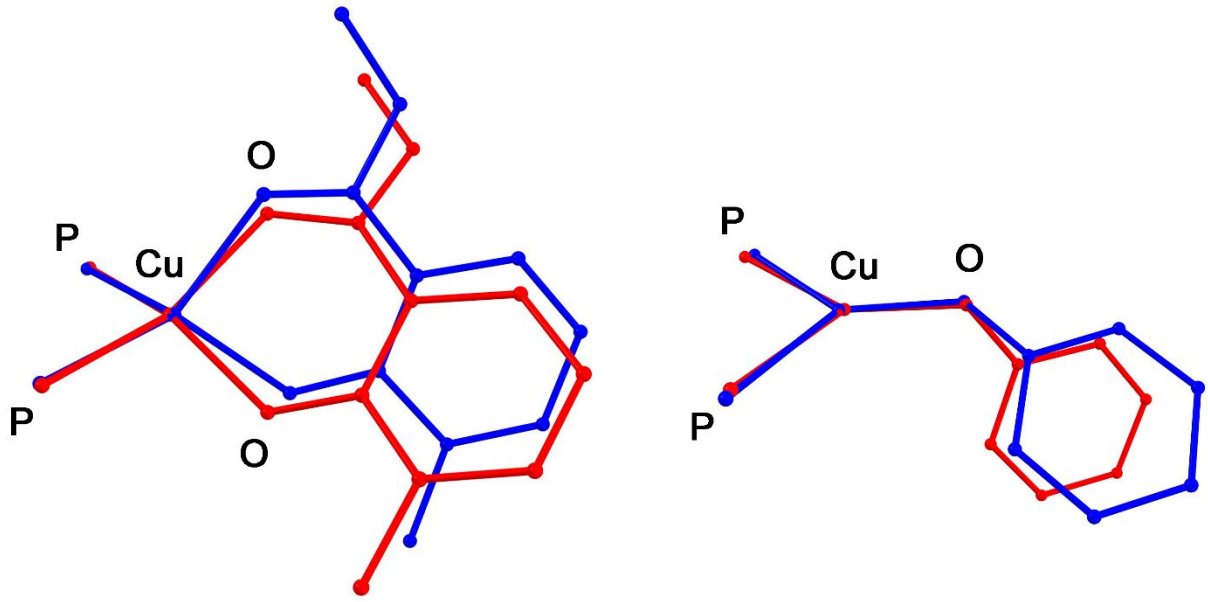

Figure 2.1.4: Geometric overlap between the ground state (blue) and excited state (red) for **P**Cu^{I}OPh (right) and **P**Cu^{I}**L** (left).

2.3: Computational investigations of the C—N coupling step

We were also interested to study the nature of the C—N coupling step. EPR spectroscopy showed that the primary Cu^{II} species in solution was the species **L**Cu^{II}(morpholine)$_2$OPh, when morpholine was used as the nucleophile. Using the alternative base cesium 2-phenylphenoxide,

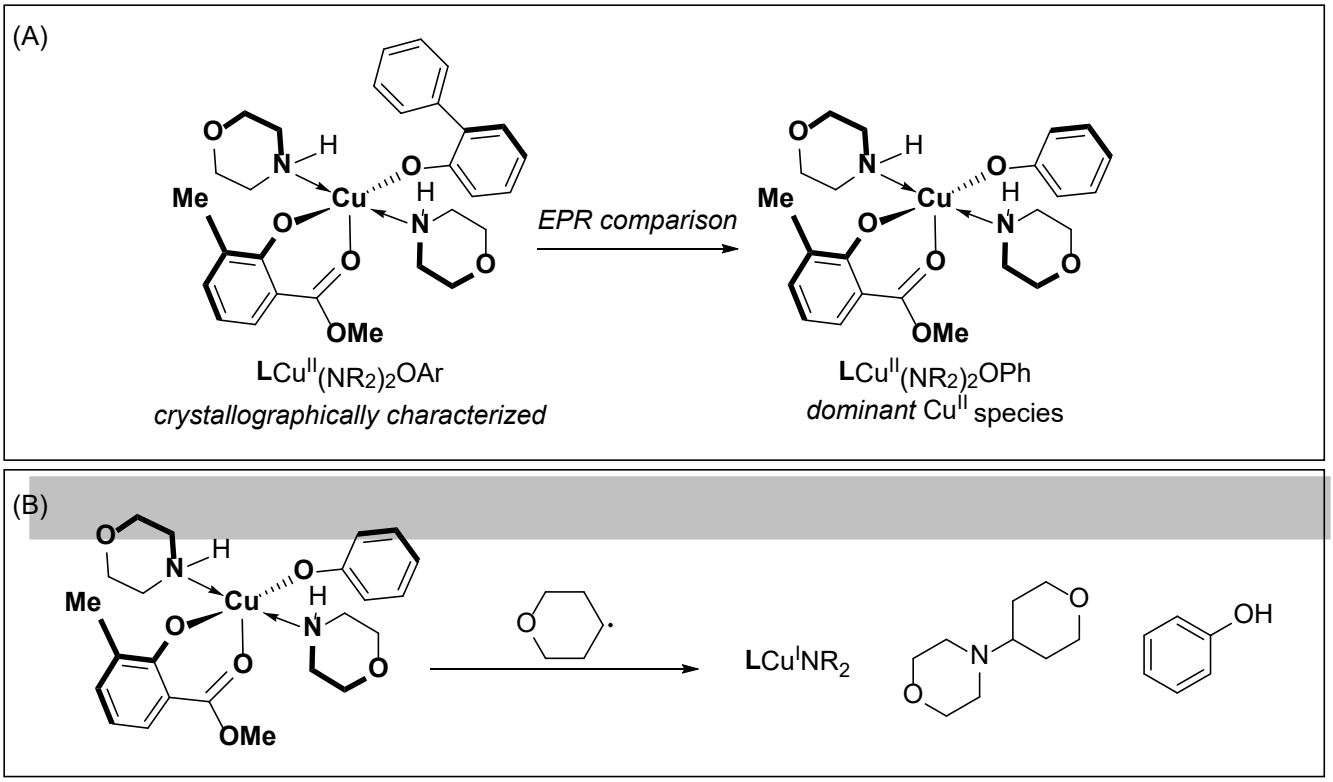

Figure 2.3.1 (A) Structure of the main copper paramagnet in solution (right), inferred from the crystallographically characterized **L**$Cu^{II}(NR_2)$Oar (right). (B) Model reaction used for computational studies.

the analogous complex **L**Cu^{II}(morpholine)$_2$OAr was crystallographically characterized. The EPR spectrum of this new species matched that of the catalysis, allowing the structure of **L**Cu^{II}(morpholine)OPh to be assigned by analogy (Fig 2.3.1A). Since experimental results showed evidence that there was facile interconversion of Cu^{II} species, the immediate thermodynamic landscape around the main Cu^{II} species was calculated. The results of these calculations are summarized in Figure 2.3.2. In order for C-N coupling to occur, the phenoxide base must at some point serve as the terminal base to deprotonate the nucleophile. Starting from the primary Cu^{II} species **1** in the Figure, deprotonation and loss of phenol to yield intermediate **3** was found to be uphill by 17.5 kcal•mol^{-1}, and thus not feasible under the reaction conditions. No evidence of any copper-amido species was found in experimental studies, consistent with this calculation. Loss of

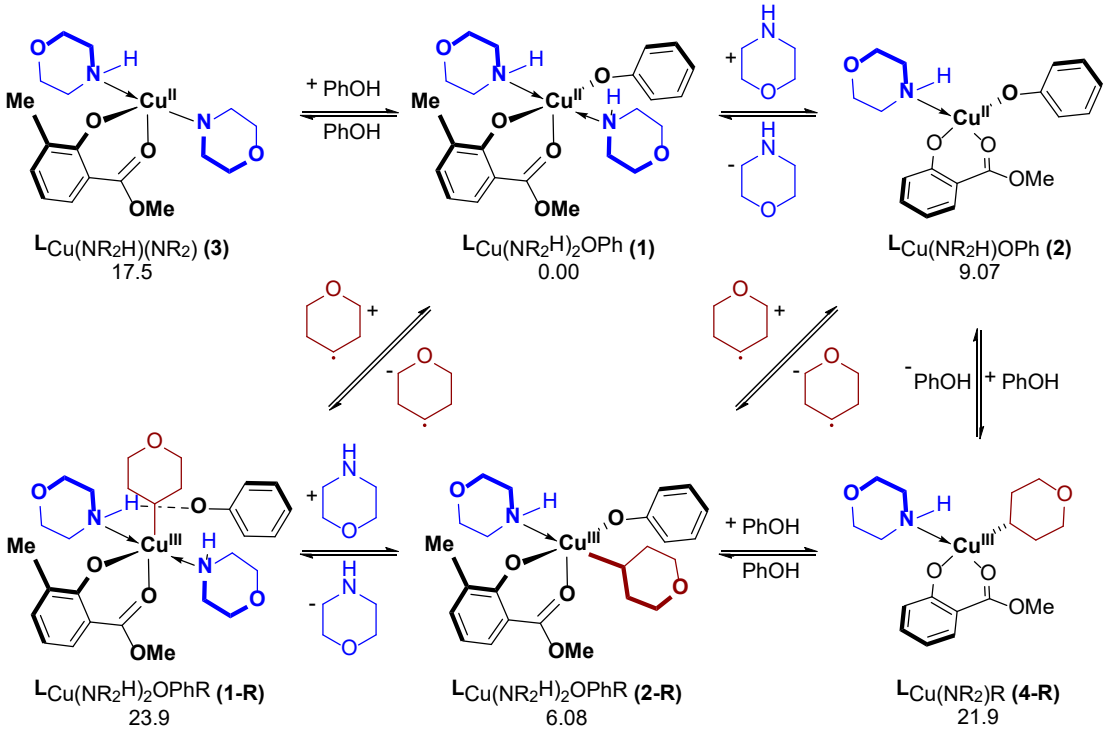

Figure 2.3.2: Computational calculations of prospective Cu^{II} species. All values are ΔG values for 263.15K relative to species **1**.

one morpholine unit to form species **was** also found to be unfavorable by 9.07 kcal•mol^{-1}, and therefore **2** is likely not a relevant species to C—N bond formation. Direct radical capture by **1** to generate species **1-R** was found to be highly unfavorable, and uphill by 23.9 kcal•mol^{-1}. In addition, during geometry optimization spontaneous dissociation of the phenoxide was noted. Likely, **1-R**, to avoid being a 20-electron complex, is driven to dissociate a ligand to stabilize. Correspondingly, dissociation of a morpholine unit from **1-R** to generate **2-R** is much more favorable, relatively, being only 6.08 kcal•mol^{-1} uphill from **1**. Deprotonation from this species to form **4-R** is also not favorable and is not relevant to the reaction conditions. This analysis leaves two possibilities for C—N bond formation. Either the process occurs through an inner-sphere process from **2-R**, or it occurs through species **1** via an outer-sphere process. In either case, deprotonation of the amine is likely to be synchronous with C—N bond formation. An extensive search of outer-sphere coupling mechanisms did not yield a transition state with an activation

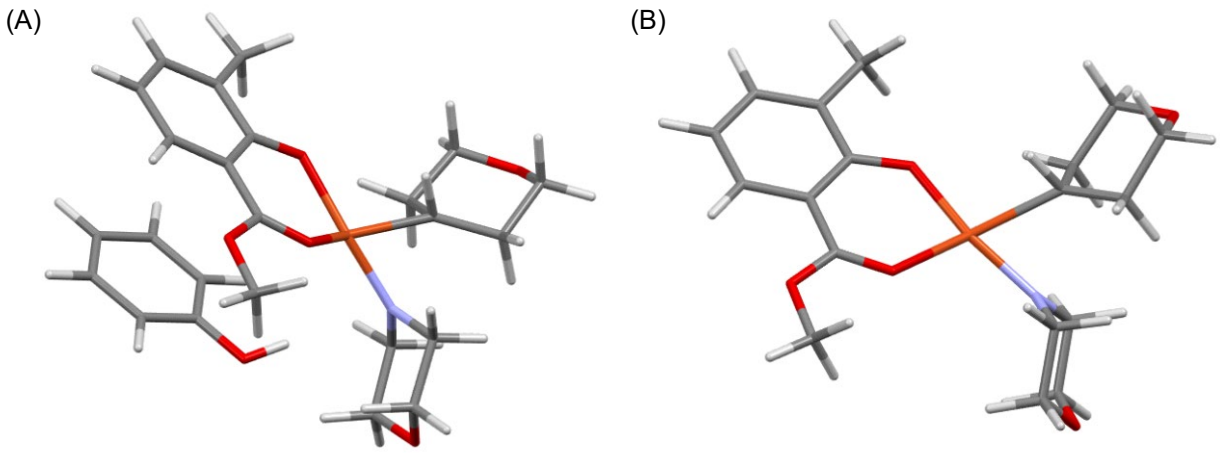

Figure 2.3.3: (A) Calculated transition state for C—N bond formation from **2-R**. (B) Calculated transition state A, but without phenol.

energy of less than 30 kcal•mol^{-1} from **1**. An inner-sphere reductive elimination from **2-R** was lower in energy, and was the lowest transition state found in this study. After the initial optimization of the transition state, it was found that a phenol molecule was concurrently generated, and was loosely associated with the complex at the calculated transition state (Fig 2.3.3A). Recalculation of this transition state with the phenol removed, which provides a lowering of the activation energy by an increase in entropy, resulting in the transition state detailed in Figure 2.3.3B. The calculated energy barrier for this process is 24.5 kcal•mol^{-1} higher in energy relative to **1**. While this energy barrier is still somewhat high for the reaction conditions, it is currently the best model for the C—N coupling step.

2.4: Computational details

2.4.1: General methods

All calculations were performed using the Orca 5.0.3 software package.[28–31] Geometry optimizations were performed using the B3LYP functional, utilizing the D4 dispersion correction.[32–34] The def2-TZVP basis set was used for all atoms except copper where applicable, with which def2-QZVPPD was used.[35,36] The RIJCOSX approximation was used with the def2/J auxiliary basis set in all calculations.[37] Frequency calculations were performed to ensure that all molecular geometries were energy minima by confirming the absence of imaginary vibrational modes.[38] All calculations included the implicit CPCM solvation model. A dielectric constant of 4.33 and a refractive index of 1.35 were chosen for the diethyl ether solvent, based on the literature.[60] TD-DFT calculations were performed to estimate the excitation energies of **P**Cu^{I}OPh and **P**Cu^{I}**L** from their ground states. For both complexes, the number of roots was taken to be 20, and triplets were included. Transitions with energies greater than 350 nm were not considered, as they were deemed irrelevant to the reaction conditions (irradiation with 440 nm LED).

For calculations of Cu^{II} species and organic molecules and fragments, the above options were using for geometry optimization, followed by an electronic energy optimization using the wB97M-V[61] functional with the DEF2-TZVPD basis set, and the def2-QZFPPD basis set on copper. The SMD solvation model was used using diethyl ether as the option solvent.[62]

2.4.2: Calculated structures

DTBM-SEGPHOS-CuOPh, singlet state

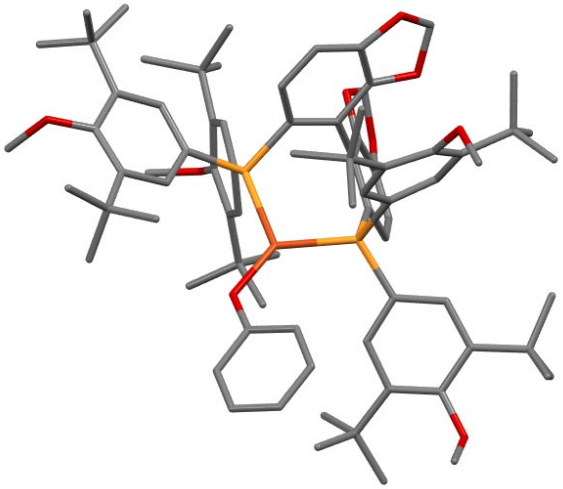

Calculated geometry

Atom	X	Y	Z
Cu1	0	0	0
P2	1.1952	1.4224	1.2916
P3	1.5877	-1.346	-0.8418
C4	-2.2688	-2.3239	-0.486
C5	-3.1197	-3.3484	-0.8758
H6	-2.7435	-4.3653	-0.9043
C7	-4.4419	-3.0879	-1.229
H8	-5.1024	-3.8898	-1.5332
C9	-4.896	-1.7704	-1.1796
H10	-5.9219	-1.544	-1.4491
C11	-4.0529	-0.7385	-0.7938
O12	-1.9292	0.0171	-0.0769
C13	-2.7064	-0.9816	-0.4398
C14	0.2564	2.1388	2.6726
C15	-1.0704	1.7562	2.7637
H16	-1.4549	1.0675	2.0252
C17	-1.923	2.2314	3.7641
C18	-3.3338	1.6048	3.816
C19	-4.0912	1.814	5.1385
H20	-4.4215	2.8366	5.2929
H21	-3.483	1.5204	5.995
H22	-4.9817	1.1818	5.1259
C23	-4.1796	2.1338	2.6417

H24	-5.1648	1.661	2.6483
H25	-3.7035	1.9079	1.6864
H26	-4.323	3.2136	2.7017
C27	-3.1931	0.0717	3.6525
H28	-2.5502	-0.344	4.431
H29	-2.7878	-0.2147	2.6839
H30	-4.1782	-0.3898	3.7432
C31	-1.3957	3.2059	4.6254
C32	-2.9905	4.9152	4.9307
H33	-2.3543	5.6126	4.3824
H34	-3.4792	5.4356	5.7526
H35	-3.7473	4.5208	4.2524
O36	-2.2125	3.8683	5.5169
C37	0.6202	4.3835	5.7574
C38	-0.0158	3.5337	4.6403
C39	0.3342	3.7209	7.1206
H40	0.8049	4.2998	7.9191
H41	0.7478	2.7101	7.1484
H42	-0.7332	3.6636	7.3216
C43	0.0997	5.8335	5.7651
H44	0.6914	6.4268	6.4663
H45	-0.9384	5.8936	6.0771
H46	0.1955	6.2887	4.777
C47	2.1486	4.4594	5.602
H48	2.4434	4.97	4.6833
H49	2.612	3.4712	5.6099
H50	2.5587	5.0254	6.4399
C51	0.7798	2.992	3.6418
H52	1.8298	3.2264	3.6174
C53	1.999	2.808	0.4322
C54	1.6772	3.0114	-0.9025
H55	1.0056	2.3112	-1.3737
C56	2.2071	4.0678	-1.6341
C57	1.8969	4.1828	-3.1397
C58	3.209	4.2419	-3.9476
H59	2.9792	4.2831	-5.0152
H60	3.8086	3.3489	-3.7679
H61	3.8036	5.114	-3.689
C62	1.0345	5.4202	-3.4517
H63	0.7154	5.3865	-4.4963
H64	1.5764	6.3489	-3.3046
H65	0.1385	5.4375	-2.8274
C66	1.1142	2.9565	-3.6432

H67	0.1223	2.8867	-3.1928
H68	1.6451	2.0238	-3.4512
H69	0.9775	3.0473	-4.7219
C70	3.0435	4.9747	-0.9444
O71	3.4741	6.085	-1.6398
C72	2.799	7.3174	-1.3789
H73	2.8051	7.889	-2.3065
H74	3.3165	7.8936	-0.6112
H75	1.7685	7.1445	-1.066
C76	3.4787	4.7398	0.3779
C77	4.4953	5.6039	1.1572
C78	5.567	6.2573	0.2633
H79	5.1811	7.0524	-0.3649
H80	6.0366	5.5199	-0.3897
C81	3.7416	6.6834	1.9607
H82	3.0457	6.2181	2.6612
H83	3.1712	7.355	1.3222
H84	4.4507	7.2845	2.5357
C85	5.2659	4.7387	2.18
H86	6.0518	5.3453	2.6325
H87	5.7277	3.8724	1.7069
H88	4.6319	4.3843	2.9922
C89	2.9249	3.6427	1.0353
H90	3.2346	3.4262	2.0437
C91	3.0774	-0.3708	-1.2413
C92	3.3868	-0.1296	-2.5776
H93	2.8145	-0.6256	-3.3476
C94	4.4138	0.735	-2.9707
H95	4.6355	0.9127	-4.0136
C96	5.1211	1.3396	-1.9646
O97	6.1438	2.2445	-2.0595
O98	5.682	1.8278	0.1577
C99	4.8347	1.0974	-0.6307
C100	3.8148	0.2736	-0.2118
C101	3.6476	0.0496	1.2475
C102	4.6441	-0.637	1.9025
O103	5.7823	-1.1689	1.3532
O104	5.7129	-1.6683	3.5942
C105	4.6019	-0.9409	3.2542
C106	3.5469	-0.5567	4.0405
H107	3.4969	-0.8019	5.0923
C108	2.543	0.1902	3.4134
H109	1.7137	0.5332	4.0136

C110	2.5794	0.5122	2.0596
C111	1.1863	-2.2429	-2.3678
C112	0.1577	-1.7266	-3.1354
H113	-0.3329	-0.8276	-2.7906
C114	-0.2656	-2.3246	-4.3236
C115	-1.3099	-1.5491	-5.156
C116	-2.6831	-1.6098	-4.4617
H117	-2.6329	-1.2203	-3.4446
H118	-3.0623	-2.6304	-4.4038
H119	-3.4088	-1.0121	-5.0189
C120	-0.8667	-0.0677	-5.2268
H121	-1.5662	0.487	-5.8551
H122	0.1291	0.02	-5.6667
H123	-0.8502	0.4168	-4.2524
C124	-1.4474	-2.008	-6.6182
H125	-1.9254	-2.9768	-6.7247
H126	-0.4773	-2.0512	-7.115
H127	-2.0648	-1.2794	-7.1482
C128	0.3226	-3.5599	-4.6445
O129	-0.1805	-4.3259	-5.6743
C130	-1.3699	-5.0463	-5.3381
H131	-1.2221	-5.6406	-4.4344
H132	-1.5808	-5.7052	-6.1787
H133	-2.2151	-4.3757	-5.1836
C134	1.4495	-4.0631	-3.9493
C135	2.2604	-5.2729	-4.4516
C136	2.7536	-4.9932	-5.8858
H137	3.3524	-5.8352	-6.2419
H138	3.3823	-4.1	-5.9067
H139	1.923	-4.8478	-6.5729
C140	1.4436	-6.579	-4.429
H141	2.1047	-7.423	-4.6398
H142	0.6564	-6.5825	-5.1765
H143	0.9944	-6.7421	-3.4469
C144	3.5055	-5.5111	-3.5804
H145	3.2442	-5.7766	-2.5544
H146	4.1605	-4.6385	-3.5523
H147	4.0755	-6.3411	-4.0011
C148	1.8539	-3.38	-2.8102
H149	2.6939	-3.7424	-2.2432
C150	2.0946	-2.6068	0.3587
C151	3.2683	-3.3457	0.2782
H152	3.9835	-3.0984	-0.4892

C153	3.5316	-4.3876	1.1594
C154	4.8436	-5.1861	1.0303
C155	5.7874	-4.5457	-0.0031
H156	6.0141	-3.5065	0.2363
H157	5.3748	-4.5818	-1.0128
C158	4.5685	-6.6238	0.5486
H159	3.9889	-6.6179	-0.3766
H160	4.0322	-7.2108	1.2875
H161	5.5164	-7.1294	0.348
C162	5.5967	-5.223	2.3754
H163	5.0476	-5.78	3.1291
H164	5.7604	-4.2146	2.7566
C165	2.5611	-4.666	2.1528
O166	2.7843	-5.7634	2.9555
C167	1.9991	-6.9302	2.7005
H168	1.6616	-6.9594	1.6635
H169	1.1336	-6.9723	3.3626
H170	2.6329	-7.794	2.9
C171	1.4428	-3.8359	2.3606
C172	0.443	-3.9296	3.5332
C173	-0.7642	-4.797	3.1244
H174	-1.4824	-4.8482	3.9467
H175	-0.4773	-5.814	2.8641
H176	-1.2705	-4.3601	2.2612
C177	1.0789	-4.4567	4.8331
H178	1.9736	-3.8831	5.0845
H179	1.3573	-5.5039	4.7889
H180	0.3629	-4.3361	5.6486
C181	-0.1037	-2.5251	3.8764
H182	-0.7279	-2.1075	3.088
H183	0.7047	-1.823	4.081
H184	-0.7266	-2.5985	4.7693
C185	1.2258	-2.84	1.4105
H186	0.354	-2.2103	1.4954
H187	6.3437	6.6848	0.9006
C188	6.6703	2.3596	-0.7313
C189	6.5965	-1.5257	2.4742
H190	7.0962	-2.47	2.2778
H191	7.3086	-0.7185	2.6768
H192	6.5716	-5.6963	2.2362
H193	6.8444	3.407	-0.4985
H194	7.5867	1.766	-0.6516
H195	6.725	-5.1039	-0.0133

H196	-1.2436	-2.5433	-0.2177
H197	-4.4122	0.2838	-0.7621

DTBM-SEGPHOS-CuOPh, triplet state

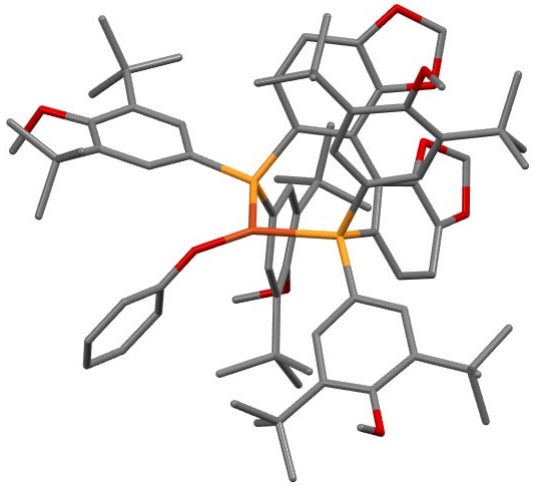

Calculated geometry

Atom	X	Y	Z
Cu1	0	0	0
P2	1.3251	1.0897	1.4625
P3	1.6208	-1.4374	-0.6128
C4	-2.6528	-1.8675	0.2309
C5	-3.7687	-2.6568	0.4625
H6	-3.6553	-3.5934	0.9957
C7	-5.0257	-2.2572	0.0156
H8	-5.8956	-2.8747	0.1986
C9	-5.1462	-1.0529	-0.6758
H10	-6.1174	-0.7309	-1.0328
C11	-4.0351	-0.2599	-0.9179
O12	-1.7158	0.1287	-0.7
C13	-2.7627	-0.6474	-0.4602
C14	0.253	1.7051	2.7867
C15	-1.0363	1.2099	2.8878
H16	-1.3539	0.4436	2.1962
C17	-1.942	1.663	3.8493
C18	-3.3039	0.936	3.9195
C19	-4.1124	1.1788	5.2061
H20	-4.5257	2.18	5.2768
H21	-3.5099	0.9952	6.0963

H22	-4.9508	0.4789	5.2171
C23	-4.1588	1.3167	2.6955
H24	-5.1031	0.7674	2.7139
H25	-3.6483	1.0707	1.7642
H26	-4.3888	2.3831	2.682
C27	-3.0457	-0.5879	3.8771
H28	-2.4174	-0.897	4.7141
H29	-2.5706	-0.9135	2.9547
H30	-3.9982	-1.1158	3.952
C31	-1.5086	2.7224	4.666
C32	-3.2257	4.3262	4.8327
H33	-2.6207	5.0491	4.2823
H34	-3.791	4.8384	5.6092
H35	-3.9168	3.8451	4.1401
O36	-2.3962	3.3689	5.4977
C37	0.3868	4.0992	5.7757
C38	-0.1612	3.1566	4.6873
C39	0.1149	3.4801	7.1622
H40	0.5255	4.1269	7.9415
H41	0.5975	2.5037	7.246
H42	-0.9503	3.357	7.3443
C43	-0.2325	5.5079	5.7036
H44	0.3017	6.1732	6.386
H45	-1.2789	5.5101	5.9932
H46	-0.1466	5.9217	4.6965
C47	1.9093	4.2723	5.6475
H48	2.188	4.7679	4.7163
H49	2.4369	3.3183	5.7007
H50	2.2628	4.8952	6.4707
C51	0.6907	2.6431	3.7191
H52	1.7158	2.9698	3.6851
C53	2.1657	2.5024	0.6785
C54	1.8417	2.8516	-0.6222
H55	1.1162	2.2507	-1.1487
C56	2.4514	3.9222	-1.2652
C57	2.1461	4.1922	-2.7515
C58	3.4551	4.1973	-3.5669
H59	3.2254	4.3438	-4.6253
H60	3.9713	3.2417	-3.4637
H61	4.1271	4.9892	-3.2472
C62	1.3988	5.5248	-2.9449
H63	1.0794	5.6151	-3.986
H64	2.0211	6.3844	-2.7172

H65	0.507	5.5653	-2.3154
C66	1.2536	3.0883	-3.3469
H67	0.2639	3.0639	-2.8867
H68	1.7058	2.1008	-3.2474
H69	1.1155	3.2877	-4.4109
C70	3.3671	4.6915	-0.5125
O71	3.8933	5.8101	-1.1223
C72	3.3542	7.0804	-0.7525
H73	3.3522	7.7033	-1.6466
H74	3.9745	7.5617	0.0044
H75	2.3347	6.9831	-0.3769
C76	3.7906	4.3079	0.7793
C77	4.9006	5.0029	1.5991
C78	6.0337	5.5748	0.7254
H79	5.7371	6.4414	0.1447
H80	6.4061	4.8212	0.0295
C81	4.2846	6.1141	2.4725
H82	3.5476	5.6915	3.1571
H83	3.7894	6.8834	1.8843
H84	5.0642	6.5947	3.0694
C85	5.573	3.9964	2.5594
H86	6.421	4.4856	3.0416
H87	5.9359	3.118	2.0265
H88	4.9047	3.6644	3.3536
C89	3.1546	3.2056	1.3458
H90	3.4553	2.8621	2.3221
C91	3.0815	-0.5009	-1.031
C92	3.3208	-0.2234	-2.3838
H93	2.633	-0.6117	-3.1218
C94	4.4173	0.5059	-2.825
H95	4.592	0.7079	-3.8713
C96	5.2811	0.9483	-1.8269
O97	6.3635	1.7873	-1.9722
O98	6.0025	1.3725	0.2533
C99	5.0637	0.693	-0.4957
C100	3.9564	0.0032	0.0042
C101	3.8032	-0.1829	1.4345
C102	4.8513	-0.7159	2.1839
O103	6.0391	-1.2124	1.6842
O104	5.9117	-1.669	3.9263
C105	4.7728	-1.003	3.5245
C106	3.6248	-0.7634	4.2739
H107	3.5623	-1.0024	5.3256

C108	2.577	-0.1603	3.5873
H109	1.6838	0.0962	4.138
C110	2.645	0.1614	2.228
C111	1.1318	-2.3904	-2.0735
C112	-0.0962	-2.1642	-2.667
H113	-0.7208	-1.3791	-2.2722
C114	-0.5458	-2.9142	-3.7577
C115	-1.8834	-2.4833	-4.4002
C116	-3.063	-2.9974	-3.5517
H117	-3.0035	-2.6197	-2.5311
H118	-3.0887	-4.0859	-3.5055
H119	-4.0077	-2.6564	-3.9824
C120	-1.9578	-0.9378	-4.4239
H121	-2.8658	-0.6345	-4.9482
H122	-1.102	-0.5136	-4.9536
H123	-1.9978	-0.4979	-3.4296
C124	-2.0545	-2.928	-5.8642
H125	-2.2152	-3.9949	-5.9787
H126	-1.1863	-2.6508	-6.4644
H127	-2.9265	-2.4182	-6.2794
C128	0.2756	-3.9788	-4.1714
O129	-0.1534	-4.8687	-5.1318
C130	-1.053	-5.8791	-4.6684
H131	-0.7111	-6.3027	-3.7225
H132	-1.067	-6.656	-5.4311
H133	-2.0619	-5.4883	-4.5391
C134	1.5834	-4.168	-3.6595
C135	2.5833	-5.1664	-4.2744
C136	2.7947	-4.819	-5.7619
H137	3.5204	-5.507	-6.2027
H138	3.1865	-3.8045	-5.8653
H139	1.867	-4.8909	-6.3254
C140	2.1127	-6.6276	-4.142
H141	2.9247	-7.2963	-4.4369
H142	1.2609	-6.8442	-4.7787
H143	1.8459	-6.8606	-3.1088
C144	3.9562	-5.079	-3.5857
H145	3.9062	-5.3658	-2.5334
H146	4.3857	-4.0777	-3.6491
H147	4.6421	-5.7665	-4.0831
C148	1.9759	-3.3647	-2.5997
H149	2.9539	-3.4907	-2.1681
C150	2.0734	-2.6773	0.6301

C151	3.2746	-3.3745	0.5614
H152	4.0154	-3.0579	-0.1547
C153	3.5243	-4.4612	1.387
C154	4.8868	-5.1779	1.3326
C155	5.8477	-4.4741	0.3594
H156	5.9983	-3.4261	0.617
H157	5.4951	-4.5289	-0.6726
C158	4.7589	-6.6373	0.8549
H159	4.2015	-6.6948	-0.0827
H160	4.2701	-7.2687	1.5906
H161	5.7559	-7.0473	0.6767
C162	5.5369	-5.1438	2.7305
H163	4.9409	-5.6871	3.4604
H164	5.6507	-4.1165	3.0787
C165	2.5049	-4.8323	2.2985
O166	2.6693	-6.0147	2.9886
C167	1.8825	-7.0959	2.4829
H168	2.066	-7.2461	1.4173
H169	0.8168	-6.9227	2.6351
H170	2.1854	-7.9845	3.0342
C171	1.3698	-4.0348	2.5203
C172	0.3422	-4.1798	3.6645
C173	-1.0013	-4.6778	3.0983
H174	-1.7427	-4.745	3.8983
H175	-0.9055	-5.6647	2.643
H176	-1.3867	-3.9951	2.3398
C177	0.7757	-5.0878	4.8283
H178	1.7639	-4.8142	5.1986
H179	0.7885	-6.1432	4.5739
H180	0.062	-4.9581	5.645
C181	0.1198	-2.7851	4.2931
H182	-0.2622	-2.0538	3.5843
H183	1.0514	-2.3973	4.7064
H184	-0.608	-2.8674	5.1026
C185	1.1635	-2.9865	1.6213
H186	0.2716	-2.3827	1.7067
H187	6.861	5.8736	1.3723
C188	6.9988	1.7592	-0.6894
C189	6.8267	-1.4742	2.8432
H190	7.4147	-2.3763	2.6923
H191	7.4587	-0.6036	3.0585
H192	6.5287	-5.6009	2.6875
H193	7.3734	2.7496	-0.4434

H194	7.8001	1.0098	-0.7019
H195	6.8163	-4.9755	0.402
H196	-1.6741	-2.187	0.5674
H197	-4.1268	0.6753	-1.4565

DTBM-SEGPHOS-L, singlet state

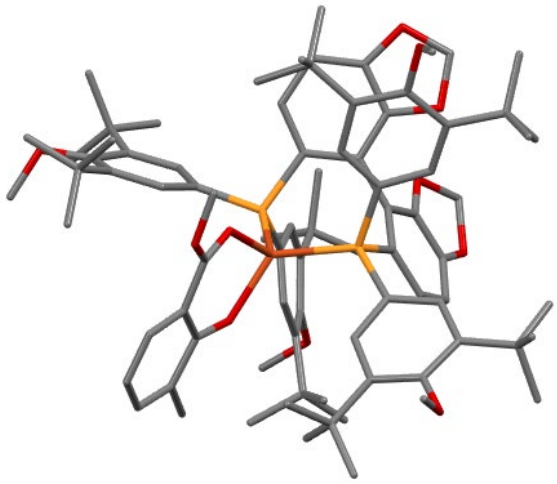

Calculated geometry

Atom	X	Y	Z
Cu1	0	0	0
P2	1.1621	1.4247	1.3191
O3	-1.5855	-1.2136	0.8196
P4	1.6457	-1.3283	-0.7812
C5	-2.8755	-3.3428	1.6008
H6	-1.9111	-3.704	1.2466
H7	-3.5847	-4.1632	1.672
H8	-2.7501	-2.8701	2.5738
O9	-3.4497	-2.4222	0.6643
C10	-3.3736	-0.4557	-0.6082
C11	-2.7054	-1.3489	0.3256
C12	-4.7416	-0.6735	-0.8857
H13	-5.2382	-1.5075	-0.4124
C14	-5.4476	0.1514	-1.7239
H15	-6.4965	-0.0281	-1.9203
C16	-4.7899	1.2462	-2.3105
H17	-5.3461	1.9128	-2.9618
C18	-3.4594	1.5036	-2.082
C19	-2.7732	2.684	-2.7005

H20	-2.3375	3.3312	-1.935
H21	-3.4737	3.2723	-3.2947
H22	-1.947	2.3764	-3.3446
O23	-1.4299	0.8932	-1.1062
C24	-2.6821	0.6389	-1.2324
C25	0.1839	2.2668	2.598
C26	-1.0734	1.7453	2.8435
H27	-1.3783	0.8715	2.2871
C28	-1.9531	2.3068	3.7715
C29	-3.2633	1.5301	4.0279
C30	-4.0348	1.943	5.2929
H31	-4.5036	2.9192	5.2151
H32	-3.3879	1.945	6.1707
H33	-4.8297	1.213	5.4617
C34	-4.1853	1.6488	2.7986
H35	-5.0942	1.0623	2.9547
H36	-3.6958	1.276	1.8979
H37	-4.4797	2.6832	2.6152
C38	-2.9081	0.0364	4.2253
H39	-2.223	-0.0907	5.0663
H40	-2.4502	-0.4096	3.3453
H41	-3.8196	-0.5245	4.4416
C42	-1.5397	3.5031	4.3797
C43	-3.3387	5.023	4.3892
H44	-2.8082	5.6775	3.695
H45	-3.8974	5.6246	5.1041
H46	-4.0306	4.3983	3.8238
O47	-2.4198	4.2341	5.1502
C48	0.3262	5.1484	5.1184
C49	-0.2189	4.0008	4.2465
C50	0.1814	4.7633	6.6049
H51	0.5888	5.5582	7.2348
H52	0.7358	3.8466	6.8185
H53	-0.8603	4.6092	6.8781
C54	-0.3934	6.4853	4.8572
H55	0.1363	7.2883	5.3753
H56	-1.4162	6.4772	5.2212
H57	-0.4024	6.7235	3.7914
C58	1.8222	5.3889	4.8535
H59	2.0099	5.7225	3.8312
H60	2.4207	4.495	5.0376
H61	2.177	6.171	5.5266
C62	0.6146	3.3644	3.3373

H63	1.6172	3.7279	3.1893
C64	1.9995	2.7469	0.396
C65	1.5734	2.9809	-0.9008
H66	0.8058	2.3391	-1.3038
C67	2.1148	3.993	-1.6938
C68	1.6529	4.0822	-3.1647
C69	2.7583	4.5845	-4.1131
H70	2.4221	4.4563	-5.1442
H71	3.6719	4.0003	-3.9832
H72	3.0099	5.6303	-3.973
C73	0.399	4.9712	-3.2745
H74	0.0486	4.9953	-4.3097
H75	0.5853	5.9956	-2.9595
H76	-0.4047	4.5703	-2.6557
C77	1.2643	2.68	-3.6846
H78	0.3852	2.272	-3.1904
H79	2.0836	1.9715	-3.563
H80	1.0298	2.7517	-4.7481
C81	3.0524	4.8439	-1.0764
O82	3.5433	5.9485	-1.7382
C83	2.7109	7.1069	-1.8094
H84	2.2473	7.1885	-2.7934
H85	3.3475	7.9779	-1.6515
H86	1.9332	7.0833	-1.0449
C87	3.5801	4.5776	0.2094
C88	4.7082	5.417	0.8414
C89	5.9033	5.5687	-0.1216
H90	5.6562	6.184	-0.9813
H91	6.2289	4.5963	-0.492
C92	4.1834	6.8088	1.2433
H93	3.3304	6.7184	1.9192
H94	3.8787	7.399	0.3842
H95	4.9691	7.3616	1.7647
C96	5.2437	4.7557	2.1245
H97	6.0772	5.35	2.5027
H98	5.6036	3.7426	1.9425
H99	4.4895	4.7149	2.912
C100	3.0362	3.5117	0.9157
H101	3.4226	3.2639	1.8908
C102	3.162	-0.3425	-1.0466
C103	3.5656	-0.0246	-2.3411
H104	3.0038	-0.4144	-3.1768
C105	4.6814	0.775	-2.6129

H106	4.9726	1.0151	-3.6261
C107	5.392	1.2183	-1.5276
O108	6.5148	2.0061	-1.4902
O109	5.8601	1.5072	0.6526
C110	4.9964	0.9165	-0.2345
C111	3.8746	0.1766	0.066
C112	3.5684	-0.0312	1.5053
C113	4.4562	-0.7659	2.2581
O114	5.5642	-1.4344	1.8098
O115	5.3226	-1.7825	4.0718
C116	4.3177	-0.9669	3.6219
C117	3.2828	-0.41	4.3265
H118	3.1709	-0.5559	5.3916
C119	2.3741	0.361	3.5934
H120	1.549	0.8163	4.1212
C121	2.4929	0.561	2.2207
C122	1.3201	-2.1356	-2.3811
C123	0.1191	-1.8124	-2.9887
H124	-0.5223	-1.0961	-2.4955
C125	-0.2803	-2.3644	-4.21
C126	-1.5657	-1.7859	-4.841
C127	-2.7942	-2.2255	-4.0223
H128	-2.7104	-1.9113	-2.982
H129	-2.9199	-3.3095	-4.0398
H130	-3.6995	-1.7734	-4.4343
C131	-1.4675	-0.2432	-4.7851
H132	-2.3602	0.1923	-5.238
H133	-0.5961	0.1075	-5.3427
H134	-1.3969	0.1382	-3.7703
C135	-1.7868	-2.1331	-6.3231
H136	-2.0514	-3.1729	-6.4904
H137	-0.9049	-1.9048	-6.9224
H138	-2.6132	-1.5231	-6.6946
C139	0.5528	-3.3557	-4.75
O140	0.138	-4.1034	-5.8318
C141	-0.7824	-5.1445	-5.4952
H142	-0.3608	-5.8054	-4.7351
H143	-0.9625	-5.7073	-6.4096
H144	-1.7262	-4.7414	-5.1266
C145	1.8469	-3.6158	-4.2337
C146	2.877	-4.4794	-4.9864
C147	3.0847	-3.9025	-6.4018
H148	3.8362	-4.491	-6.9341

H149	3.4421	-2.8717	-6.3455
H150	2.1637	-3.9181	-6.9799
C151	2.4457	-5.9551	-5.0835
H152	3.2696	-6.5482	-5.4877
H153	1.5905	-6.0886	-5.7391
H154	2.197	-6.3547	-4.0979
C155	4.2452	-4.4579	-4.2844
H156	4.2055	-4.9096	-3.2919
H157	4.6391	-3.4448	-4.1852
H158	4.9549	-5.0341	-4.8804
C159	2.194	-2.9965	-3.0424
H160	3.1665	-3.1781	-2.6202
C161	2.1919	-2.6397	0.3613
C162	3.3161	-3.4187	0.1389
H163	3.931	-3.2048	-0.7183
C164	3.6887	-4.4536	0.994
C165	4.9488	-5.2707	0.6333
C166	5.9509	-4.3996	-0.1566
H167	6.1941	-3.4816	0.3786
H168	5.5833	-4.1298	-1.1461
C169	4.5527	-6.4457	-0.2838
H170	4.0846	-6.074	-1.1969
H171	3.853	-7.1279	0.1945
H172	5.4414	-7.0163	-0.5661
C173	5.717	-5.794	1.8623
H174	5.2009	-6.5912	2.3858
H175	5.901	-4.993	2.58
C176	2.8633	-4.6791	2.116
O177	3.112	-5.7363	2.9658
C178	2.6151	-7.0197	2.5836
H179	1.7818	-6.9301	1.8855
H180	2.2756	-7.5208	3.49
H181	3.4035	-7.6211	2.1283
C182	1.8011	-3.8116	2.4541
C183	1.0251	-3.9041	3.7836
C184	0.1031	-5.1376	3.8031
H185	-0.5194	-5.116	4.7012
H186	0.6603	-6.0698	3.8114
H187	-0.5592	-5.14	2.9348
C188	1.9924	-3.9531	4.9837
H189	2.6477	-3.0812	4.9823
H190	2.6108	-4.8458	4.9745
H191	1.4172	-3.9384	5.9127

C192	0.1312	-2.6681	3.99
H193	-0.6541	-2.5926	3.2407
H194	0.7077	-1.7441	3.9701
H195	-0.3516	-2.7436	4.966
C196	1.4684	-2.8243	1.5319
H197	0.6361	-2.1669	1.7227
H198	6.7417	6.0295	0.4061
C199	6.9848	1.8945	-0.1407
C200	6.2591	-1.852	2.9888
H201	6.6006	-2.8766	2.8672
H202	7.0893	-1.1648	3.183
H203	6.6841	-6.1815	1.5353
H204	7.3597	2.8552	0.1999
H205	7.7511	1.1131	-0.0891
H206	6.8709	-4.9676	-0.3035

DTBM-SEGPHOS-L, triplet state

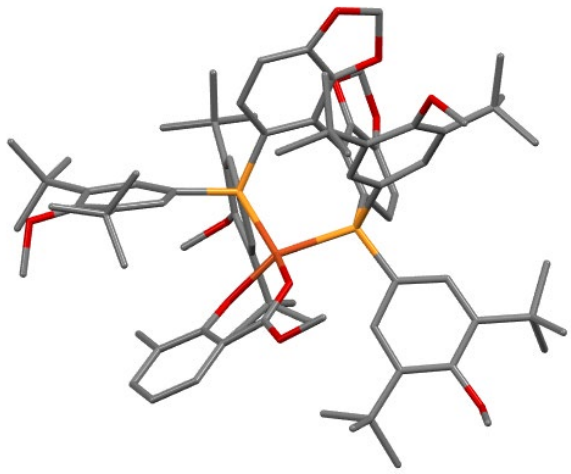

Calculated geometry

Atom	X	Y	Z
Cu1	0	0	0
P2	1.2393	1.4657	1.2421
O3	-1.2776	-1.4587	0.0449
P4	1.7724	-1.2682	-0.7431
C5	-2.6275	-3.6614	-0.0597

H6	-1.9282	-3.7957	-0.8878
H7	-3.3958	-4.4318	-0.1015
H8	-2.0761	-3.743	0.8791
O9	-3.3204	-2.4231	-0.1576
C10	-3.2566	-0.0676	-0.2451
C11	-2.5492	-1.2756	-0.1296
C12	-4.687	-0.0574	-0.2626
H13	-5.2106	-1.0023	-0.2548
C14	-5.3991	1.1256	-0.2477
H15	-6.4832	1.094	-0.2396
C16	-4.7392	2.3564	-0.2271
H17	-5.3015	3.2825	-0.1974
C18	-3.3339	2.4004	-0.2675
C19	-2.6076	3.7169	-0.3011
H20	-1.8701	3.79	0.5013
H21	-3.3099	4.5462	-0.2001
H22	-2.0578	3.8537	-1.2369
O23	-1.2756	1.3247	-0.4861
C24	-2.5884	1.2184	-0.3194
C25	0.1241	2.3394	2.3614
C26	-0.933	1.6303	2.908
H27	-0.997	0.5672	2.7225
C28	-1.9226	2.2434	3.6736
C29	-2.9379	1.3118	4.3711
C30	-3.7735	1.9714	5.4819
H31	-4.5182	2.6664	5.1065
H32	-3.1426	2.5005	6.1971
H33	-4.3054	1.1835	6.02
C34	-3.8753	0.6765	3.3291
H35	-4.5632	-0.0153	3.8218
H36	-3.3192	0.1215	2.5737
H37	-4.4676	1.4257	2.8041
C38	-2.1421	0.1812	5.0658
H39	-1.4342	0.5916	5.7894
H40	-1.5885	-0.4362	4.3615
H41	-2.8347	-0.4725	5.5995
C42	-1.8767	3.648	3.7482
C43	-4.0498	4.4684	3.3655
H44	-3.7332	4.9086	2.4193
H45	-4.7732	5.1211	3.8508
H46	-4.5092	3.5011	3.1632
O47	-2.9422	4.349	4.2668
C48	-0.5814	5.889	3.6083

C49	-0.7563	4.389	3.3076
C50	-0.6327	6.1095	5.1336
H51	-0.4916	7.1693	5.3597
H52	0.1649	5.5502	5.6282
H53	-1.5865	5.7937	5.5505
C54	-1.6575	6.752	2.9216
H55	-1.3951	7.8076	3.0253
H56	-2.6382	6.6102	3.3653
H57	-1.7206	6.5241	1.8557
C58	0.7837	6.4013	3.1182
H59	0.8808	6.3403	2.0325
H60	1.6135	5.8525	3.5672
H61	0.8875	7.4502	3.4008
C62	0.231	3.7017	2.6133
H63	1.0804	4.2363	2.2244
C64	2.0945	2.7244	0.2785
C65	1.6742	2.9303	-1.0235
H66	0.8992	2.2922	-1.4161
C67	2.2159	3.9315	-1.8282
C68	1.7561	3.9861	-3.3014
C69	2.8161	4.571	-4.2536
H70	2.4917	4.4022	-5.2825
H71	3.777	4.0705	-4.1182
H72	2.975	5.6367	-4.1294
C73	0.4343	4.7704	-3.4121
H74	0.0997	4.7921	-4.4523
H75	0.53	5.7984	-3.0671
H76	-0.3434	4.2891	-2.8169
C77	1.4826	2.5541	-3.8153
H78	0.6398	2.078	-3.3182
H79	2.3581	1.9163	-3.6922
H80	1.2414	2.6012	-4.8785
C81	3.1407	4.7994	-1.2159
O82	3.6107	5.91	-1.8799
C83	2.7337	7.0375	-1.9499
H84	2.14	7.0185	-2.8638
H85	3.3609	7.9282	-1.9577
H86	2.0669	7.0704	-1.0873
C87	3.6659	4.5553	0.0764
C88	4.8049	5.3961	0.6843
C89	6.018	5.4267	-0.2671
H90	5.7872	5.9426	-1.1951
H91	6.3415	4.4155	-0.5156

C92	4.3404	6.835	0.9821
H93	3.4428	6.8329	1.6035
H94	4.1328	7.397	0.0772
H95	5.1256	7.3645	1.5275
C96	5.2849	4.8011	2.0196
H97	6.1305	5.3886	2.3806
H98	5.6116	3.7662	1.9155
H99	4.5086	4.8392	2.7863
C100	3.1218	3.5016	0.7994
H101	3.4842	3.2829	1.791
C102	3.3089	-0.3237	-0.9494
C103	3.779	-0.009	-2.2203
H104	3.2385	-0.3627	-3.0853
C105	4.9397	0.7447	-2.4257
H106	5.2887	0.9876	-3.4196
C107	5.6168	1.1416	-1.3013
O108	6.7638	1.8805	-1.2051
O109	5.9864	1.3966	0.903
C110	5.15	0.844	-0.0294
C111	3.9874	0.1478	0.2041
C112	3.568	-0.0626	1.612
C113	4.3429	-0.8572	2.4245
O114	5.4483	-1.5738	2.0646
O115	4.9686	-1.9555	4.2867
C116	4.0609	-1.0794	3.7639
C117	2.9936	-0.4819	4.3834
H118	2.7741	-0.6456	5.4289
C119	2.199	0.3516	3.5905
H120	1.3516	0.8396	4.0489
C121	2.4599	0.568	2.2397
C122	1.3393	-1.9396	-2.3692
C123	0.1266	-1.5469	-2.9083
H124	-0.481	-0.8507	-2.3557
C125	-0.3502	-2.0307	-4.1272
C126	-1.6917	-1.451	-4.6283
C127	-2.8614	-2.1491	-3.9061
H128	-2.7921	-2.0041	-2.8275
H129	-2.8859	-3.221	-4.1011
H130	-3.8105	-1.7231	-4.2404
C131	-1.7654	0.0541	-4.2769
H132	-2.6695	0.4754	-4.7193
H133	-0.9067	0.595	-4.6788
H134	-1.8195	0.2405	-3.2057

C135	-1.8799	-1.5334	-6.1538
H136	-2.0361	-2.5428	-6.5195
H137	-1.0195	-1.1142	-6.6787
H138	-2.7586	-0.9452	-6.4261
C139	0.4428	-2.9984	-4.7686
O140	-0.0049	-3.6408	-5.9013
C141	-0.9253	-4.7124	-5.675
H142	-0.6104	-5.3254	-4.8289
H143	-0.9284	-5.3162	-6.581
H144	-1.933	-4.3409	-5.4906
C145	1.7451	-3.3294	-4.3145
C146	2.7237	-4.1783	-5.1493
C147	2.9285	-3.51	-6.5244
H148	3.643	-4.0901	-7.1136
H149	3.3323	-2.5022	-6.4025
H150	1.9968	-3.4441	-7.0813
C151	2.2326	-5.6262	-5.3389
H152	3.0281	-6.2216	-5.793
H153	1.3664	-5.6843	-5.9902
H154	1.9793	-6.0817	-4.3791
C155	4.1052	-4.2618	-4.4781
H156	4.0646	-4.7814	-3.5191
H157	4.5447	-3.2757	-4.3174
H158	4.7775	-4.8233	-5.1286
C159	2.1536	-2.8017	-3.0982
H160	3.1254	-3.0549	-2.7109
C161	2.2188	-2.6553	0.33
C162	3.3383	-3.4378	0.1009
H163	3.9924	-3.1789	-0.7151
C164	3.6519	-4.5351	0.9008
C165	4.9275	-5.3333	0.5501
C166	5.9952	-4.3957	-0.0586
H167	6.2029	-3.5478	0.5937
H168	5.7083	-4.0101	-1.0364
C169	4.5921	-6.3916	-0.5203
H170	4.2066	-5.9116	-1.4214
H171	3.8452	-7.1056	-0.1785
H172	5.4931	-6.948	-0.7913
C173	5.5975	-6.0033	1.7648
H174	5.0348	-6.8403	2.1629
H175	5.7464	-5.2891	2.5762
C176	2.7606	-4.8268	1.9557
O177	2.9392	-5.9483	2.7361

C178	2.4543	-7.1851	2.2069
H179	1.5999	-7.0235	1.5483
H180	2.1481	-7.7969	3.0545
H181	3.2363	-7.7121	1.6594
C182	1.6902	-3.9689	2.2974
C183	0.8452	-4.1396	3.5747
C184	-0.0286	-5.4066	3.5174
H185	-0.7145	-5.4129	4.3679
H186	0.5602	-6.3173	3.5645
H187	-0.6271	-5.4252	2.6041
C188	1.7632	-4.1894	4.8128
H189	2.356	-3.2766	4.8866
H190	2.441	-5.0384	4.7798
H191	1.1536	-4.2679	5.7162
C192	-0.1085	-2.948	3.7719
H193	-0.8604	-2.8839	2.9837
H194	0.4281	-1.9997	3.8124
H195	-0.6357	-3.0744	4.7187
C196	1.4266	-2.9075	1.441
H197	0.5902	-2.2555	1.6297
H198	6.8512	5.9414	0.2174
C199	7.156	1.7788	0.1712
C200	5.9804	-2.1113	3.2816
H201	6.1988	-3.1679	3.1473
H202	6.8695	-1.5435	3.5711
H203	6.5779	-6.3767	1.4624
H204	7.509	2.7439	0.5239
H205	7.9184	0.9998	0.2726
H206	6.9195	-4.9585	-0.1979

LCu(NR_2H)$_2$OPh **(1)**

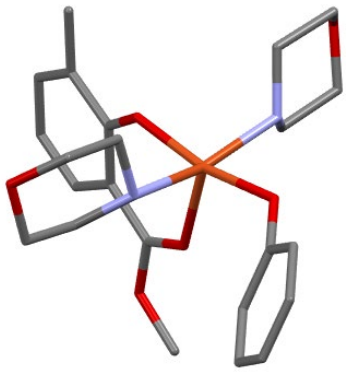

Calculated geometry

Atom	X	Y	Z
Cu1	0	0	0
O2	2.3161	1.4975	-3.9562
O3	-1.3023	1.7641	0.3892
O4	1.3337	-0.0035	1.4188
O5	-1.2042	-0.401	-1.4736
O6	-3.0256	3.1429	0.1176
O7	-2.8008	-3.4952	1.8746
N8	1.3171	0.9234	-1.3307
N9	-0.9489	-1.4097	1.2103
C10	3.5937	0.598	1.8121
C11	-2.9905	1.2286	-1.2425
C12	-3.0807	-0.6483	-2.8176
C13	-2.3675	0.0642	-1.7975
C14	2.2451	0.9406	1.5827
C15	-2.3505	2.0223	-0.1983
C16	1.9901	-0.1025	-2.1564
C17	2.9643	0.5267	-3.1402
C18	-4.2625	1.6283	-1.7089
C19	0.7213	1.9725	-2.1835
C20	1.7395	2.5324	-3.1637
C21	4.5612	1.5766	1.9912
C22	-4.9261	0.9264	-2.6838
C23	1.9228	2.3143	1.5347
C24	-2.3517	-1.1261	1.5697
C25	-0.814	-2.7786	0.6716
C26	-2.4375	-1.8682	-3.409
C27	-1.4385	-3.8085	1.6005

C28	-4.3193	-0.2141	-3.2318
C29	-2.9232	-2.2077	2.4728
C30	4.2287	2.9293	1.9369
C31	2.9022	3.2846	1.7063
C32	-2.4589	3.9654	1.1497
H33	2.0135	1.3625	-0.7296
H34	1.2161	-0.6536	-2.6928
H35	2.5148	-0.7934	-1.495
H36	3.7947	0.998	-2.5957
H37	3.3728	-0.2292	-3.8114
H38	-4.7175	2.5069	-1.2765
H39	0.3365	2.7646	-1.5417
H40	-0.1148	1.5283	-2.7221
H41	1.2624	3.2289	-3.8536
H42	2.5336	3.0649	-2.6212
H43	5.5891	1.2809	2.169
H44	-5.9023	1.2454	-3.0242
H45	0.8919	2.597	1.3596
H46	-2.9303	-1.0717	0.6472
H47	-2.3985	-0.1547	2.0614
H48	0.2455	-2.9945	0.5257
H49	-1.307	-2.7994	-0.3009
H50	-1.4759	-1.6265	-3.8697
H51	-3.0822	-2.3156	-4.166
H52	-2.23	-2.6185	-2.6416
H53	-1.4283	-4.7964	1.1393
H54	-0.8751	-3.8562	2.5433
H55	-4.8375	-0.7742	-4.0031
H56	-2.4055	-2.2019	3.4425
H57	-3.9866	-2.04	2.6453
H58	4.9878	3.689	2.0718
H59	2.6242	4.3318	1.6631
H60	-1.4728	4.3233	0.8558
H61	-2.3779	3.4095	2.0831
H62	-3.1462	4.7993	1.2627
H63	-0.3629	-1.3193	2.038
H64	3.8575	-0.4526	1.8475

LCu(NR_2H)OPh **(2)**

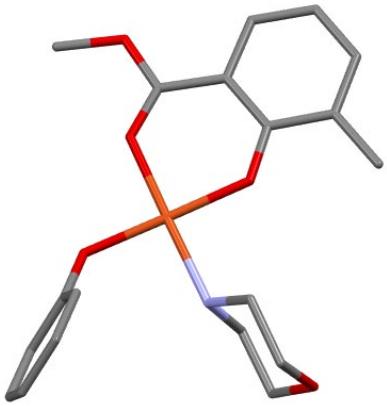

Calculated geometry

Atom	X	Y	Z
Cu1	0	0	0
O2	2.9797	-1.6726	-3.3635
O3	-1.6469	0.3209	1.0741
O4	1.0327	0.3297	1.57
O5	-1.0738	-0.3635	-1.5356
O6	-3.7943	0.439	1.6038
N7	1.6627	-0.516	-1.0957
C8	3.2782	0.2916	2.3319
C9	-3.2949	-0.2089	-0.5924
C10	-2.8817	-0.8628	-2.9149
C11	-2.3651	-0.4657	-1.6423
C12	2.2456	0.8594	1.5578
C13	-2.8298	0.1929	0.7187
C14	1.7051	-1.9803	-1.3179
C15	2.9291	-2.3784	-2.128
C16	-4.6807	-0.3458	-0.8264
C17	1.8024	0.2118	-2.3779
C18	3.0232	-0.2649	-3.1487
C19	4.553	0.8402	2.336
C20	-5.1549	-0.7283	-2.0553
C21	2.5627	1.9975	0.787
C22	-1.9106	-1.1364	-4.0255
C23	-4.2421	-0.9842	-3.0915
C24	4.8519	1.9615	1.5638
C25	3.8446	2.5323	0.7905
C26	-3.3902	0.8329	2.93

H27	2.4466	-0.2577	-0.4982
H28	0.7942	-2.2594	-1.8478
H29	1.7132	-2.4799	-0.3483
H30	3.8432	-2.1792	-1.5512
H31	2.8949	-3.4407	-2.37
H32	-5.3669	-0.1463	-0.0164
H33	1.883	1.2781	-2.1648
H34	0.8942	0.0386	-2.9525
H35	3.0576	0.2046	-4.1318
H36	3.9409	-0.0036	-2.6032
H37	5.3255	0.3835	2.9442
H38	-6.218	-0.8336	-2.2263
H39	1.7797	2.4529	0.1904
H40	-1.3095	-0.2521	-4.2525
H41	-2.4362	-1.4392	-4.9313
H42	-1.2062	-1.9256	-3.7511
H43	-4.6158	-1.2879	-4.0635
H44	5.8491	2.3823	1.5669
H45	4.0567	3.4071	0.1865
H46	-2.8172	1.7579	2.8925
H47	-2.7915	0.0494	3.3916
H48	-4.3171	0.9786	3.4765
H49	3.0509	-0.5845	2.9276

LCu(NR_2H)(NR_2)**(3)**

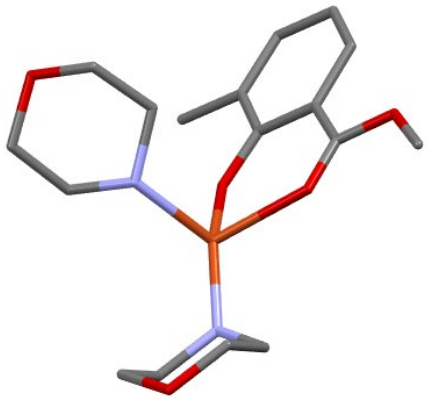

Calculated geometry

Atom	X	Y	Z
Cu1	0	0	0
O2	4.2144	0.2967	-1.4852
O3	-1.3205	0.4941	-1.8484
O4	-1.6481	-0.026	0.8824
O5	-3.1551	0.1815	-3.0776
N6	1.5956	0.7679	-0.3768
C7	-3.2338	-0.5779	-0.8575
C8	-3.5574	-1.2275	1.4806
C9	-2.7606	-0.5864	0.488
C10	-2.4684	0.0726	-1.9269
C11	1.9506	1.1595	-1.7341
C12	3.0763	0.3311	-2.3436
C13	-4.4631	-1.188	-1.1672
C14	2.7797	0.6108	0.452
C15	3.8726	-0.2271	-0.2044
C16	-5.2194	-1.8023	-0.1949
C17	-3.0613	-1.2473	2.897
C18	-4.7567	-1.8132	1.1257
C19	-2.4631	0.7796	-4.1856
H20	2.2844	2.2085	-1.704
H21	1.0677	1.1185	-2.3724
H22	2.737	-0.6913	-2.5445
H23	3.4074	0.7748	-3.2835
H24	-4.8081	-1.174	-2.1905
H25	2.5059	0.181	1.4168
H26	3.1969	1.6104	0.6498

H27	4.7833	-0.2071	0.3957
H28	3.5475	-1.2695	-0.3082
H29	-6.1594	-2.2744	-0.4487
H30	-2.9481	-0.2347	3.2923
H31	-2.0762	-1.7156	2.963
H32	-3.7513	-1.7945	3.5395
H33	-5.3482	-2.2997	1.8937
H34	-3.1718	0.7664	-5.0089
H35	-1.5748	0.2016	-4.4385
H36	-2.175	1.803	-3.9482
H37	-0.8894	-2.1848	0.0109
C38	0.8931	-4.0354	1.0918
C39	0.9159	-2.4939	1.1417
C40	0.1788	-1.9779	-0.0661
C41	0.7283	-2.5297	-1.3556
C42	0.6868	-4.0662	-1.2582
O43	1.4247	-4.5225	-0.1319
H44	-0.1365	-4.3946	1.2199
H45	1.511	-4.4512	1.8882
H46	1.9573	-2.168	1.1449
H47	0.4504	-2.1653	2.0728
H48	0.1454	-2.2074	-2.2205
H49	1.7632	-2.231	-1.5092
H50	-0.3525	-4.4139	-1.1893
H51	1.1493	-4.5166	-2.137

LCu(NR_2)R **(4-R)**

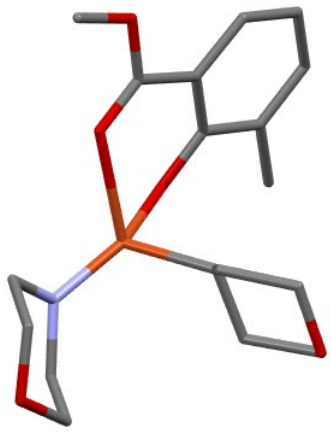

Calculated geometry

Atom	X	Y	Z
Cu1	0	0	0
O2	4.2144	0.2967	-1.4852
O3	-1.3205	0.4941	-1.8484
O4	-1.6481	-0.026	0.8824
O5	-3.1551	0.1815	-3.0776
N6	1.5956	0.7679	-0.3768
C7	-3.2338	-0.5779	-0.8575
C8	-3.5574	-1.2275	1.4806
C9	-2.7606	-0.5864	0.488
C10	-2.4684	0.0726	-1.9269
C11	1.9506	1.1595	-1.7341
C12	3.0763	0.3311	-2.3436
C13	-4.4631	-1.188	-1.1672
C14	2.7797	0.6108	0.452
C15	3.8726	-0.2271	-0.2044
C16	-5.2194	-1.8023	-0.1949
C17	-3.0613	-1.2473	2.897
C18	-4.7567	-1.8132	1.1257
C19	-2.4631	0.7796	-4.1856
H20	2.2844	2.2085	-1.704
H21	1.0677	1.1185	-2.3724
H22	2.737	-0.6913	-2.5445
H23	3.4074	0.7748	-3.2835

H24	-4.8081	-1.174	-2.1905
H25	2.5059	0.181	1.4168
H26	3.1969	1.6104	0.6498
H27	4.7833	-0.2071	0.3957
H28	3.5475	-1.2695	-0.3082
H29	-6.1594	-2.2744	-0.4487
H30	-2.9481	-0.2347	3.2923
H31	-2.0762	-1.7156	2.963
H32	-3.7513	-1.7945	3.5395
H33	-5.3482	-2.2997	1.8937
H34	-3.1718	0.7664	-5.0089
H35	-1.5748	0.2016	-4.4385
H36	-2.175	1.803	-3.9482
H37	-0.8894	-2.1848	0.0109
C38	0.8931	-4.0354	1.0918
C39	0.9159	-2.4939	1.1417
C40	0.1788	-1.9779	-0.0661
C41	0.7283	-2.5297	-1.3556
C42	0.6868	-4.0662	-1.2582
O43	1.4247	-4.5225	-0.1319
H44	-0.1365	-4.3946	1.2199
H45	1.511	-4.4512	1.8882
H46	1.9573	-2.168	1.1449
H47	0.4504	-2.1653	2.0728
H48	0.1454	-2.2074	-2.2205
H49	1.7632	-2.231	-1.5092
H50	-0.3525	-4.4139	-1.1893
H51	1.1493	-4.5166	-2.137

LCu(NR_2H)$_2$(OPh)R **(1-R)**

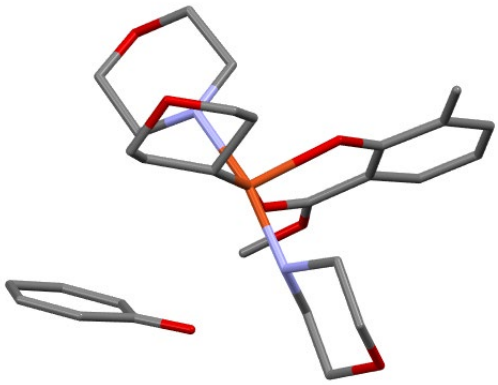

Calculated geometry

Atom	X	Y	Z
Cu1	0	0	0
O2	1.8922	3.2707	-2.8921
O3	-1.1678	1.6898	0.0893
O4	1.0214	-1.1333	3.4555
O5	-1.4736	-0.672	-1.4068
O6	-2.8479	3.1226	-0.0779
O7	-2.9873	-2.082	3.1179
N8	1.1317	0.9937	-1.331
N9	-0.8597	-0.8938	1.5839
C10	3.2886	-0.5007	3.7911
C11	-3.1293	1.0615	-1.1603
C12	-3.5571	-1.0123	-2.4081
C13	-2.6454	-0.2129	-1.6282
C14	1.9425	-0.2166	3.433
C15	-2.2997	1.9309	-0.3582
C16	0.4086	1.3704	-2.573
C17	1.3415	2.1157	-3.515
C18	-4.4445	1.4794	-1.4784
C19	1.7575	2.1937	-0.7162
C20	2.6299	2.9213	-1.7274
C21	4.2878	0.4542	3.6908
C22	-5.2837	0.693	-2.2217
C23	1.6793	1.1184	3.0181
C24	-1.9488	-0.0905	2.1881

C25	-1.3716	-2.255	1.3074
C26	-3.0716	-2.3442	-2.8988
C27	-1.9509	-2.886	2.5674
C28	-4.8233	-0.5566	-2.6809
C29	-2.4969	-0.7831	3.4299
C30	4.0083	1.7479	3.2451
C31	2.6899	2.0648	2.9222
C32	-2.0811	4.0212	0.7412
H33	1.8815	0.3709	-1.6139
H34	-0.4304	2.0048	-2.3002
H35	0.0215	0.4659	-3.0359
H36	2.1525	1.4525	-3.8482
H37	0.7908	2.4577	-4.391
H38	-4.7858	2.4381	-1.116
H39	2.3482	1.8851	0.1445
H40	0.9534	2.8392	-0.3691
H41	3.007	3.8485	-1.2964
H42	3.4867	2.2916	-2.0062
H43	5.3046	0.1879	3.9599
H44	-6.2882	1.0227	-2.4522
H45	0.6626	1.3902	2.759
H46	-2.7489	0.0327	1.4589
H47	-1.5639	0.8908	2.4565
H48	-0.5625	-2.8863	0.9442
H49	-2.1302	-2.1882	0.5284
H50	-2.1863	-2.235	-3.5313
H51	-3.8474	-2.853	-3.4718
H52	-2.7745	-2.9882	-2.0667
H53	-2.3923	-3.8533	2.3265
H54	-1.1584	-3.0322	3.3115
H55	-5.4888	-1.1813	-3.268
H56	-1.7152	-0.8522	4.1956
H57	-3.3367	-0.2134	3.8284
H58	4.7927	2.49	3.1687
H59	2.4451	3.0683	2.5896
H60	-1.1472	4.2863	0.2472
H61	-1.8662	3.5702	1.7089
H62	-2.7071	4.9006	0.8629
H63	-0.0976	-0.966	2.325
H64	3.5212	-1.506	4.1249
H65	1.2045	-1.8388	1.0683
C66	3.7971	-2.1291	0.3812
C67	2.9023	-0.8742	0.2454

C68	1.4944	-1.3821	0.1284
C69	1.31	-2.2956	-1.049
C70	2.3183	-3.4587	-0.8801
O71	3.6439	-2.9784	-0.7449
H72	3.549	-2.6661	1.3036
H73	4.8448	-1.8319	0.4151
H74	3.2559	-0.3441	-0.6406
H75	3.0482	-0.2434	1.1186
H76	0.3031	-2.7073	-1.1101
H77	1.5243	-1.7912	-1.9941
H78	2.0422	-4.0577	-0.0034
H79	2.3007	-4.096	-1.7641

LCu(NR_2H)(OPh)R **(2-R)**

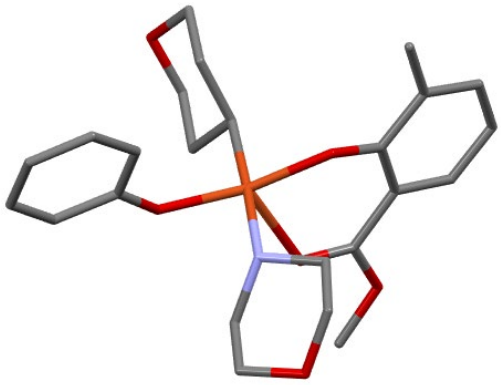

Calculated geometry

Atom	X	Y	Z
Cu1	0	0	0
O2	1.7609	4.5747	-0.225
O3	-1.3195	1.0181	-1.5864
O4	1.4523	-0.758	-0.9044
O5	-1.3058	0.5964	1.211
O6	-3.2911	1.6179	-2.4323
N7	1.1186	1.8087	0.2074
C8	3.7214	-1.3627	-1.0279
C9	-3.2612	1.0092	-0.1644
C10	-3.3892	0.5459	2.2374
C11	-2.5967	0.7097	1.0622
C12	2.588	-1.0051	-0.2692
C13	-2.5187	1.2006	-1.4144
C14	1.6025	2.3093	-1.0974
C15	2.4611	3.552	-0.929
C16	-4.6642	1.1358	-0.18
C17	0.4542	2.8937	0.9554
C18	1.3463	4.1211	1.0601
C19	4.936	-1.6245	-0.4136
C20	-5.4108	0.9784	0.9639
C21	2.7373	-0.9307	1.1295
C22	-2.6951	0.2247	3.5288
C23	-4.76	0.6862	2.1685
C24	5.0724	-1.5435	0.9721
C25	3.9615	-1.1969	1.7327

C26	-2.6376	1.8077	-3.6981
H27	1.9291	1.5013	0.7429
H28	0.7276	2.5361	-1.7073
H29	2.1657	1.5173	-1.5879
H30	3.385	3.3001	-0.3887
H31	2.7301	3.9664	-1.901
H32	-5.1539	1.3596	-1.116
H33	0.1864	2.5293	1.9456
H34	-0.4683	3.1436	0.4302
H35	0.8075	4.9464	1.5267
H36	2.2308	3.8914	1.6719
H37	5.7895	-1.8952	-1.0246
H38	-6.4881	1.0753	0.9336
H39	1.8793	-0.6805	1.743
H40	-2.001	1.0189	3.8155
H41	-2.1001	-0.6875	3.4403
H42	-3.4193	0.0924	4.3328
H43	-5.3442	0.557	3.0731
H44	6.0233	-1.7498	1.4458
H45	4.0419	-1.1338	2.8118
H46	-3.4184	2.1358	-4.3785
H47	-2.1977	0.8734	-4.0451
H48	-1.8602	2.5663	-3.6162
H49	3.6195	-1.426	-2.1044
H50	-1.9432	-1.4327	0.1476
C51	-1.1234	-4.048	0.7815
C52	-0.3707	-2.7064	0.9026
C53	-0.9423	-1.7645	-0.1186
C54	-0.8998	-2.3213	-1.5126
C55	-1.6264	-3.6825	-1.4897
O56	-1.0454	-4.5622	-0.5386
H57	-2.1746	-3.9142	1.0691
H58	-0.6725	-4.7937	1.4366
H59	0.6885	-2.891	0.7202
H60	-0.4881	-2.3262	1.9191
H61	-1.4011	-1.6666	-2.2271
H62	0.1261	-2.4758	-1.8424
H63	-2.6909	-3.5392	-1.2619
H64	-1.5389	-4.1698	-2.4611

Morpholine **(NR_2H)**

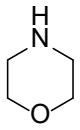

Calculated geometry

Atom	X	Y	Z
O1	0	0	0
N2	-0.2916	2.6568	-1.0631
C3	-0.0751	1.4884	-1.9232
C4	-0.5746	0.1947	-1.292
C5	0.2127	2.4063	0.2913
C6	-0.2933	1.0915	0.872
H7	-1.2875	2.853	-1.0148
H8	-1.6709	0.2201	-1.2041
H9	-0.294	-0.6739	-1.8903
H10	-0.0741	3.2365	0.9408
H11	1.3062	2.3796	0.2478
H12	0.1892	0.8656	1.8244
H13	-1.3799	1.1476	1.0343
H14	0.9994	1.4007	-2.1137
H15	-0.5707	1.652	-2.8829

Phenol **(PhOH)**

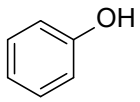

Calculated geometry

Atom	X	Y	Z
O1	0	0	0
C2	2.2569	0.6381	0.2604
C3	0.9514	0.9763	-0.0905
C4	3.2583	1.5972	0.1834
C5	0.653	2.2696	-0.5151
C6	2.9711	2.8924	-0.2402
C7	1.6651	3.2207	-0.588
H8	4.2712	1.3286	0.4572
H9	-0.3651	2.5259	-0.7866
H10	3.7556	3.6356	-0.2981
H11	1.4267	4.224	-0.9192
H12	2.4716	-0.3709	0.5887
H13	-0.8584	0.3536	-0.2669

Organic radical **(R)**

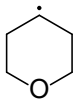

Calculated geometry

Atom	X	Y	Z
C1	0	0	0
C2	-1.4941	-0.025	-0.3388
O3	-2.2835	0.4326	0.7557
C4	-2.1418	-0.4031	1.9012
C5	-0.6982	-0.4083	2.4151
C6	0.2537	-0.6758	1.3021
H7	0.3155	1.0556	0.0495
H8	0.5711	-0.4585	-0.8114
H9	-1.7991	-1.0459	-0.6061
H10	-1.7193	0.635	-1.1769
H11	-2.8266	-0.0113	2.6537
H12	-2.4508	-1.426	1.6462
H13	-0.497	0.5803	2.8607
H14	-0.5949	-1.1402	3.2203
H15	1.1964	-1.173	1.4907

3: Copper-catalyzed asymmetric azidation of alkyl halides

3.1: Background

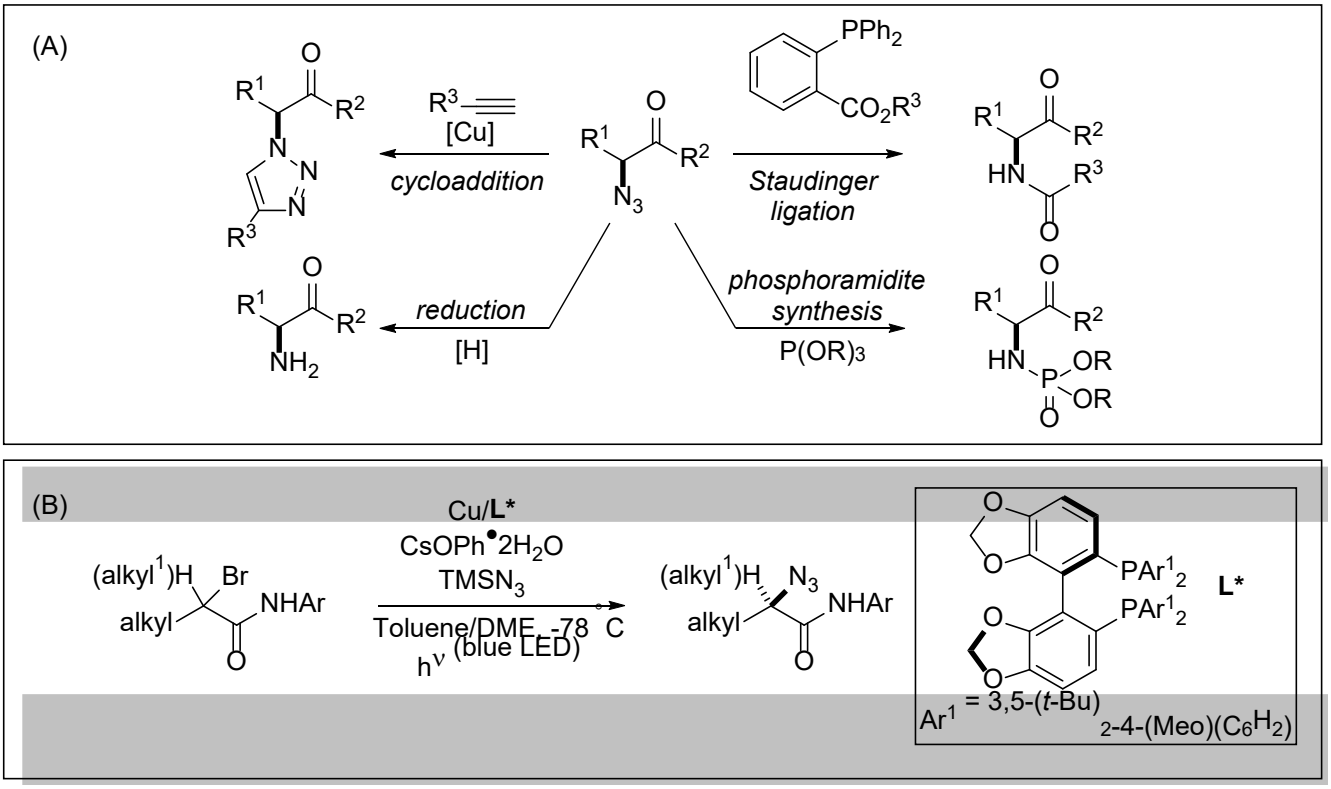

Figure 3.1.1: (A) Selected useful transformations of alkyl azides. (B) Enantioconvergent azidation of secondary and tertiary α-bromo amides.

Azides are valuable motifs in synthetic organic chemistry and find wide use as a synthetic intermediate, for example as an intermediate in the Curtius rearrangement.[63] In particular, chiral alkyl azides are interemediates in click chemistry reactions[64] such as Huisgen cycloaddition,[65] and Staudinger ligation.[66–68] Other useful transformations include reduction to amines,[69] tetrazole,[70] and phosphoramide synthesis, and others (Fig. 3.1.1A). A variety of methods have been reported for the synthesis of enantioenriched alkyl azides including ring-opening approaches,[71,72] azidofunctionalization of olefins,[73–76] decarboxylation,[77,78] and C-H functionalization.[79–81] Conceptually, the most simple synthesis approach is the nucleophilic substitution by azide, however few asymmetric methods of this type have been reported.[82–84] Given this literature

backdrop, our group sought to developed a general method for the asymmetric synthesis of α-azido carbonyl compounds from racemic α-halo carbonyl precursors. After optimization, we devised a catalytic protocol using a copper-photocatalyst to achieve the enantioconvergent synthesis of α-azido amides from secondary and tertiary alkyl halides using $TMSN_3$ as an azide source in the presence of the base cesium phenoxide. Using this protocol, a diverse range of secondary and tertiary azides could be synthesized. (Fig 3.1.1B). EPR and ^{31}P-NMR spectroscopy indicates that the primary Cu^{II} species in solution was a DTBM-SEGPHOS-Cu-azide complex. However, it was ambiguous whether or not the Cu^{II} species was the neutral diazide species $\mathbf{L}Cu^{II}(N_3)_2$ or the cationic species $\mathbf{L}Cu^{II}(N_3)^+$.

3.2: EPR calculations of Cu^{II}-azide species

To disambiguate the identity of the dominant Cu^{II} species in solution, a dual strategy of EPR measurements as well as DFT experiments was undertaken. The geometry of both putative Cu^{II} species were computed, and their EPR hyperfine couplings calculated. Figure 3.2.1 shows the results of both the reported and calculated EPR values. From the table, the measured ^{31}P couplings of the two phosphorus atoms are close together, which matches closely with the computed values for $\mathbf{L}Cu^{II}(N_3)_2$. In contrast, these values are divergent from each other in the case of $\mathbf{L}Cu(N_3)^+$. Further, the experimental couplings for ^{14}N nuclei is closer in value to the calculated values for

Parameter	x				y				z				isotropic			
g	2.0172				2.0150				2.111				2.0477			
A(MHz)	Exp.	DFT			Exp.	DFT			Exp.	DFT			Exp.	DFT		
		$\mathbf{L}Cu(N_3)_2$		$[\mathbf{L}Cu(N_3)]^+$		$\mathbf{L}Cu(N_3)_2$		$[\mathbf{L}Cu(N_3)]^+$		$\mathbf{L}Cu(N_3)_2$		$[\mathbf{L}Cu(N_3)]^+$		$\mathbf{L}Cu(N_3)_2$		$[\mathbf{L}Cu(N_3)]^+$
A($^{63/65}$Cu)	±74	-42		71	±44	-46		94	±344	-468		-314	±154	-185		-50
A($^{31}P_1$)	525	495		243	374	356		158	385	358		163	428	403		188
A($^{31}P_2$)	368	339		431	505	479		672	428	340		432	434	386		512
A(^{14}N)	9.3	α	7.9, 8.2	-4.0	9.3	8.1, 8.5		-4.5	31	17.0, 18.2		9.4	16.5	11.0, 11.6		0.3
		β	-0.4, -0.6	-1.2		-2.0, -2.2		-3.3		-3.0, -3.2		-5.3		-1.6, -2.0		-3.3
		γ	-2.9, -2.8	-3.7		-3.2, -3.1		-4.3		10.0, 9.6		12.9		1.3, 1.2		1.6

Figure 3.2.1: Comparison of experimental EPR parameters with calculated values for $\mathbf{L}Cu^{II}(N_3)_2$ and $\mathbf{L}Cu^{II}(N_3)^+$.

L$Cu^{II}(N_3)_2$. Based on this evidence and further analogy to the previously reported **L**$Cu^{II}Cl_2$, the structure of the dominant Cu^{II} species in solution was assigned to **L**$Cu^{II}(N_3)_2$.[85]

3.3: Computational details

3.3.1: Computational methods

All calculations were performed using the Orca 6.0.1 software package.[28,29,86] All molecular structure images were generated using the Mercury software package.[27] Geometry optimizations were carried out using the B3LYP[87] functional with the D4 dispersion correction. ` The Def2-SVP basis set was used for all atoms except copper, for which the Def2-QZVPPD basis set was used.[35,36] The RIJCOSX approximation was used with the def2/J auxiliary basis set in all calculations.[88,89] All calculations included the implicit CPCM solvation model.[39] A dielectric constant of 7.20,[90] a refractive index of 1.38,[91] and a solvent radius of 2.42 Å were used to approximate 1,2-dimethoxyethane. EPR values for **L**$Cu^{II}(N_3)_2$ and [**L**$Cu^{II}(N_3)$]$^+$ were calculated using the TPSSh functional[92,93] based on literature examples showing its effectiveness in modeling spin states of bioinorganic compounds.[94] The Def2-TZVPD basis set was used for all atoms except copper, for which def2-QZVPPD was used. EPR values were calculated for all Cu, P, and N atoms.

3.3.3.2: Calculated structures

L$Cu^{II}(N_3)_2$

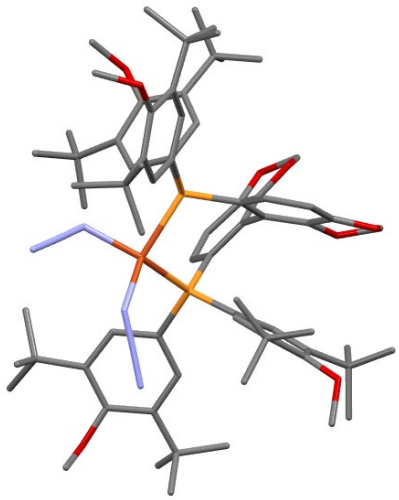

Calculated geometry

Atom	X	Y	Z
Cu1	0	0	0
P2	1.2806	1.3682	1.3574
N3	-1.3068	-1.4807	-0.0662
P4	1.8845	-1.1402	-0.7107
N5	-1.3139	1.4299	-0.4596
C6	0.2627	2.1375	2.6558
C7	-0.9604	1.5526	2.9731
H8	-1.2603	0.6538	2.4395
C9	-1.8099	2.0813	3.9569
C10	-3.1133	1.3078	4.2755
C11	-3.5114	1.3985	5.7649
H12	-3.8181	2.401	6.0781
H13	-2.6749	1.0867	6.4113
H14	-4.3542	0.7143	5.9524
C15	-4.2593	1.8097	3.3672
H16	-5.1848	1.2513	3.5866
H17	-4.0121	1.6496	2.3062
H18	-4.4707	2.8776	3.5059
C19	-2.9257	-0.2004	3.9805
H20	-2.058	-0.6128	4.5186
H21	-2.8018	-0.4169	2.9099
H22	-3.8225	-0.7448	4.3136
C23	-1.3952	3.2885	4.5768

C24	-3.291	4.7079	5.0097
H25	-3.1288	5.035	3.9708
H26	-3.3773	5.5942	5.6559
H27	-4.2354	4.145	5.069
O28	-2.1982	3.9291	5.4871
C29	0.4327	5.0626	5.1404
C30	-0.1112	3.8582	4.3388
C31	0.4088	4.7386	6.6511
H32	0.8141	5.5894	7.2236
H33	1.0354	3.8576	6.8671
H34	-0.6099	4.5351	7.0033
C35	-0.3811	6.3435	4.8558
H36	0.1115	7.2083	5.33
H37	-1.4005	6.2903	5.2517
H38	-0.4378	6.54	3.7728
C39	1.8962	5.3704	4.7627
H40	2.0004	5.6775	3.7104
H41	2.5602	4.5092	4.9354
H42	2.2597	6.2018	5.3861
C43	0.6886	3.2655	3.3596
H44	1.6614	3.6903	3.1325
C45	2.0626	2.7261	0.4361
C46	1.5875	3.0092	-0.8403
H47	0.8284	2.3604	-1.2706
C48	2.0476	4.1082	-1.581
C49	1.534	4.2269	-3.0374
C50	2.3091	5.2201	-3.9269
H51	1.9873	5.0733	-4.9706
H52	3.3938	5.0433	-3.8797
H53	2.1217	6.2699	-3.676
C54	0.0352	4.6001	-3.0275
H55	-0.3513	4.6491	-4.0589
H56	-0.1354	5.5798	-2.5547
H57	-0.5588	3.8531	-2.478
C58	1.6933	2.8442	-3.7182
H59	1.1267	2.0486	-3.2169
H60	2.7508	2.5413	-3.743
H61	1.328	2.9012	-4.7556
C62	2.9422	4.9835	-0.9246
O63	3.26	6.1975	-1.4841
C64	2.2653	7.2048	-1.3252
H65	1.3451	6.9643	-1.88
H66	2.6892	8.1378	-1.722

H67	2.0065	7.3456	-0.2633
C68	3.5583	4.6451	0.3142
C69	4.7328	5.4618	0.8985
C70	5.8482	5.5822	-0.165
H71	5.5126	6.1706	-1.028
H72	6.1503	4.5897	-0.5304
C73	4.2893	6.8713	1.3473
H74	3.4279	6.815	2.0322
H75	4.0218	7.5134	0.5007
H76	5.1156	7.363	1.8867
C77	5.3308	4.7626	2.1356
H78	6.2041	5.3356	2.484
H79	5.6621	3.7391	1.9109
H80	4.6133	4.7183	2.9699
C81	3.0952	3.5041	0.9731
H82	3.5349	3.2116	1.9239
C83	3.3788	-0.139	-0.9964
C84	3.7664	0.1656	-2.3065
H85	3.1842	-0.2294	-3.14
C86	4.8966	0.9541	-2.5888
H87	5.1921	1.185	-3.6131
C88	5.6242	1.4017	-1.5034
O89	6.7524	2.1691	-1.4734
O90	6.1184	1.6885	0.6725
C91	5.239	1.1069	-0.1934
C92	4.1128	0.3653	0.1174
C93	3.8034	0.0952	1.5424
C94	4.746	-0.5813	2.2988
O95	5.9572	-1.0556	1.8869
O96	5.6431	-1.6148	4.0831
C97	4.5516	-0.927	3.6376
C98	3.3881	-0.5967	4.305
H99	3.2252	-0.871	5.3481
C100	2.4313	0.132	3.5763
H101	1.5165	0.4379	4.0849
C102	2.6204	0.489	2.2343
C103	1.4363	-1.9385	-2.2784
C104	0.4245	-1.3447	-3.0284
H105	0.0421	-0.3756	-2.7133
C106	-0.1452	-1.9714	-4.1438
C107	-1.2623	-1.2074	-4.8936
C108	-2.609	-1.4372	-4.1693
H109	-2.5572	-1.0715	-3.1312

H110	-2.888	-2.499	-4.135
H111	-3.4158	-0.8887	-4.6832
C112	-0.9705	0.3132	-4.8627
H113	-1.7176	0.8366	-5.479
H114	0.0273	0.5397	-5.2701
H115	-1.034	0.7425	-3.853
C116	-1.3713	-1.5852	-6.386
H117	-1.7389	-2.6014	-6.5574
H118	-0.394	-1.4919	-6.8863
H119	-2.0694	-0.8901	-6.8792
C120	0.3247	-3.2733	-4.4484
O121	-0.2868	-4.0331	-5.4145
C122	-1.5024	-4.6863	-5.0521
H123	-1.5456	-4.877	-3.9685
H124	-1.5387	-5.6444	-5.5908
H125	-2.379	-4.0886	-5.3474
C126	1.453	-3.8427	-3.7926
C127	2.109	-5.1625	-4.2556
C128	2.4942	-5.0556	-5.748
H129	2.9763	-5.9904	-6.0791
H130	3.2102	-4.2323	-5.9054
H131	1.614	-4.8764	-6.3781
C132	1.1724	-6.3701	-4.0323
H133	1.7246	-7.3059	-4.2195
H134	0.3086	-6.36	-4.7053
H135	0.8055	-6.396	-2.9936
C136	3.4028	-5.4465	-3.4662
H137	3.2078	-5.6208	-2.3967
H138	4.1312	-4.6251	-3.553
H139	3.8757	-6.3564	-3.8669
C140	1.9737	-3.1586	-2.6919
H141	2.7902	-3.5938	-2.1229
C142	2.3603	-2.4583	0.4431
C143	3.5793	-3.1339	0.3554
H144	4.3065	-2.809	-0.3851
C145	3.8741	-4.2093	1.1991
C146	5.2412	-4.9217	1.082
C147	6.203	-4.1281	0.1732
H148	6.3475	-3.0976	0.5288
H149	5.8504	-4.0872	-0.869
C150	5.0692	-6.3175	0.4446
H151	4.5959	-6.2361	-0.5468
H152	4.4609	-6.9897	1.0597

H153	6.0558	-6.7914	0.3102
C154	5.917	-5.0495	2.4669
H155	5.3943	-5.7638	3.1123
H156	5.9259	-4.0805	2.9876
C157	2.8827	-4.5983	2.1452
O158	3.1556	-5.6907	2.9287
C159	2.536	-6.9391	2.6403
H160	2.0894	-6.9472	1.6341
H161	1.7562	-7.1658	3.3849
H162	3.3052	-7.7247	2.6981
C163	1.6932	-3.8506	2.3383
C164	0.6399	-4.1063	3.4426
C165	-0.376	-5.1663	2.9586
H166	-1.1671	-5.3038	3.7146
H167	0.0859	-6.1439	2.7753
H168	-0.8521	-4.8392	2.0206
C169	1.2823	-4.5222	4.7832
H170	2.0179	-3.7676	5.1075
H171	1.7951	-5.488	4.739
H172	0.5001	-4.5839	5.5567
C173	-0.164	-2.8165	3.7339
H174	-0.8079	-2.516	2.8951
H175	0.4955	-1.9706	3.9801
H176	-0.8254	-2.9946	4.5953
C177	1.4576	-2.7994	1.4451
H178	0.5453	-2.2179	1.5368
H179	6.7338	6.0741	0.2699
C180	7.2346	2.0723	-0.1301
C181	6.6475	-1.4012	3.0874
H182	7.2231	-2.3221	2.9328
H183	7.2957	-0.5589	3.394
H184	6.9598	-5.3842	2.3439
H185	7.6135	3.0471	0.2021
H186	8.0137	1.2891	-0.0747
H187	7.1832	-4.6294	0.1647
N188	-1.1919	-2.606	-0.4597
N189	-1.1212	-3.702	-0.8259
N190	-2.4889	1.206	-0.3713
N191	-3.6281	1.019	-0.2971

L$Cu^{II}(N_3)^+$

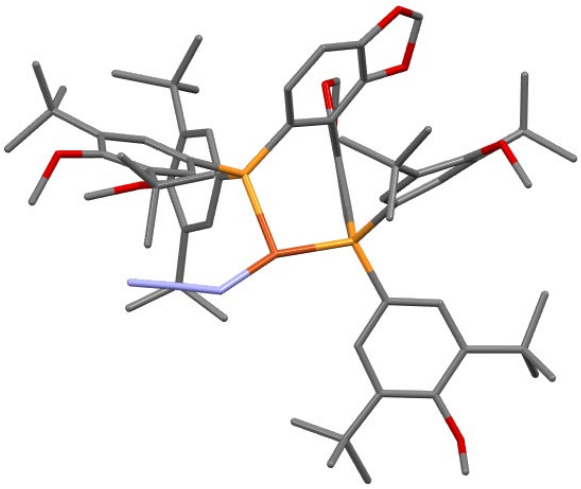

Calculated geometry

Atom	X	Y	Z
Cu1	0	0	0
P2	1.2021	1.4248	1.2758
N3	-1.5084	-0.9095	-0.6313
P4	1.8309	-1.1174	-0.8497
C5	0.1891	2.1726	2.5892
C6	-0.9717	1.5189	2.9984
H7	-1.235	0.5738	2.5255
C8	-1.8032	2.0352	4.0048
C9	-3.0219	1.1845	4.4405
C10	-3.4037	1.3841	5.9236
H11	-3.8239	2.3701	6.1424
H12	-2.528	1.2388	6.5762
H13	-4.1582	0.6308	6.2002
C14	-4.2253	1.4889	3.5199
H15	-5.091	0.8708	3.8102
H16	-3.9777	1.2559	2.4717
H17	-4.5319	2.5424	3.5646
C18	-2.6925	-0.3206	4.2923
H19	-1.7798	-0.5894	4.8464
H20	-2.5628	-0.6321	3.2462

H21	-3.5252	-0.9139	4.6995
C22	-1.4496	3.3012	4.5376
C23	-3.4157	4.6154	4.9363
H24	-3.2659	4.9504	3.898
H25	-3.5872	5.4928	5.5766
H26	-4.3076	3.9719	4.9843
O27	-2.2628	3.9411	5.4354
C28	0.2809	5.2089	4.942
C29	-0.2185	3.941	4.2135
C30	0.3479	4.9394	6.4623
H31	0.7222	5.8352	6.9847
H32	1.04	4.109	6.678
H33	-0.6383	4.6858	6.8706
C34	-0.6281	6.4241	4.6555
H35	-0.1632	7.3362	5.0638
H36	-1.6166	6.327	5.1164
H37	-0.7603	6.5703	3.5712
C38	1.7014	5.593	4.481
H39	1.7344	5.8655	3.4149
H40	2.4275	4.7826	4.6504
H41	2.0402	6.4686	5.0553
C42	0.5724	3.3577	3.2222
H43	1.5012	3.8361	2.9278
C44	1.9382	2.7879	0.3356
C45	1.4193	3.0843	-0.9214
H46	0.6705	2.4184	-1.3527
C47	1.8395	4.2069	-1.6522
C48	1.3182	4.3317	-3.1051
C49	2.0117	5.4024	-3.9715
H50	1.6917	5.2572	-5.0158
H51	3.1063	5.307	-3.9369
H52	1.7459	6.4283	-3.6931
C53	-0.2031	4.5954	-3.0917
H54	-0.5879	4.6504	-4.1231
H55	-0.4423	5.5457	-2.589
H56	-0.7485	3.7921	-2.5715
C57	1.5894	2.9826	-3.8151
H58	1.1088	2.1309	-3.3165
H59	2.6697	2.7781	-3.8603
H60	1.2035	3.0219	-4.8454
C61	2.7275	5.0907	-0.9971
O62	2.9932	6.3235	-1.5351
C63	1.9687	7.2936	-1.3286

H64	1.0265	7.0048	-1.8198
H65	2.3286	8.2352	-1.7654
H66	1.7731	7.4412	-0.2542
C67	3.3888	4.7401	0.2143
C68	4.5645	5.5691	0.777
C69	5.6479	5.711	-0.3166
H70	5.2804	6.3001	-1.1663
H71	5.9544	4.7253	-0.6963
C72	4.1158	6.9706	1.246
H73	3.2678	6.902	1.9458
H74	3.8289	7.6173	0.4094
H75	4.9477	7.4637	1.7747
C76	5.2019	4.8682	1.9928
H77	6.0739	5.4514	2.3264
H78	5.5444	3.852	1.7518
H79	4.5039	4.8054	2.8426
C80	2.971	3.5749	0.8598
H81	3.4406	3.274	1.7936
C82	3.2757	-0.0673	-1.1433
C83	3.6351	0.2528	-2.4597
H84	3.0516	-0.1513	-3.2876
C85	4.7447	1.0629	-2.7536
H86	5.0226	1.3027	-3.7805
C87	5.4801	1.5178	-1.6755
O88	6.5932	2.2981	-1.6609
O89	6.0004	1.8025	0.4938
C90	5.1195	1.211	-0.359
C91	4.0132	0.4476	-0.034
C92	3.7343	0.1665	1.3958
C93	4.7023	-0.4944	2.1335
O94	5.9113	-0.9473	1.6994
O95	5.6481	-1.507	3.9031
C96	4.539	-0.841	3.4776
C97	3.384	-0.5302	4.1681
H98	3.2474	-0.8056	5.2146
C99	2.4016	0.1838	3.459
H100	1.4936	0.4774	3.9866
C101	2.5608	0.541	2.1143
C102	1.3417	-1.9439	-2.3843
C103	0.5006	-1.2803	-3.2772
H104	0.2427	-0.2418	-3.0779
C105	-0.0484	-1.9239	-4.3937
C106	-0.9541	-1.0921	-5.3335

C107	-2.4057	-1.1189	-4.8018
H108	-2.4499	-0.6887	-3.7883
H109	-2.8173	-2.1348	-4.7504
H110	-3.06	-0.5187	-5.4557
C111	-0.4949	0.3847	-5.3407
H112	-1.0765	0.9407	-6.0918
H113	0.5717	0.4759	-5.5996
H114	-0.6576	0.8876	-4.3779
C115	-0.8948	-1.5573	-6.8047
H116	-1.3429	-2.5402	-6.976
H117	0.1478	-1.5972	-7.159
H118	-1.4346	-0.8289	-7.4303
C119	0.2452	-3.3052	-4.5469
O120	-0.3545	-4.0465	-5.5302
C121	-1.6945	-4.4901	-5.3176
H122	-1.9381	-4.527	-4.2449
H123	-1.7834	-5.4999	-5.7439
H124	-2.4136	-3.8336	-5.8314
C125	1.194	-3.9717	-3.723
C126	1.6773	-5.4135	-3.9955
C127	2.2539	-5.5041	-5.426
H128	2.6115	-6.5284	-5.6217
H129	3.11	-4.8194	-5.5429
H130	1.4992	-5.2498	-6.1807
C131	0.5358	-6.4379	-3.8144
H132	0.948	-7.4595	-3.8516
H133	-0.2224	-6.3634	-4.6008
H134	0.0409	-6.3086	-2.8383
C135	2.8006	-5.8177	-3.019
H136	2.4527	-5.8532	-1.9749
H137	3.6632	-5.1351	-3.0701
H138	3.158	-6.8253	-3.2806
C139	1.7079	-3.2685	-2.6318
H140	2.3897	-3.7627	-1.947
C141	2.2926	-2.4161	0.3188
C142	3.5291	-3.0646	0.2531
H143	4.2793	-2.6973	-0.4433
C144	3.7957	-4.1841	1.0451
C145	5.1777	-4.8709	0.9715
C146	6.1485	-4.0682	0.0823
H147	6.267	-3.0316	0.4282
H148	5.8205	-4.0453	-0.9689
C149	5.0693	-6.2827	0.3551

H150	4.5768	-6.2436	-0.6293
H151	4.5151	-6.9795	0.9927
H152	6.0793	-6.6999	0.2104
C153	5.7954	-4.9558	2.3859
H154	5.2184	-5.6231	3.037
H155	5.8218	-3.9639	2.861
C156	2.7644	-4.6377	1.9182
O157	2.9953	-5.8004	2.6036
C158	2.3192	-6.9787	2.1697
H159	2.0708	-6.9261	1.0981
H160	1.397	-7.1456	2.7475
H161	2.9947	-7.8292	2.342
C162	1.5693	-3.9021	2.1178
C163	0.4938	-4.1903	3.192
C164	-0.6225	-5.07	2.5852
H165	-1.4131	-5.2494	3.3325
H166	-0.249	-6.0458	2.2469
H167	-1.0807	-4.5682	1.7176
C168	1.0702	-4.8349	4.4707
H169	1.9109	-4.2401	4.8627
H170	1.424	-5.8602	4.327
H171	0.285	-4.8574	5.2429
C172	-0.158	-2.8615	3.6474
H173	-0.755	-2.3829	2.8587
H174	0.5969	-2.138	3.9921
H175	-0.8442	-3.0641	4.4832
C176	1.3504	-2.8174	1.2598
H177	0.4171	-2.2636	1.3348
H178	6.5378	6.2135	0.0964
C179	7.0955	2.222	-0.3217
C180	6.6304	-1.2951	2.8843
H181	7.1992	-2.2179	2.7158
H182	7.2871	-0.4548	3.1755
H183	6.8283	-5.3349	2.3223
H184	7.4438	3.2104	0.0031
H185	7.9008	1.4664	-0.2749
H186	7.1375	-4.5511	0.1056
N187	-1.6552	-2.0466	-0.9934
N188	-1.8355	-3.1262	-1.3505

4. References

(1) Cherney, A. H.; Kadunce, N. T.; Reisman, S. E. Enantioselective and Enantiospecific Transition-Metal-Catalyzed Cross-Coupling Reactions of Organometallic Reagents To Construct C–C Bonds. *Chem. Rev.* **2015**, *115* (17), 9587–9652. https://doi.org/10.1021/acs.chemrev.5b00162.

(2) Yus, M.; Nájera, C.; Foubelo, F.; Sansano, J. M. Metal-Catalyzed Enantioconvergent Transformations. *Chem. Rev.* **2023**, *123* (20), 11817–11893. https://doi.org/10.1021/acs.chemrev.3c00059.

(3) Choi, J.; Fu, G. C. Transition Metal–Catalyzed Alkyl-Alkyl Bond Formation: Another Dimension in Cross-Coupling Chemistry. *Science* **2017**, *356* (6334), eaaf7230. https://doi.org/10.1126/science.aaf7230.

(4) Fu, G. C. Transition-Metal Catalysis of Nucleophilic Substitution Reactions: A Radical Alternative to S $_N$ 1 and S $_N$ 2 Processes. *ACS Cent. Sci.* **2017**, *3* (7), 692–700. https://doi.org/10.1021/acscentsci.7b00212.

(5) Bera, S.; Fan, C.; Hu, X. Enantio- and Diastereoselective Construction of Vicinal C(Sp3) Centres via Nickel-Catalysed Hydroalkylation of Alkenes. *Nat. Catal.* **2022**, *5* (12), 1180–1187. https://doi.org/10.1038/s41929-022-00894-0.

(6) Chen, J.; Wu, L.; Zhao, Y.; Zhu, S. Enantio- and Diastereoselective NiH-Catalyzed Hydroalkylation of Enamides or Enecarbamates with Racemic *α* -Bromoamides**. *Angew. Chem. Int. Ed.* **2023**, *62* (44), e202311094. https://doi.org/10.1002/anie.202311094.

(7) Dong, Z.; Xu, C.; Chang, J.; Zhou, S.; Sun, P.; Li, Y.; Chen, L.-A. Enantioselective Directed Nickel-Catalyzed Three-Component Reductive Arylalkylation of Alkenes via the Carbometalation/Radical Cross-Coupling Sequence. *ACS Catal.* **2024**, *14* (7), 4395–4406. https://doi.org/10.1021/acscatal.4c00477.

(8) Tan, S.-Z.; Zhang, D.-F.; Zhu, L.; Ouyang, Q.; Du, W.; Chen, Y.-C. Divergent Asymmetric Dialkylation of Dienoic Acids with Carbonyls and Zinc Reagents via Tandem Ni(0) and Ni(II) Catalysis. *J. Am. Chem. Soc.* **2025**, *147* (24), 20947–20956. https://doi.org/10.1021/jacs.5c05284.

(9) Xi, Y.; Huang, W.; Wang, C.; Ding, H.; Xia, T.; Wu, L.; Fang, K.; Qu, J.; Chen, Y. Catalytic Asymmetric Diarylation of Internal Acyclic Styrenes and Enamides. *J. Am. Chem. Soc.* **2022**, *144* (18), 8389–8398. https://doi.org/10.1021/jacs.2c03411.

(10) Wang, L.; Lin, C.; Chong, Q.; Zhang, Z.; Meng, F. Photoredox Cobalt-Catalyzed Regio-, Diastereo- and Enantioselective Propargylation of Aldehydes via Propargyl Radicals. *Nat. Commun.* **2023**, *14* (1), 4825. https://doi.org/10.1038/s41467-023-40488-3.

(11) Li, Z.; Liu, B.; Yao, C.-Y.; Gao, G.-W.; Zhang, J.-Y.; Tong, Y.-Z.; Zhou, J.-X.; Sun, H.-K.; Liu, Q.; Lu, X.; Fu, Y. Ligand-Controlled Cobalt-Catalyzed Regio-, Enantio-, and Diastereoselective Oxyheterocyclic Alkene Hydroalkylation. *J. Am. Chem. Soc.* **2024**, *146* (5), 3405–3415. https://doi.org/10.1021/jacs.3c12881.

(12) Ghosh, S.; Mukherjee, S. Doubly Stereoconvergent Propargylic Alkylation of α-Cyanocarbonyls: Enantioselective Construction of Vicinal Stereocenters. *Org. Lett.* **2024**, *26* (36), 7733–7738. https://doi.org/10.1021/acs.orglett.4c02880.

(13) Zhang, J.; Zhu, W.; Chen, Z.; Zhang, Q.; Guo, C. Dual-Catalyzed Stereodivergent Electrooxidative Homocoupling of Benzoxazolyl Acetate. *J. Am. Chem. Soc.* **2024**, *146* (2), 1522–1531. https://doi.org/10.1021/jacs.3c11429.

(14) He, J.; Yoon, W. S.; Yun, J. Cu-Catalyzed Diastereo- and Enantioselective Synthesis of Homopropargyl Amines Bearing All-Carbon Quaternary Stereocenters via Chirality Transfer of Hindered Allenylcopper Species. *ACS Catal.* **2025**, *15* (1), 578–584. https://doi.org/10.1021/acscatal.4c06631.
(15) Han, J.; Liu, X.; Jin, H.; Guo, P.; Xu, L.; Li, P.; Zhan, M. Iridium-Catalyzed Doubly Stereoconvergent Allylic Alkylation of Racemic α-Boryl Organozinc Reagents. *Chem Catal.* **2024**, *4* (2), 100858. https://doi.org/10.1016/j.checat.2023.100858.
(16) Xi, Y.; Huang, W.; Wang, C.; Ding, H.; Xia, T.; Wu, L.; Fang, K.; Qu, J.; Chen, Y. Catalytic Asymmetric Diarylation of Internal Acyclic Styrenes and Enamides. *J. Am. Chem. Soc.* **2022**, *144* (18), 8389–8398. https://doi.org/10.1021/jacs.2c03411.
(17) Tosatti, P.; Campbell, A. J.; House, D.; Nelson, A.; Marsden, S. P. Catalyst Control in Sequential Asymmetric Allylic Substitution: Stereodivergent Access to *N,N* -Diprotected Unnatural Amino Acids. *J. Org. Chem.* **2011**, *76* (13), 5495–5501. https://doi.org/10.1021/jo200720c.
(18) Mu, X.; Shibata, Y.; Makida, Y.; Fu, G. C. Control of Vicinal Stereocenters through Nickel-Catalyzed Alkyl–Alkyl Cross-Coupling. *Angew. Chem. Int. Ed.* **2017**, *56* (21), 5821–5824. https://doi.org/10.1002/anie.201702402.
(19) Huo, H.; Gorsline, B. J.; Fu, G. C. Catalyst-Controlled Doubly Enantioconvergent Coupling of Racemic Alkyl Nucleophiles and Electrophiles. *Science* **2020**, *367* (6477), 559–564. https://doi.org/10.1126/science.aaz3855.
(20) Hossain, A.; Anderson, R. L.; Zhang, C. S.; Chen, P.-J.; Fu, G. C. Nickel-Catalyzed Enantioconvergent and Diastereoselective Allenylation of Alkyl Electrophiles: Simultaneous Control of Central and Axial Chirality. *J. Am. Chem. Soc.* **2024**, *146* (11), 7173–7177. https://doi.org/10.1021/jacs.4c00593.
(21) Pu, X.; Qi, X.; Ready, J. M. Allenes in Asymmetric Catalysis: Asymmetric Ring Opening of *Meso* -Epoxides Catalyzed by Allene-Containing Phosphine Oxides. *J. Am. Chem. Soc.* **2009**, *131* (30), 10364–10365. https://doi.org/10.1021/ja9041127.
(22) Ban, H. S.; Onagi, S.; Uno, M.; Nabeyama, W.; Nakamura, H. Allene as an Alternative Functional Group for Drug Design: Effect of C□C Multiple Bonds Conjugated with Quinazolines on the Inhibition of EGFR Tyrosine Kinase. *ChemMedChem* **2008**, *3* (7), 1094–1103. https://doi.org/10.1002/cmdc.200800073.
(23) Souli, C.; Avlonitis, N.; Calogeropoulou, T.; Tsotinis, A.; Maksay, G.; Bíró, T.; Politi, A.; Mavromoustakos, T.; Makriyannis, A.; Reis, H.; Papadopoulos, M. Novel 17β-Substituted Conformationally Constrained Neurosteroids That Modulate $GABA_A$ Receptors. *J. Med. Chem.* **2005**, *48* (16), 5203–5214. https://doi.org/10.1021/jm050271q.
(24) Rivera-Fuentes, P.; Diederich, F. Allenes in Molecular Materials. *Angew. Chem. Int. Ed.* **2012**, *51* (12), 2818–2828. https://doi.org/10.1002/anie.201108001.
(25) Yin, H.; Fu, G. C. Mechanistic Investigation of Enantioconvergent Kumada Reactions of Racemic α-Bromoketones Catalyzed by a Nickel/Bis(Oxazoline) Complex. *J. Am. Chem. Soc.* **2019**, *141* (38), 15433–15440. https://doi.org/10.1021/jacs.9b08185.
(26) Schley, N. D.; Fu, G. C. Nickel-Catalyzed Negishi Arylations of Propargylic Bromides: A Mechanistic Investigation. *J. Am. Chem. Soc.* **2014**, *136* (47), 16588–16593. https://doi.org/10.1021/ja508718m.
(27) Macrae, C. F.; Sovago, I.; Cottrell, S. J.; Galek, P. T. A.; McCabe, P.; Pidcock, E.; Platings, M.; Shields, G. P.; Stevens, J. S.; Towler, M.; Wood, P. A. *Mercury 4.0* : From Visualization

to Analysis, Design and Prediction. *J. Appl. Crystallogr.* **2020**, *53* (1), 226–235. https://doi.org/10.1107/S1600576719014092.
(28) Neese, F. Software Update: The ORCA Program System—Version 5.0. *WIREs Comput. Mol. Sci.* **2022**, *12* (5), e1606. https://doi.org/10.1002/wcms.1606.
(29) Neese, F. The SHARK Integral Generation and Digestion System. *J. Comput. Chem.* **2023**, *44* (3), 381–396. https://doi.org/10.1002/jcc.26942.
(30) Neese, F.; Wennmohs, F.; Hansen, A.; Becker, U. Efficient, Approximate and Parallel Hartree–Fock and Hybrid DFT Calculations. A 'Chain-of-Spheres' Algorithm for the Hartree–Fock Exchange. *Chem. Phys.* **2009**, *356* (1–3), 98–109. https://doi.org/10.1016/j.chemphys.2008.10.036.
(31) Neese, F. An Improvement of the Resolution of the Identity Approximation for the Formation of the Coulomb Matrix. *J. Comput. Chem.* **2003**, *24* (14), 1740–1747. https://doi.org/10.1002/jcc.10318.
(32) Wittmann, L.; Gordiy, I.; Friede, M.; Helmich-Paris, B.; Grimme, S.; Hansen, A.; Bursch, M. Extension of the D3 and D4 London Dispersion Corrections to the Full Actinides Series. *Phys. Chem. Chem. Phys.* **2024**, *26* (32), 21379–21394. https://doi.org/10.1039/D4CP01514B.
(33) Garcia-Ratés, M.; Neese, F. Efficient Implementation of the Analytical Second Derivatives of Hartree–Fock and Hybrid DFT Energies within the Framework of the Conductor-like Polarizable Continuum Model. *J. Comput. Chem.* **2019**, *40* (20), 1816–1828. https://doi.org/10.1002/jcc.25833.
(34) Caldeweyher, E.; Bannwarth, C.; Grimme, S. Extension of the D3 Dispersion Coefficient Model. *J. Chem. Phys.* **2017**, *147* (3), 034112. https://doi.org/10.1063/1.4993215.
(35) Rappoport, D.; Furche, F. Property-Optimized Gaussian Basis Sets for Molecular Response Calculations. *J. Chem. Phys.* **2010**, *133* (13), 134105. https://doi.org/10.1063/1.3484283.
(36) Weigend, F.; Ahlrichs, R. Balanced Basis Sets of Split Valence, Triple Zeta Valence and Quadruple Zeta Valence Quality for H to Rn: Design and Assessment of Accuracy. *Phys. Chem. Chem. Phys.* **2005**, *7* (18), 3297. https://doi.org/10.1039/b508541a.
(37) Helmich-Paris, B.; De Souza, B.; Neese, F.; Izsák, R. An Improved Chain of Spheres for Exchange Algorithm. *J. Chem. Phys.* **2021**, *155* (10), 104109. https://doi.org/10.1063/5.0058766.
(38) Heidrich, D.; Quapp, W. Saddle Points of Index 2 on Potential Energy Surfaces and Their Role in Theoretical Reactivity Investigations. *Theor. Chim. Acta* **1986**, *70* (2), 89–98. https://doi.org/10.1007/BF00532206.
(39) Garcia-Ratés, M.; Neese, F. Effect of the Solute Cavity on the Solvation Energy and Its Derivatives within the Framework of the Gaussian Charge Scheme. *J. Comput. Chem.* **2020**, *41* (9), 922–939. https://doi.org/10.1002/jcc.26139.
(40) Zhao, Y.; Truhlar, D. G. The M06 Suite of Density Functionals for Main Group Thermochemistry, Thermochemical Kinetics, Noncovalent Interactions, Excited States, and Transition Elements: Two New Functionals and Systematic Testing of Four M06-Class Functionals and 12 Other Functionals. *Theor. Chem. Acc.* **2008**, *120* (1–3), 215–241. https://doi.org/10.1007/s00214-007-0310-x.
(41) St. John, P. C.; Guan, Y.; Kim, Y.; Etz, B. D.; Kim, S.; Paton, R. S. Quantum Chemical Calculations for over 200,000 Organic Radical Species and 40,000 Associated Closed-Shell Molecules. *Sci. Data* **2020**, *7* (1), 244. https://doi.org/10.1038/s41597-020-00588-x.

(42) McGrath, N. A.; Brichacek, M.; Njardarson, J. T. A Graphical Journey of Innovative Organic Architectures That Have Improved Our Lives. *J. Chem. Educ.* **2010**, *87* (12), 1348–1349. https://doi.org/10.1021/ed1003806.
(43) Finlay, M. R. V.; Anderton, M.; Ashton, S.; Ballard, P.; Bethel, P. A.; Box, M. R.; Bradbury, R. H.; Brown, S. J.; Butterworth, S.; Campbell, A.; Chorley, C.; Colclough, N.; Cross, D. A. E.; Currie, G. S.; Grist, M.; Hassall, L.; Hill, G. B.; James, D.; James, M.; Kemmitt, P.; Klinowska, T.; Lamont, G.; Lamont, S. G.; Martin, N.; McFarland, H. L.; Mellor, M. J.; Orme, J. P.; Perkins, D.; Perkins, P.; Richmond, G.; Smith, P.; Ward, R. A.; Waring, M. J.; Whittaker, D.; Wells, S.; Wrigley, G. L. Discovery of a Potent and Selective EGFR Inhibitor (AZD9291) of Both Sensitizing and T790M Resistance Mutations That Spares the Wild Type Form of the Receptor. *J. Med. Chem.* **2014**, *57* (20), 8249–8267. https://doi.org/10.1021/jm500973a.
(44) O'Brien, C. F.; Jimenez, R.; Hauser, R. A.; Factor, S. A.; Burke, J.; Mandri, D.; Castro-Gayol, J. C. NBI-98854, a Selective Monoamine Transport Inhibitor for the Treatment of Tardive Dyskinesia: A Randomized, Double-blind, Placebo-controlled Study. *Mov. Disord.* **2015**, *30* (12), 1681–1687. https://doi.org/10.1002/mds.26330.
(45) Letchuman, S.; Madhuranga, H. D. T.; Madhurangi, B. L. N. K.; Premarathna, A. D.; Saravanan, M. Alkaloids Unveiled: A Comprehensive Analysis of Novel Therapeutic Properties, Mechanisms, and Plant-Based Innovations. *Intell. Pharm.* **2025**, *3* (4), 268–276. https://doi.org/10.1016/j.ipha.2024.09.007.
(46) Heinrich, M.; Mah, J.; Amirkia, V. Alkaloids Used as Medicines: Structural Phytochemistry Meets Biodiversity—An Update and Forward Look. *Molecules* **2021**, *26* (7), 1836. https://doi.org/10.3390/molecules26071836.
(47) Kim, A. N.; Ngamnithiporn, A.; Du, E.; Stoltz, B. M. Recent Advances in the Total Synthesis of the Tetrahydroisoquinoline Alkaloids (2002–2020). *Chem. Rev.* **2023**, *123* (15), 9447–9496. https://doi.org/10.1021/acs.chemrev.3c00054.
(48) Brown, D. G.; Boström, J. Analysis of Past and Present Synthetic Methodologies on Medicinal Chemistry: Where Have All the New Reactions Gone?: Miniperspective. *J. Med. Chem.* **2016**, *59* (10), 4443–4458. https://doi.org/10.1021/acs.jmedchem.5b01409.
(49) Afanasyev, O. I.; Kuchuk, E.; Usanov, D. L.; Chusov, D. Reductive Amination in the Synthesis of Pharmaceuticals. *Chem. Rev.* **2019**, *119* (23), 11857–11911. https://doi.org/10.1021/acs.chemrev.9b00383.
(50) Fu, G. C. Transition-Metal Catalysis of Nucleophilic Substitution Reactions: A Radical Alternative to S_N 1 and S_N 2 Processes. *ACS Cent. Sci.* **2017**, *3* (7), 692–700. https://doi.org/10.1021/acscentsci.7b00212.
(51) Bissember, A. C.; Lundgren, R. J.; Creutz, S. E.; Peters, J. C.; Fu, G. C. Transition-Metal-Catalyzed Alkylations of Amines with Alkyl Halides: Photoinduced, Copper-Catalyzed Couplings of Carbazoles. *Angew. Chem. Int. Ed.* **2013**, *52* (19), 5129–5133. https://doi.org/10.1002/anie.201301202.
(52) Do, H.-Q.; Bachman, S.; Bissember, A. C.; Peters, J. C.; Fu, G. C. Photoinduced, Copper-Catalyzed Alkylation of Amides with Unactivated Secondary Alkyl Halides at Room Temperature. *J. Am. Chem. Soc.* **2014**, *136* (5), 2162–2167. https://doi.org/10.1021/ja4126609.
(53) Peacock, D. M.; Roos, C. B.; Hartwig, J. F. Palladium-Catalyzed Cross Coupling of Secondary and Tertiary Alkyl Bromides with a Nitrogen Nucleophile. *ACS Cent. Sci.* **2016**, *2* (9), 647–652. https://doi.org/10.1021/acscentsci.6b00187.

(54) Cho, H.; Tong, X.; Zuccarello, G.; Anderson, R. L.; Fu, G. C. Synthesis of Tertiary Alkyl Amines via Photoinduced Copper-Catalysed Nucleophilic Substitution. *Nat. Chem.* **2025**, *17* (2), 271–278. https://doi.org/10.1038/s41557-024-01692-w.
(55) Chen, C.; Peters, J. C.; Fu, G. C. Photoinduced Copper-Catalysed Asymmetric Amidation via Ligand Cooperativity. *Nature* **2021**, *596* (7871), 250–256. https://doi.org/10.1038/s41586-021-03730-w.
(56) Matier, C. D.; Schwaben, J.; Peters, J. C.; Fu, G. C. Copper-Catalyzed Alkylation of Aliphatic Amines Induced by Visible Light. *J. Am. Chem. Soc.* **2017**, *139* (49), 17707–17710. https://doi.org/10.1021/jacs.7b09582.
(57) Dang, Q.-Q.; Tian, X.; Li, H.; Liu, X.-N.; Wen, Z.-K. Copper-Catalyzed Reductive Alkylation of β-Acyl Allylic Thioethers with Alkyl Bromides to Access α-Branched Enones with Flexible Alkyl Chains. *Org. Lett.* **2025**, *27* (16), 4355–4360. https://doi.org/10.1021/acs.orglett.5c01098.
(58) Huang, S.; Trevino, R.; Zuo, D.; Tian, X.; Yang, W.; Hughes, W. B.; Fremin, S. O.; Porey, A.; Nguyen, V. T. B.; Gao, B.; Xu, X.; Dhungana, B. R.; Jiang, Y.; Sun, Y.; Huang, C.; He, M.; Giri, C.; Dhakal, S. K.; Qin, B.; Liu, Y.; Cheng, M.; Larionov, O. V.; Jin, S. Cobalt-Catalyzed Enantioconvergent Decarboxylative N-Alkylation. *J. Am. Chem. Soc.* **2025**, *147* (24), 21097–21108. https://doi.org/10.1021/jacs.5c06317.
(59) Lin, S.; Peng, Q.; Ou, Q.; Shuai, Z. Strong Solid-State Fluorescence Induced by Restriction of the Coordinate Bond Bending in Two-Coordinate Copper(I)–Carbene Complexes. *Inorg. Chem.* **2019**, *58* (21), 14403–14409. https://doi.org/10.1021/acs.inorgchem.9b01705.
(60) Wyman, J. Dielectric Constants: Ethanol—Diethyl Ether and Urea—Water Solutions between 0 and 50°. *J. Am. Chem. Soc.* **1933**, *55* (10), 4116–4121. https://doi.org/10.1021/ja01337a029.
(61) Mardirossian, N.; Head-Gordon, M. *ω* B97M-V: A Combinatorially Optimized, Range-Separated Hybrid, Meta-GGA Density Functional with VV10 Nonlocal Correlation. *J. Chem. Phys.* **2016**, *144* (21), 214110. https://doi.org/10.1063/1.4952647.
(62) Marenich, A. V.; Cramer, C. J.; Truhlar, D. G. Universal Solvation Model Based on Solute Electron Density and on a Continuum Model of the Solvent Defined by the Bulk Dielectric Constant and Atomic Surface Tensions. *J. Phys. Chem. B* **2009**, *113* (18), 6378–6396. https://doi.org/10.1021/jp810292n.
(63) Ghosh, A. K.; Sarkar, A.; Brindisi, M. The Curtius Rearrangement: Mechanistic Insight and Recent Applications in Natural Product Syntheses. *Org. Biomol. Chem.* **2018**, *16* (12), 2006–2027. https://doi.org/10.1039/C8OB00138C.
(64) Kolb, H. C.; Sharpless, K. B. The Growing Impact of Click Chemistry on Drug Discovery. *Drug Discov. Today* **2003**, *8* (24), 1128–1137. https://doi.org/10.1016/S1359-6446(03)02933-7.
(65) Rostovtsev, V. V.; Green, L. G.; Fokin, V. V.; Sharpless, K. B. A Stepwise Huisgen Cycloaddition Process: Copper(I)-Catalyzed Regioselective "Ligation" of Azides and Terminal Alkynes. *Angew. Chem. Int. Ed.* **2002**, *41* (14), 2596–2599. https://doi.org/10.1002/1521-3773(20020715)41:14%253C2596::AID-ANIE2596%253E3.0.CO;2-4.
(66) Sletten, E. M.; Bertozzi, C. R. From Mechanism to Mouse: A Tale of Two Bioorthogonal Reactions. *Acc. Chem. Res.* **2011**, *44* (9), 666–676. https://doi.org/10.1021/ar200148z.
(67) Bednarek, C.; Wehl, I.; Jung, N.; Schepers, U.; Bräse, S. The Staudinger Ligation. *Chem. Rev.* **2020**, *120* (10), 4301–4354. https://doi.org/10.1021/acs.chemrev.9b00665.

(68) Schilling, C. I.; Jung, N.; Biskup, M.; Schepers, U.; Bräse, S. Bioconjugation via Azide–Staudinger Ligation: An Overview. *Chem. Soc. Rev.* **2011**, *40* (9), 4840. https://doi.org/10.1039/c0cs00123f.
(69) Corey, E. J.; Link, J. O. A General, Catalytic, and Enantioselective Synthesis of .Alpha.-Amino Acids. *J. Am. Chem. Soc.* **1992**, *114* (5), 1906–1908. https://doi.org/10.1021/ja00031a069.
(70) Himo, F.; Demko, Z. P.; Noodleman, L.; Sharpless, K. B. Mechanisms of Tetrazole Formation by Addition of Azide to Nitriles. *J. Am. Chem. Soc.* **2002**, *124* (41), 12210–12216. https://doi.org/10.1021/ja0206644.
(71) Nugent, W. A. Chiral Lewis Acid Catalysis. Enantioselective Addition of Azide to Meso Epoxides. *J. Am. Chem. Soc.* **1992**, *114* (7), 2768–2769. https://doi.org/10.1021/ja00033a090.
(72) Li, Z.; Fernández, M.; Jacobsen, E. N. Enantioselective Ring Opening of Meso Aziridines Catalyzed by Tridentate Schiff Base Chromium(III) Complexes. *Org. Lett.* **1999**, *1* (10), 1611–1613. https://doi.org/10.1021/ol990992h.
(73) Zhong, F.; Zhao, X.; Liao, L. Catalytic Asymmetric Azidative Functionalization of Alkenes. *Eur. J. Org. Chem.* **2025**, *28* (17), e202500015. https://doi.org/10.1002/ejoc.202500015.
(74) Myers, J. K.; Jacobsen, E. N. Asymmetric Synthesis of β-Amino Acid Derivatives via Catalytic Conjugate Addition of Hydrazoic Acid to Unsaturated Imides. *J. Am. Chem. Soc.* **1999**, *121* (38), 8959–8960. https://doi.org/10.1021/ja991621z.
(75) Wu, L.; Zhang, Z.; Wu, D.; Wang, F.; Chen, P.; Lin, Z.; Liu, G. Anionic Bisoxazoline Ligands Enable Copper-Catalyzed Asymmetric Radical Azidation of Acrylamides. *Angew. Chem. Int. Ed.* **2021**, *60* (13), 6997–7001. https://doi.org/10.1002/anie.202015083.
(76) Ge, L.; Wang, H.; Liu, Y.; Feng, X. Asymmetric Three-Component Radical Alkene Carboazidation by Direct Activation of Aliphatic C–H Bonds. *J. Am. Chem. Soc.* **2024**, *146* (19), 13347–13355. https://doi.org/10.1021/jacs.4c02012.
(77) Wang, K.; Li, Y.; Li, X.; Li, D.; Bao, H. Iron-Catalyzed Asymmetric Decarboxylative Azidation. *Org. Lett.* **2021**, *23* (22), 8847–8851. https://doi.org/10.1021/acs.orglett.1c03355.
(78) Rui, J.; Mu, X.; Soler, J.; Paris, J. C.; Guo, Y.; Garcia-Borràs, M.; Huang, X. Merging Photoredox with Metalloenzymatic Catalysis for Enantioselective Decarboxylative C(Sp3)–N3 and C(Sp3)–SCN Bond Formation. *Nat. Catal.* **2024**, *7* (12), 1394–1403. https://doi.org/10.1038/s41929-024-01257-7.
(79) Rui, J.; Zhao, Q.; Huls, A. J.; Soler, J.; Paris, J. C.; Chen, Z.; Reshetnikov, V.; Yang, Y.; Guo, Y.; Garcia-Borràs, M.; Huang, X. Directed Evolution of Nonheme Iron Enzymes to Access Abiological Radical-Relay C(Sp^3)−H Azidation. *Science* **2022**, *376* (6595), 869–874. https://doi.org/10.1126/science.abj2830.
(80) Deng, Q.-H.; Bleith, T.; Wadepohl, H.; Gade, L. H. Enantioselective Iron-Catalyzed Azidation of β-Keto Esters and Oxindoles. *J. Am. Chem. Soc.* **2013**, *135* (14), 5356–5359. https://doi.org/10.1021/ja402082p.
(81) Wang, R.; Liang, Y.-J.; Bian, K.-J.; Xu, J.; Zhou, S.-Y.; Jin, R.-X.; Guan, W.; Wang, X.-S. Bioinspired Copper/Amine Cooperative Catalysis Enables Asymmetric Radical Azidation. *J. Am. Chem. Soc.* **2025**, *147* (8), 6644–6653. https://doi.org/10.1021/jacs.4c15840.
(82) Zhang, X.; Ren, J.; Tan, S. M.; Tan, D.; Lee, R.; Tan, C.-H. An Enantioconvergent Halogenophilic Nucleophilic Substitution (S_N 2X) Reaction. *Science* **2019**, *363* (6425), 400–404. https://doi.org/10.1126/science.aau7797.

(83) Ren, J.; Ban, X.; Zhang, X.; Tan, S. M.; Lee, R.; Tan, C. Kinetic and Dynamic Kinetic Resolution of Racemic Tertiary Bromides by Pentanidium-Catalyzed Phase-Transfer Azidation. *Angew. Chem. Int. Ed.* **2020**, *59* (23), 9055–9058. https://doi.org/10.1002/anie.202000138.
(84) Wang, J.; Horwitz, M. A.; Dürr, A. B.; Ibba, F.; Pupo, G.; Gao, Y.; Ricci, P.; Christensen, K. E.; Pathak, T. P.; Claridge, T. D. W.; Lloyd-Jones, G. C.; Paton, R. S.; Gouverneur, V. Asymmetric Azidation under Hydrogen Bonding Phase-Transfer Catalysis: A Combined Experimental and Computational Study. *J. Am. Chem. Soc.* **2022**, *144* (10), 4572–4584. https://doi.org/10.1021/jacs.1c13434.
(85) Cho, H.; Suematsu, H.; Oyala, P. H.; Peters, J. C.; Fu, G. C. Photoinduced, Copper-Catalyzed Enantioconvergent Alkylations of Anilines by Racemic Tertiary Electrophiles: Synthesis and Mechanism. *J. Am. Chem. Soc.* **2022**, *144* (10), 4550–4558. https://doi.org/10.1021/jacs.1c12749.
(86) Neese, F. Software Update: The ORCA Program System—Version 6.0. *WIREs Comput. Mol. Sci.* **2025**, *15* (2), e70019. https://doi.org/10.1002/wcms.70019.
(87) Stephens, P. J.; Devlin, F. J.; Chabalowski, C. F.; Frisch, M. J. Ab Initio Calculation of Vibrational Absorption and Circular Dichroism Spectra Using Density Functional Force Fields. *J. Phys. Chem.* **1994**, *98* (45), 11623–11627. https://doi.org/10.1021/j100096a001.
(88) Lehtola, S.; Steigemann, C.; Oliveira, M. J. T.; Marques, M. A. L. Recent Developments in Libxc — A Comprehensive Library of Functionals for Density Functional Theory. *SoftwareX* **2018**, *7*, 1–5. https://doi.org/10.1016/j.softx.2017.11.002.
(89) Weigend, F. Accurate Coulomb-Fitting Basis Sets for H to Rn. *Phys. Chem. Chem. Phys.* **2006**, *8* (9), 1057. https://doi.org/10.1039/b515623h.
(90) Pereira, S. M.; Rivas, M. A.; Iglesias, T. P. Speeds of Sound, Densities, and Isentropic Compressibilities of the System Methanol + Tetraethylene Glycol Dimethyl Ether at the Temperatures from 293.15 K to 333.15 K. *J. Chem. Eng. Data* **2002**, *47* (6), 1363–1366. https://doi.org/10.1021/je020028l.
(91) Franchini, G.; Marchetti, A.; Seeber, R.; Tassi, L.; Zannini, P. Refractive Properties of Binary Mixtures Containing *N,N*- Dimethylformamide + 2-Methoxyethanol or 1,2-Dimethoxyethane. *Phys. Chem. Liq.* **2001**, *39* (3), 277–300. https://doi.org/10.1080/00319100108031663.
(92) Perdew, J. P.; Kurth, S.; Zupan, A.; Blaha, P. Accurate Density Functional with Correct Formal Properties: A Step Beyond the Generalized Gradient Approximation. *Phys. Rev. Lett.* **1999**, *82* (12), 2544–2547. https://doi.org/10.1103/PhysRevLett.82.2544.
(93) Perdew, J. P.; Tao, J.; Staroverov, V. N.; Scuseria, G. E. Meta-Generalized Gradient Approximation: Explanation of a Realistic Nonempirical Density Functional. *J. Chem. Phys.* **2004**, *120* (15), 6898–6911. https://doi.org/10.1063/1.1665298.
(94) Jensen, K. P. Bioinorganic Chemistry Modeled with the TPSSh Density Functional. *Inorg. Chem.* **2008**, *47* (22), 10357–10365. https://doi.org/10.1021/ic800841t.